



HAL
open science

Trafic endomembranaire des protéines membranaires chez les plantes

Doan D. Luu

► **To cite this version:**

Doan D. Luu. Trafic endomembranaire des protéines membranaires chez les plantes. Biologie végétale. 2014. tel-02799124

HAL Id: tel-02799124

<https://hal.inrae.fr/tel-02799124>

Submitted on 5 Jun 2020

HAL is a multi-disciplinary open access archive for the deposit and dissemination of scientific research documents, whether they are published or not. The documents may come from teaching and research institutions in France or abroad, or from public or private research centers.

L'archive ouverte pluridisciplinaire **HAL**, est destinée au dépôt et à la diffusion de documents scientifiques de niveau recherche, publiés ou non, émanant des établissements d'enseignement et de recherche français ou étrangers, des laboratoires publics ou privés.



Distributed under a Creative Commons Attribution - ShareAlike 4.0 International License

**UNIVERSITE MONTPELLIER II
SCIENCES ET TECHNIQUES**

NOTICE

pour obtenir le diplôme

HABILITATION A DIRIGER DES RECHERCHES

***Ecole Doctorale :
Systèmes Intégrés en Biologie, Agronomie, Géosciences,
Hydrosciences, Environnement***

présentée et soutenue publiquement

par

Doan Trung LUU

Année 2014

PLAN

| | |
|--|----|
| REMERCIEMENTS..... | 2 |
| 1 – CURRICULUM VITAE | 3 |
| 2 – LISTE DES PUBLICATIONS..... | 4 |
| 3 - ACTIVITES D’ENCADREMENT ET D’ENSEIGNEMENT | 10 |
| 4 - TRAVAUX D’EXPERTISE..... | 12 |
| 5 – CONTRATS DE RECHERCHE..... | 12 |
| 6 – ORGANISATION DE COLLOQUES..... | 12 |
| 7 - ACTIVITES DE VULGARISATION SCIENTIFIQUE | 12 |
| 8 - RESUME DES TRAVAUX ANTERIEURS | 14 |
| 8.1 - DEA-Doctorat (1993-1997) et premier post-doctorat (1997-2000) : Adhésion pollen-stigmate, évolution de la famille multigénique <i>S</i> et barrières interspécifiques chez les Brassicaceae..... | 14 |
| 8.2 – Deuxième post-doctorat (2000-2002) : Transformation chloroplastique et phytoremédiation | 15 |
| 9 – RECHERCHES EN COURS | 16 |
| 9.1 – Motifs protéiques portés par <i>AtPIP2;1</i> et impliqués dans son trafic endomembranaire | 16 |
| 9.2 – Effet de stimuli sur la localisation sub-cellulaire des aquaporines..... | 17 |
| 9.2.1 – Effet du NaCl par analyse « FRAP » | 17 |
| 9.2.2 – Effet du NaCl par analyse «SPT et FCS»..... | 19 |
| 9.2.3 – Effets de l’H ₂ O ₂ | 19 |
| 9.3 – Rôle des aquaporines dans l’émergence racinaire | 20 |
| 9.4 – Biologie cellulaire des aquaporines chez le riz | 21 |
| 9.5 Bilan | 22 |
| 10 – PROJET DE RECHERCHE | 23 |
| 10.1 – Remarques liminaires..... | 23 |
| 10.2 – Dynamique membranaire et cyclage des aquaporines dans les cellules de la racine d’ <i>Arabidopsis</i> sous stress salin. | 24 |
| 10.2.1 – Développement du sptPALM en biologie cellulaire chez les plantes. | 24 |
| 10.2.2 – Identification des acteurs moléculaires impliqués dans le cyclage d’ <i>AtPIP2;1</i> | 24 |
| 10.3 – Biologie cellulaire des aquaporines chez le riz. | 25 |
| REFERENCES CITEES | 27 |
| CINQ PUBLICATIONS SIGNIFICATIVES DU PARCOURS | 30 |

REMERCIEMENTS

Je souhaiterais tout d'abord remercier mes collègues membres du jury pour le temps qu'ils ont consacré à juger cette habilitation à diriger des recherches. Je voudrais aussi remercier les collègues qui, grâce aux discussions informelles que nous avons eues, ont permis de faire avancer mes réflexions sur mes recherches.

Mes remerciements vont aussi en direction des membres des laboratoires avec lesquels j'ai interagi depuis mes premiers pas dans ce métier de chercheur :

- Laboratoire Reconnaissance Cellulaire et Amélioration des Plantes, devenu par la suite Reproduction & Développement des Plantes à Lyon,
- Institut de Recherche en Biologie Végétale à Montréal,
- Laboratoire d'Ecophysiologie de la Photosynthèse du CEA de Cadarache,
- Laboratoire Biochimie & Physiologie Moléculaire des Plantes à Montpellier.

Mes pensées vont aussi en direction des personnels scientifiques, techniques et administratifs, mais aussi des étudiants que j'ai encadrés.

Plus particulièrement, j'ai une pensée pour M. Philippe Heizmann, mon Directeur de thèse, M. Mario Cappadocia et M. Gilles Peltier, mes Directeurs de stages post-doctoraux, respectivement, à Montréal et à Cadarache. Je voudrais aussi souligner mes remerciements à M. Christophe Maurel, chef de l'équipe "Aquaporines" dans laquelle je développe mes recherches depuis mon recrutement au CNRS, pour son soutien et sa précieuse expérience dont il m'a toujours fait bénéficier.

1 – CURRICULUM VITAE

Monsieur Doan-Trung LUU

Résidence :

22, impasse des oliviers
34070 Montpellier
Tél : 06 66 53 18 47

Laboratoire :

Biochimie & Physiologie Moléculaire des Plantes
SupAgro/INRA/CNRS/UMII UMR5004
2, Place Viala
34060 Montpellier
Tél : 04 99 61 20 20 / Fax : 04 67 52 57 37
E-mail : luu@supagro.inra.fr



Né le 10/12/1969, à Tan Thuan Dong (Vietnam) ; célibataire ; nationalité française.

➤ Diplômes :

| | | | |
|------|---------------------|----------------------------------|---------------------------------|
| 1997 | Doctorat | Ecole Normale Supérieure de LYON | Sciences de la Vie |
| 1994 | DEA | Université LYON I | Différenciation/Génétique Immu. |
| 1994 | Magistère | Université & E.N.S. LYON | Bio. Moléculaire et Cellulaire |
| 1992 | Maîtrise | Université LYON I | Bio. Moléculaire et Cellulaire |
| 1991 | Licence | Université LYON I | Bio. Moléculaire et Cellulaire |
| 1990 | DUT | IUT Université LYON I | Biologie Appliquée (Agronomie) |
| 1988 | Baccalauréat | Académie de NICE | Sc. Naturelles et Mathématiques |

➤ Expériences en recherche :

| Durée : | Etablissement : | Nom du responsable : | Sujet : |
|--|--|----------------------|---|
| Depuis 2002 | Montpellier SupAgro | Dr MAUREL C. | Transport de l'eau dans la plante |
| Recrutement au CNRS en tant que Chargé de recherche 1 ^{er} classe | | | |
| 2012-2013 | Mise à disposition d'un an à l'Agricultural Genetics Institute-LMI-RICE (Vietnam). | | |
| 2000-2001 | CEA Cadarache | Dr PELTIER G. | Phytoremédiation Stage post-doctoral |
| 1997-2000 | IRBV-Univ. de Montréal | Pr CAPPADOCIA M. | Signalisation mol. Stage post-doctoral |
| 1993-1997 | E.N.S. Lyon | Dr HEIZMANN Ph. | Dével & Reprod. Stage DEA et thèse |

➤ Bourses obtenues :

- Bourse Marie Curie Actions – International outgoing fellowship (Commission européenne) (2012-2014).
- Bourse Post-doctorale d'excellence du ministère de l'Éducation Québec (Canada) (1998-2000).
- Bourse Post-doctorale Jean Walter-Zellidja de l'Académie Française (1997-1998).
- Bourse de voyage du Centre Jacques Cartier (1997).
- Bourse de DEA et de Doctorat du Ministère de la Recherche (France) (1993-1997).

Distinctions :

Médaillé du service national et des Nations Unies pour volontariat service long en Bosnie-Herzégovine (1993). Titre de reconnaissance de la Nation (2003). Carte et Médaille du combattant (2012).

2 – LISTE DES PUBLICATIONS

□ *Revue à comité de lecture*

• Travaux sur le transport de l'eau dans la plante :

- Wudick, M.M., Luu D-T, Tournaire-Roux, C., Sakamoto, W., and Maurel, C. (In press). Vegetative and sperm cell-specific aquaporins of *Arabidopsis thaliana* highlight the vacuolar equipment of pollen and contribute to plant reproduction. **Plant Physiology**.
- Sanchez-Romera B, Ruiz-Lozano JM, Li G, Luu D-T, Martínez-Ballesta MDC, Carvajal M, Zamarreño AM, García-Mina JM, Maurel C, Aroca R. (2014). Enhancement of root hydraulic conductivity by methyl jasmonate and the role of calcium and abscisic acid in this process. **Plant Cell Environment** 37, 995-1008..
- Li X, Luu D-T, Maurel C and Lin J. (2013). Probing plasma membrane dynamics at the single-molecule level. **Trends in Plant Science** 18(11), 617-624
- Luu D-T, Maurel C. (2013). Aquaporin trafficking in plant cells: an emerging membrane-protein model. **Traffic** 14, 629-635.
- Péret B, Li G, Zhao J, Band LR, Voßl U, Postaire O, Luu D-T, Da Ines O, Casimiro I, Lucas M, Wells DM, Lazzerini L, Nacry P, King JR, Jensen OE, Schäffner AR, Maurel C, Malcolm JB. (2012). Auxin regulates aquaporin function to facilitate lateral root emergence. **Nature Cell Biology** 14(10), 991-998.
- Martiniere A, Lavag I, Nageswaran G, Rolfe DJ, Maneta-Peyret L, Luu D-T, Botchway SW, Webb SED, Mongrand S, Maurel C, Martin-Fernandez ML, Kleine-Vehn J, Friml J, Moreau P and Runions J. (2012). The cell wall constrains lateral diffusion of plant plasma-membrane proteins. **Proceedings of the National Academy of Sciences USA** 109, 12805-12810.
- Martiniere A, Li X, Runions J, Lin J, Maurel C, Luu D-T. (2012). Salt stress triggers enhanced cycling of *Arabidopsis* root plasma-membrane aquaporins. **Plant Signaling & Behavior** 7, 529-532
- Luu D-T, Martiniere A, Sorieul M, Runions J, Maurel C. (2012). Fluorescence recovery after photobleaching reveals high cycling dynamics of plasma membrane aquaporins in *Arabidopsis* roots under salt stress. **The Plant Journal** 69, 894-905
- Li X, Wang X, Yang Y, Li R, He Q, Fang X, Luu D-T, Maurel C, Lin J. (2011). Single-molecule analysis of PIP2;1 dynamics and partitioning reveals multiple modes of *Arabidopsis* plasma membrane aquaporin regulation. **The Plant Cell** 23, 3780-3797
- Sorieul M, Santoni V, Maurel C, Luu D-T. (2011). Mechanisms and effects of retention of over-expressed aquaporin AtPIP2;1 in the endoplasmic reticulum. **Traffic** 12, 473-482
- Leborgne-Castel N, Luu D-T. (2009). Regulation of endocytosis by external stimuli. **Plant Biosystems** 143(3), 630-635
- Wudick MM, Luu D-T, Maurel C. (2009). A look inside: localization patterns and functions of intracellular plant aquaporins. **The New Phytologist** 184, 289-302.
- Maurel C, Santoni V, Luu D-T, Wudick MM, Verdoucq L. (2009). The cellular dynamics of plant aquaporin expression and functions. **Current Opinion in Plant Biology** 12, 690-698

- Boursiac Y, Prak S, Boudet J, Postaire O, Luu D-T, Tournaire-Roux C, Santoni V, Maurel C. (2008). The response of Arabidopsis root water transport to a challenging environment implicates reactive oxygen species- and phosphorylation-dependent internalization of aquaporins. **Plant Signaling Behavior** 3, 1096-1098.

- Boursiac Y., Boudet J., Postaire O., Luu D-T, Tournaire-Roux C., Maurel C. (2008). Stimulus-induced downregulation of root water transport involves reactive oxygen species-activated cell signalling and plasma membrane intrinsic protein internalization. **Plant Journal** 56(2), 207-18.

- Maurel, C., Verdoucq, L, Luu D-T, Santoni, V. (2008). Plant aquaporins: membrane channels with multiple integrated functions. **Annual Review of Plant Biology** 59, 595-624.

- Boursiac Y, Chen S, Luu D-T, Sorieul M, van den Dries N, Maurel C. (2005). Early Effects of Salinity on Water Transport in Arabidopsis Roots. Molecular and Cellular Features of Aquaporin Expression. **Plant Physiology** 139, 790-805

- Luu D-T, Maurel C. (2005). Aquaporins in a challenging environment: molecular gears for adjusting plant water status. **Plant, Cell & Environment** 28(1), 85-96

- Tournaire C, Sutka M, Javot, H, Gout E, Gerbeau P, Luu D-T, Bligny R, Maurel C. (2003). Gating of aquaporins by cytosolic pH regulates root water transport during anoxic stress. **Nature** 425(6956), 393-7

- Travaux sur la phytoremédiation :

- Picault N, Cazale AC, Beyly A, Cuine S, Carrier P, Luu D-T, Forestier C, Peltier G. (2006). Chloroplast targeting of phytochelatin synthase in Arabidopsis: effects on heavy metal tolerance and accumulation. **Biochimie** 88(11), 1743-50.

- Sauge-Merle S, Cuiné S, Carrier P, Lecomte-Pradines C, Luu D-T, Peltier G. (2003). Enhanced Toxic Metal Accumulation in Engineered Bacterial Cells Expressing *Arabidopsis thaliana* Phytochelatin Synthase. **Applied & Environmental Microbiology** 69(1), 490–494

- Travaux sur l'auto-incompatibilité gamétophytique :

- Luu D-T, Qin X, Laublin G, Yang Q, Morse D, Cappadocia M. (2001). Rejection of S-heteroallelic pollen by a dual-specific s-RNase in *Solanum chacoense* predicts a multimeric SI pollen component. **Genetics** 159(1), 329-35.

- Qin X, Luu D-T, Yang Q, Maes O, Matton DP, Morse D, Cappadocia M. (2001). Genotype-dependent differences in S12-RNase expression lead to sporadic self-compatibility. **Plant Molecular Biology** 45(3), 295-305.

- Luu D-T, Qin X, Laublin G, Morse D and Cappadocia M. (2000). S-RNase uptake by compatible pollen tubes in gaméophytic self-incompatibility. **Nature** 407(6804), 649-651.

- Matton D, Luu D-T, Qin X, Laublin G, O'Brien M, Maes O, Morse D and Cappadocia M. (1999). The production of an S-RNase with dual specificity suggests a novel hypothesis for generation of new S-alleles. **The Plant Cell** 11, 2087-2098.

- Travaux sur les barrières interspécifiques :

- Luu D-T, Hugues S, Passelegue E, Heizmann P. (2001). Evidence for orthologous *S-locus-related I* genes in several genera of Brassicaceae. **Molecular & General Genetics** 264(6), 735-45.

- Heizmann P, Luu D-T, Dumas C. (2000). The clues to species specificity of pollination among Brassicaceae. **Sexual Plant Reproduction** 13, 157-161.
- Heizmann P, Luu D-T, Dumas C. (2000) Pollen-stigma adhesion in the Brassicaceae. **Annals of Botany** 85, 23-27.
- Luu D-T, Marty-Mazars D, Trick M, Dumas C and Heizmann P. (1999). Pollen-stigma adhesion in *Brassica* involves SLG and SLR1 glycoproteins. **The Plant Cell** 11, 251-262.
- Luu D-T, Passelègue E, Dumas C and Heizmann P. (1998). Pollen-stigma capture is not species discriminant within the Brassicaceae family. **Comptes Rendus de l'Académie des Sciences Paris sciences de la vie / life science** 321, 747-755.
- Luu D-T, Heizmann P and Dumas C. (1997). Pollen-stigma adhesion in *Brassica oleracea* is not dependent on the self-(in)compatibility genotype. **Plant Physiology** 115, 1221-1230.
- Luu D-T, Trick M, Heizmann P, Dumas C and Cappadocia M. (1997). Involvement of *SLR1* genes in pollen adhesion to stigmatic surface in Brassicaceae. **Sexual Plant Reproduction** 10, 227-235.

- Travaux issues de collaborations techniques :

- van Aarle IM, Viennois G, Amenc LK, Taty MV, Luu DT, Plassard C. (2007). Fluorescent *in situ* RT-PCR to visualise the expression of a phosphate transporter gene from an ectomycorrhizal fungus. **Mycorrhiza** 17, 487-494.
- Cellier F, Conejero G, Ricaud L, Luu D-T, Lepetit M, Gosti F, Casse F. (2004). Characterization of AtCHX17, a member of the cation/H⁺ exchangers, CHX family, from *Arabidopsis thaliana* suggests a role in K⁺ homeostasis. **The Plant Journal** 39(6):834-46.

- *Principales communications*

Les conférenciers et les personnes qui présentent les affiches sont indiqués en italique.

- Travaux sur le transport de l'eau dans la plante :

- Hosal E, Martinière A, Perrot-Rechenmann C, Choquet D, Maurel C, Luu D-T. (2013). Super-resolved and dynamic imaging in plant cell. High resolution imaging & applications workshop. Institut Pasteur, Paris (affiche)
- Luu D-T. (2013). Intracellular trafficking of aquaporins in *Arabidopsis thaliana*. Institut de Biologie Intégrative des Plantes, Montpellier (séminaire).
- Luu D-T. (2013). Intracellular trafficking of aquaporins in *Arabidopsis thaliana*. Laboratoire de Biogenèse membranaire, Bordeaux (séminaire).
- Maurel C, Prado K, Li G, Grondin A, Rodrigues O, Verdoucq L, Tournaire-Roux C, Boursiac Y, Santoni V, Luu D-T. (2013). Emerging functions of aquaporins in Arabidopsis. 16th International Workshop on Plant Membrane Biology. Kurashiki (Japon) (conférence).
- Wudick MM, Li XJ, Valentini V, Geldner N, Chory J, Lin J, Maurel C, Luu D-T. (2013). Plant aquaporin endomembrane trafficking and dynamics. 16th International Workshop on Plant Membrane Biology. Kurashiki (Japon) (affiche)
- Valentini V, Dichio B, Maurel C, Luu D-T. (2012). Study of the degradation of aquaporin AtPIP2;1 in *Arabidopsis thaliana*. 23rd International Conference on Arabidopsis research. Vienne (Autriche) (affiche)
- Luu D-T. (2012). Root water transport in *Arabidopsis thaliana* - Are there similar mechanisms in rice ? Conférencier invité. Agricultural Genetics Institute, Hanoi (Vietnam) (séminaire).

- *Wudick MM, Luu D-T and Maurel C* (2010) Sub-cellular pathway and role of hydrogen peroxide-induced redistribution of root aquaporins. 15th International Workshop on Plant Membrane Biology. Adelaide (Australie). (affiche)
- *Maurel C, Postaire O, Tournaire-Roux C, Boursiac Y, Li GW, Sutka M, Prado K, Santoni V, Wudick MM, Luu D-T, Schäffner AR, Monnet F and Genty B* (2010). The variety of aquaporin functions in roots and leaves. 15th International Workshop on Plant Membrane Biology. Adelaide (Australie) (conférence)
- *Maurel C, Postaire O, Tournaire-Roux C, Boursiac Y, Sutka M, Li G, Santoni V, Wudick MM, Luu D-T* (2010) Physiological and genetic dissection of aquaporin functions in roots and leaves. FESPB. Valence (Espagne). (conférence)
- *Vialet S, Sorieul M, Maurel C, Luu D-T.* (2009) Potential role of tyrosine motif in *AtPIP* trafficking. XIIth ENPER Meeting. Montpellier (conférence)
- *Wudick MW, Luu D-T, Maurel C.* (2009) Stimulus-dependent plant aquaporin redistribution. XIIth ENPER Meeting. Montpellier (conférence)
- *Luu D-T, Sorieul M, Boursiac Y, Tournaire-Roux C, Maurel C.* (2008) Fonction et régulation des aquaporines d'*Arabidopsis thaliana*. Institut de Recherche en Biologie Végétale, Montréal (Canada) (séminaire).
- *Boudet J, Boursiac Y, Luu D-T, Postaire O, Tournaire-Roux C, Maurel C.* (2007) Regulation of root water transport by hydrogen peroxide involves cell signalling mechanisms and altered aquaporin trafficking. ROS in Plants 2007 Conference. Ghent (Belgique) (affiche)
- *Luu D-T, Boursiac Y, Tournaire-Roux C, Maurel C.* (2007) Regulation of root water transport by hydrogen peroxyde involves cell signalling mechanisms and altered aquaporin trafficking. 14th International workshop on plant membrane biology. Valence (Espagne) (affiche)
- *Sorieul M, Luu D-T, Santoni V, Verdoucq L, Maurel C.* (2007) Role of N-terminal tail of *Arabidopsis* aquaporin *AtPIP2;1* in protein sub-cellular trafficking. 14th International workshop on plant membrane biology. Valence (Espagne) (affiche)
- *Luu D-T, Boursiac Y, Chen S., Sorieul M, Tournaire-Roux C, Maurel C.* (2007) Regulation of plant aquaporins in response to water stress. Annual meeting of the Society for Experimental Biology. Glasgow (Royaume-Uni). Actes publiés dans *Comparative Biochemistry and Physiology* 146A (4 suppl), page S152. (conférence)
- *Luu D-T, Tournaire-Roux C, Boursiac Y, Chen S, Sorieul M, Dries N, Javot H, Bligny R, Santoni V, Maurel C* (2005) Regulation of root water transport by quaporins under anoxic and salt stresses. Xth France-Japan workshop on plant sciences. Toulouse (conférence)
- *Santoni V, Tournaire-Roux C, Verdoucq L, Luu D-T, Sorieul M, Prak S, Sommerer N, Maurel C.* (2005) Mechnisms of post-translational regulation of plant aquaporins. The 4th international Conference on Aquaporins. Genval (Belgique) (affiche)
- *Luu, D-T, Tournaire-Roux, C, Boursiac, Y, Chen, S, Javot, H, Bligny, R, Santoni, V, Maurel, C.* (2004). Regulation of root water transport by quaporins under anoxic and salt stresses. *Acta Physiologiae Plantarum* 26(3), 78. Actes du 14th FESPB Congress. Cracovie (Pologne) (conférence)
- *Luu D-T, Sorieul M, van den Dries N, Viennois G, Alcon C, Maurel C.* (2004). *In vivo* sub-cellular localisation studies in the *Arabidopsis* aquaporin family. 13th International workshop on plant membrane biology. Montpellier (affiche)

- Boursiac Y, Chen S, Luu D-T, Maurel C. (2004). Early effect of salinity on water transport and aquaporin transcriptome in the Arabidopsis roots suggest a dual mechanism of regulation. 13th International workshop on plant membrane biology. Montpellier (affiche)
- Tournaire-Roux C., Sutka M, Javot H, Gout E, Luu D-T, Postaire O , Bligny R, Maurel C. (2004). Gating of aquaporins by cytosolic pH regulates Arabidopsis root water transport during anoxic stress. 13th International workshop on plant membrane biology. Montpellier (affiche)
- Boursiac Y, Luu D-T, Maurel C. (2003). Early effect of salinity on water transport and aquaporin gene expression in the Arabidopsis root. 7th International Congress of Plant Molecular Biology. Barcelone (Espagne) (affiche)

- Travaux sur la phytoremédiation :

- Picault N, Cazalé AC, Luu DT, Beyly A, Cuiné S, Carrier P, Peltier G. (2005). Overproduction of heavy metal chelating peptides in *Arabidopsis thaliana*. 6^{ème} colloque National de la SFBV, Arcachon (affiche)
- Picault N, Beyly A, Cuine S, Carrier P, Luu D-T, Forestier C, Peltier G. (2004). Effects of over-expressing metal binding peptides and transporters on heavy metal tolerance and accumulation in *A. thaliana*. 13th International workshop on plant membrane biology. Montpellier (affiche)
- Luu D-T & Peltier G. (2001). Plastid products and environment : phytoremediation. Meeting du 5^{ème} PCRD. Vico Equense (Italie) (conférence)

- Travaux sur l'auto-incompatibilité gamétophytique :

- Matton D, Luu D-T, Morse D, Cappadocia M. (2000). Establishing a paradigm for the generation of new S alleles. The Plant Cell 12, 313-316 (Lettre à l'éditeur)
- Luu D-T. (2000). L'auto-incompatibilité chez *Solanum chacoense* : spécificité allélique et recherche du ligand pollinique. ENSA-Montpellier. (séminaire)
- Luu D-T. (2000). L'auto-incompatibilité chez *Solanum chacoense* : spécificité allélique et recherche du ligand pollinique. CEA Cadarache. (séminaire)
- Luu, D-T, Matton, D, Qin, X, Yang, Q, Pelletier, N, Laublin, G, Morse, D, Cappadocia, M (1999). Use of the two-hybrid system to identify the pollen-S component in *Solanum chacoense* Bitt. Pollen-Stigma Interactions Conference. Oxford (Royaume-Uni). (affiche)
- Cappadocia M, Luu D-T, Matton D, Morse D, Qin X. (1999). Self-incompatibility studies in *Solanum chacoense* : generation of an S-allele with dual specificity. Abstracts 14th Triennial Conf. European Assoc potato research, pp72-73. Sorrento (Italie) (conférence)

- Travaux sur les barrières interspécifiques :

- Luu D-T (1999). Pollen-stigma adhesion. Pollen-Stigma Interactions Conference. Oxford (Royaume-Uni). (conférence)
- Luu D-T, Passelègue E, Dumas C, Heizmann P. (1999). Conservation, expression and function of *S-Locus Related 1* among Brassicaceae. Pollen-Stigma Interactions Conference. Oxford (Royaume-Uni) (affiche)
- Luu D-T (1998). L'adhésion pollen-stigmate chez les Brassicaceae. Institut de Recherche en Biologie Végétale, Montréal (Canada) (séminaire)

- Luu D-T (1997). Molecular evolution of S(=Self-incompatibility) family in the Brassicaceae. Evolutionary Biology Meeting. Barcelone (Espagne) (conférence)

- Luu D-T (1997). Adhesion pollen-stigmate : aspects intraspécifiques et interspécifiques. École Normale Supérieure de Lyon (séminaire)

- Travaux issues de collaborations :

- Amenc J, van Aarle I, Viennois G, Bouhmama L, Kouas S., Luu D-T, Plassard C, Drevon J-J (2007). Visualisation and localisation of acid phosphatase transcripts in common bean nodules (*Phaseolus vulgaris*) by in situ RT-PCR. Rhizosphere2 International Conference. Montpellier (affiche)

- Bianco-Trinchant J, Luu D-T, Le Page-Degivry M-T (1996). Abscisic acid accumulation in cells and protoplasts of *Amaranthus tricolor* in response to osmotic stress. Xth FESPP congress. Florence (Italie) (affiche)

- *Chapitres d'ouvrages*

- Travaux sur le transport de l'eau dans la plante :

- Luu D-T and Maurel C. (2012) Dynamic behaviour and internalization of aquaporins at the surface of plant cells. *Plant Endocytosis*, Plant Cell Monographs, ed Samaj J (Springer-Verlag Berlin Heidelberg), pp185-199

- *Thèse et principaux rapports*

- Luu D-T. (1997) Adhésion pollen-stigmate chez les Brassicaceae : implication des gènes *S-Locus Glycoprotein* et *S-Locus Related 1*. Thèse. Ecole Normale Supérieure de Lyon. Jury : A-M CHEVRE (rapp), P-H GOUYON (rapp), M. HERZOG, C. DUMAS, Ph. HEIZMANN.

- Luu D-T, Heizmann, P. et Dumas, C. (1995) Implication de gènes de la famille "S" dans le contrôle des croisements interspécifiques chez les Crucifères. *In* Dissémination des plantes génétiquement modifiées : bilan des recherches soutenues par le Ministère de l'Agriculture et le Ministère de l'Environnement, sur proposition du comité scientifique du CTPS. 43-50.

- Luu D-T. (1994) Implication des gènes *SLR* dans les croisements interspécifiques chez les Crucifères. Mémoire de DEA.

3 - ACTIVITES D'ENCADREMENT ET D'ENSEIGNEMENT

❑ Encadrements d'étudiants stagiaires de niveau Licence

- Melle Anne-Sophie Fremont (2ème année Montpellier SupAgro), un mois en 2006.
- M. Jean-François Estève (2ème année DEUG, Université de Montpellier 2), trois semaines en 2005.
- Melle Juliette Peres (2ème année AgroM), 5 semaines en 2002.
- M. Nicolas Pelletier (étudiant bachelier en sciences, Université de Montréal, Canada), deux mois en 1999.
- Melle Claire Le Penhuizic (Magistère, Université de Lyon), trois mois en 1996
- Etudiantes en BTS : Melle Muriel Fouilloux, Melle Béatrice Moyroud, Melle Isabelle Tamisé, Melle Elisabeth Ferrera, trois mois entre 1994 et 1997.

❑ Encadrements d'étudiants stagiaires de niveau Master

- M. Duy Chi Trinh (Master 2, University of Science & Technology, USTH, Hanoï, Vietnam), six mois en 2014.
 - Mme Hong Chien Nguyen (Master 2, Agricultural Genetics Institute-LMI-RICE, Hanoï, Vietnam), trois mois en 2012.
 - Melle Sandrine Vialet (Master 2 Professionnel, Université de Montpellier 2), six mois en 2009.
 - M. Mathias Sorieul (DEA, Université de Montpellier 2), six mois en 2004. Co-encadrement avec le Dr. Christophe Maurel.
 - M. Niels van den Dries (Master 2, Programme ERASMUS, Université d'Amsterdam, Pays-Bas), six mois en 2003.
- Publication issu de cet encadrement :

- Boursiac Y, Chen S, Luu D-T, Sorieul M, van den Dries N, Maurel C. (2005). Early Effects of Salinity on Water Transport in Arabidopsis Roots. Molecular and Cellular Features of Aquaporin Expression. **Plant Physiology** 139, 790-805

- M. Xike Qin (Master 2, Université de Montréal, Canada), deux ans entre 1998 et 2000. Publications issus de cet encadrement :

- Luu D-T, Qin X, Laublin G, Yang Q, Morse D, Cappadocia M. (2001). Rejection of S-heteroallelic pollen by a dual-specific s-RNase in *Solanum chacoense* predicts a multimeric SI pollen component. **Genetics** 159(1), 329-35.

- Qin X, Luu D-T, Yang Q, Maes O, Matton DP, Morse D, Cappadocia M. (2001). Genotype-dependent differences in S12-RNase expression lead to sporadic self-compatibility. **Plant Molecular Biology** 45(3), 295-305.

- Luu D-T, Qin X, Laublin G, Morse D and Cappadocia M. (2000). S-RNase uptake by compatible pollen tubes in gameophytic self-incompatibility. **Nature** 407(6804), 649-651.

- Matton D, Luu D-T, Qin X, Laublin G, O'Brien M, Maes O, Morse D and Cappadocia M. (1999). The production of an S-RNase with dual specificity suggests a novel hypothesis for generation of new S-alleles. **The Plant Cell** 11, 2087-2098.

❑ Encadrements de Doctorants

- Le sujet de Doctorat « Cell biology of aquaporins in rice » a été sélectionné par l'USTH pour être proposé aux étudiants vietnamiens. La sélection du doctorant se déroulera avant l'été 2014, pour un début des travaux de recherche avant la fin 2014. Le doctorant sélectionné se verra attribuer une bourse de Doctorat du Gouvernement vietnamien de trois ans sous ma direction.

- M. Michael Wudick (Montpellier SupAgro), entre 2007 et 2010. Co-encadrement avec le Dr. Christophe Maurel. Titre : Intracellular aquaporins of Arabidopsis thaliana: dynamic expression in pollen and in roots under oxidative stress. Thèse soutenue le 28 avril 2010. Publications issues de ce co-encadrement :

- Wudick, M.M., Luu, D.-T., Tournaire-Roux, C., Sakamoto, W., and Maurel, C. (In press). Vegetative and sperm cell-specific aquaporins of Arabidopsis thaliana highlight the vacuolar equipment of pollen and contribute to plant reproduction. **Plant Physiology**.

- Wudick MM, Luu D-T, Maurel C. (2009). A look inside: localization patterns and functions of intracellular plant aquaporins. **The New Phytologist** 184, 289-302.

- Maurel C, Santoni V, Luu D-T, Wudick MM, Verdoucq L. (2009). The cellular dynamics of plant aquaporin expression and functions. **Current Opinion in Plant Biology** 12, 690-698

- M. Mathias Sorieul, (Université de Montpellier 2), entre 2004 et 2007. Co-encadrement avec le Dr. Christophe Maurel. Titre : Localisation et Dynamique Sub-cellulaires des Aquaporines d'Arabidopsis thaliana. Thèse soutenue le 19 décembre 2007. Publications issues de ce co-encadrement :

- Luu D-T, Martiniere A, Sorieul M, Runions J, Maurel C. (2012). Fluorescence recovery after photobleaching reveals high cycling dynamics of plasma membrane aquaporins in Arabidopsis roots under salt stress. **The Plant Journal** 69, 894-905

- Sorieul M, Santoni V, Maurel C, Luu D-T. (2011). Mechanisms and effects of retention of over-expressed aquaporin AtPIP2;1 in the endoplasmic reticulum. **Traffic** 12, 473-482

- Boursiac Y, Chen S, Luu D-T, Sorieul M, van den Dries N, Maurel C. (2005). Early Effects of Salinity on Water Transport in Arabidopsis Roots. Molecular and Cellular Features of Aquaporin Expression. **Plant Physiology** 139, 790-805

- Melle Valeria Valentini, (Università degli Studi della Basilicata, Potenza, Italie). Stage européen de novembre 2011 à avril 2012.

□ Enseignements

- Cours et travaux pratiques (42 h) sur « Plant cell biotechnology » aux Bachelors 2 and 3 de l'USTH (2013 et 2014).

- Cours (3 h) sur « Molecular Biology » aux Masters 1 de l'USTH (2013).

- Cours (2 h) donnés dans le cadre de l'école thématique du Master Biologie Fonctionnelle des Plantes (2010, 2011 et 2013).

- Cours (3 h) sur "Fundamental knowledge on plant cell signaling in response to abiotic stresses" aux Masters 2 de l'Université des Sciences et Technologie de Hanoi (USTH) (2012).

- Cours (3 h) donné à l'Agence universitaire de la francophonie (Hanoi, Vietnam) sur la préparation d'une soutenance (2012).

- Cours et travaux pratiques (13 h) donnés dans le cadre de l'école thématique « Transmembrane water transport in plants » (2011).

- Participations aux cours magistraux (3 h) dans le cadre du cours BIO3701 du Pr M. Cappadocia (Université de Montréal). (Automnes 1997, 1998, 1999).

4 - TRAVAUX D'EXPERTISE

- Examineur-rapporteur pour les thèses de M. Jonathan Soulard (Université de Montréal, Canada) en 2014 et de Melle Valérie Van Wilder (Université Catholique de Louvain, Belgique) en 2005.
- Membre du Comité de thèse de M. Thibaud Adam (Université de Bourgogne). Thèse soutenue en 2012
- Membre du Jury d'admissibilité de l'Ecole doctorale SIBAGHE (Montpellier), depuis 2011.
- Reviewer pour les journaux Traffic, Plant Science, BBA Membrane, Cell Research, Planta, Plant Science, Scientia Horticulturae, Tree Physiology.
- Reviewer pour le Concil for Earth and life sciences (Pays-Bas)

5 – CONTRATS DE RECHERCHE

- Partenariat Hubert Curien franco-vietnamien « Hoa Sen-Lotus », “Application of functional genomics and association genetics to characterize genes involved in abiotic stresses tolerance in rice” de 2015-2016. Ce projet est coordonné par le Pr. Pascal Gantet, côté français, et par le Dr. Hoang Thi Giang, côté vietnamien. Je suis l'un des participants.
- J'ai bénéficié d'une bourse Marie Curie Actions (FP7-PEOPLE-2011-IOF) – International Outgoing Fellowships (#300150 ORYZAQUA), “Cell biology of rice aquaporins”, de 2012 à 2014. Les recherches menées seront détaillées dans les parties qui suivent.
- J'ai participé au Réseau Marie Curie (MRTN-CT-2006-035833) , Vacuolar Transport Equipment for Growth Regulation in Plant (VaTEP), de 2006 à 2010. Ce réseau a permis le financement de la thèse de M. Michael Wudick.
- De 2004 à 2007, j'ai été en relation avec la société BiotechMarines (ex-SECMA Biotechnologies Marines) ayant son siège à Pontrieux (France) pour coordonner un contrat de recherche portant sur «La recherche des effets agonistes ou antagonistes de substances naturelles d'origines algale ou végétale sur les aquaporines chez Arabidopsis thaliana ». Ce contrat a permis de recruter successivement M. Lionel Verdoucq, Melle Moira Sutka et Melle Julie Boudet comme stagiaires post-doctoraux dans l'équipe.

6 – ORGANISATION DE COLLOQUES

J'ai été l'organisateur principal du XIIème colloque European Network of Plant Endomembrane Research (ENPER) du 8-11 septembre 2009. Ce colloque qui s'est tenu sur le campus de SupAgro/INRA Montpellier a réuni 130 scientifiques de 11 nationalités différentes. Des spécialistes mondialement reconnus tels que Mike Blatt, Federica Brandizzi, Niko Geldner, Chris Hawes, Natasha Raikhel, ... ont participé aux débats sur le trafic endomembranaire chez les plantes. Le principe des colloques ENPER est de favoriser la prise de parole des non-permanents et les échanges informels. Les présentations orales ont ainsi été exclusivement assurées par les non-permanents et les encadrants n'ont fait que de courtes introductions.

7 - ACTIVITES DE VULGARISATION SCIENTIFIQUE

- Membre du comité de rédaction de « Regards », anciennement appelé « Echos de la Gaillarde », le journal interne du Centre Inra de Montpellier, depuis 2005.
- Organisation de visites du laboratoire pour le grand public. Par exemple, j'ai présenté les activités de recherche du laboratoire à une délégation de la Direction régionale de l'alimentation, de l'agriculture et de la forêt.

- Organisation d'ateliers scientifiques à direction du grand public et des scolaires dans le cadre de la Fête de la science, depuis 1996. Par exemple en 2008, j'ai organisé un atelier sur le thème des plantes et de l'eau avec le Jardin des Plantes de Montpellier, à la MJC de Castelnau-le-Lez. En 2009, j'ai organisé un atelier sur l'anatomie des plantes pour une classe de la maternelle Mozart, située à proximité du Campus. En 2013, j'ai coordonné un cycle de conférences sur les plantes qui ont marqué l'Humanité, données par le Pr. M. Cappadocia de l'Université de Montréal (Canada).

- Chroniques de biologie végétale, à "Radio Pluriel" (91.5MHz, St-Priest) en 1995 et 1996.

8 - RESUME DES TRAVAUX ANTERIEURS

8.1 - DEA-Doctorat (1993-1997) et premier post-doctorat (1997-2000) : Adhésion pollen-stigmate, évolution de la famille multigénique *S* et barrières interspécifiques chez les Brassicaceae

Dans le cadre de mon travail de DEA et de Doctorat (Luu, 1997) au laboratoire de Reproduction et Développement des Plantes (Ecole Normale Supérieure, Lyon) dirigé par le Pr Christian Dumas, je me suis intéressé aux barrières interspécifiques, à l'adhésion pollen-stigmate ainsi qu'à l'évolution des séquences de la famille *S* chez le chou et des espèces proches de la famille des Brassicaceae. Mon travail a été encadré par le Dr Philippe Heizmann. Notre contribution à la compréhension de ces thématiques a fait l'objet de deux articles de revue (Heizmann et al., 2000a; Heizmann et al., 2000b) et de cinq articles (Luu et al., 1997a; Luu et al., 2001a; Luu et al., 1999; Luu et al., 1998; Luu et al., 1997b). Après mon Doctorat, j'ai effectué un stage post-doctoral dans le laboratoire du Pr Cappadocia à l'Institut de Recherche en Biologie Végétale (Montréal, Canada). Ce laboratoire caractérise des processus de signalisation moléculaire dans le cadre de ses études sur l'auto-incompatibilité gamétophytique chez une Solanaceae, *Solanum chacoense*. Ce post-doctorat a donné lieu à 4 articles scientifiques (Luu et al., 2001b; Luu et al., 2000; Matton et al., 1999; Qin et al., 2001). Je résume dans la partie ci-dessous mes travaux.

L'hermaphroditisme, très largement répandu parmi les plantes à fleurs, favorise la proximité des organes mâles (étamines) et femelles (pistils), ce qui faciliterait l'autopollinisation et la "consanguinité". Or, des barrières à l'autofécondation assurent le brassage génétique et la variabilité au sein de certaines espèces végétales. Ces barrières, définies par des bases génétiques et moléculaires très précises et regroupées sous le terme d'auto-incompatibilité, contrôlent la reconnaissance et l'acceptation du "non-soi" ou le rejet du "soi" (auto-pollen). Chez le chou *Brassica oleracea* et chez *Solanum chacoense*, un parent sauvage de la pomme de terre, l'auto-incompatibilité est contrôlée par un locus unique *Self-incompatibility (S)*. Chez le chou, le gène *S-Locus Receptor Kinase (SRK)*, lié au locus *S* et exprimé dans les stigmates, intervient dans la reconnaissance et le rejet de l'autopollen, à travers une cascade d'événements qui implique SCR/SP11 (pour *S-locus Cysteine-Rich protein / S-locus Protein 11*) un composé d'origine pollinique (Schopfer et al., 1999; Shiba et al., 2001; Takayama et al.). Le gène *S-Locus Glycoprotein (SLG)* est lui aussi lié au locus *S* et présente un polymorphisme, mais sa fonction dans l'auto-incompatibilité n'est pas encore précisée. D'autres membres de cette famille, les gènes *S-Locus Related 1 et 2 (SLR)*, présentent un monomorphisme qui contraste avec le polymorphisme des gènes *SLG* et *SRK* et ils ne sont pas liés au locus *S*. Ils ne doivent donc pas intervenir dans l'auto-incompatibilité, mais plutôt dans des phénomènes généraux lors de la pollinisation. La contribution de mon travail de DEA et de thèse a été de découvrir et de démontrer expérimentalement que les glycoprotéines SLR1, mais aussi SLG, sont impliquées dans l'adhésion entre le pollen et le stigmate, la partie apicale du pistil qui reçoit le pollen.

Nous avons analysé le monomorphisme du gène *SLR1* dans plusieurs espèces de la famille des Brassicaceae (*Brassica insularis*, *Hirschfeldia incana*, *Raphanus raphanistrum*, *Sinapis arvensis*) (Luu et al., 2001a). Par ailleurs, nous avons ainsi mis au point un test biomécanique, pour mesurer l'intensité des forces nécessaires à l'arrachement des grains de pollen de la surface stigmatique (Luu et al., 1997a). Ce test est basé sur le principe physique simple des forces de flottaison, plus connues sous le terme de poussée d'Archimède. A l'aide de ce test, nous avons montré que, chez *Brassica oleracea*, l'adhésion est indépendante du phénotype d'auto-compatibilité ou d'incompatibilité. Nous avons alors réalisé une étude approfondie du phénomène d'adhésion en montrant, d'une part, le rôle des protéines formant la pellicule de surface du stigmate, et d'autre part, le rôle des lipides et des protéines de la surface

pollinique ou manteau. Ces études permettent de déterminer les participations respectives du stigmate et du pollen dans la formation du ménisque qui assure l'adhésion puis l'hydratation du pollen. Cette analyse a été étendue à des relations pollen-stigmates interspécifiques, où nous avons observé qu'au sein des Brassicaceae, les forces d'adhésion sont de même ordre que celles observées en situation intraspécifique (Luu et al., 1998). Enfin, nous avons aussi démontré que cette adhésion pollen-stigmate fait aussi intervenir la glycoprotéine SLG (Luu et al., 1999).

Chez les Solanaceae, le rejet de l'auto-pollen implique une interaction entre une *S*-Locus RiboNucléase (*S*-RNase) exprimée dans les tissus du style et une protéine de type F-box exprimée côté pollen (Sijacic et al., 2004). Deux modèles opposés proposent de rendre compte du rejet de l'auto-pollen. D'une part, le modèle du récepteur spécifique suppose qu'une *S*-RNase, par exemple la *S11*-RNase est excrétée dans la paroi des cellules du style et importée dans le cytoplasme du tube pollinique de génotype (haploïde) *S11* par un récepteur membranaire pollinique. Par contre, cette *S11*-RNase ne peut pas être importée dans des tubes polliniques de génotype différent. Le modèle de l'inhibiteur, quant à lui, suppose que les *S*-RNases ont la capacité de pénétrer dans n'importe quel tube pollinique indépendamment de son génotype. Un ou des inhibiteurs spécifiques inactivent alors les *S*-RNases d'haploïde différent de celui du tube pollinique. Une manière de trancher entre ces deux modèles est de localiser les *S*-RNases dans les tubes polliniques : dans le modèle du récepteur, seule la *S11*-RNase peut pénétrer dans un tube pollinique de type *S11* ; dans le modèle de l'inhibiteur, la *S11*-RNase peut pénétrer dans n'importe quel tube pollinique. Nous avons alors fait produire un anticorps polyclonal spécifiquement dirigé contre la *S11*-RNase. L'utilisation de cet anticorps en immunolocalisation et marquage à l'or colloïdal, montre clairement la présence de la *S11*-RNase aussi bien dans les tubes polliniques de génotype *S11* que ceux de génotype *S12*, *S13* et *S14* (Luu et al., 2000).

Nous avons aussi participé à mieux comprendre l'apparition de nouveaux allèles *S*. Ainsi, les *S11*- et *S13*-RNases ne diffèrent dans leur forme mature que de 10 acides aminés. Des expériences de mutagenèse dirigée et expression dans les pistils de *S. chacoense* nous ont permis de montrer que la *S*-RNase mutée présentait une double spécificité, c'est à dire qu'elles rejettent aussi bien le pollen *S11* que *S13*. En d'autres termes, le composant pollinique *S11* est reconnu à la fois par la *S11*-RNase et la *S*-RNase doublement spécifique, et le composant pollinique *S13* est reconnu à la fois par la *S13*-RNase et la *S*-RNase doublement spécifique. Ce résultat est important pour proposer des schémas d'apparition-évolution des allèles d'auto-incompatibilité (Matton et al., 1999) : un allèle *Sa* évolue vers une forme intermédiaire *Sa/b* qui lui permet de garder sa spécificité initiale (*a*), tout en acquérant une nouvelle spécificité (*b*) ; ensuite l'intermédiaire *Sa/b* évolue à nouveau en perdant la spécificité initiale (*a*) et en ne conservant que la nouvelle spécificité (*b*).

8.2 – Deuxième post-doctorat (2000-2002) : Transformation chloroplastique et phytoremédiation

J'ai effectué un deuxième stage post-doctoral au CEA de Cadarache, dans le Laboratoire d'Ecophysiologie de la Photosynthèse dirigé par le Dr Gilles Peltier. Mon objectif était de déterminer dans quelle mesure il est possible de provoquer une hyper-accumulation de métaux lourds, et de cadmium en particulier, dans du tabac transgénique produisant des molécules chélatantes de type métallothionéines ou phytochélatines. La transformation du chloroplaste a été choisie puisqu'elle permet une plus forte expression des transgènes comparée à la transformation nucléaire. Deux stratégies ont été engagées : d'une part, la surexpression d'un gène codant la métallothionéine (MT) de mouton déjà disponible au laboratoire et, d'autre part, l'introduction de gènes qui codent une *g*-Glutamylcystéine Synthase (*g*-ECS) et une Phytochélatine Synthase (PCS), deux enzymes de la voie de

biosynthèse des phytochélatines. Les stratégies utilisées ne nous ont pas permis d'obtenir une hyper-accumulation attendue. Une autre stratégie menée au laboratoire utilisant la *AtPCS* d'*Arabidopsis thaliana* et exprimée dans *Escherichia coli* a permis d'observer une accumulation de métaux lourds (Sauge-Merle et al., 2003). Enfin, son expression chez *A. thaliana*, dans le compartiment cytosolique ou dans les plastes à l'aide d'un peptide d'adressage n'a pas permis d'observer une hyper-accumulation (Picault et al., 2006).

9 – RECHERCHES EN COURS

Recruté depuis janvier 2002 au CNRS, j'ai intégré l'équipe 'Aquaporines' dirigée par le Dr. Christophe Maurel, au sein de l'Unité Biochimie & Physiologie Moléculaire des Plantes (B&PMP) actuellement dirigée par le Dr. Alain Gojon. Un des axes majeurs proposés dans mon projet de recherche, lors de mon recrutement, a été d'étudier la dynamique de la localisation sub-cellulaire des aquaporines d'*Arabidopsis* en conditions standard et sous contraintes de l'environnement. Alors qu'en 2002 très peu de données supportaient l'hypothèse que la localisation sub-cellulaire de protéines membranaires pouvait être régulée par des stimuli, actuellement, plusieurs exemples chez les plantes illustrent l'importance du trafic endomembranaire dans la régulation de leurs fonctions biologiques. La contribution de notre travail dans ce domaine a été de mettre en lumière la dynamique de la localisation des aquaporines de la membrane plasmique (MP). Par ailleurs, notre stratégie s'est portée sur des fusions des aquaporines avec des marqueurs fluorescents exprimées de façon stable dans la plante. Un effort important a donc été nécessaire pour obtenir le matériel végétal exprimant les aquaporines d'intérêt ainsi que les marqueurs sub-cellulaires *ad hoc*. Plusieurs publications de l'équipe discutent des fonctions et des régulations des aquaporines et peuvent être consultées comme un cadre général de mon travail de recherche (Boursiac et al., 2008b; Leborgne-Castel and Luu, 2009; Li et al., 2013; Luu and Maurel, 2005; Luu and Maurel, 2012; Luu and Maurel, 2013; Martiniere et al., 2012; Maurel et al., 2009; Maurel et al., 2008; Wudick et al., 2009). Dans le cadre de ces recherches, j'ai co-signé dix articles de recherche et dix articles de revues ou commentaires, et ai (co-)encadré douze étudiants dont deux Doctorants et trois étudiants en Master.

Les aquaporines forment une famille multigénique de 35 membres chez *Arabidopsis*. Deux des cinq sous-familles qui la composent, les Plasma membrane Intrinsic Proteins (PIP) et les Tonoplast Intrinsic Proteins (TIP), possèdent certains membres localisés, respectivement, dans la MP et le tonoplaste. Mon travail se concentre sur la première de ces deux sous-familles, en prenant l'isoforme *AtPIP2;1* comme protéine modèle du fait de données sur son expression (transcrits et protéines) dans la racine d'*Arabidopsis* et accumulées par d'autres études du groupe (di Pietro et al., 2013; Prado et al., 2013; Prak et al., 2008; Sahr et al., 2010; Santoni et al., 2006; Verdoucq et al., 2008).

9.1 – Motifs protéiques portés par *AtPIP2;1* et impliqués dans son trafic endomembranaire

Ce sujet a été réalisé dans le cadre de la thèse de M. Mathias Sorieul que j'ai co-encadrée avec le Dr. Christophe Maurel. En résumé, l'existence de motifs di-acides, composés de deux résidus acides séparés par un résidu indéterminé portés par les protéines membranaires et leur permettant d'être exportées hors du reticulum endoplasmique (RE), avait déjà été décrite dans le domaine animal et la levure. Depuis, les groupes du Dr. Federica Bandizzi, du Dr. Ulrike Homann et du Pr. François Chaumont ont décrit le rôle d'un tel motif entre autres pour KAT1 chez *A. thaliana* et les aquaporines PIP de maïs (Hanton et al., 2005; Mikosch et al., 2006; Zelazny et al., 2009).

Nous avons à notre tour tenté d'identifier le rôle potentiel du motif diacide DVE (Asp⁴Val⁵Glu⁶) porté par l'extrémité N-terminale de l'aquaporine modèle *AtPIP2;1* en sur-exprimant sous le contrôle du promoteur *35SCaMV* doublé une séquence fusion *AtPIP2;1*-GFP soit sauvage soit mutée. L'originalité de ce travail reposait aussi sur l'étude de l'effet des mutations du motif di-acide sur la fonction des aquaporines. Dans un premier temps, nous avons analysé l'effet des séquences mutées AVE, DVA, AVA, EVE, DVD sur la localisation sub-cellulaire des constructions. Dans les tissus observés (cellules de l'épiderme de racine, d'hypocotyle ou de jeunes cotylédons), toutes les fusions mutées montrent un marquage intracellulaire qui contraste avec celui de la fusion sauvage. Nous avons apporté des preuves que le marquage intracellulaire concerne le RE. Ensuite, nous avons cherché à évaluer l'impact de la rétention des fusions *AtPIP2;1*-GFP dans les capacités de transport d'eau racinaire. Cet aspect a permis d'aborder un point original et fortement discuté dans notre domaine (Zelazny *et al.* 2009). En effet, on sait que, chez le maïs, les membres de la sous-famille PIP1 ont besoin d'interagir avec des PIP2 pour être exportés hors du RE (Zelazny *et al.*, 2009). La sur-expression d'une forme d'*AtPIP2;1*-GFP mutée et retenue dans le RE pourrait donc avoir un effet sur l'export hors du RE des PIP endogènes. De fait, des mesures réalisées sur des plantes sur-exprimant les formes mutées AVA et DVD montrent une réduction de conductivité hydraulique racinaire (L_{pr}) d'environ 40% par rapport aux plantes exprimant une forme contrôle non-mutée. Nous avons donc voulu évaluer directement si la sur-expression de la construction *AtPIP2;1*-GFP mutée conduit à une rétention des PIP endogènes et, par conséquent, à une réduction de leur densité à la surface des cellules. De fait, la construction *AtPIP1;4*-mCherry montre une accumulation intracellulaire quand elle est co-exprimée avec la construction E6D. Par ailleurs, l'expression de la construction *AtPIP2;1*-GFP mutée ne provoque pas de rétention dans le RE d'un marqueur de l'appareil de Golgi ou d'une TIP, ce qui suggère que les interactions potentielles, dans le RE, entre la construction *AtPIP2;1*-GFP mutée et les PIP endogènes sont spécifiques. Toutefois, notons que la réduction de la L_{pr} est la même chez les plantes qui expriment les formes mutées AVA et DVD alors que leurs accumulations intracellulaires ne sont pas similaires. L'ensemble de ce travail a permis de préciser que pour l'aquaporine *AtPIP2;1*, le motif di-acide est en réalité un motif DVE et que toute mutation de ce motif conduit à une rétention stricte dans le RE (pas de fuite possible vers l'appareil de Golgi). Les effets d'une telle rétention sur la conductivité hydraulique ont été évalués et renforcent le modèle d'une possible interaction entre les isoformes PIP1 et PIP2. Ce travail a été publié dans la revue *Traffic* (Sorieul *et al.*, 2011).

9.2 – Effet de stimuli sur la localisation sub-cellulaire des aquaporines

9.2.1 – Effet du NaCl par analyse « FRAP »

Une étude précédente de l'équipe (Boursiac *et al.*, 2005), a permis de conclure en un effet coordonné du stress salin sur l'expression et la localisation sub-cellulaire des PIP pour expliquer la baisse induite de la L_{pr} . Toutefois, après 45 min de traitement par 100 mM NaCl, la L_{pr} est réduite de 50% alors qu'on n'observe ni de baisse réelle des transcrits d'aquaporines ni de relocalisation massive des PIP. Nous avons obtenu, grâce à la coloration par le FM4-64 de racines traitées ou non par le sel, l'information que l'endocytose des membranes lipidiques était accrue en condition de stress salin en accord avec les résultats de (Leshem *et al.*, 2007). Ces arguments ainsi que d'autres nous ont conduits, dans le cadre de la thèse de M. Mathias Sorieul, à mieux comprendre les étapes précoces du trafic endomembranaire des PIP par une approche de Fluorescence Recovery

After Photobleaching (FRAP). La technique du FRAP a été appliquée aux cellules de l'épiderme de racines exprimant des fusions d'*AtPIP1;2* et *AtPIP2;1* avec la GFP. Brièvement, le principe de notre analyse est le suivant. Les expériences de FRAP indiquent que le retour à la fluorescence est très lent, ce qui renseigne sur une diffusion latérale des PIP extrêmement réduite. Après photoblanchiment, les courbes de retour à la fluorescence présentent deux composantes cinétiques. La composante rapide correspond à la diffusion des endosomes marqués par les protéines fusions ; la composante tardive correspond à la réalimentation par cyclage des protéines fusions vers la MP. Cette interprétation, étayée par une solide analyse pharmacologique, nous a permis de proposer un modèle de cyclage des PIP d'*Arabidopsis*, très proche de celui proposé pour les transporteurs d'auxines (Luu et al., 2012), à l'exception de l'effet de cette phytohormone. En effet, les auxines inhibent l'endocytose dépendante de la clathrine des PIN, via une fixation sur l'Auxin Binding Protein (ABP1) (Dhonukshe et al., 2007; Paciorek et al., 2005; Robert et al., 2010; Sauer and Kleine-Vehn, 2011) et, combinées avec la Bréfeldine A (BFA), empêchent le marquage des corps BFA par diverses constructions de protéines membranaires (*AtPIP2;1* entre autres) (Paciorek et al., 2005). Or nos données obtenues avec le FRAP ne sont pas en accord avec le modèle proposé pour les PIN, mais suggèrent plutôt que les auxines inhiberaient une étape du cyclage des PIP qui se trouve en aval de l'endocytose. La deuxième originalité de ce travail est de proposer que le traitement salin provoque une dynamique accrue du cyclage des PIP. Un retour à la fluorescence plus élevé dans la composante tardive des courbes de retour à la fluorescence est en effet observé avec le traitement salin (100 mM NaCl). Des expériences de traitement avec de la BFA nous ont permis d'observer qu'en présence de sel, les corps BFA étaient plus rapidement marqués qu'en absence de sel. Réciproquement, en rinçant avec une solution saline des racines précédemment traitées avec de la BFA, nous avons observé une disparition plus rapide du marquage des corps BFA qu'en rinçant avec une solution contrôle. Ces expériences supportent l'hypothèse d'une cinétique accrue d'internalisation (endocytose) et d'externalisation (exocytose) des PIP sous stress salin. De plus, nos expériences suggèrent que l'endocytose induite sous stress salin semble ne pas être dépendante de la clathrine. L'ensemble de ces résultats soulignent que les mécanismes de trafic des PIP sont partiellement similaires à ceux d'autres protéines membranaires modèles. Ils proposent aussi que des mécanismes originaux d'internalisation des protéines membranaires sont mis en place sous stress salin. Ils nous incitent donc à mettre en évidence les spécificités du modèle des aquaporines et les déterminants moléculaires mis en place sous stress salin. Ce travail a été publié dans la revue *The Plant Journal* (Luu et al., 2012).

Enfin, rappelons que ce travail a été réalisé en collaboration avec les Pr. Chris Hawes et John Runions (School of Life Sciences, Oxford Brookes University, R.U.) et en particulier avec le Dr. Alexandre Martinière, stagiaire post-doctoral de cet institut et récemment recruté Chargé de recherche CNRS dans l'équipe. Les expériences de FRAP ont été menées de concert entre Oxford et Montpellier.

Cette collaboration s'est poursuivie par un autre travail, qui n'a pas porté spécifiquement sur les aquaporines, mais sur un des points que nous avons soulevés dans le précédent article. En effet, la faible diffusion latérale de certaines protéines membranaires (dont les PIP) dans le plan de la MP contraste avec la dynamique de diffusion du marqueur GFP-LTi6a, un marqueur de référence de la MP. Le Dr. Martinière s'est intéressé à comprendre les déterminants moléculaires de cette faible mobilité, en posant dans un premier temps, la question d'interactions potentielles avec le cytosquelette. Il a pu écarter cette piste pour révéler que la faible mobilité des protéines de la MP était due à leurs interactions avec la paroi. Cette découverte originale suggère

que la paroi pourrait contrôler la dynamique de diffusion des protéines à la surface des cellules. Ce travail a fait l'objet d'un article publié dans les Proceedings of National Academy of Sciences USA (Martinière et al., 2012).

9.2.2 – Effet du NaCl par analyse «SPT et FCS»

Une collaboration a été établie entre notre équipe et le laboratoire du Pr. Jinxin Lin (Key Laboratory of Plant Molecular Physiology, Institute of Botany, Chinese Academy of Sciences, Beijing, Chine), pour étudier la dynamique sub-cellulaire des PIP en réponse à la salinité (100 mM NaCl). Alors que nous avons contribué à cette étude par notre expertise des aquaporines et de leur adressage sub-cellulaire, notre partenaire a apporté son expertise pour les techniques de Single Particle Tracking (SPT) et Fluorescence Correlation Spectroscopy (FCS) (voir (Li et al., 2013) pour plus d'explications sur ces deux techniques). Pour le SPT, l'effet obtenu par « Total Internal Reflective Fluorescence » (TIRF) aussi dénommé onde évanescence ou variable (cf. (Konopka and Bednarek, 2008) pour plus d'explications), a permis de pister dans la MP de cellules d'épiderme de racines d'*Arabidopsis* des molécules uniques de la construction *AtPIP2;1-GFP* exprimée sous le contrôle du promoteur *35S CaMV*. Bien que de faible vitesse, la diffusion latérale de ces molécules peut se manifester selon 4 modes : diffusion brownienne, dirigée, restreinte (confinée), ou mixte (combinaison entre brownienne et restreinte) et les valeurs du coefficient de diffusion reflète la dynamique de diffusion dans le plan de la MP. Ainsi, les constructions *AtPIP2;1-GFP* diffusent 10 fois moins que *GFP-LTi6a*, confirmant d'autres données de la littérature et nos propres données (Luu et al., 2012; Sutter et al., 2006). Par une approche pharmacologique et en utilisant un marqueur de référence des micro-domaines lipidiques, nous avons montré que les constructions *AtPIP2;1-GFP* se répartissent à l'intérieur de tels micro-domaines. Le traitement salin augmente la dynamique de diffusion des constructions *AtPIP2;1-GFP* et la déstructuration des micro-domaines lipidiques, par un traitement pharmacologique, modifie significativement la diffusion latérale des constructions en situation de salinité. De plus, la technique de FCS qui permet de mesurer la densité des constructions *AtPIP2;1-GFP* dans la MP révèle que le traitement salin réduit de moitié la valeur cette densité. Cet ensemble de données suggère que le traitement salin augmente la dynamique des PIP à la surface des cellules en favorisant une internalisation qui serait en partie contrôlée au niveau des micro-domaines lipidiques. Il est aussi concordant avec les données du travail basé sur la technique de FRAP (cf. § 9.2.1) et renforce le modèle d'une dynamique accrue de cyclage des PIP en réponse au stress salin. Ce travail a fait l'objet d'un article dans la revue *The Plant Cell* (Li et al., 2011).

9.2.3 – Effets de l' H_2O_2

Dans une précédente étude du laboratoire (Boursiac et al., 2008a), nous avons montré qu'un traitement par 0.5 mM d'acide salicylique ou 150 mM de NaCl provoque une réduction de la L_{p_r} de façon concomitante à une production d'espèces activées de l'oxygène (EAO). Le rôle central des EAO dans la signalisation conduisant à l'internalisation des PIP et à l'inhibition de la L_{p_r} avait été disséqué, entre autres, par un apport exogène d' H_2O_2 . Ici, nous avons poursuivi la dissection des mécanismes de relocalisation sub-cellulaire des aquaporines en réponse à un apport exogène d' H_2O_2 . Ce sujet a été effectué dans le cadre de la thèse de M. Micha Wudick que j'ai co-encadré avec le Dr. Christophe Maurel, en y incluant une collaboration avec nos collègues chinois.

Un fractionnement sub-cellulaire par gradients de saccharose de racines traitées ou non par l' H_2O_2 , couplé à des Western-blots, nous a permis de révéler que 15 min après l'apport exogène de 0.5 mM H_2O_2 , les

anticorps anti-PIP1 et anti-PIP2 ne marquent plus de fractions correspondant à la MP. Ceci nous a suggéré, une redistribution de ces marqueurs dans des compartiments intracellulaires. Pour les analyses par SPT, une construction *AtPIP2;1-GFP* a été exprimée sous le contrôle d'une séquence de 1,5 kpb du promoteur d'*AtPIP2;1* dans les cellules de l'épiderme de racines. Le traitement de ces cellules avec de l' H_2O_2 induit une augmentation de deux fois de la valeur du coefficient de diffusion par rapport au contrôle. Nous avons aussi observé, par la technique de FCS, une réduction significative de la densité des constructions sous traitement H_2O_2 , confirmant une dynamique accrue vers des compartiments intracellulaires. L'identification de ces derniers a été rendue possible par co-expression de la construction *AtPIP2;1-mCherry* et de marqueurs endomembranaires de référence (Geldner et al., 2009). Nous avons ainsi observé une co-localisation de la construction *AtPIP2;1-mCherry* avec des marqueurs des endosomes tardifs/corps multivésiculaires/prévacuoles (Late endosomes/Multivesicular bodies/Prevacuolar compartments, LE/MVB/PVC). La relocalisation de la construction peut être empêchée par un co-traitement avec de l'auxine, mais pas avec de la tyrphostine A23. Cette dernière drogue est connue pour perturber l'endocytose dépendante de la clathrine, ce qui suggère que la relocalisation des PIP provoquée par un stress oxydant pourrait emprunter une voie indépendante de celle avec la clathrine. Il est à noter qu'un cas d'endocytose indépendante de la clathrine a été récemment décrit dans le processus du transport du glucose dans les cellules BY2 de tabac (Bandmann and Homann, 2012). Enfin, la question de la dégradation ou de la séquestration des PIP a aussi été abordée par deux approches indépendantes. Des tests ELISA avec des anticorps anti-PIP1 et anti-PIP2, réalisés sur des protéines totales, indiquent qu'il n'y a pas de diminution de la quantité des aquaporines dans les racines traitées pendant 2 h par de l' H_2O_2 . Par ailleurs, des plantes sur-exprimant une fusion entre la *AtPIP2;1* et une GFP photo-activable ont été photo-activées lors d'un traitement par de l' H_2O_2 . Aucune réduction du signal de la GFP n'a été observée, que ce soit dans des cellules contrôles ou traitées. Ces deux résultats suggèrent que le traitement par de l' H_2O_2 ne conduirait pas à une dégradation rapide des PIP, mais plutôt à leur séquestration. Ce travail établit aussi que les effets du sel sur la dynamique de trafic des PIP (voir paragraphes précédents) peuvent être expliqués par une production intermédiaire d'EAO. Ce travail est en cours de révision.

Notons que la deuxième partie de la thèse de Micha Wudick porte sur la description de la localisation et de la fonction des isoformes *AtTIP1;3* et *AtTIP5;1* dans le pollen, sous l'encadrement du Dr. Christophe Maurel. Ce travail, auquel j'ai également contribué, est sous presse (Wudick et al., In press). Il décrit notamment l'expression spécifique d'*AtTIP1;3* et *AtTIP5;1* au cours de la maturation et la germination du pollen dans, respectivement, les vacuoles de la cellule végétative et des cellules de sperme.

9.3 – Rôle des aquaporines dans l'émergence racinaire

Issu d'une collaboration tripartite entre notre laboratoire et ceux du Dr. Malcolm Bennett (Centre for Plant Integrative Biology, University of Nottingham, R.U.) et du Dr. Anton Schäffner (Institute of Biochemical Plant Pathology, Helmholtz Zentrum München, Neuherberg, Allemagne), ce travail a permis de mettre en évidence que l'expression de la plupart des *PIP* est réprimée pendant l'émergence racinaire. Cette répression peut être mimée par un apport exogène d'auxine. En accord avec ces effets, l'auxine inhibe le transport d'eau racinaire en agissant sur la fonction des aquaporines. Une modélisation mathématique, se basant sur les territoires d'expression de l'isoforme *AtPIP2;1*, a permis de prédire que des perturbations de son expression modifieraient le flux d'eau vers le primordium émergent, ralentissant ainsi l'émergence racinaire. L'analyse de

mutants réprimés ou sur-expresseurs de *AtPIP2;1* confirme le modèle obtenu. Ces travaux sont très importants car ils mettent en évidence un nouveau contrôle hydraulique de la croissance des racines secondaires. Plus précisément, nous avons démontré que l'action de l'auxine sur l'émergence racinaire s'effectuerait en partie par l'intermédiaire d'une régulation spatio-temporelle très fine de la fonction des aquaporines. Ma contribution dans ce travail a consisté à (i) décrire l'expression d'*AtPIP2;1* au cours des stades primaires de l'émergence d'un primordium racinaire et (ii) à analyser, avec une doctorante du laboratoire du Dr. Schöffner, des mutants KO de *pip2;1* complétés avec notre construction *AtPIP2;1-mCherry*. Ce travail a été publié dans la revue *Nature Cell Biology* (Péret et al., 2012) et constitue la base du projet de recherche du Dr. Philippe Nacry, Chargé de recherche INRA, nouvellement arrivé dans l'équipe.

9.4 – Biologie cellulaire des aquaporines chez le riz

Natif du Vietnam et pleinement intégré dans la communauté française, j'ai voulu mettre mes compétences professionnelles au service du développement scientifique de mon pays d'origine, en privilégiant une collaboration entre nos deux pays. En contact avec le Pr. Pascal Gantet, co-directeur du Laboratoire Mixte International (LMI-RICE) hébergé dans l'Agricultural Genetics Institute (Hanoï, Vietnam), et en accord avec mon laboratoire d'origine, j'ai candidaté à l'appel à projets Marie Curie Actions – International Outgoing Fellowships (IOF). Une bourse d'une durée de deux ans m'a été attribuée pour développer un projet sur la « Biologie cellulaire des aquaporines chez le riz » ; la première année, dite phase sortante, me permet d'être accueilli dans le laboratoire de Hanoï ; la deuxième année, dite phase rentrante, me permet de finaliser les travaux dans mon laboratoire de Montpellier. Ainsi, entre mai 2012 et mai 2013, j'ai été mis à disposition dans le LMI-RICE. Toutefois, en accord avec le Dr. Maurel et le Pr. Gantet, j'ai continué à développer mon projet de recherche sur le modèle d'*Arabidopsis* (cf. les paragraphes ci-dessus), pour me permettre de faire des allers-retours scientifiques entre les deux modèles.

L'expression et la fonction des aquaporines, chez le riz, a fait l'objet de plusieurs travaux d'équipes étrangères (Guo et al., 2006; Lian et al., 2006; Lian et al., 2004; Lu and Neumann, 1999; Miyamoto et al., 2001; Ranathunge et al., 2004; Ranathunge et al., 2011; Ranathunge et al., 2003; Sakurai-Ishikawa et al., 2011; Sakurai et al., 2008; Sakurai et al., 2005; Yu et al., 2006). Toutefois, les sujets que nous souhaiterions traiter ne sont pas encore documentés. En résumé, une collection de riz transgéniques exprimant chacun une isoforme sélectionnée d'*O_sPIP* fusionnée à la GFP ou à la mCherry est en cours d'obtention. L'expression racinaire et la localisation sub-cellulaire des constructions seront analysées en conditions normales, sous stress salin (NaCl) et sous stress hydrique (mimé par l'application de polyéthylène glycol). A terme, nous souhaiterions aussi disposer, chez le riz, d'une collection de marqueurs d'autres compartiments sub-cellulaires de référence (RE, appareil de Golgi, Trans-Golgi Network (TGN), PVC, tonoplaste). La *Lp_r* sera également caractérisée dans la variété irriguée NipponBare et la variété pluviale Azucena. Le choix de ces deux variétés repose sur le fait que la variété NipponBare a été la première variété à être séquencée et utilisée pour générer des banques de mutants d'insertion, alors que la variété Azucena est utilisée par la communauté scientifique comme la variété de riz pluviale de référence pour l'étude du développement racinaire. Ces deux variétés, phylogénétiquement proches, appartiennent au groupe des riz *japonica*. L'objectif est, à terme, de mieux comprendre la fonction et la régulation des aquaporines chez une céréale modèle. Actuellement, des lignées de riz transgéniques exprimant les constructions *O_sPIP1;1-GFP*, *GFP-O_sPIP1;1*, *O_sPIP1;1-mCherry*, *O_sPIP2;1-GFP*, *O_sRab5-mCherry* sont en

cours de sélection. Nous discuterons dans la partie “Objectifs/Projets de recherche” la suite des travaux initiés dans ce cadre.

9.5 Bilan

Nos travaux sur la dynamique endomembranaire des aquaporines PIP indiquent que celle-ci est déterminée par des mécanismes généraux et spécifiques. Ainsi, le signal d’export hors du RE de l’isoforme *AtPIP2;1* se trouve bien être un motif di-acide, mais dont la séquence DVE ne peut subir de substitution par aucune autre combinaison de résidus acides. De plus, le cyclage de cette isoforme entre la PM et les compartiments intracellulaires suit le modèle établi pour la famille des PIN bien que les effets de l’auxine sur le cyclage d’*AtPIP2;1* semblent s’exercer à un niveau qui n’a pas été décrit. Par ailleurs, deux de nos études suggèrent, par des approches indépendantes, que l’endocytose ne ferait pas intervenir la clathrine sous stress salin. Nous projetons de vérifier cette hypothèse par des approches génétiques. La dissection d’un mécanisme d’endocytose indépendant de la clathrine chez les plantes serait de toute évidence originale.

Nos travaux suggèrent aussi un modèle dans lequel un stress salin (150 mM NaCl) provoquerait la production et l’accumulation d’EAO qui aurait pour conséquence l’internalisation accrue des PIP et la réduction de la conductivité hydraulique. Toutefois, plusieurs arguments laissent à penser que ces mécanismes sont plus complexes. Ainsi un stress salin plus modéré (100 mM NaCl) bien que provoquant une réduction de la conductivité hydraulique ne permet pas de détecter, avec nos outils, d’accumulation d’EAO et ne provoque pas d’internalisation massive de PIP. Ceci laisse à penser qu’un mécanisme d’inhibition intrinsèque des PIP serait aussi impliqué dans la réduction de la conductivité hydraulique.

Nous avons la conviction que bien que très largement admises comme protéines membranaires modèles pour le trafic endomembranaire chez les plantes, les membres de la famille des PIN ne peuvent rendre compte à elles seules de la multitude des mécanismes et des régulations moléculaires que subissent les autres transporteurs et les canaux. Aussi, les PIP pourraient valablement compléter ces connaissances. Pour conclure, les efforts de la communauté des biologistes cellulaires dans le futur devront porter sur l’émergence d’autres modèles que les PIN (*BOR1*, *BRI1*, *FLS2*, *KAT1*, *IRT1*, ... et bien sûr *AtPIP2;1*), conduisant à une meilleure connaissance de la multiplicité de mécanismes et de régulations.

10 – PROJET DE RECHERCHE

Le projet de recherche que je souhaiterais développer continuera à porter sur les aquaporines, et plus particulièrement les PIP, comme objets moléculaires. Il portera sur la découverte des mécanismes moléculaires qui gouvernent leur trafic endomembranaire et les régulations qui contrôlent leur localisation en réponse aux contraintes de l'environnement. En préambule, je mentionnerai les verrous technologiques que je serais amené à lever. De plus, compte tenu du recrutement du Dr. Alexandre Martinière comme Chargé de recherche CNRS dans notre équipe, sur la thématique « Perception et réponses précoces des cellules végétales à la contrainte hydrique », j'indiquerai aussi au jury comment nous comptons travailler.

10.1 – Remarques liminaires

Comme mentionnées plus haut (§ 9.2.2 et 9.2.3), les techniques de SPT et FCS s'imposent comme outils d'analyse du comportement des protéines à la MP. Ces techniques ont été utilisées dans le cadre de collaboration avec des collègues Chinois et nous devons dans le futur proche les maîtriser. Concernant le SPT, une collaboration a déjà été initiée depuis quelques mois avec les Dr. Eric Hosity et Jean-Baptiste Sibarita du laboratoire du Dr. Daniel Choquet (Institut interdisciplinaire de neuroscience, Bordeaux) sur la technique du spt-Photoactivated localization microscopy (sptPALM), et nous permettant d'évaluer sa faisabilité dans le modèle végétal. Le sptPALM permet d'obtenir à partir de la mobilité des molécules uniques une résolution à l'échelle nano-métrique et à haute densité (Li et al., 2013). Il s'affranchit ainsi de la diffraction qui limite la résolution (environ 200 nm pour des observations au microscope confocal à balayage laser) ; en mesurant la position des marqueurs fluorescents une par une, on peut reconstruire une image précise au nanomètre près de l'objet observé (résolution d'environ 40 nm). Entre nos mains, cette technique s'est avérée applicable aux protéines membranaires dans la cellule de l'épiderme de racine d'*Arabidopsis* (cf. plus loin). Toutefois, développée à Bordeaux, nous devons maintenant avoir accès à cette technique en local. Des contacts ont ainsi été pris avec la plate-forme MARS (www.cbs.cnrs.fr/mars). Cette dernière en plus d'offrir l'équipement nécessaire au sptPALM dans le plan de la membrane (deux dimensions) le développe aussi dans trois dimensions (3D). Je devrai évaluer si le sptPALM 3D s'avère utile à l'étude de l'endocytose des PIP. De plus, le sptPALM n'est actuellement applicable qu'avec un seul marqueur fluorescent à la fois ; il sera utile que des images super-résolutives avec au moins deux marqueurs soient disponibles. Enfin, le logiciel d'analyse des trajectoires PALM-TRACER a été développé et est la propriété intellectuelle du Dr. Jean-Baptiste Sibarita. Nous avons obtenu son accord pour l'utiliser exclusivement dans le cadre de nos recherches et pensons que cela, ainsi que les équipements de la plate-forme MARS, nous garantiront une avance technologique.

Le recrutement du Dr. Alexandre Martinière lui permettra de développer une thématique originale dont les objectifs sont :

- (i) Identifier le/les messageur(s) secondaires ou les processus biochimiques permettant la transduction du signal osmotique et aboutissant d'une part à l'augmentation de la diffusion membranaire des protéines et d'autre part à l'induction de l'endocytose.
- (ii) Déterminer le rôle du continuum paroi/MP/cytosquelette dans le mécanisme de perception du stress osmotique.
- (iii) Identifier les facteurs moléculaires impliqués dans la perception et transduction du signal osmotique

Il se servira donc des phénomènes de diffusion latérale et d'endocytose des PIP comme marqueurs du signal osmotique pour caractériser les mécanismes moléculaires impliqués. Nous serons amenés à interagir étroitement, puisque les informations que nous obtiendrons permettront de nourrir nos thématiques respectives. Par exemple, l'un de ses objectifs est de caractériser les éléments moléculaires précis impliqués dans la chaîne de perception/signalisation, en développant une approche génétique. Je serai peut-être amené à m'intéresser à l'un des gènes candidats qu'il identifiera dans l'endocytose des PIP ? Il est à noter que notre collaboration a déjà permis la publication de trois articles (Luu et al., 2012; Martinière et al., 2012; Martinière et al., 2012).

10.2 – Dynamique membranaire et cyclage des aquaporines dans les cellules de la racine d'Arabidopsis sous stress salin.

10.2.1 – Développement du sptPALM en biologie cellulaire chez les plantes.

Comme mentionné plus haut, nous pensons que le sptPALM aidera à caractériser la localisation et la dynamique d'*AtPIP2;1* dans le plan de la MP avec une résolution jamais atteinte auparavant et pourra être appliquée aussi bien en conditions contrôles que sous stress salin. *AtPIP2;1* a été fusionnée à la protéine fluorescente convertible mEOS2 et la construction a été exprimée de façon stable dans *Arabidopsis*. Nous avons aussi testé la faisabilité du sptPALM avec des constructions *LTi6a-mEOS2* et *AtTIP1;1-mEOS2*. Les résultats préliminaires indiquent que des images super-résolutives et les trajectoires pour ces trois constructions sont accessibles dans la cellule de l'épiderme de la racine de jeunes plantules. Alors que la localisation d'*AtPIP2;1-mEOS2* est concentrée dans des régions d'environ 100 nm de diamètre, celles de *LTi6a-mEOS2* et d'*AtTIP1;1-mEOS2* sont réparties, respectivement, dans l'ensemble de la MP et du tonoplaste. Le contraste entre les localisations d'*AtPIP2;1*, d'une part, et de *LTi6a-mEOS2* et *AtTIP1;1-mEOS2*, d'autre part, traduit leur différence de mobilité. En effet, nous avons estimé que seules $23.3 \pm 2.8\%$ des constructions *AtPIP2;1-mEOS2* sont mobiles alors que cette proportion est de $86.0 \pm 1.8\%$ et $89.7 \pm 2.8\%$, respectivement, pour *LTi6a-mEOS2* et *AtTIP1;1-mEOS2*. La distribution des coefficients de diffusion se présente sous la forme d'une courbe en cloche dont les valeurs des pics sont de 4×10^{-3} , 6.3×10^{-2} et $6.31 \times 10^{-1} \mu\text{m}^2 \text{s}^{-1}$, respectivement, pour *AtPIP2;1*, *LTi6a*, et *AtTIP1;1*. La faisabilité technique du sptPALM appliqué à des protéines membranaires dans des cellules végétales ainsi démontrée, nous pourrions envisager de comprendre, avec une meilleure résolution qu'auparavant, les mécanismes moléculaires responsables du confinement d'*AtPIP2;1*. Nous questionnerons la relation hypothétique entre mobilité et densité des molécules PIP à la MP, en exprimant la construction *AtTIP1;1-mEOS2* à des niveaux d'expression modéré et fort avec, respectivement, son promoteur natif et le promoteur *CaMV35S*. Les PIP forment des tétramères qui peuvent se multimériser à leur tour, limitant les propriétés de diffusion. Bien que la présence d'*AtPIP2;1* ait déjà été documentée dans des micro-domaines lipidiques (Li et al., 2011), nous tirerons avantage de la super-résolution du sptPALM pour préciser cette localisation et avec quels autres molécules *AtPIP2;1* colocalise. Pour rappel, dans le cadre d'une collaboration avec le laboratoire du Dr John Runions (cf. § 9.2.1, (Martinière et al., 2012)), il avait été établi que le cytosquelette et la paroi ont des rôles contrastés dans le confinement de protéines chimères de la MP, sans pour autant aborder celui d'*AtPIP2;1*. Cette lacune sera comblée avec le renfort du sptPALM.

10.2.2 – Identification des acteurs moléculaires impliqués dans le cyclage d'AtPIP2;1.

Ce sujet sera abordé dans le cadre d'une collaboration avec le Dr. Catherine Perrot-Rechenmann (Institut des sciences du végétal, Gif-sur-Yvette), le Dr. Eric Hosy (Institut interdisciplinaire de neuroscience, Bordeaux) et le

Dr. Alexandre Martinière. Nos approches précédentes reposaient essentiellement sur des traitements pharmacologiques ; nous souhaitons utiliser des fonds génétiques altérés dans certaines fonctions du trafic endomembranaire et analyser le cyclage par technique de FRAP (cf. § .9.2.1) et SPT. Comme nous l'avons mentionné dans les remarques liminaires, nous évaluerons si le sptPALM 3D permettra une analyse fine de l'endocytose.

L'endocytose de *AtPIP2;1* en conditions contrôles et salines sera évaluée dans des cellules affectées de façon conditionnelle dans la fonction de la clathrine par expression d'une séquence anti-sens de la chaîne lourde ou du fragment HUB sous un promoteur inductible.

L'ABP1 joue un rôle inconnu dans l'endocytose des PIN ou son inhibition en réponse à l'auxine. Nous évaluerons si l'ABP1 a un tel rôle dans l'endocytose d'*AtPIP2;1*, en utilisant un ensemble de fonds génétiques altérés de façon conditionnelle dans la fonction d'ABP1. Par exemple, le Dr Catherine Perrot-Rechenmann a mis à disposition des plantes d'*Arabidopsis* exprimant un système d'immunisation cellulaire consistant à la production de fragments recombinants d'immunoglobulines construits à partir d'anticorps monoclonaux anti-*NtABP1* capables de bloquer la protéine dans une configuration inactive.

D'autres fonds génétiques altérés dans l'expression de GNOM (Geldner et al., 2003), et EXO70A1 (Synek et al., 2006) sont envisagés pour aborder l'exocytose d' *AtPIP2;1*. Par exemple, le Dr. Viktor Zarsky (Université Charles, Prague, République Tchèque) a mis à notre disposition le mutant *exo70a1*. Toutefois, sous la forme homozygote les plantes mutantes présentent un défaut important de développement et ne sont pas analysable par FRAP ; aussi, nous devons envisager d'altérer sa fonction de façon conditionnelle.

Ce sujet a fait l'objet de deux dépôts de projet blanc à l'ANR et d'une soumission d'une pré-proposition en 2014. Compte tenu du coût important des approches de biologie cellulaire, il sera crucial d'obtenir un moyen de financement *ad hoc*.

10.3 – Biologie cellulaire des aquaporines chez le riz.

En plus des lignées de riz transgéniques exprimant les constructions *OsPIP1;1-GFP*, *GFP-OsPIP1;1*, *OsPIP1;1-mCherry*, *OsPIP2;1-GFP*, *OsRab5-mCherry*, nous devons aussi considérer les isoformes *OsPIP2;4* et *OsPIP2;5*, ainsi que d'autres marqueurs des compartiments intracellulaires :

- une protéine fluorescente fusionnée au polypeptide HDEL permettra de marquer le RE,
- *OsNST1* (Nucleotide Sugar Transporter) pourra marquer l'appareil de Golgi (Zhang et al., 2011),
- *OsRMR1* (Receptor homology region-transmembrane domain-RING-H2) marque les PVC (Shen et al., 2011),
- *OsGAP1* (Rab-specific rice GTPase-activating protein) marque des compartiments endosomaux (Heo et al., 2005),
- *OsSCAMP1* (Secretory Carrier Membrane Protein) est localisée dans des compartiments endosomaux (Cai et al., 2011)
- *OsTIP2;1* et *OsTIP4;1* seront utilisés pour marquer les vacuoles.

Notons que l'étude de la fonction des aquaporines de riz en situation de salinité est déjà abordée par d'autres équipes internationales. En particulier, la sur-expression de l'isoforme *OsPIP1;1* favoriserait la résistance à la salinité de jeunes plantules (Liu et al., 2013). Ces informations ainsi que d'autres nous alertent sur l'état de la concurrence scientifique et orientent notre choix des isoformes intéressantes. Un effort devra être fait pour avancer dans la caractérisation du trafic des aquaporines chez le riz, par les approches que nous avons développées chez *Arabidopsis*. Précisément, depuis le commencement du projet ORYZAQUA, nous avons pu

compter sur l'aide du Dr Hoang Thi Giang, qui supervise la plate-forme de transgénèse du riz au LMI-RICE. De plus, à partir de mars 2014, nous pourrons compter sur l'aide de M. Trinh Duy Chi, stagiaire de Master 2 de l'USTH. Notre sujet de thèse a été récemment validé par l'USTH et sera proposé au concours des bourses de thèse de cet établissement. Enfin, dans le cadre du Partenariat Hubert Curien franco-vietnamien « Hoa Sen-Lotus » et prenant la suite du projet ORYZAQUA, des échanges de personnels entre notre laboratoire et le LMI-RICE seront financés en 2015-2016. En résumé, nous espérons pouvoir compter sur l'ensemble de cette aide pour avancer sur cette thématique.

REFERENCES CITEES

- Bandmann, V., and Homann, U. (2012). Clathrin-independent endocytosis contributes to uptake of glucose into BY-2 protoplasts. *Plant J* 70:578-584.
- Boursiac, Y., Boudet, J., Postaire, O., Luu, D.-T., Tournaire-Roux, C., and Maurel, C. (2008a). Stimulus-induced downregulation of root water transport involves reactive oxygen species-activated cell signalling and plasma membrane intrinsic protein internalization. *Plant J* 56:207-218.
- Boursiac, Y., Chen, S., Luu, D.-T., Sorieul, M., van den Dries, N., and Maurel, C. (2005). Early effects of salinity on water transport in Arabidopsis roots. Molecular and cellular features of aquaporin expression. *Plant Physiol* 139:790-805.
- Boursiac, Y., Prak, S., Boudet, J., Postaire, O., Luu, D.-T., Tournaire-Roux, C., Santoni, V., and Maurel, C. (2008b). The response of Arabidopsis root water transport to a challenging environment implicates reactive oxygen species- and phosphorylation-dependent internalization of aquaporins. *Plant Signal Behav* 3:1096-1098.
- Cai, Y., Jia, T., Lam, S.K., Ding, Y., Gao, C., San, M.W., Pimpl, P., and Jiang, L. (2011). Multiple cytosolic and transmembrane determinants are required for the trafficking of SCAMP1 via an ER-Golgi-TGN-PM pathway. *Plant J* 65:882-896.
- Dhonukshe, P., Aniento, F., Hwang, I., Robinson, D.G., Mravec, J., Stierhof, Y.D., and Friml, J. (2007). Clathrin-mediated constitutive endocytosis of PIN auxin efflux carriers in Arabidopsis. *Curr Biol* 17:520-527.
- di Pietro, M., Vialaret, J., Li, G.W., Hem, S., Prado, K., Rossignol, M., Maurel, C., and Santoni, V. (2013). Coordinated post-translational responses of aquaporins to abiotic and nutritional stimuli in Arabidopsis roots. *Mol Cell Proteomics* 12:3886-3897.
- Geldner, N., Anders, N., Wolters, H., Keicher, J., Kornberger, W., Muller, P., Delbarre, A., Ueda, T., Nakano, A., and Jurgens, G. (2003). The Arabidopsis GNOM ARF-GEF mediates endosomal recycling, auxin transport, and auxin-dependent plant growth. *Cell* 112:219-230.
- Geldner, N., Denervaud-Tendon, V., Hyman, D.L., Mayer, U., Stierhof, Y.D., and Chory, J. (2009). Rapid, combinatorial analysis of membrane compartments in intact plants with a multicolor marker set. *Plant J* 59:169-178.
- Guo, L., Wang, Z.Y., Lin, H., Cui, W.E., Chen, J., Liu, M., Chen, Z.L., Qu, L.J., and Gu, H. (2006). Expression and functional analysis of the rice plasma-membrane intrinsic protein gene family. *Cell Res* 16:277-286.
- Hanton, S.L., Renna, L., Bortolotti, L.E., Chatre, L., Stefano, G., and Brandizzi, F. (2005). Diacidic motifs influence the export of transmembrane proteins from the endoplasmic reticulum in plant cells. *Plant Cell* 17:3081-3093.
- Heizmann, P., Luu, D.-T., and Dumas, C. (2000a). The clues to species specificity of pollination among Brassicaceae. *Sex. Plant Reprod.* 13:157-161.
- Heizmann, P., Luu, D.-T., and Dumas, C. (2000b). Pollen-stigma adhesion in the Brassicaceae. *Ann. Bot.* 85:23-27.
- Heo, J.B., Rho, H.S., Kim, S.W., Hwang, S.M., Kwon, H.J., Nahm, M.Y., Bang, W.Y., and Bahk, J.D. (2005). OsGAP1 functions as a positive regulator of OsRab11-mediated TGN to PM or vacuole trafficking. *Plant Cell Physiol* 46:2005-2018.
- Konopka, C.A., and Bednarek, S.Y. (2008). Variable-angle epifluorescence microscopy: a new way to look at protein dynamics in the plant cell cortex. *Plant J* 53:186-196.
- Leborgne-Castel, N., and Luu, D.-T. (2009). Regulation of endocytosis by external stimuli in plant cells. *Plant Biosystems* 143:630 - 635.
- Leshem, Y., Seri, L., and Levine, A. (2007). Induction of phosphatidylinositol 3-kinase-mediated endocytosis by salt stress leads to intracellular production of reactive oxygen species and salt tolerance. *Plant J* 51:185-197.
- Li, X., Luu, D.-T., Maurel, C., and Lin, J. (2013). Probing plasma membrane dynamics at the single-molecule level. *Trends in Plant Science* 18:617-624.
- Li, X., Wang, X., Yang, Y., Li, R., He, Q., Fang, X., Luu, D.-T., Maurel, C., and Lin, J. (2011). Single-molecule analysis of PIP₂;1 dynamics and partitioning reveals multiple modes of Arabidopsis plasma membrane aquaporin regulation. *Plant Cell* 23:3780-3797.
- Lian, H.-L., Yu, X., Lane, D., Sun, W.-N., Tang, Z.-C., and Su, W.-A. (2006). Upland rice and lowland rice exhibited different PIP expression under water deficit and ABA treatment. *Plant Cell Physiol* 47:651-660.
- Lian, H.-L., Yu, X., Ye, Q., Ding, X.-S., Kitagawa, Y., Kwak, S.-S., Su, W.-A., and Tang, Z.-C. (2004). The Role of Aquaporin RWC3 in Drought Avoidance in Rice. *Plant Cell Physiol* 45:481-489.
- Liu, C., Fukumoto, T., Matsumoto, T., Gena, P., Frascaria, D., Kaneko, T., Katsuhara, M., Zhong, S., Sun, X., Zhu, Y., et al. (2013). Aquaporin OsPIP1;1 promotes rice salt resistance and seed germination. *Plant Physiology and Biochemistry* 63:151-158.
- Lu, Z.J., and Neumann, P.M. (1999). Water stress inhibits hydraulic conductance and leaf growth in rice seedlings but not the transport of water via mercury-sensitive water channels in the root. *Plant Physiol* 120:143-151.
- Luu, D.-T. (1997). Adh sion pollen-stigmate chez les Brassicaceae : implication des g nes S-Locus Glycoprotein et S-Locus Related 1: Ecole Normale Sup rieure de Lyon.

- Luu, D.-T., Heizmann, P., and Dumas, C. (1997a). Pollen-stigma adhesion in kale is not dependent on the self-(in)compatibility genotype. *Plant Physiol* 115:1221-1230.
- Luu, D.-T., Hugues, S., Passelegue, E., and Heizmann, P. (2001a). Evidence for orthologous S-locus-related I genes in several genera of Brassicaceae. *Mol Gen Genet* 264:735-745.
- Luu, D.-T., Martinière, A., Sorieul, M., Runions, J., and Maurel, C. (2012). Fluorescence recovery after photobleaching reveals high cycling dynamics of plasma membrane aquaporins in Arabidopsis roots under salt stress. *Plant J* 69:894-905.
- Luu, D.-T., Marty-Mazars, D., Trick, M., Dumas, C., and Heizmann, P. (1999). Pollen-stigma adhesion in Brassica spp involves SLG and SLR1 glycoproteins. *Plant Cell* 11:251-262.
- Luu, D.-T., and Maurel, C. (2005). Aquaporins in a challenging environment: molecular gears for adjusting plant water status. *Plant Cell Environ* 28:85-96.
- Luu, D.-T., and Maurel, C. (2012). Dynamic behaviour and internalization of aquaporins at the surface of plant cells. In: *Endocytosis in Plant* --Samaj, J., ed. Heidelberg New York Dorrecht London: Springer-Verlag. 185-199.
- Luu, D.-T., and Maurel, C. (2013). Aquaporin trafficking in plant cells: an emerging membrane-protein model. *Traffic* 14:629-635.
- Luu, D.-T., Passelègue, E., Dumas, C., and Heizmann, P. (1998). Pollen-stigma capture is not species discriminant within the Brassicaceae family. *C. R. Acad. Sci. Paris* 321:747-755.
- Luu, D.-T., Qin, X., Laublin, G., Yang, Q., Morse, D., and Cappadocia, M. (2001b). Rejection of S-heteroallelic pollen by a dual-specific s-RNase in Solanum chacoense predicts a multimeric SI pollen component. *Genetics* 159:329-335.
- Luu, D.-T., Qin, X., Morse, D., and Cappadocia, M. (2000). S-RNase uptake by compatible pollen tubes in gametophytic self-incompatibility. *Nature* 407:649-651.
- Luu, D.-T., Trick, M., Heizmann, P., Dumas, C., and Cappadocia, M. (1997b). Involvement of SLR1 genes in pollen adhesion to stigmatic surface in Brassicaceae. *Sex. Plant Reprod.* 10:227-235.
- Martinière, A., Lavagi, I., Nageswaran, G., Rolfe, D.J., Maneta-Peyret, L., Luu, D.-T., Botchway, S.W., Webb, S.E.D., Mongrand, S., Maurel, C., et al. (2012). Cell wall constrains lateral diffusion of plant plasma-membrane proteins. *Proceedings of the National Academy of Sciences of the United States of America* 109:12805-12810.
- Martinière, M., Li, X., Runions, J., Lin, J., Maurel, C., and Luu, D.-T. (2012). Salt stress triggers enhanced cycling of Arabidopsis root plasma-membrane aquaporins. *Plant Signal Behav* 7:529 - 532.
- Matton, D.P., Luu, D.-T., Xike, Q., Laublin, G., O'Brien, M., Maes, O., Morse, D., and Cappadocia, M. (1999). Production of an S RNase with dual specificity suggests a novel hypothesis for the generation of new S alleles. *Plant Cell* 11:2087-2097.
- Maurel, C., Santoni, V., Luu, D.-T., Wudick, M.M., and Verdoucq, L. (2009). The cellular dynamics of plant aquaporin expression and functions. *Curr Opin Plant Biol* 12:690-698.
- Maurel, C., Verdoucq, L., Luu, D.-T., and Santoni, V. (2008). Plant aquaporins: membrane channels with multiple integrated functions. *Annu Rev Plant Biol* 59:595-624.
- Mikosch, M., Hurst, A.C., Hertel, B., and Homann, U. (2006). Diacidic Motif Is Required for Efficient Transport of the K⁺ Channel KAT1 to the Plasma Membrane. *Plant Physiol* 142:923-930.
- Miyamoto, N., Steudle, E., Hirasawa, T., and Lafitte, R. (2001). Hydraulic conductivity of rice roots. *J Exp Bot* 52:1835-1846.
- Paciorek, T., Zazimalova, E., Ruthardt, N., Petrasek, J., Stierhof, Y.D., Kleine-Vehn, J., Morris, D.A., Emans, N., Jurgens, G., Geldner, N., et al. (2005). Auxin inhibits endocytosis and promotes its own efflux from cells. *Nature* 435:1251-1256.
- Péret, B., Li, G., Zhao, J., Band, L.R., Voß, U., Postaire, O., Luu, D.-T., Da Ines, O., Casimiro, I., Lucas, M., et al. (2012). Auxin regulates aquaporin function to facilitate lateral root emergence. *Nat Cell Biol* 14:991-998.
- Picault, N., Cazale, A.C., Beyly, A., Cuine, S., Carrier, P., Luu, D.-T., Forestier, C., and Peltier, G. (2006). Chloroplast targeting of phytochelatin synthase in Arabidopsis: effects on heavy metal tolerance and accumulation. *Biochimie* 88:1743-1750.
- Prado, K., Boursiac, Y., Tournaire-Roux, C., Monneuse, J.-M., Postaire, O., Da Ines, O., Schaffner, A.R., Hem, S., Santoni, V., and Maurel, C. (2013). Regulation of Arabidopsis leaf hydraulics involves light-dependent phosphorylation of aquaporins in veins. *The Plant Cell* 25:1029-1039.
- Prak, S., Hem, S., Boudet, J., Viennois, G., Sommerer, N., Rossignol, M., Maurel, C., and Santoni, V. (2008). Multiple phosphorylations in the C-terminal tail of plant plasma membrane aquaporins: role in subcellular trafficking of AtPIP2;1 in response to salt stress. *Mol Cell Proteomics* 7:1019-1030.
- Qin, X., Luu, D.-T., Yang, Q., Maes, O., Matton, D.P., Morse, D., and Cappadocia, M. (2001). Genotype-dependent differences in S12-RNase expression lead to sporadic self-compatibility. *Plant Mol Biol* 45:295-305.
- Ranathunge, K., Kotula, L., Steudle, E., and Lafitte, R. (2004). Water permeability and reflection coefficient of the outer part of young rice roots are differently affected by closure of water channels (aquaporins) or blockage of apoplastic pores. *J. Exp. Bot.* 55:433-447.

- Ranathunge, K., Lin, J., Steudle, E., and Schreiber, L. (2011). Stagnant deoxygenated growth enhances root suberization and lignifications, but differentially affects water and NaCl permeabilities in rice (*Oryza sativa* L.) roots. *Plant, Cell & Environment* 34:1223-1240.
- Ranathunge, K., Steudle, E., and Lafitte, R. (2003). Control of water uptake by rice (*Oryza sativa* L.): role of the outer part of the root. *Planta* 217:193-205.
- Robert, S., Kleine-Vehn, J., Barbez, E., Sauer, M., Paciorek, T., Baster, P., Vanneste, S., Zhang, J., Simon, S., Covanova, M., et al. (2010). ABP1 mediates auxin inhibition of clathrin-dependent endocytosis in *Arabidopsis*. *Cell* 143:111-121.
- Sahr, T., Adam, T., Fizames, C., Maurel, C., and Santoni, V. (2010). O-carboxyl- and N-methyltransferases active on plant aquaporins. *Plant Cell Physiol* 51:2092-2104.
- Sakurai-Ishikawa, J., Murai-Hatano, M., Hayashi, H., Ahamed, A., Fukushi, K., Matsumoto, T., and Kitagawa, Y. (2011). Transpiration from shoots triggers diurnal changes in root aquaporin expression. *Plant Cell Environ* 34:1150-1163.
- Sakurai, J., Ahamed, A., Murai, M., Maeshima, M., and Uemura, M. (2008). Tissue and Cell-Specific Localization of Rice Aquaporins and Their Water Transport Activities. *Plant and Cell Physiology* 49:30-39.
- Sakurai, J., Ishikawa, F., Yamaguchi, T., Uemura, M., and Maeshima, M. (2005). Identification of 33 rice aquaporin genes and analysis of their expression and function. *Plant Cell Physiol* 46:1568-1577.
- Santoni, V., Verdoucq, L., Sommerer, N., Vinh, J., Pflieger, D., and Maurel, C. (2006). Methylation of aquaporins in plant plasma membrane. *Biochem J* 400:189-197.
- Sauer, M., and Kleine-Vehn, J. (2011). AUXIN BINDING PROTEIN1: The Outsider. *Plant Cell* 23:2033-2043.
- Sauge-Merle, S., Cuine, S., Carrier, P., Lecomte-Pradines, C., Luu, D.-T., and Peltier, G. (2003). Enhanced toxic metal accumulation in engineered bacterial cells expressing *Arabidopsis thaliana* phytochelatin synthase. *Appl Environ Microbiol* 69:490-494.
- Schopfer, C., Nasrallah, M., and Nasrallah, J. (1999). The male determinant of self-incompatibility in *Brassica*. *Science* 286:1697-1700.
- Shen, Y., Wang, J., Ding, Y., Lo, S.W., Gouzerh, G., Neuhaus, J.-M., and Jiang, L. (2011). The Rice RMR1 Associates with a Distinct Prevacuolar Compartment for the Protein Storage Vacuole Pathway. *Molecular Plant*.
- Shiba, H., Takayama, S., Iwano, M., Shimosato, H., Funato, M., T, N., Che, F., Suzuki, F., Watanabe, M., Hinata, K., et al. (2001). A pollen coat protein, SP11/SCR, determines the pollen S-specificity in the self-incompatibility of *Brassica* species. *Plant Physiology* 125:2095-2103.
- Sijacic, P., Wang, X., Skirpan, A., Wang, Y., Dowd, P., McCubbin, A., Huang, S., and Kao, T.-H. (2004). Identification of the pollen determinant of S-RNase-mediated self-incompatibility. *Nature* 429:302-305
- Sorieul, M., Santoni, V., Maurel, C., and Luu, D.-T. (2011). Mechanisms and effects of retention of over-expressed aquaporin AtPIP2;1 in the endoplasmic reticulum. *Traffic* 12:473-482.
- Sutter, J.U., Campanoni, P., Tyrrell, M., and Blatt, M.R. (2006). Selective mobility and sensitivity to SNAREs is exhibited by the *Arabidopsis* KAT1 K⁺ channel at the plasma membrane. *Plant Cell* 18:935-954.
- Synek, L., Schlager, N., Elias, M., Quentin, M., Hauser, M.T., and Zarsky, V. (2006). AtEXO70A1, a member of a family of putative exocyst subunits specifically expanded in land plants, is important for polar growth and plant development. *Plant J* 48:54-72.
- Takayama, S., Shiba, H., Iwano, M., Shimosato, H., Che, F., Kai, N., Watanabe, M., Suzuki, G., Hinata, K., and Isogai, A. (2000). The pollen determinant of self-incompatibility in *Brassica campestris*. *Proceedings of the National Academy of Sciences of the United States of America* 97:1920-1925.
- Verdoucq, L., Grondin, A., and Maurel, C. (2008). Structure-function analysis of plant aquaporin AtPIP2;1 gating by divalent cations and protons. *Biochem J* 415:409-416.
- Wudick, M.M., Luu, D.-T., and Maurel, C. (2009). A look inside: localization patterns and functions of intracellular plant aquaporins. *New Phytol* 184:289-302.
- Wudick, M.M., Luu, D.-T., Tournaire-Roux, C., Sakamoto, W., and Maurel, C. (In press). Vegetative and sperm cell-specific aquaporins of *Arabidopsis thaliana* highlight the vacuolar equipment of pollen and contribute to plant reproduction. *Plant Physiol*.
- Yu, X., Peng, Y.H., Zhang, M.H., Shao, Y.J., Su, W.A., and Tang, Z.C. (2006). Water relations and an expression analysis of plasma membrane intrinsic proteins in sensitive and tolerant rice during chilling and recovery. *Cell Res* 16:599-608.
- Zelazny, E., Miecielica, U., Borst, J.W., Hemminga, M.A., and Chaumont, F. (2009). An N-terminal diacidic motif is required for the trafficking of maize aquaporins ZmPIP2;4 and ZmPIP2;5 to the plasma membrane. *Plant J* 57:346-355.
- Zhang, B., Liu, X., Qian, Q., Liu, L., Dong, G., Xiong, G., Zeng, D., and Zhou, Y. (2011). Golgi nucleotide sugar transporter modulates cell wall biosynthesis and plant growth in rice. *Proc Natl Acad Sci U S A* 108:5110-5115.

CINQ PUBLICATIONS SIGNIFICATIVES DU PARCOURS

Fluorescence recovery after photobleaching reveals high cycling dynamics of plasma membrane aquaporins in *Arabidopsis* roots under salt stress

Doan-Trung Luu^{1,*†}, Alexandre Martinière^{2,†}, Mathias Sorieul^{1,†}, John Runions² and Christophe Maurel¹

¹Biochimie et Physiologie Moléculaire des Plantes, Institut de Biologie Intégrative des Plantes, UMR 5004 CNRS/UMR 0386 INRA/Montpellier SupAgro/Université Montpellier 2, F-34060 Montpellier Cedex 2, France, and

²School of Life Sciences, Oxford Brookes University, Oxford OX3 0BP, UK

Received 15 September 2011; revised 27 October 2011; accepted 31 October 2011; published online 16 December 2011.

*For correspondence (fax +33 467525737; e-mail luu@supagro.inra.fr).

†These authors contributed equally to this work.

*Present address: University of Warwick, Department of Biological Sciences, Warwick, UK.

SUMMARY

The constitutive cycling of plant plasma membrane (PM) proteins is an essential component of their function and regulation under resting or stress conditions. Transgenic *Arabidopsis* plants that express GFP fusions with AtPIP1;2 and AtPIP2;1, two prototypic PM aquaporins, were used to develop a fluorescence recovery after photobleaching (FRAP) approach. This technique was used to discriminate between PM and endosomal pools of the aquaporin constructs, and to estimate their cycling between intracellular compartments and the cell surface. The membrane trafficking inhibitors tyrphostin A23, naphthalene-1-acetic acid and brefeldin A blocked the latter process. By contrast, a salt treatment (100 mM NaCl for 30 min) markedly enhanced the cycling of the aquaporin constructs and modified their pharmacological inhibition profile. Two distinct models for PM aquaporin cycling in resting or salt-stressed root cells are discussed.

Keywords: *Arabidopsis*, aquaporins, constitutive cycling, salt stress, fluorescence recovery after photobleaching.

INTRODUCTION

In eukaryotic cells, endocytosis is an essential phenomenon whereby extracellular substances and/or plasma membrane (PM) proteins are internalized by using membrane vesicles for transport to endosomes. In plants, the functional importance of endocytosis has been demonstrated in the PIN-FORMED (PIN) auxin transport system by the analysis of developmental mutants and by means of pharmacological interference (Geldner *et al.*, 2001, 2003). Polarity of auxin transport is achieved by the coordinated localization of PIN efflux transporters to one end of a cell, which requires continuous cycling between the plasma membrane and endosomal compartments. In these studies, and others, the fungal toxin brefeldin A (BFA), which supposedly blocks exocytosis, has been extensively used to demonstrate the cycling of PM proteins. Other studies, using the tyrosine analogue tyrphostin A23 (A23) as a tentative blocker of endocytosis, have addressed this other step of constitutive cycling (Ortiz-Zapater *et al.*, 2006; Dhonukshe *et al.*, 2007;

Konopka *et al.*, 2008; Leborgne-Castel *et al.*, 2008; Fujimoto *et al.*, 2010). Other molecular tools for studying membrane and protein endocytosis in plants (reviewed by Samaj, 2006) include the lipophilic styryl dyes FM1-43 and FM4-64, used as endocytic tracers.

Under challenging biotic or abiotic environmental conditions, regulation of endocytosis is essential in plant cells (Leborgne-Castel and Luu, 2009). When rice cells were subjected to a saline stress, the endocytosis of biotinylated bovine serum albumin was initially inhibited but then activated after a 24-h period (Bahaji *et al.*, 2003). By contrast, a study in *Arabidopsis* roots (Leshem *et al.*, 2007) demonstrated an induction of FM1-43 uptake shortly after salt treatment, which was interpreted as an enhancement of endocytosis. Treatment with 100 mM NaCl also induced the partial accumulation in intracellular compartments of aquaporins, which are expressed at the PM of epidermal and cortical cells in resting conditions (Boursiac *et al.*, 2005). Salt

treatment induced a concomitant (half-time 45 min) and significant (~70%) decrease in root hydraulic conductivity (Boursiac *et al.*, 2005).

AtPIP1;2 and AtPIP2;1 belong to two distinct sub-groups of the plasma membrane intrinsic protein family and are among the most highly expressed aquaporins in Arabidopsis roots (Santoni *et al.*, 2003; Boursiac *et al.*, 2005; Prak *et al.*, 2008). To determine the components controlling the cycling of aquaporins in roots under resting and salt-stress conditions, we investigated these two model PM aquaporins in Arabidopsis root epidermal cells. Recently, we used fluorescence recovery after photobleaching (FRAP) to discriminate between the subcellular localization of a wild-type isoform of AtPIP2;1 fused to GFP (AtPIP2;1-GFP), and that of AtPIP2;1 mutated at a diacidic motif involved in AtPIP2;1 trafficking to the PM (Sorieu *et al.*, 2011). The FRAP kinetics were faster in the mutated forms than in the PM-localized control construct and were used as an estimate of the retention of the former in the endoplasmic reticulum (ER). Here, we have used FRAP on AtPIP-GFP constructs to further dissect the exchange between the PM and intracellular pools of AtPIP1;2 and AtPIP2;1.

RESULTS AND DISCUSSION

Fluorescence recovery after photobleaching reveals an extremely low lateral diffusion of PM-localised aquaporins

When observed by laser scanning confocal microscopy, a tangential optical section of root epidermal cells expressing the PM marker GFP-LTI6a (Cutler *et al.*, 2000; Grebe *et al.*, 2003) exhibited a uniform signal corresponding to homogeneous distribution of protein at the cell surface. Yet the labelling of intracellular compartments associated with the endomembrane trafficking of GFP-LTI6a could not be excluded. The FRAP experiments showed that the signal within a region of interest (ROI) recovered by ~55% at 50 sec and almost completely at 7 min after photobleaching (Figure S1a–c). Such a fast and full recovery has previously been observed (Grebe *et al.*, 2003). For comparison, we also investigated the kinetics of recovery of a soluble GFP (sGFP), used as a cytosolic marker, and of the tonoplast intrinsic protein AtTIP1;1 aquaporin fused to GFP (AtTIP1;1-GFP and GFP-AtTIP1;1) (Figure S1a,b,d). The recovery of fluorescence of these markers was even faster than for GFP-LTI6a and was virtually complete within a few seconds after photobleaching. Very active cytoplasmic streaming carrying sGFP molecules results in facilitated diffusion and might partially explain the extremely fast recovery observed for this marker.

By contrast, AtPIP1;2-GFP, GFP-AtPIP1;2, AtPIP2;1-GFP or GFP-AtPIP2;1 displayed very slow FRAP kinetics, the recovery of fluorescence remained below 60% even at 30 min after photobleaching (Figure 1a). The FRAP kinetics were biphasic, however, with a fast process completed at 60 sec and a slower process that developed for up to 30 min and

beyond (Figures 1b,c and S2). The recovery values at these reference time points were in the range of 9–15% after 60 sec and 46–58% after 30 min (Figure 1b,c).

A kymographic analysis was performed to further discriminate between the kinetic behaviour of GFP-LTI6a, AtTIP1;1-GFP, AtPIP1;2-GFP and AtPIP2;1-GFP constructs (Figure 2a). In agreement with their fast recovery after photobleaching, GFP-LTI6a and AtTIP1;1-GFP showed a fast lateral diffusion. For GFP-LTI6a in particular, the recovery of fluorescence clearly occurred from the border of the bleached area to the centre. By contrast, the lateral diffusion of AtPIP-GFP constructs appeared to be much lower, as kymographs did not show any diffusion of the AtPIP-GFP signal from the border into the bleached area. Moreover, we did not observe any intense dots corresponding to endosomes crossing the ROI, suggesting that AtPIPs do not predominantly accumulate in such compartments. To evaluate further the possible contribution of lateral diffusion to the recovery of fluorescence of AtPIP-GFP, we compared in long-term FRAP the signals at the centre of the bleached areas with those either in the whole ROI or at the periphery (Figure 2b). It was assumed that the former should increase more slowly than the latter if fluorescence recovery was due to lateral diffusion of AtPIP-GFP constructs. The kinetic profiles were identical for these regions, suggesting that the lateral diffusion of AtPIP-GFP constructs does not contribute importantly to the recovery of the entire ROI.

An additional estimate of the contribution of lateral diffusion to signal recovery was made by means of photoactivation. Arabidopsis constitutively expressing photoactivatable GFP (paGFP; Patterson and Lippincott-Schwartz, 2002) fused either to LTI6a (paGFP-LTI6a; Martiniere *et al.*, 2011) or to AtPIP2;1 (AtPIP2;1-paGFP) were photoactivated and signal decreases were compared (Figure 2d,e). While the signal of paGFP-LTI6a exhibited a fast decrease, the AtPIP2;1-paGFP signal decreased much more slowly. Importantly, the signal was observed to spread from the photoactivated ROI in the case of paGFP-LTI6a (see $t = 120$ sec) but not of AtPIP2;1-paGFP (Figure 2e).

Altogether, the data show that lateral diffusion of AtPIP-GFP constructs in the PM of Arabidopsis root epidermal cells is negligible over 30 min of monitoring. Most importantly, the lateral diffusion of AtPIP-GFP constructs cannot be invoked to explain, over this period of time, the recovery of fluorescence after photobleaching.

Pharmacological and FRAP approaches combined to study AtPIP-GFP cycling

To explain the two-phase kinetics of AtPIP-GFP fluorescence recovery (see Figures 1b,c and S2), we suggest a model (Figure 3) whereby the fast mobility of cytoplasmic streaming, which carries endomembrane compartments labelled with AtPIP-GFP into focus within the bleached ROI, provokes

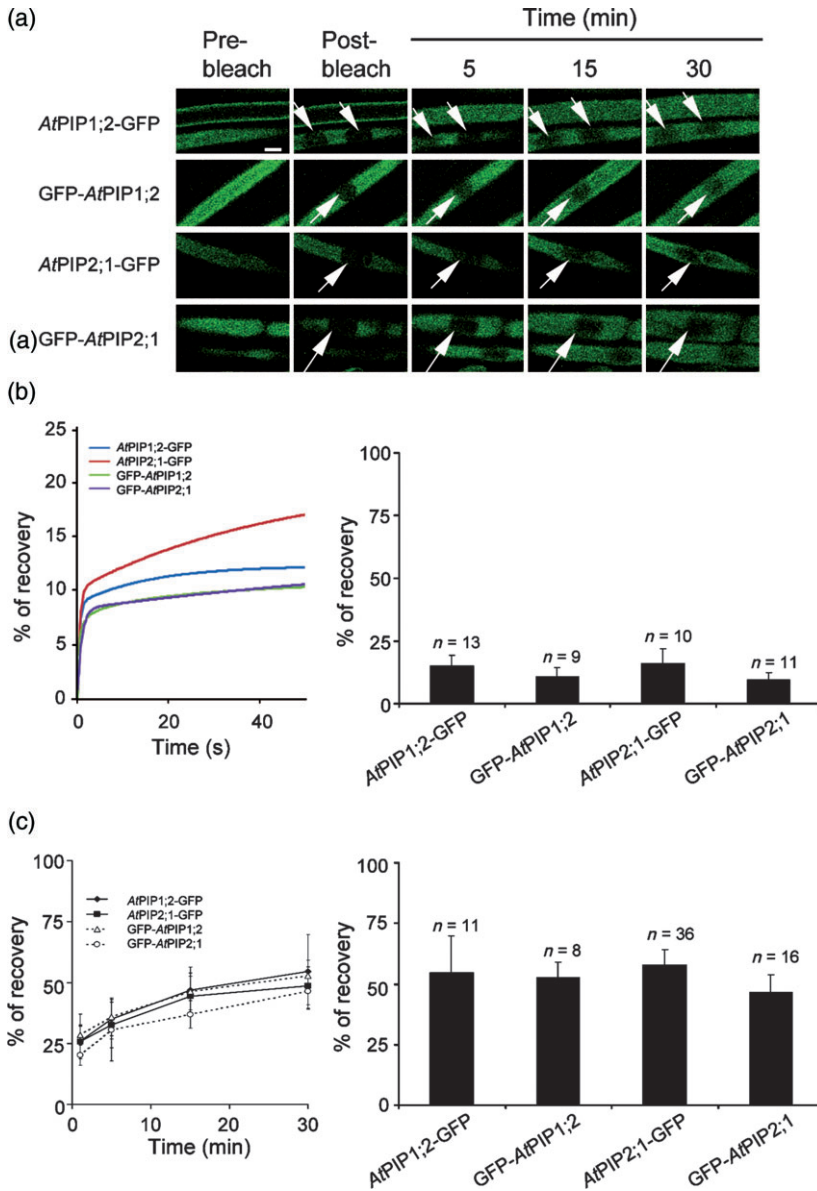


Figure 2. Non-significant contribution of the lateral diffusion to the recovery after photobleaching of AtPIPs fused to GFP.

(a) Comparative kymographic analysis by fluorescence recovery after photobleaching (FRAP) of the mobility of membrane proteins fused to GFP in either mock- or salt-treated epidermal root cells. Confocal images were collected at 246-ms intervals before and after photobleaching in localized areas ($\sim 10 \mu\text{m}$ in diameter). Pixel values along a line which goes through the photobleached region were taken over the whole time course of the experiment. Position along the line determines the horizontal axis, whereas time progresses downward. The time of photobleaching is indicated by the arrow (left). In the case of salt data, FRAP was monitored after a 30 min treatment in the presence of 100 mM NaCl.

(b) Comparative FRAP analysis of the fluorescence recovery of the whole surface of photobleached areas, each representing about 7700 pixels (Total), and of a selected area representing 350 pixels, at the centre (Center) or at the periphery (Periphery) of the photobleached areas. The graph shows analysis of FRAP recordings of a AtPIP2;1-GFP construct, as documented in Figure 1(c). Recovery values of the whole surface and of areas selected at the centre and at the periphery were compared for each time point and no significant differences ($P > 0.05$) were observed, based on Student's *t*-test. The inset shows a schematic representation of the total area, and of the areas at the centre or at the periphery.

(c) Same as in (b) except that the recordings were done in the presence of 100 mM NaCl added at time 0. Standard errors and the numbers of ROIs analysed (*n*) are shown.

(d), (e) Photoactivation of paGFP fused either to LTI6a (paGFP-LTI6a) or to AtPIP2;1 (AtPIP2;1-paGFP) and stably expressed under the 35S promoter in Arabidopsis root epidermal cells. In (d), a circular ROI of $7.4 \mu\text{m}$ in diameter was photoactivated. Pixel intensities in a $25 \times 25 \mu\text{m}$ square were obtained by means of the Surface plot 3D plugin of ImageJ software and monitored at the indicated time-frames in either mock or 100 mM NaCl conditions. The height indicates the intensity of the signal. For visual aspect, warm to cold false colours that vary from low to high intensity signal were superposed. In (e) we show plot profiles obtained using the plugin of ImageJ software and Gaussian fitting on images acquired in (d). The time-frames are indicated. Note that for AtPIP2;1-paGFP in salt-treated cells, signal was only recorded until 15 min, since it became indistinguishable from the noise at later times.

Figure 1. Fluorescence recovery after photobleaching (FRAP) of constructs with AtPIPs fused to GFP and stable expression in Arabidopsis root epidermal cells.

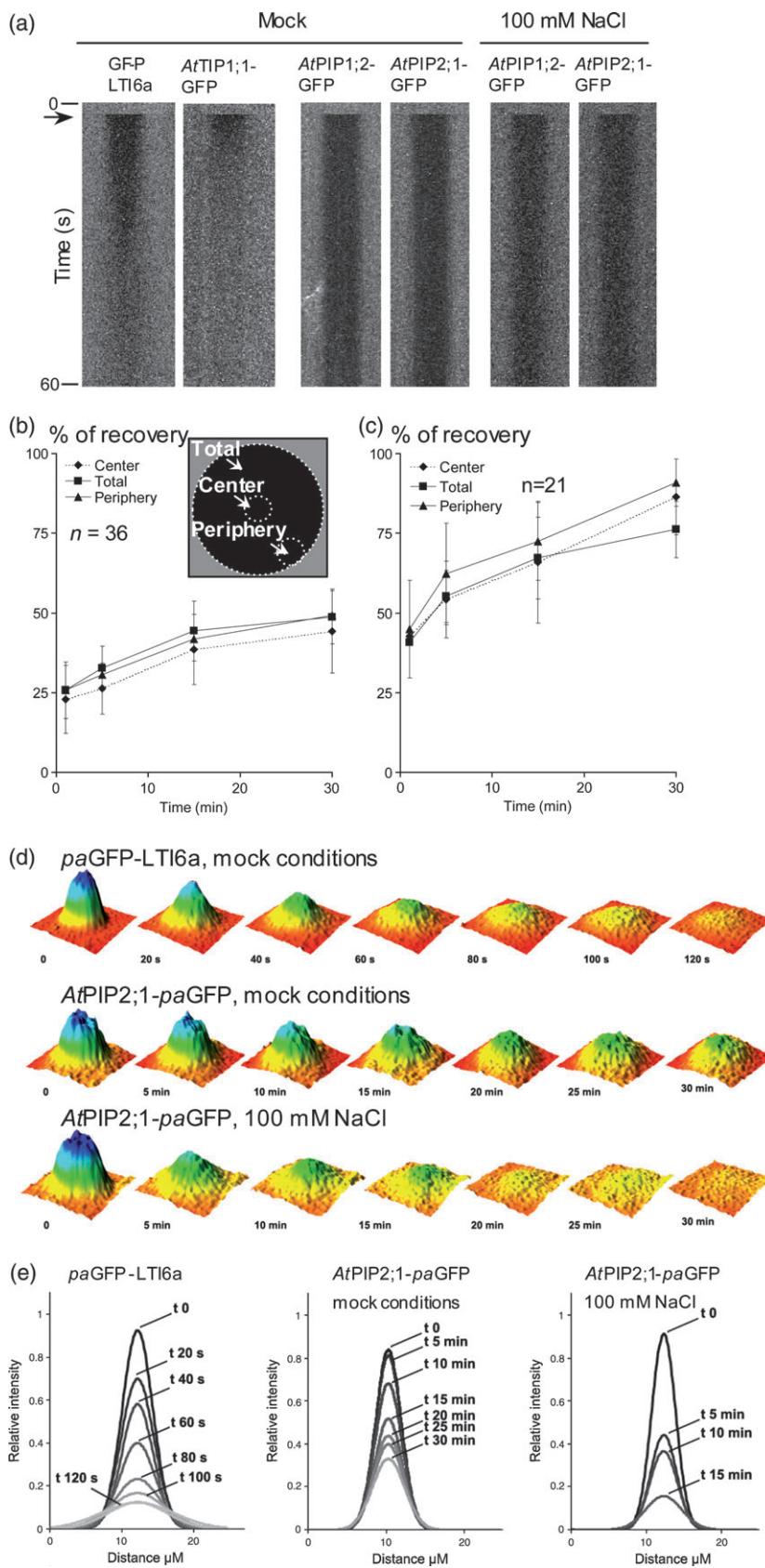
Stably transformed Arabidopsis plants expressing AtPIP1;2 or AtPIP2;1 fused with GFP at either the N- or C-terminal domain were observed by means of laser scanning confocal microscopy.

(a) The focus was set to obtain a tangential optical section of epidermal root cells and a region of interest (ROI) was photobleached (arrows). The first post-bleach image was obtained manually immediately after photobleaching and would therefore correspond to less than a minute after photobleaching. Time series of images taken before, immediately after, and 5, 15 and 30 min after photobleaching are presented.

(b) In the left part, the curves represent the best fits from a data set of 20 cells. In the right part, the values represent percentages of recovery at 60 sec after photobleaching of a ROI.

(c) In the left part, the curves represent recoveries after photobleaching monitored manually in time series for 30 min. In the right part, the values represent percentage of recovery at 30 min after photobleaching.

Standard errors and the numbers of ROIs analysed (*n*) are shown. Bar = $10 \mu\text{m}$.



an apparent fast but limited recovery at early stages. The slower recovery observed for the next 30 min would be mainly due to the recycling of AtPIP-GFP constructs from endosomal compartments to the PM. Once at the PM, AtPIP-GFP is relatively fixed in place with very little lateral diffusion potential, but is still endocytosed. As a consequence, the amplitude of the early recovery phase reports on the labelling intensity of endomembrane compartments. The slow recovery phase reports on the cycling of AtPIP-GFP constructs including sequential steps in endocytosis, sorting in the endosomal compartments and exocytosis. Anterograde secretory process may also contribute to the recovery. This tentative model was first investigated using a pharmacological dissection of FRAP responses.

Animal cells exhibit various uptake mechanisms for surface proteins, such as clathrin-dependent endocytosis, caveolae-mediated endocytosis, pinocytosis and phagocytosis. In plant cells, the existence of related mechanisms was unclear until genetic approaches established that clathrin is required for internalisation of PIN1, PIN2 and AtPIP2;1 (Dhonukshe *et al.*, 2007; Tahara *et al.*, 2007; Kitakura *et al.*, 2011). Further evidence that similar uptake mechanisms exist in plant cells comes from pharmacological interference using A23. One of the potential effects of A23 in mammalian cells is to prevent interaction between the μ 2 subunit of the clathrin-binding adaptor protein (AP)-2 complex and cytosolic motifs of cargo PM proteins (Banbury *et al.*, 2003). Tyrosine-based YXX Φ motifs (where Y is Tyr, X is any amino acid and Φ is an amino acid with a bulky hydrophobic side chain) mediate recruitment into clathrin-coated vesicles by binding to the μ 2-subunit of the AP complex and have been identified in both animal and plant proteins (Happel *et al.*, 2004; Ron and Avni, 2004; daSilva *et al.*, 2006; Takano *et al.*, 2010). Although A23 side-effects could not be excluded (see Robinson *et al.*, 2008), evidence that A23 inhibition allows one to dissect membrane trafficking processes in plants has been provided by several laboratories (Ortiz-Zapater *et al.*, 2006; Dhonukshe *et al.*, 2007; Konopka *et al.*, 2008; Leborgne-Castel *et al.*, 2008; Fujimoto *et al.*, 2010). The synthetic auxin analogue naphthalene-1-acetic acid (NAA) has been shown to inhibit endocytosis of PIN, AtPIP2;1 and PM H⁺-ATPase (Paciorek *et al.*, 2005; Pan *et al.*, 2009). A role of membrane sterols in the endocytosis of PIN proteins and other PM markers such as AtPIP2;1 has also been described (Kleine-Vehn *et al.*, 2006; Men *et al.*, 2008; Pan *et al.*, 2009).

Here, the endocytosis of AtPIP-GFP was targeted using either A23 or NAA (Paciorek *et al.*, 2005; Dhonukshe *et al.*, 2007). Exocytosis was probed using BFA, which inhibits functioning of ARF-GEF and provokes, among other effects, an aggregation of endosomal vesicles including the trans-Golgi network (TGN) (collectively known as BFA compartments) (Geldner *et al.*, 2001; Grebe *et al.*, 2003; Dettmer

et al., 2006; Robinson *et al.*, 2008; Naramoto *et al.*, 2010; Viotti *et al.*, 2010).

When treated with BFA, AtPIP1;2-GFP and AtPIP2;1-GFP constructs labelled intracellular structures typical of BFA compartments (Figure 4, Table 1). This indicates that although not resident in the TGN compartment, the AtPIP-GFP constructs traffic through it, in agreement with previous studies (Paciorek *et al.*, 2005; Kleine-Vehn *et al.*, 2006; Dhonukshe *et al.*, 2007; Pan *et al.*, 2009). Co-treatment with BFA and either A23 or NAA provoked a marked reduction of the labelling of these structures. These data extend previous observations (Paciorek *et al.*, 2005; Dhonukshe *et al.*, 2007) and indicate that, under our experimental conditions, AtPIP-GFP constructs undergo active endocytosis and cycling between the plasma membrane and the endosomes.

Next, we performed FRAP experiments on roots which had been pretreated with various drugs for 30 min. AtPIP-GFP constructs exhibited significantly reduced short-term recovery ($t = 60$ sec) when roots were treated with A23 (AtPIP1;2-GFP, $P = 0.025$; AtPIP2;1-GFP, $P < 0.01$; Figure 5a). At 30 min after photobleaching, the recovery of fluorescence was also reduced significantly compared with the control situation (Figures 5b and S3). Thus, A23 alters the internalization of AtPIP1;2 and AtPIP2;1, and consequently impairs their recycling to the PM.

When roots were pretreated with NAA, we did not observe any significant reduction in fluorescence recovery at 60 sec after photobleaching for either construct (Figure 5a). Thus, NAA does not reduce the labelling of endosomal compartments. By contrast, recovery of fluorescence at 30 min after photobleaching was found to be lower compared with control conditions, suggesting that, in a longer time frame, AtPIP1;2-GFP and AtPIP2;1-GFP did not recycle properly from endosomal compartments to the PM (Figures 5b and S3). Because NAA prevented the labelling of BFA compartments by the AtPIP-GFP constructs (Figure 4) (Paciorek *et al.*, 2005; Pan *et al.*, 2009; Robert *et al.*, 2010), the data suggest that NAA alters their cycling downstream of endocytosis and upstream of the TGN.

Treatment with BFA did not significantly alter the fluorescence recovery at 60 sec for AtPIP1;2-GFP and AtPIP2;1-GFP (Figure 5a). This indicates that the BFA-induced aggregation of endosomal vesicles and TGN labelled by AtPIP-GFP occurs simultaneously with continuous AtPIP-GFP endocytosis, thereby maintaining a significant level of intracellular labelling. This also indicates that BFA does not inhibit endocytosis of AtPIP-GFP, providing an indication that BFA truly interferes with trafficking of PM proteins downstream of endocytosis. GNOM-LIKE1 (GNL1), a BFA-resistant ARF-GEF, has no function in recycling from endosomes, and has been shown to act selectively in the endocytosis of PIN2 (Teh and Moore, 2007). Further investigations are needed to examine whether GNL1 is involved in the cycling of AtPIP-GFP. Finally, we noticed that a BFA

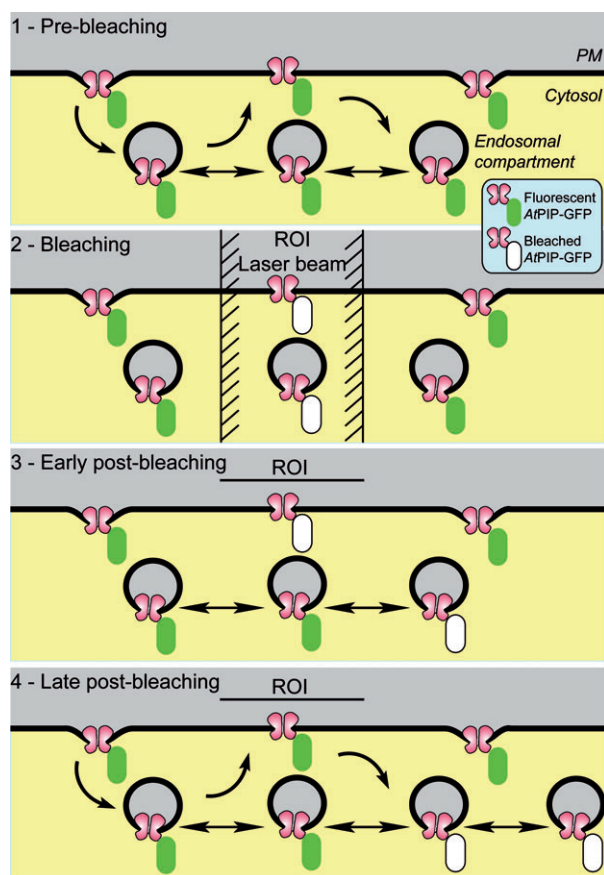


Figure 3. Model to explain fluorescence recovery after photobleaching (FRAP) experiments with AtPIP-GFP constructs.

The schemes represent a cross section in the vicinity of the plasma membrane (PM) of the epidermal root cell. The experiments in the present paper relate to tangential optical sections about 1 μm thick. Yet, due to the space that it occupies, the vacuole pushes the cell cytoplasm against the PM and reduces its thickness to about 200 nm. Thus, the tangential optical sections collect the signal from compartments between the PM and the tonoplast, including the intracellular compartments. Upon strong initial illumination, the fluorophores present in the PM and in the endosomal compartment in the ROI are photobleached. Next, at the early post-bleach stage, the endosomal compartment rapidly comes to homogeneity through intense cytoplasmic streaming (two-headed arrows). Thus, in the early stages, the fluorescent signal in the region of interest (ROI) comes mainly from intracellular (endosomal) compartments. Next, recycling of AtPIP-GFP from endosomal compartments to the PM allows the signal to recover in the PM. Thus, in the latter step, the fluorescent signal captured in the ROI comes from both the intracellular compartment and the PM. Note that lateral diffusion of AtPIP-GFP constructs in the PM does not significantly contribute to recovery of the fluorescent signal in the ROI.

pretreatment reduced significantly the amount of fluorescence recovery of AtPIP1;2-GFP and AtPIP2;1-GFP at 30 min (Figures 5b and S3). In accordance with our model (Figure 3), BFA inhibits the cycling of AtPIP-GFP and, more specifically, the exocytosis step, preventing the long-term recovery of fluorescence at the PM. The overall data validate the use of FRAP for exploring the mode of PIP aquaporin cycling.

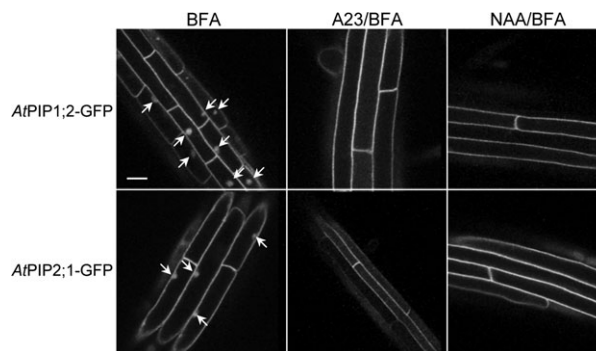


Figure 4. Pharmacological disruption of AtPIP-GFP constitutive cycling in root epidermal cells.

The confocal images show the effects on the subcellular localization of the AtPIP1;2-GFP or the AtPIP2;1-GFP construct of brefeldin A (BFA) on its own or in combination with either tyrphostin A23 (A23) or naphthalene-1-acetic acid (NAA). Prior to observation, roots were incubated for 30 min in $\frac{1}{2}$ MS medium supplemented with 50 μM BFA alone or in combination with 30 μM A23 or 5 μM NAA. Arrows indicate intracellular aggregates containing AtPIP-GFP and tentatively identified as BFA compartments. Bar = 20 μm .

Table 1 Effects of drug treatments on brefeldin A (BFA) compartment labelling by AtPIP-GFP

| | AtPIP1;2-GFP | | | | AtPIP2;1-GFP | | | |
|------|--------------|----------|------|----------|--------------|----------|------|----------|
| | -BFA | | +BFA | | -BFA | | +BFA | |
| | % | <i>n</i> | % | <i>n</i> | % | <i>n</i> | % | <i>n</i> |
| Mock | 0 | 28 | 84 | 32 | 0 | 27 | 83 | 25 |
| A23 | 0 | 28 | 4 | 19 | 0 | 27 | 0 | 20 |
| NAA | 0 | 32 | 5 | 22 | 0 | 22 | 8 | 22 |

A23, tyrphostin A23; NAA, naphthalene-1-acetic acid.

Values indicate the percentages of cells labelled with at least one BFA compartment. The conditions of treatment were as indicated in Figure 4. The number of cells analysed (*n*) are indicated.

Enhanced cycling of AtPIP-GFP constructs upon salt stress

A stimulation of vesicle trafficking, as monitored using FM1-43 labelling, was previously reported in *Arabidopsis* roots under salt stress (Leshem *et al.*, 2007). Here, we obtained similar observations ourselves using FM4-64 (Figure S4). These results suggested that a salt treatment (100 mM NaCl) may also impact on the trafficking of AtPIP-GFP constructs.

These putative effects were investigated by means of FRAP. In a first series of experiments, the stress and photobleaching treatments were applied at the same initial time. Quantification of the recovery after photobleaching at 30 min for AtPIP1;2-GFP and AtPIP2;1-GFP constructs indicated values of 82 and 76%, respectively (Figure 6a,b). Thus, the late recovery of fluorescence under salt stress was high, corresponding to an increase of 1.3–1.5 times compared with the values for control mock treatments. These

findings led us to evaluate in close detail the lateral diffusion of AtPIP-GFP constructs under salt stress conditions. Kymographic analysis showed that fluorescence recovery was uniformly distributed within the ROI (Figure 2a, right panels). More precisely, there was no difference between values of recovery estimated on the whole surface of the photobleached ROI or on selected areas at its centre or its periphery (Figure 2c). Finally, photoactivation experiments did not reveal any spreading of the AtPIP2;1-paGFP signal over the photoactivated ROI (Figure 2d,e). This series of experiments strongly suggests that the lateral diffusion of AtPIP-GFP constructs in salt stress conditions is similar to mock conditions, and negligible over 30 min of monitoring.

We therefore hypothesized that the faster kinetics of recovery may reflect an enhanced cycling of the AtPIP-GFP constructs. To check whether salt increases the intracellular accumulation of AtPIP-GFP constructs, we performed FRAP analysis after 30 min of a salt treatment and monitored the values of recovery at 60 sec. By comparison with the control, a slight but not significant increase was observed under salt conditions (Figure 6c). These results suggest that the overall endosomal labelling is not increased, but the rates of AtPIP-GFP cycling (endocytosis and exocytosis) were simultaneously increased, leading to a faster targeting to the PM. In addition, when roots of transgenic plants expressing LTI6a, AtPIP1;2 or AtPIP2;1 fused to GFP were treated by 100 mM NaCl for 45 min, confocal microscopy imaging revealed that the PM localization of these markers was not altered (Boursiac *et al.*, 2005). These latter observations do not

demonstrate an accumulation of PM proteins in intracellular compartments during the early response of root cells to salt. Collectively, the data suggest that salt treatment enhances the rate of AtPIP-GFP cycling.

To possibly corroborate these ideas, we investigated the effect of a salt treatment on BFA compartment labelling by AtPIP1;2-GFP and AtPIP2;1-GFP constructs. In a first set of experiments, roots were incubated in a salt or a standard solution (half-strength Murashige and Skoog; ½ MS) supplemented with BFA, and BFA compartment labelling was monitored as a function of time. The BFA compartments were observed in almost every epidermal cell of the control and salt-treated roots, although they appeared much earlier in the latter situation (Figure 7a). For instance, after 20 min, the percentage of labelling of AtPIP2;1-GFP was three times as high with the salt solution as with ½ MS. Moreover, AtPIP1;2-GFP labelling appeared as early as 10 min, only in salt-treated roots. The results indicate that salt treatment stimulated the accumulation of AtPIP1;2-GFP and AtPIP2;1-GFP constructs in BFA compartments. Because the molecular targets of BFA in salt treatment conditions are not known, the results obtained here have to be interpreted with caution, and we propose that salt treatment enhanced the endocytosis of AtPIPs.

Next, we tested the effect of a removal of BFA on BFA compartment labelling. After 30 min of BFA treatment in ½ MS, followed by extensive washings in either ½ MS or a salt solution (100 mM NaCl), we monitored the labelling of root epidermal cells by AtPIP1;2-GFP and AtPIP2;1-GFP con-

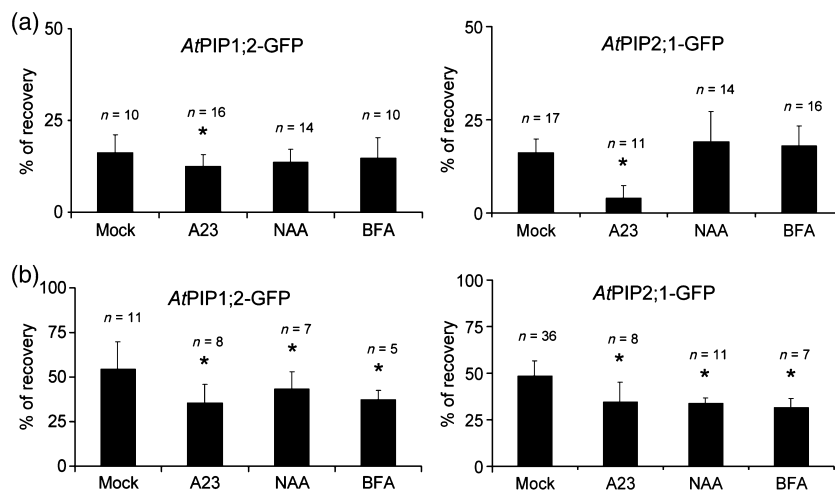


Figure 5. Effects of drug pretreatments on the recovery after photobleaching of AtPIP-GFP constructs.

Roots expressing either AtPIP1;2-GFP or AtPIP2;1-GFP were pretreated for 30 min with the indicated drugs at the same concentrations as in Figure 4 and then photobleached. Recovery of fluorescence was monitored in the continuous presence of the indicated drugs.

(a) Percentage of recovery at 60 sec after photobleaching.

(b) Percentage of recovery at 30 min after photobleaching. The values were obtained by analysing images acquired manually.

In the case of brefeldin A (BFA), fluorescence recovery after photobleaching (FRAP) analysis excluded the few regions of interest (ROIs) that exhibited a BFA compartment.

The graphs show mean values with standard errors and the number of ROIs analysed (*n*). Asterisks indicate significant differences between mock and drug treatments (Student's *t*-test, *P* < 0.05).

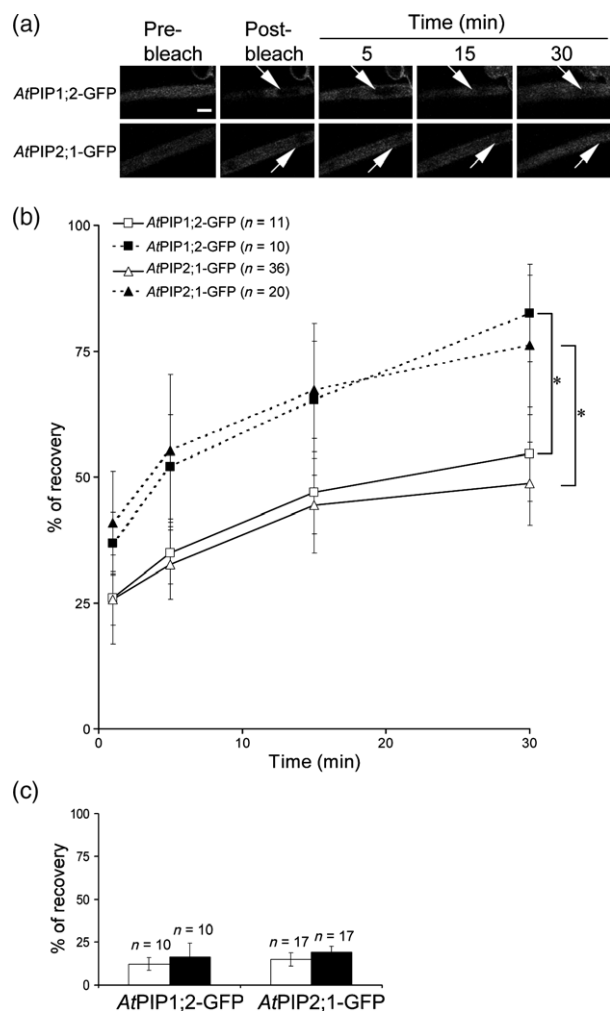


Figure 6. Fluorescence recovery after photobleaching (FRAP) of AtPIP-GFP constructs upon 100 mM NaCl treatment.

(a) Roots were immersed in a salt solution between a microscope slide and cover slip. Fluorescent images were recorded prior to, immediately following, and at 5, 15 and 30 min after photobleaching (arrows).

(b) Roots were immersed in a salt solution as described in (a) and then immediately photobleached. The recoveries after photobleaching were monitored in time series for 30 min with cells expressing AtPIP-GFP constructs in mock (open symbols) and salt (closed symbols) treatments.

(c) Roots were pretreated in a salt solution for 30 min and then subjected to FRAP analysis. The values represent percentages of recovery at 60 sec after photobleaching in mock (open bars) and salt (closed bars) treatment conditions.

The graphs show mean values with standard errors and the numbers of regions of interest analysed (*n*). Asterisks indicate significant differences between mock and drug treatments (Student's *t*-test, $P < 0.05$). Bar = 10 μm .

structures. Although a wash-out provoked the disappearance of the BFA compartment labelling in all root materials and conditions, the process was faster when a salt solution was applied (Figure 7b). For instance, the percentage of labelling by AtPIP2;1-GFP was reduced to 10% at 120 min after wash-out with $\frac{1}{2}$ MS, whereas 90 min were sufficient under salt-treated conditions to get the same order of reduction. These

results suggest that salt treatment also enhanced the exocytosis of AtPIPs.

Collectively, these results indicate that salt stress interferes with vesicle trafficking and probably enhances both the endocytosis and exocytosis of AtPIPs.

We also note that the proteinaceous defence elicitor cryptogein stimulated FM4-64 endocytosis and increased the number of clathrin-coated pits in BY-2 tobacco cells (Leborgne-Castel *et al.*, 2008). Thus, endocytosis regulation occurs early in plant cells under challenging biotic or abiotic environmental conditions (reviewed by Leborgne-Castel and Luu, 2009).

Combination of pharmacological and FRAP approaches to study AtPIP-GFP cycling in salt stress conditions

To get a better understanding of the increase in PM aquaporin cycling under salt stress, roots of plants expressing AtPIP1;2-GFP or AtPIP2;1-GFP were treated first with a solution containing a drug for 30 min, and then challenged with the same solution but supplemented with 100 mM NaCl. In the following 30 min FRAP was monitored with roots bathing in the latter solution. Using this procedure, we can consistently compare the effects of a drug in the absence and in the presence of a salt treatment.

Under salt stress conditions, no significant difference in fluorescence recovery, whether at 60 sec or 30 min, was observed between roots with and without A23, suggesting, in contrast to the control conditions, that the endocytosis of AtPIP-GFP constructs was not inhibited by A23 (Figures 8 and S5). Thus, an endocytic mechanism, which is insensitive to A23, specifically operates in salt stress conditions. We cannot exclude that enhanced endocytosis (with more clathrin pits) could overcome the effect of this drug. Higher drug concentrations might be used, but would probably impair the vitality of the cells (see Robinson *et al.*, 2008).

Root cells expressing AtPIP-GFP constructs pretreated by NAA and challenged in salt for 30 min exhibited values of fluorescence recovery at 60 sec not significantly different compared with controls without NAA (Figure 8a). This suggests that NAA does not alter the endocytosis of AtPIP-GFP under salt stress. Yet, the fluorescence recovery at 30 min was significantly reduced by NAA (Figures 8b and S5). One possible explanation for this result is that, under salt stress and similar to standard conditions, NAA alters the cycling of AtPIP-GFP constructs in a step downstream of endocytosis and upstream of the TGN compartment.

In roots expressing AtPIP2;1-GFP and exposed to salt, pretreatment by BFA did not change fluorescence recovery at 60 sec, suggesting that, similar to standard conditions, intracellular accumulation of the fusion proteins was insensitive to BFA (Figure 8a). Yet, the recovery of fluorescence at 30 min after photobleaching (Figures 8b and S5) was markedly reduced, indicating that the sup-

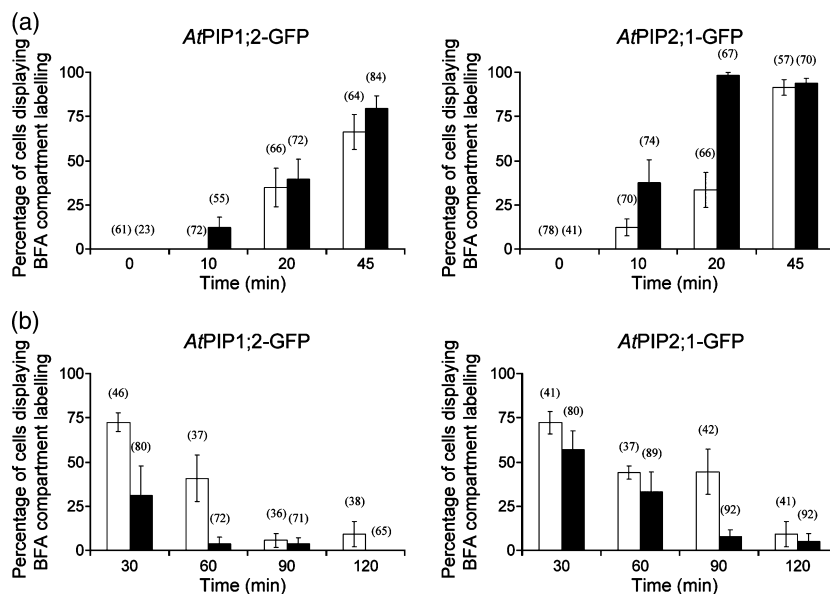


Figure 7. Effect of a 100 mM NaCl treatment on the dynamics of labelling the brefeldin A (BFA) compartment by AtPIP-GFP constructs.

(a) Roots were incubated, from time 0, in a 1/2 MS (open bars) or a 100 mM NaCl (closed bars) medium supplemented with BFA and the percentage of cells with at least one labelled BFA compartment was counted by microscopy after the indicated time.

(b) Roots were treated with BFA in 1/2 MS for 30 min, washed out with a 1/2 MS (open bars) or a 100 mM NaCl (closed bars) medium for the indicated time, and the percentage of cells displaying BFA compartment labelling was counted as above.

Results for AtPIP1;2-GFP and AtPIP2;1-GFP constructs are presented in the left and right parts, respectively. The number of cells counted for each assay is indicated in parentheses.

posedly intense recycling from endosomal and TGN compartments to the PM was strongly impaired. By contrast, root cells expressing AtPIP1;2-GFP did not show, under salt stress, any significant inhibition by BFA of fluorescence recovery at 30 min even though AtPIP1;2-GFP labelled BFA compartments. These last results indicate that, under salt treatment, BFA exerted only a partial inhibition of AtPIP1;2-GFP recycling to the PM. This property slightly influences the interpretation of BFA compartment labelling kinetics (Figure 7), but further supports the idea of salt-enhanced AtPIP1;2-GFP endocytosis.

Direct measurement of endocytosis using labelled receptor ligands has proved difficult to develop in plant cells. Here, we present an alternative and simple technique based on FRAP to estimate the intracellular labelling and the cycling parameters of two prototypical PM proteins. In root cells in particular, it may help to uncover differences in the cycling path of other PM proteins. We also believe that this method can easily be extended to other plant and animal systems.

Our data provide general insights into the turnover mechanism of plant PM aquaporins (Figure 9). Most importantly, our data indicate that salt treatment enhances the cycling of PIP aquaporins by stimulating an A23-insensitive endocytosis. All subsequent steps, including an auxin-sensitive transfer into early endosome/TGN, and BFA-sensitive exocytosis were also stimulated under salt stress.

Several details of this mechanism are still to be uncovered. For instance, salt treatment induces a rapid decrease in root hydraulic conductivity (Boursiac *et al.*, 2005). We wonder about the early molecular mechanisms involved. Since our data do not support the hypothesis of a massive internalisation of PIPs, we would rather invoke an inactivation of their intrinsic activity (gating), possibly linked to their enhanced cycling. The activity of aquaporins is dependent on their phosphorylation status and various cell parameters including cytosolic proton and calcium concentration (Maurel *et al.*, 2008). The next step would be to determine the molecular basis of this enhanced salt-induced cycling. In mammalian cells, early endosomes comprise two distinct populations: a dynamic population that is highly mobile on microtubules and matures rapidly towards late endosomes and a static population that matures much more slowly (Lakadamyali *et al.*, 2006). The dynamic population was found to be linked to an AP-2-independent endocytic machinery and transports cargoes such as low-density lipoprotein receptors. Our data suggest that a similar pathway may be activated in plant cells under salt stress.

EXPERIMENTAL PROCEDURES

Plant materials and growth conditions

All plants used in this work are *Arabidopsis thaliana* L. (Heyn.) accession Columbia 0. Plants were grown *in vitro*, vertically on 1/2

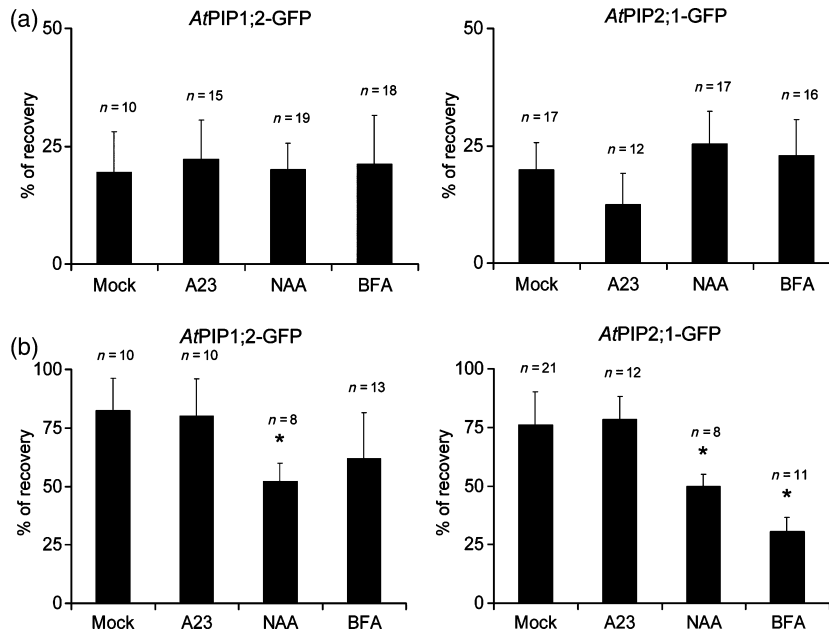


Figure 8. Effect of drug pretreatments on the recovery after photobleaching of AtPIP-GFP constructs under salt stress conditions. Roots expressing either AtPIP1;2-GFP or AtPIP2;1-GFP were pretreated for 30 min in solutions of ½ MS medium supplemented with the indicated drugs at the same concentrations as in Figure 4. Then, the pretreated roots were transferred in the same solution but supplemented with 100 mM NaCl. (a) Roots pretreated with drug were transferred in the same solutions but supplemented with 100 mM NaCl, and the salt challenge was maintained for 30 min. Then, root cells were photobleached and the recoveries of fluorescence at 60 sec after photobleaching were monitored. (b) After drug pretreatments, roots were transferred in the same solutions but supplemented with 100 mM NaCl and immediately photobleached. The recoveries of fluorescence were recorded at 30 min after photobleaching. The values were obtained by analysing images acquired manually. In the case of BFA, fluorescence recovery after photobleaching (FRAP) analysis excluded the few regions of interest (ROIs) that exhibited a BFA compartment. The graphs show mean values with standard errors and the numbers of ROIs analysed (n). Asterisks indicate significant differences between mock and drug treatments (Student's t-test, $P < 0.05$).

MS medium supplemented with sucrose (10 g l^{-1}) and agar (7 g l^{-1}) (Murashige and Skoog, 1962), in a growth chamber with cycles of 16 h light ($\sim 150 \mu\text{E m}^{-2} \text{ sec}^{-1}$) and 8 h dark at 21°C. Transgenic plants used in this study are described elsewhere (Boursiac *et al.*,

2005, 2008). paGFP-LTI6a (Martiniere *et al.*, 2011) and AtPIP2;1-paGFP constructs were expressed under the control of a cauliflower mosaic virus 35S promoter.

Drug treatments

The BFA, A23, NAA and cycloheximide (CHX) were all from Sigma (<http://www.sigmaaldrich.com/>). The BFA and A23 were from 50 and 30 mM dimethylsulphoxide stock solutions, respectively. The NAA and cycloheximide were from 5 and 200 mM ethanol stock solutions, respectively. Drugs were added to the liquid ½ MS medium (agar free) for the indicated times at final concentrations of 50 μM BFA, 30 μM A23, 5 μM NAA or 50 μM CHX. The CHX was added to solutions to prevent protein biosynthesis.

Microscopy

Observations were performed on epidermal cells of the primary root (at about 1 cm from the apex) of transgenic seedlings cultivated

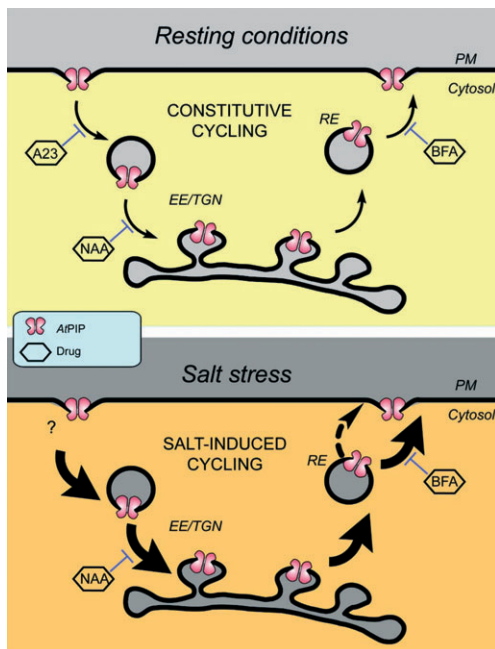


Figure 9. Subcellular trafficking mechanisms controlling AtPIP cycling in resting and salt stress conditions.

(a) In resting conditions, AtPIPs constitutively cycle between the plasma membrane (PM) and the endosomal compartments [early endosome (EE)/trans-Golgi network (TGN)]. The endocytosis is sensitive to tyrphostin A23 (A23). Trafficking of AtPIPs within the EE/TGN compartments is sensitive to naphthalene-1-acetic acid (NAA). Brefeldin A (BFA) prevents the cycling of AtPIPs by inhibiting a trafficking process downstream their exit out of the TGN.

(b) Under salt stress, the rate of AtPIP cycling is increased compared with the resting conditions. The endocytosis is insensitive to A23. AtPIP1;2 exocytosis is partially insensitive to BFA (dashed arrow). RE, recycling endosome.

for 9–12 days. For each condition or treatment, 5–36 cells were analysed from at least four different seedlings. Images were captured with an inverted confocal laser-scanning microscope (Inverse 1 Axiovert 200M Zeiss/LSM 510 META confocal, <http://www.zeiss.com/>). The argon laser excitation wavelength was 488 nm; GFP emission was detected with the filter set for fluorescein isothiocyanate (bandpass 500–530 nm).

A 63× objective (1.4 NA) was used at a digital zoom setting of five. Pre-bleaching and post-bleaching imaging was done using a 488 nm beam set at 50% output and 1% transmission. Ten scan images were made to establish the pre-bleach intensity and then a circular ROI of 25 μm^2 in a cortical optical section of the fluorescent plasma membrane was bleached. Five scans of the ROI at 100% transmission were used for bleaching. Recovery of fluorescence was recorded for up to 30 min. Images were collected at 128 pixels² with a scan speed of 0.246 sec/frame. We checked that the energy of the 488 nm laser used to record post-bleach data was low enough to have no bleaching effect by recording unbleached ROIs. For analysis of the FRAP the data were normalised using the equation

$$I_n = [(I_t - I_{\min}) / (I_{\max} - I_{\min})] \times 100$$

where I_n is the normalised intensity, I_t is the intensity at any time t , I_{\min} is the minimum post-photobleaching intensity and I_{\max} is the maximum pre-photobleaching intensity. Nonlinear regression was used to model the normalised FRAP data. In this case, a two-phase exponential association equation was used:

$$Y(t) = A + B[1 + \exp(-K_1t)] + C[1 - \exp(-K_2t)]$$

where $Y(t)$ is normalised intensity, A , B , C , K_1 and K_2 are parameters of the curve, and t is time. Then, the value of Y was calculated at 60 sec and used as an approximate of the relative mobile fraction.

The recovery of fluorescence was quantified by means of ImageJ software (Rasband W.S., NIH, <http://imagej.nih.gov/ij/>) which allows the measurement of the mean grey value within a ROI; GraphPad software (GraphPad Software Inc., <http://www.graphpad.com/>) was used for curve fitting.

For photoactivation experiments, circles of radius 3.7 μm were photoactivated with one iteration of a 405 nm laser diode set at 100%. Then, we recorded over time the decrease of fluorescence with 14% of a 488 nm argon laser and the emission was detected with a filter BP of 500–530 nm. For each time series, pixel intensities were measured along the diameter of the ROI with ImageJ. The first frame after photoactivation was used to normalise the data set. Gaussian curves were fit on the data with GraphPad software and plotted on a graph. At least five cells from five plantlets were tested for each treatment.

ACKNOWLEDGEMENTS

JR and AM are funded by the UK Biotechnology and Biological Sciences Research Council (BB/F01407/1) and MS received a doctoral fellowship from the French Ministry of Research. We thank Angélique Adivèze for assistance in Arabidopsis transformations and staff members of the Institut de Biologie Intégrative des Plantes for technical assistance in biological material culture. Confocal observations were made at the Montpellier RIO imaging facility.

SUPPORTING INFORMATION

The following supplementary material is available for this article online:

Figure S1. Fast recovery after photobleaching of GFP-LTI6a, soluble GFP, and AtPIP1;1 fused to GFP.

Figure S2. Comparison between fluorescence recovery after photobleaching (FRAP) experiments with AtPIPs fused to GFP combinations and other markers.

Figure S3. Kinetics of recovery after photobleaching of AtPIP-GFP constructs upon drug pretreatment.

Figure S4. Quantification of relative FM4-64 uptake in mock- and salt-treated root epidermal cells.

Figure S5. Effects of drug pretreatments on the kinetics of recovery after photobleaching of AtPIP-GFP constructs under salt stress conditions.

Please note: As a service to our authors and readers, this journal provides supporting information supplied by the authors. Such materials are peer-reviewed and may be re-organized for online delivery, but are not copy-edited or typeset. Technical support issues arising from supporting information (other than missing files) should be addressed to the authors.

REFERENCES

- Bahaji, A., Aniento, F. and Cornejo, M.J. (2003) Uptake of an endocytic marker by rice cells: variations related to osmotic and saline stress. *Plant Cell Physiol.* **44**, 1100–1111.
- Banbury, D.N., Oakley, J.D., Sessions, R.B. and Banting, G. (2003) Tyrothostin A23 inhibits internalization of the transferrin receptor by perturbing the interaction between tyrosine motifs and the medium chain subunit of the AP-2 adaptor complex. *J. Biol. Chem.* **278**, 12022–12028.
- Boursiac, Y., Chen, S., Luu, D.T., Sorieul, M., van den Dries, N. and Maurel, C. (2005) Early effects of salinity on water transport in Arabidopsis roots. Molecular and cellular features of aquaporin expression. *Plant Physiol.* **139**, 790–805.
- Boursiac, Y., Boudet, J., Postaire, O., Luu, D.T., Tournaire-Roux, C. and Maurel, C. (2008) Stimulus-induced downregulation of root water transport involves reactive oxygen species-activated cell signalling and plasma membrane intrinsic protein internalization. *Plant J.* **56**, 207–218.
- Cutler, S., Ehrhardt, D., Griffitts, J. and Somerville, C. (2000) Random GFP::cDNA fusions enable visualisation of subcellular structures in cells of Arabidopsis at a high frequency. *Proc. Natl Acad. Sci. USA*, **97**, 3718–3723.
- Dettmer, J., Hong-Hermesdorf, A., Stierhof, Y.D. and Schumacher, K. (2006) Vacuolar H⁺-ATPase activity is required for endocytic and secretory trafficking in Arabidopsis. *Plant Cell*, **18**, 715–730.
- Dhonukshe, P., Aniento, F., Hwang, L., Robinson, D.G., Mravec, J., Stierhof, Y.D. and Friml, J. (2007) Clathrin-mediated constitutive endocytosis of PIN auxin efflux carriers in Arabidopsis. *Curr. Biol.* **17**, 520–527.
- Fujimoto, M., Arimura, S.-i., Ueda, T., Takanashi, H., Hayashi, Y., Nakano, A. and Tsutsumi, N. (2010) Arabidopsis dynamin-related proteins DRP2B and DRP1A participate together in clathrin-coated vesicle formation during endocytosis. *Proc. Natl Acad. Sci. USA*, **107**, 6094–6099.
- Geldner, N., Friml, J., Stierhof, Y.-D., Jurgens, G. and Palme, K. (2001) Auxin transport inhibitors block PIN1 cycling and vesicle trafficking. *Nature*, **413**, 425–428.
- Geldner, N., Anders, N., Wolters, H., Keicher, J., Kornberger, W., Müller, P., Delbarre, A., Ueda, T., Nakano, A. and Jurgens, G. (2003) The Arabidopsis GNOM ARF-GEF mediates endosomal recycling, auxin transport, and auxin-dependent plant growth. *Cell*, **112**, 219–230.
- Grebe, M., Xu, J., Mobius, W., Ueda, T., Nakano, A., Geuze, H.J., Rook, M.B. and Scheres, B. (2003) Arabidopsis sterol endocytosis involves actin-mediated trafficking via ARA6-positive early endosomes. *Curr. Biol.* **13**, 1378–1387.
- Happel, N., Honing, S., Neuhaus, J.M., Paris, N., Robinson, D.G. and Holstein, S.E. (2004) Arabidopsis mu A-adaptin interacts with the tyrosine motif of the vacuolar sorting receptor VSR-PS1. *Plant J.* **37**, 678–693.
- Kitakura, S., Vanneste, S., Robert, S., Lofke, C., Teichmann, T., Tanaka, H. and Friml, J. (2011) Clathrin mediates endocytosis and polar distribution of PIN auxin transporters in Arabidopsis. *Plant Cell*, **23**, 1920–1931.
- Kleine-Vehn, J., Dhonukshe, P., Swarup, R., Bennett, M. and Friml, J. (2006) Subcellular trafficking of the Arabidopsis auxin influx carrier AUX1 uses a novel pathway distinct from PIN1. *Plant Cell*, **18**, 3171–3181.
- Konopka, C.A., Backues, S.K. and Bednarek, S.Y. (2008) dynamics of Arabidopsis dynamin-related protein 1C and a clathrin light chain at the plasma membrane. *Plant Cell*, **20**, 1363–1380.

- Lakadamyali, M., Rust, M.J. and Zhuang, X. (2006) Ligands for clathrin-mediated endocytosis are differentially sorted into distinct populations of early endosomes. *Cell*, **124**, 997–1009.
- Leborgne-Castel, N. and Luu, D.-T. (2009) Regulation of endocytosis by external stimuli in plant cells. *Plant Biosystems*, **143**, 630–635.
- Leborgne-Castel, N., Lherminier, J., Der, C., Fromentin, J., Houot, V. and Simon-Plas, F. (2008) The plant defense elicitor cryptogein stimulates clathrin-mediated endocytosis correlated with reactive oxygen species production in bright Yellow-2 tobacco cells. *Plant Physiol.* **146**, 1255–1266.
- Leshem, Y., Seri, L. and Levine, A. (2007) Induction of phosphatidylinositol 3-kinase-mediated endocytosis by salt stress leads to intracellular production of reactive oxygen species and salt tolerance. *Plant J.* **51**, 185–197.
- Martiniere, A., Shvedunova, M., Thomson, A.J.W., Evans, N.H., Penfield, S., Runions, J. and McWatters, H.G. (2011) Homeostasis of plasma membrane viscosity in fluctuating temperatures. *New Phytol.* **192**, 328–337.
- Maurel, C., Verdoucq, L., Luu, D.T. and Santoni, V. (2008) Plant aquaporins: membrane channels with multiple integrated functions. *Annu Rev Plant Biol.* **59**, 595–624.
- Men, S., Boutte, Y., Ikeda, Y., Li, X., Palme, K., Stierhof, Y.D., Hartmann, M.A., Moritz, T. and Grebe, M. (2008) Sterol-dependent endocytosis mediates post-cytokinetic acquisition of PIN2 auxin efflux carrier polarity. *Nat. Cell Biol.* **10**, 237–244.
- Murashige, T. and Skoog, F. (1962) A revised medium for rapid growth and bioassays with tobacco tissue cultures. *Physiol. Plant*, **15**, 473–497.
- Naramoto, S., Kleine-Vehn, J., Robert, S. *et al.* (2010) ADP-ribosylation factor machinery mediates endocytosis in plant cells. *Proc. Natl. Acad. Sci. USA*, **107**, 21890–21895.
- Ortiz-Zapater, E., Soriano-Ortega, E., Marcote, M.J., Ortiz-Masia, D. and Aniento, F. (2006) Trafficking of the human transferrin receptor in plant cells: effects of tyrphostin A23 and brefeldin A. *Plant J.* **48**, 757–770.
- Paciorek, T., Zazimalova, E., Ruthardt, N. *et al.* (2005) Auxin inhibits endocytosis and promotes its own efflux from cells. *Nature*, **435**, 1251–1256.
- Pan, J., Fujioka, S., Peng, J., Chen, J., Li, G. and Chen, R. (2009) The E3 Ubiquitin Ligase SCFTIR1/AFB and membrane sterols play key roles in auxin regulation of endocytosis, recycling, and plasma membrane accumulation of the auxin efflux transporter PIN2 in *Arabidopsis thaliana*. *Plant Cell*, **21**, 568–580.
- Patterson, G.H. and Lippincott-Schwartz, J. (2002) A Photoactivatable GFP for Selective Photolabeling of Proteins and Cells. *Science*, **297**, 1873–1877.
- Prak, S., Hem, S., Boudet, J., Viennois, G., Sommerer, N., Rossignol, M., Maurel, C. and Santoni, V. (2008) Multiple phosphorylations in the C-terminal tail of plant plasma membrane aquaporins: role in subcellular trafficking of AtPIP2;1 in response to salt stress. *Mol. Cell Proteomics*, **7**, 1019–1030.
- Robert, S., Kleine-Vehn, J., Barbez, E. *et al.* (2010) ABP1 mediates auxin inhibition of clathrin-dependent endocytosis in Arabidopsis. *Cell*, **143**, 111–121.
- Robinson, D.G., Jiang, L. and Schumacher, K. (2008) The endosomal system of plants: charting new and familiar territories. *Plant Physiol.* **147**, 1482–1492.
- Ron, M. and Avni, A. (2004) The receptor for the fungal elicitor ethylene-inducing xylanase is a member of a resistance-like gene family in tomato. *Plant Cell*, **16**, 1604–1615.
- Samaj, J. (2006) Methods and molecular tools for studying endocytosis in plants—an overview. In *Plant Endocytosis* (Menzel, J.S.F.B.D., ed). Berlin Heidelberg: Springer-Verlag, pp. 1–17.
- Santoni, V., Vinh, J., Pflieger, D., Sommerer, N. and Maurel, C. (2003) A proteomic study reveals novel insights into the diversity of aquaporin forms expressed in the plasma membrane of plant roots. *Biochem. J.* **373**, 289–296.
- daSilva, L.L., Foresti, O. and Denecke, J. (2006) Targeting of the plant vacuolar sorting receptor BP80 is dependent on multiple sorting signals in the cytosolic tail. *Plant Cell*, **18**, 1477–1497.
- Sorieul, M., Santoni, V., Maurel, C. and Luu, D.T. (2011) Mechanisms and effects of retention of over-expressed aquaporin AtPIP2;1 in the endoplasmic reticulum. *Traffic*, **12**, 473–482.
- Tahara, H., Yokota, E., Igarashi, H., Orii, H., Yao, M., Sonobe, S., Hashimoto, T., Hussey, P.J. and Shimmen, T. (2007) Clathrin is involved in organization of mitotic spindle and phragmoplast as well as in endocytosis in tobacco cell cultures. *Protoplasma*, **230**, 1–11.
- Takano, J., Tanaka, M., Toyoda, A., Miwa, K., Kasai, K., Fuji, K., Onouchi, H., Naito, S. and Fujiwara, T. (2010) Polar localization and degradation of Arabidopsis boron transporters through distinct trafficking pathways. *Proc. Natl. Acad. Sci. USA*, **107**, 5220–5225.
- Teh, O.K. and Moore, I. (2007) An ARF-GEF acting at the Golgi and in selective endocytosis in polarized plant cells. *Nature*, **448**, 493–496.
- Viotti, C., Bubeck, J., Stierhof, Y.-D. *et al.* (2010) Endocytic and secretory traffic in Arabidopsis merge in the Trans-Golgi Network/Early Endosome, an independent and highly dynamic organelle. *Plant Cell*, **22**, 1344–1357.

Single-Molecule Analysis of PIP2;1 Dynamics and Partitioning Reveals Multiple Modes of *Arabidopsis* Plasma Membrane Aquaporin Regulation

Xiaojuan Li,^{a,b,1} Xiaohua Wang,^{a,b,1} Yong Yang,^c Ruili Li,^{a,b} Qihua He,^d Xiaohong Fang,^c Doan-Trung Luu,^e Christophe Maurel,^e and Jinxing Lin^{a,2}

^aKey Laboratory of Plant Molecular Physiology, Institute of Botany, Chinese Academy of Sciences, Beijing 100093, China

^bGraduate University of Chinese Academy of Sciences, Beijing 100049, China

^cBeijing National Laboratory for Molecular Sciences, Institute of Chemistry, Key Laboratory of Molecular Nanostructures and Nanotechnology, Chinese Academy of Sciences, Beijing 100190, China

^dPeking University Health Science Center, Beijing 100191, China

^eBiochimie et Physiologie Moléculaire des Plantes, Institut de Biologie Intégrative des Plantes, Unité Mixte de Recherche 5004 Centre National de la Recherche Scientifique/Unité Mixte de Recherche 0386 Institut National de la Recherche Agronomique/Montpellier SupAgro/Université Montpellier 2, F-34060 Montpellier Cedex 2, France

PIP2;1 is an integral membrane protein that facilitates water transport across plasma membranes. To address the dynamics of *Arabidopsis thaliana* PIP2;1 at the single-molecule level as well as their role in PIP2;1 regulation, we tracked green fluorescent protein–PIP2;1 molecules by variable-angle evanescent wave microscopy and fluorescence correlation spectroscopy (FCS). Single-particle tracking analysis revealed that PIP2;1 presented four diffusion modes with large dispersion of diffusion coefficients, suggesting that partitioning and dynamics of PIP2;1 are heterogeneous and, more importantly, that PIP2;1 can move into or out of membrane microdomains. In response to salt stress, the diffusion coefficients and percentage of restricted diffusion increased, implying that PIP2;1 internalization was enhanced. This was further supported by the decrease in PIP2;1 density on plasma membranes by FCS. We additionally demonstrated that PIP2;1 internalization involves a combination of two pathways: a typhostin A23-sensitive clathrin-dependent pathway and a methyl- β -cyclodextrin-sensitive, membrane raft-associated pathway. The latter was efficiently stimulated under NaCl conditions. Taken together, our findings demonstrate that PIP2;1 molecules are heterogeneously distributed on the plasma membrane and that clathrin and membrane raft pathways cooperate to mediate the subcellular trafficking of PIP2;1, suggesting that the dynamic partitioning and recycling pathways might be involved in the multiple modes of regulating water permeability.

INTRODUCTION

Aquaporins, which facilitate the diffusion of water across biological membranes, are key molecules in the regulation of water transport at the cell and organ levels, and plasma membrane intrinsic proteins (PIPs) are the most abundant aquaporins in the plant plasma membrane (Katsuhara et al., 2008; Maurel et al., 2008). Plants have multiple PIP isoforms (13 in *Arabidopsis thaliana*), and on the basis of sequence similarity, PIPs can be divided into two groups, PIP1 and PIP2. PIPs are thought to occur as tetramers, with each subunit forming an individual aqueous pore, but recent work from several laboratories has

indicated that PIP1s and PIP2s can assemble to form heterotetramers (Zelazny et al., 2007; Otto et al., 2010). The function of PIPs in plants has attracted extensive research. Certain PIP1s enhanced osmotic water transport upon expression in *Xenopus laevis* oocytes (Biela et al., 1999), and *Nicotiana tabacum* and *Arabidopsis* plants deficient in these or close PIP1 homologs showed reduced hydraulic conductivity in roots and shoots (Martre et al., 2002; Siefritz et al., 2002; Postaire et al., 2010). Yet, the water transport activity of other PIP1 homologs is still unclear (Fetter et al., 2004; Sommer et al., 2008), whereas all PIP2s examined so far have been shown to have high water channel activity (Fetter et al., 2004; Verdoucq et al., 2008), indicating that PIP2s play an important role in plant–water relations.

Many studies have also noted that the regulation properties of plant aquaporins can provide useful indications about their integrated function (Vera-Estrella et al., 2004; Chaumont et al., 2005; Boursiac et al., 2008; Maurel et al., 2008). In addition to regulated opening and closing (gating), plant aquaporins were shown to undergo highly controlled subcellular trafficking as a critical point for regulating their expression and function. In these respects, *Arabidopsis* PIP2;1 has emerged as a prototypic isoform. This aquaporin shows calcium- and proton-dependent

¹ These authors contributed equally to this work.

² Address correspondence to linjx@ibcas.ac.cn.

The author responsible for distribution of materials integral to the findings presented in this article in accordance with the policy described in the Instructions for Authors (www.plantcell.org) is: Jinxing Lin (linjx@ibcas.ac.cn).

 Some figures in this article are displayed in color online but in black and white in the print edition.

 Online version contains Web-only data.

www.plantcell.org/cgi/doi/10.1105/tpc.111.091454

gating upon reconstitution in proteoliposomes (Verdoucq et al., 2008). Its trafficking to the plasma membrane was shown to be dependent on a diacidic motif and ubiquitination (Lee et al., 2009; Sorieul et al., 2011). Studies on plant roots under salt stress also revealed a reactive oxygen species–dependent internalization of PIP2;1, which was linked to salt-induced changes in C-terminal phosphorylation (Boursiac et al., 2008; Prak et al., 2008). Several endocytic pathways for plasma membrane proteins have been identified in animal and plant cells, including clathrin-dependent and raft-associated pathways (Mayor and Pagano, 2007). The former pathway is constitutive and has been established for PIP2;1 and other plant membrane proteins (Dhonukshe et al., 2007). The latter is by far less understood in plants and may be triggered by specific signals (Mayor and Pagano, 2007). In this context, a critical issue is to understand how PIP2;1 responds to osmotic stress to regulate root hydraulic conductivity (L_{pr}), particularly the initial events that determine PIP2;1 subcellular movements immediately after cell stimulation.

Although earlier studies focused on the structure and regulation mechanisms (Törnroth-Horsefield et al., 2006; Maurel et al., 2009), few have examined the diffusion dynamics and partitioning of membrane proteins in living cells, which is important for bridging data collected at the level of individual molecules to the physical and physiological processes (Joo et al., 2008). Bulk approaches have been unable to unambiguously determine the oligomeric state and mobility of molecules within living cells. Recent progress in single-molecule measurements has enabled observation of the dynamic behavior of membrane proteins and their elementary molecular processes (Dahan et al., 2003; Douglass and Vale, 2005; Zhang et al., 2009c; Hern et al., 2010). The aim of this study was to investigate the motion of PIP2;1 at a high spatiotemporal resolution in *Arabidopsis* cell membranes using variable-angle evanescent wave microscopy (EWM), also known as variable-angle epifluorescence microscopy, and fluorescence correlation spectroscopy (FCS) and to reveal heterogeneities or physical effects usually hidden in the ensemble average. Specifically, we focused on partitioning on the membrane and recycling pathways of PIP2;1 under resting and salt stress conditions.

RESULTS

The Assembly State of PIP2;1 in *Arabidopsis* Plasma Membranes

To monitor PIP2;1 molecules in plant plasma membranes and study their assembly state, it was necessary to label them specifically with a fluorescent species having suitable biophysical characteristics in terms of absorption wavelength and resistance to photobleaching. We performed fluorescence targeting experiments in *Arabidopsis* using green fluorescent protein (GFP) fusions. Although some fluorescent signals in transgenic lines driven by the native promoter could be detected by the electron-multiplying charge-coupled device (EMCCD) (see Supplemental Figure 1A and Supplemental Movie 1 online), the signals were weak and fluorescent spots could not be used for single-molecule analysis. Thus, we stably expressed the fusion

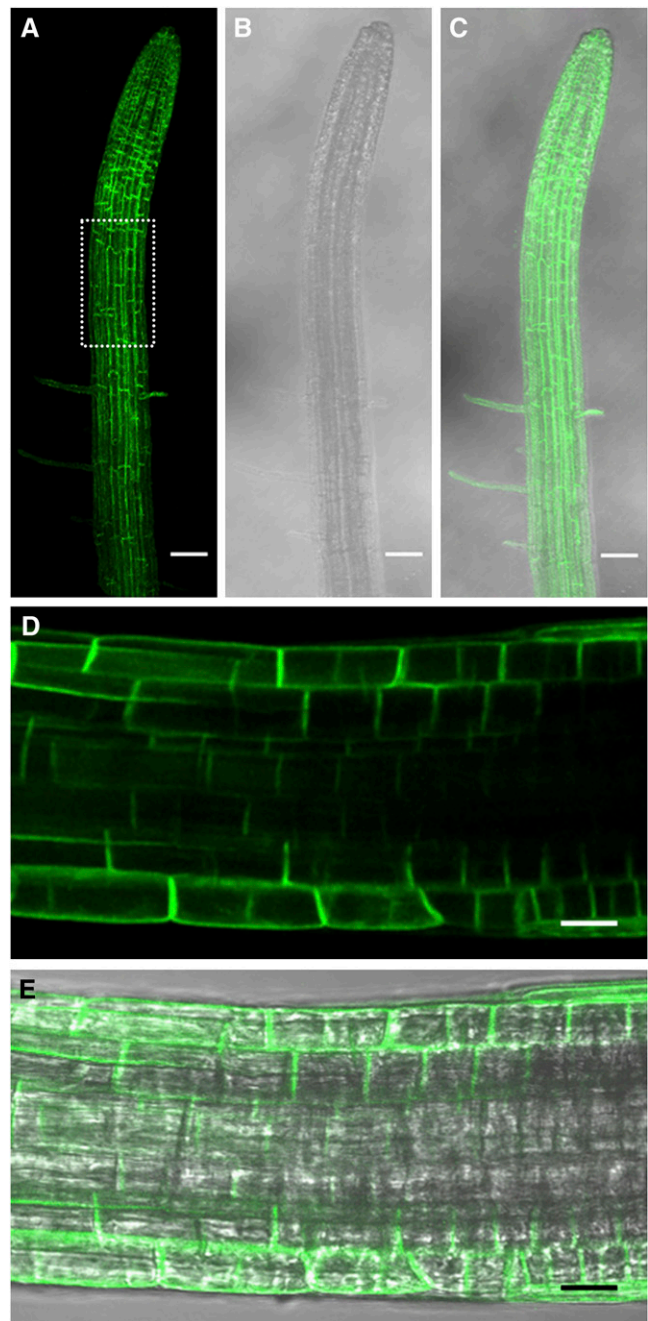


Figure 1. Confocal Microscopy Images of GFP-PIP2;1 Fusion Proteins Expressed in *Arabidopsis* Roots.

(A) to (C) Fluorescence, bright-field, and merged images showing that the GFP-PIP2;1 fusion protein could be efficiently expressed in *Arabidopsis* root cells, from the root apical meristem to the maturation zone. (D) and (E) Higher magnification of the area highlighted in (A), showing extensive plasma membrane-restricted GFP fluorescence in the epidermis. Bars = 40 μm in (A) to (C) and 20 μm in (D) and (E).

protein under control of the constitutive 35S promoter. Cells expressing GFP-labeled PIP2;1 (GFP-PIP2;1) were observed to ensure that the GFP insertion did not interfere with PIP2;1 plasma membrane targeting. Figure 1 shows that GFP-PIP2;1 was efficiently targeted to the plasma membrane of *Arabidopsis* root epidermal cells. Furthermore, the water transport activity of fluorescently tagged PIP2;1 was investigated after functional expression in *Xenopus* oocytes. Osmotic swelling assays showed that the osmotic water permeability (P_f) of oocytes injected with the GFP-PIP2;1 cRNAs was significantly higher (more than fivefold) than that of control oocytes expressing GFP alone.

When the plasma membrane of living root epidermal cells was viewed under EWM, numerous fluorescent spots were observed, most of which appeared as well-dispersed diffraction-limited fluorescent spots. Figure 2A shows a single video frame taken from a 45-s recording of the epidermal cell plasma membrane. To determine the number of GFP-PIP2;1 molecules contained in these diffraction-limited fluorescent spots, we performed calibration experiments using purified monomeric GFP, which was immobilized on cover glasses and visualized with EWM illumination. The brightness of a single GFP molecule could be detected in our measurement apparatus, and the fluorescence intensity distribution of diffraction-limited spots was analyzed. The background-corrected, area-integrated fluorescence intensities of individual spots produced a unimodal distribution with a peak intensity around 70 counts (see Supplemental Figure 1B online).

To investigate the oligomerization state of GFP-PIP2;1 in the plasma membrane of living cells, we analyzed the fluorescence intensity distribution of the GFP-PIP2;1 spots. A histogram of the intensity showed an asymmetric distribution skewed to intensities lower than that expected for four fluorophores (Figure 2B). The majority of spots had intensities ranging from 120 to 250 counts, which were approximately two- or threefold that of purified GFP, suggesting that these spots included two or three GFP-PIP2;1 molecules. To circumvent signal fluctuation due to the diffusion of GFP-PIP2;1 in living cell membranes, the photobleaching of individual spots was further analyzed in fixed cells. For each of the chosen fluorescent spots, we determined, as described previously (Ulbrich and Isacoff, 2007), the number of fluorescing GFP molecules by counting the number of bleaching steps. As shown in Figure 2C, the number of bleaching steps ranged from one to four for the analyzed puncta.

Molecular Behavior of GFP-PIP2;1 in the Plasma Membrane

We then studied the dynamic properties of PIP2;1 in more detail using single-particle tracking (SPT) in continuous images (Figures 3A and 3B; see Supplemental Movie 2 online). Some molecules covered relatively long distances (up to 0.767 μm within 100 ms), whereas others were less mobile (0.053 μm within 100 ms). The diffusion type was evaluated by analysis of mean square displacement (MSD) versus time plots of the trajectories of individual molecules (Figure 3C). The curve-fitting relationship between MSD and time showed that GFP-PIP2;1 diffusion could be classified into four categories: pure Brownian diffusion (33.75% \pm 3.3% of the total trajectories; Figure 4A);

directed diffusion (27.5% \pm 2.4% of the total trajectories; Figure 4A); pure restricted or confined diffusion (17.5% \pm 2.1% of the total trajectories; Figure 4A), with an average confinement range of 87.76% \pm 9.4 nm; or diffusion with combinations of Brownian and restricted modes referred to as a mixed trajectory. The proportion of the last category was 21.25% \pm 3.1% (Figure 4A), with the mean value of the confinement range (116.83 \pm 10.7 nm) generally larger than that of pure restricted trajectories. Although one-third of the PIP2;1 spots had a pure Brownian diffusion, most PIP2;1 molecules were restricted in confinement zones, which were emphasized by the mixed trajectory regime.

The diffusion coefficient of the GFP-PIP2;1 particles was calculated by linear fit to MSD versus time (MSD- t) plots. The distribution of the diffusion coefficients was plotted in a histogram having logarithmically spaced bins (Figure 4B). The data were fitted using Gaussians, the position of the peak (noted as \hat{G}) being considered the characteristic diffusion coefficient. Figure 4B shows that \hat{G} was around $2.46 \times 10^{-3} \mu\text{m}^2/\text{s}$ (SE 2.19 to $2.75 \times 10^{-3} \mu\text{m}^2/\text{s}$), with a large dispersion of diffusion coefficients, most of which were between $10^{-4} \mu\text{m}^2/\text{s}$ and $3 \times 10^{-2} \mu\text{m}^2/\text{s}$, indicating that the movement of PIP2;1 was heterogeneous. When the diffusion coefficients and the percentage of different diffusion modes were plotted against the fluorescence intensity (a parameter that tends to reflect the level of GFP-PIP2;1 oligomerization) (see Supplemental Figures 2A and 2B online), we found that the diffusion characters were not directly associated with the fluorescence intensity.

We were curious as to whether the dynamic characteristics of GFP-PIP2;1 were general because no such analysis of membrane proteins has been reported in plant cells. Therefore, we compared the behavior of GFP-PIP2;1 and GFP-LTI6a, a small plasma membrane marker protein (see Supplemental Figures 3A and 3B online). As illustrated in Supplemental Figure 3C online, the diffusion coefficient of GFP-LTI6a ranged from 5.62×10^{-3} to $3.16 \times 10^{-1} \mu\text{m}^2/\text{s}$, with a \hat{G} value of $2.37 \times 10^{-2} \mu\text{m}^2/\text{s}$ (SE 2.06 to $2.73 \times 10^{-2} \mu\text{m}^2/\text{s}$), which is 10-fold that of GFP-PIP2;1. To extract more information about the behavior of individual GFP-LTI6a fluorescent particles, we further analyzed the diffusion mode according to the initial selection criteria described above. Over 50% (51.27% \pm 4.4%; see Supplemental Figure 3D online) of the GFP-LTI6a molecules exhibited Brownian diffusion, whereas other GFP-LTI6a molecules underwent directed diffusion and restricted diffusion (25.91% \pm 3.9% and 21.53% \pm 6.0%, respectively; see Supplemental Figure 3D online). However, almost no mixed trajectory was detected (only one among 77 trajectories). These results show that our analysis was sensitive enough to distinguish the dynamics of two different proteins. Thus, GFP-PIP2;1 exhibited specific dynamic properties.

Partitioning of PIP2;1 Is Associated with Membrane Rafts

To understand better the molecular mechanisms underlying PIP2;1 partitioning into plasma membrane domains, we treated seedlings with methyl- β -cyclodextrin (M β CD), a sterol disrupting reagent. The subsequent reduction in sterol levels was monitored by cell staining with filipin, a fluorescent polyene antibiotic that binds to sterols. Treatment with 10 mM M β CD resulted in the effective depletion of sterol in root cells by \sim 30% (see

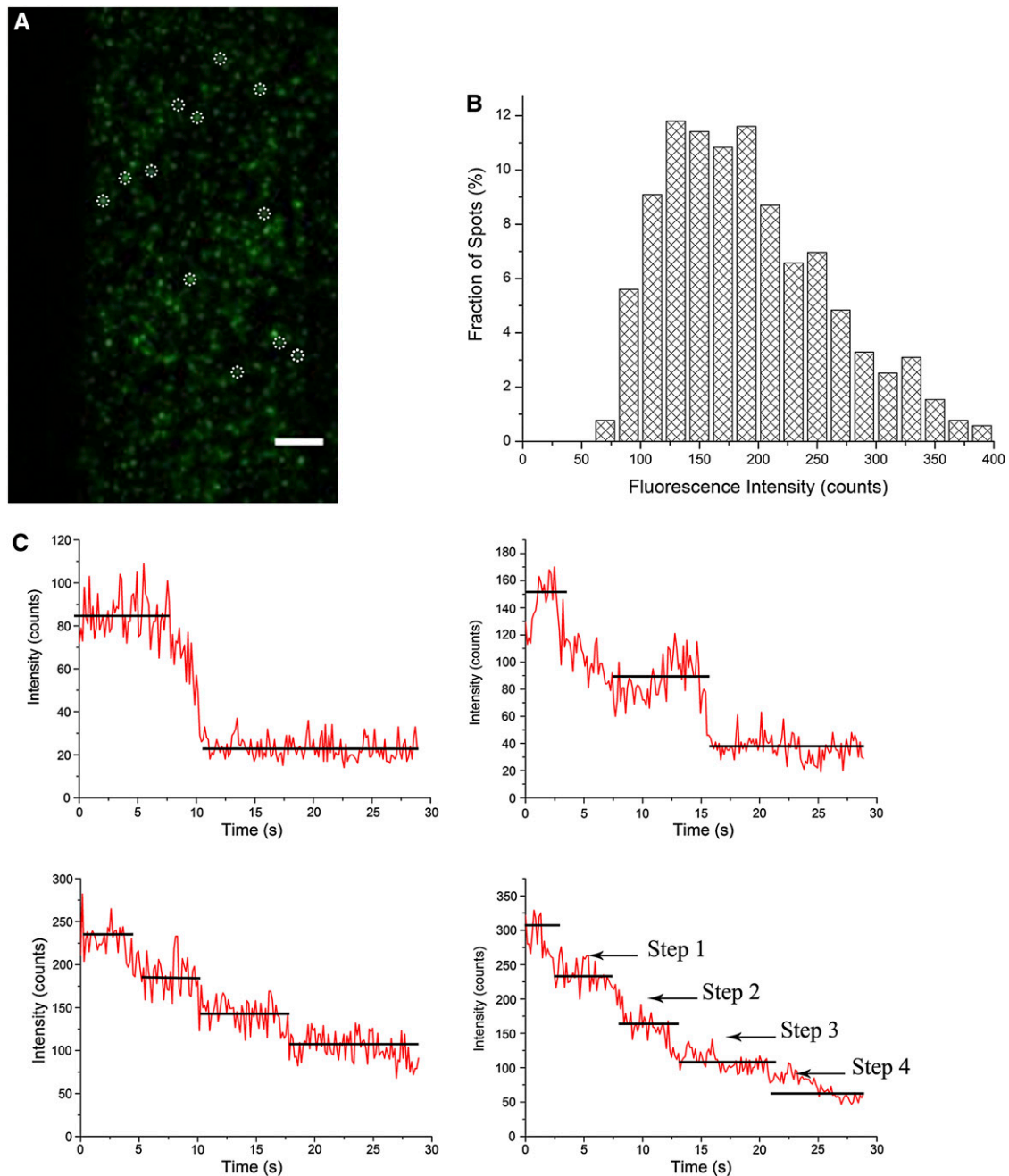


Figure 2. GFP-PIP2;1 Molecules on the Plasma Membrane of Root Epidermal Cells Imaged with EWM and Oligomeric State Analysis.

(A) A typical single-molecule image of GFP-PIP2;1 on the plasma membrane of living epidermal cells. The image is a section of the first frame of a stack of images with the background subtracted. The diffraction-limited spots (3×3 pixel regions) enclosed within white circles represent the signals from individual GFP-PIP2;1 fluorescent spots and were chosen for the fluorescence intensity analysis. Bar = $5 \mu\text{m}$.

(B) Distribution of the fluorescence intensity of diffraction-limited GFP-PIP2;1 spots from the living cell imaging ($n = 523$ spots).

(C) Time courses of GFP emission after background correction showing one-step, two-step, three-step, and four-step bleaching. The amplitude of each step was close to that of single purified GFP molecules observed on cover slips (see Supplemental Figure 1 online).

[See online article for color version of this figure.]

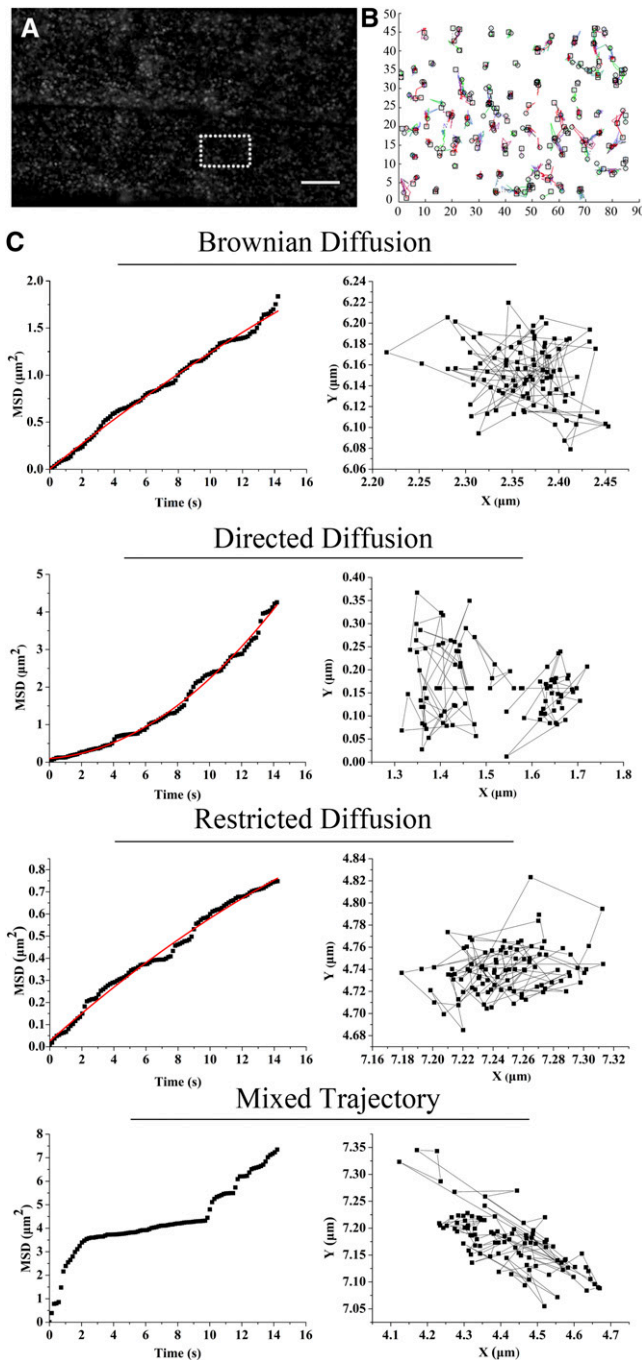


Figure 3. Automated Tracking and Statistical Analysis of GFP-PIP2;1 Spots on the Plasma Membrane.

(A) EWM image of GFP-PIP2;1 on the plasma membrane of epidermal cells. Bar = 10 μm .

(B) Trajectories of GFP-PIP2;1 molecules in the area indicated by the white box in **(A)**. The indicated trajectories result from automated tracking of individual puncta in a series of stacks.

(C) Analysis by MSD of various trajectories and classification into different diffusion modes. The resulting MSD- t curves (black squares) were fitted with pure Brownian, restricted, directed, and those exhibiting

Supplemental Figure 4 online). Under confocal laser scanning microscopy and EWM, we found that actin filaments became slightly shorter after treatment with M β CD, whereas the elongation rate and the rate of convolution frequency did not significantly change (see Supplemental Figure 5, Supplemental Movies 3 and 4, and Supplemental Table 1 online), suggesting that M β CD treatment did not significantly affect the organization of the actin cytoskeleton. As shown in Figure 5B, treatment with M β CD induced dramatic changes in the partitioning of GFP-PIP2;1 in the plasma membrane compared with that in control cells (Figure 5A). More specifically, the well dispersed patterns of diffraction-limited spots disappeared. Instead, some particles accumulated into small clusters, which were brighter than diffraction-limited spots (purple circles in Figure 5B). Disappearance of PIP2;1 molecules in certain areas was also observed. We further followed the impacts of fenpropimorph (Fen), a sterol synthesis inhibitor, and DL-threo-1-phenyl-2-palmitoylamino-3-morpholino-1-propanol (PPMP), a sphingolipid biosynthesis inhibitor, on the localization of GFP-PIP2;1. Both inhibitors resulted in GFP-PIP2;1 coalescing into larger particles with an increased fluorescence intensity (see Supplemental Figure 6 online), similar to the effect of M β CD treatment. These results suggest that the partitioning of PIP2;1 in the plasma membrane depends on membrane lipids and on the sterol content.

Because of its multiple diffusion modes and dependency on sterol, we suspected that PIP2;1 localized at least partially to sphingolipid-rich microdomains referred to as membrane rafts (Bhat and Panstruga, 2005). To validate this assumption, cells coexpressing GFP-PIP2;1 and mCherry-Flotillin1 (At-Flot1, a marker protein of membrane rafts) were imaged by dual-color EWM. Excitation was switched between two lasers so that the cells were alternatively illuminated with blue (473 nm) and green (561 nm) light, and sequential video frames were obtained. When two consecutive frames representing green and red fluorescence were overlaid, we detected some yellow regions caused by the high intensity in both the green and red channels, suggesting an overlap of the GFP-PIP2;1 and mCherry-Flot1 fluorescent foci. An example of colocalization is shown in Figures 5C to 5E, and the lateral diffusion trajectories of the overlapped fluorescent spots are shown in Figures 5F and 5G. To test the possibility that the colocalization was due to random overlap of the highly dense foci on the cell membrane, the red channel image from four different cells was rotated 180° with respect to the green channel, as reported in a previous investigation (Konopka et al., 2008). The average peak distance for the original image (4.27 ± 1.38 pixels; $n = 211$ from four cells) was significantly smaller from that of the rotated images (6.82 ± 2.18 pixels;

a combination of Brownian and restricted modes were regarded as mixed trajectories. A representative sample of the various diffusion modes of GFP-PIP2;1 on the plasma membrane is shown with the corresponding trajectories. Note that classification into various diffusion modes could not have been accurately performed using simple visual inspection of the trajectories.

[See online article for color version of this figure.]

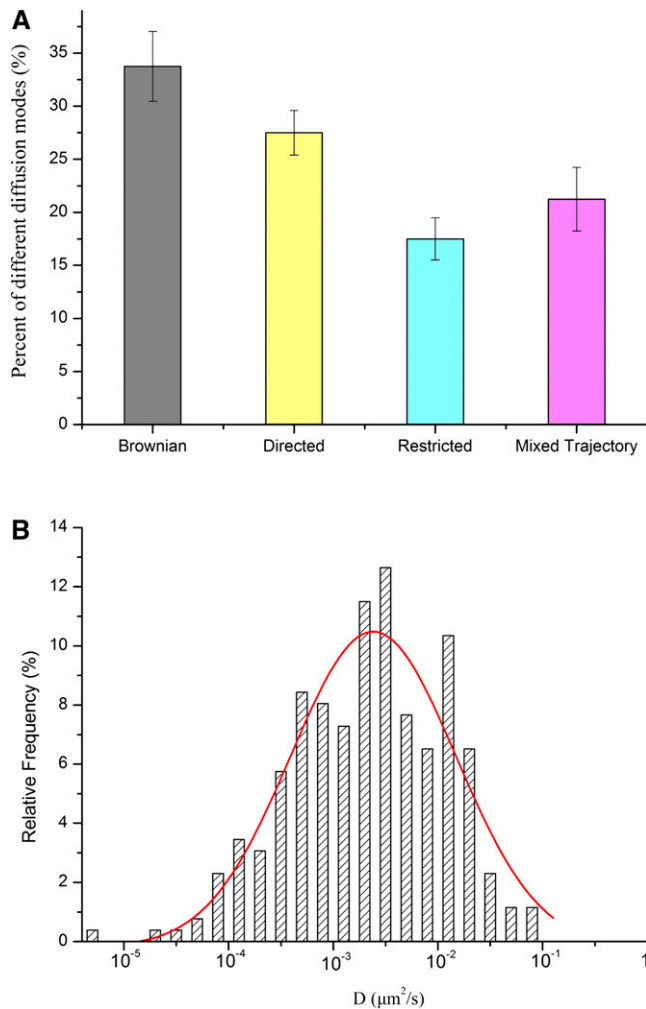


Figure 4. Statistical Analyses of GFP-PIP2;1 Lateral Dynamics on the Plasma Membrane.

(A) Relative percentage of the different diffusion modes of GFP-PIP2;1 derived from three separate analysis of a total $n = 80$ individual trajectories. Values given are mean \pm SD.

(B) Distribution of diffusion coefficients (D) for GFP-PIP2;1 on the plasma membrane of epidermal cells ($n = 261$ spots).

[See online article for color version of this figure.]

$n = 213$ from four cells, $P < 0.0001$), indicating that the colocalization was significant.

Tracking the fluorescent spots of GFP-PIP2;1 from their colocalization with mCherry-Flot1 clearly showed that the movements of these GFP-PIP2;1 spots were mainly confined within a specific area, the average displacement of the confined GFP-PIP2;1 being 88.87 ± 8.2 nm (mean \pm SE; $n = 21$). These spots also exhibited restricted or mixed trajectory diffusion (Figures 5F and 5G). Within the mixed trajectories, GFP-PIP2;1 exhibited restricted diffusion when it was confined in mCherry-Flot1-rich structures. These results imply that the partitioning of PIP2;1 on membranes is closely related to membrane rafts.

Salt Exposure Triggers Relocalization and Dynamic Changes

The effects of treating roots with 100 mM NaCl on GFP-PIP2;1 cellular dynamics were first investigated using confocal laser scanning microscopy. Whereas homogenous labeling of the plasma membrane by GFP-PIP2;1 was observed under normal conditions (Figure 1D), salt exposure resulted in a discontinuous labeling pattern after 10 min (Figures 6A and 6B); a similar phenomenon was also detected using 200 mM sorbitol as a comparable osmotic stress (see Supplemental Figure 7A online). After staining with FM4-64, a plasma membrane marker, the plasma membrane areas with discontinuous GFP labeling were found to be intact and unperturbed by the salt treatment (Figure 6C). Furthermore, we observed the appearance of intracellular structures containing GFP-PIP2;1 in a restricted number of cells (Figure 6D). Parallel experiments with seedlings expressing GFP-LTi6a, an independent marker of the plasma membrane, showed much less pronounced relocalization of GFP-LTi6a after NaCl and sorbitol treatments (see Supplemental Figures 7B to 7D online).

When observed by EWM, salt-treated epidermal cells displayed highly mobile puncta dispersed on the membrane (Figure 6E; see Supplemental Movie 5 online). The dynamic characteristics of GFP-PIP2;1 after treatment with 100 mM NaCl were also investigated using SPT analysis. As illustrated in the histogram of Figure 6F, the diffusion coefficients of GFP-PIP2;1 in NaCl-treated cells ranged mainly from 10^{-3} to 10^{-1} $\mu\text{m}^2/\text{s}$ (1×10^{-4} to 3×10^{-2} $\mu\text{m}^2/\text{s}$ in control cells); the highest value of 1.94×10^{-1} $\mu\text{m}^2/\text{s}$ was 2 times higher than in control cells (9.8×10^{-2} $\mu\text{m}^2/\text{s}$). More specifically, \hat{G} increased to 5.62×10^{-3} $\mu\text{m}^2/\text{s}$ (SE 4.57 to 6.92×10^{-3} $\mu\text{m}^2/\text{s}$), more than twofold that of the diffusion coefficient of PIP2;1 in control cells (2.5×10^{-3} $\mu\text{m}^2/\text{s}$). To investigate further the behavior of PIP2;1 in living cells exposed to salt, the percentage of different diffusion modes was also analyzed. As shown in Figure 6G, and with respect to normal conditions, Brownian diffusion, directed diffusion, and mixed trajectory decreased to 83.33, 91, and 88% of the control values, respectively, while restricted diffusion increased significantly to 160% compared with control cells (Figure 6G). These changes indicate that in relation to the modified surface and intracellular GFP-PIP2;1 labeling observed under NaCl treatment conditions, diffusion coefficients were skewed toward higher values and more GFP-PIP2;1 molecules underwent restricted diffusion.

Membrane Rafts and Clathrin Contribute to the Internalization of PIP2;1

Endocytosis is a basic cellular process used by cells to internalize a variety of molecules (Robinson et al., 2008). The discovery of clathrin-dependent endocytosis has provided a fundamental paradigm for analyzing membrane trafficking in cells (Dhonukshe et al., 2007; Pérez-Gómez and Moore, 2007; Foresti et al., 2010). Moreover, a sterol-dependent pathway has also been reported to play an important role in *Arabidopsis* (Men et al., 2008). To investigate the pathways that are involved in PIP2;1 trafficking under normal conditions and in its relocalization upon stimulation, we compared the localization of PIP2;1 to that of clathrin

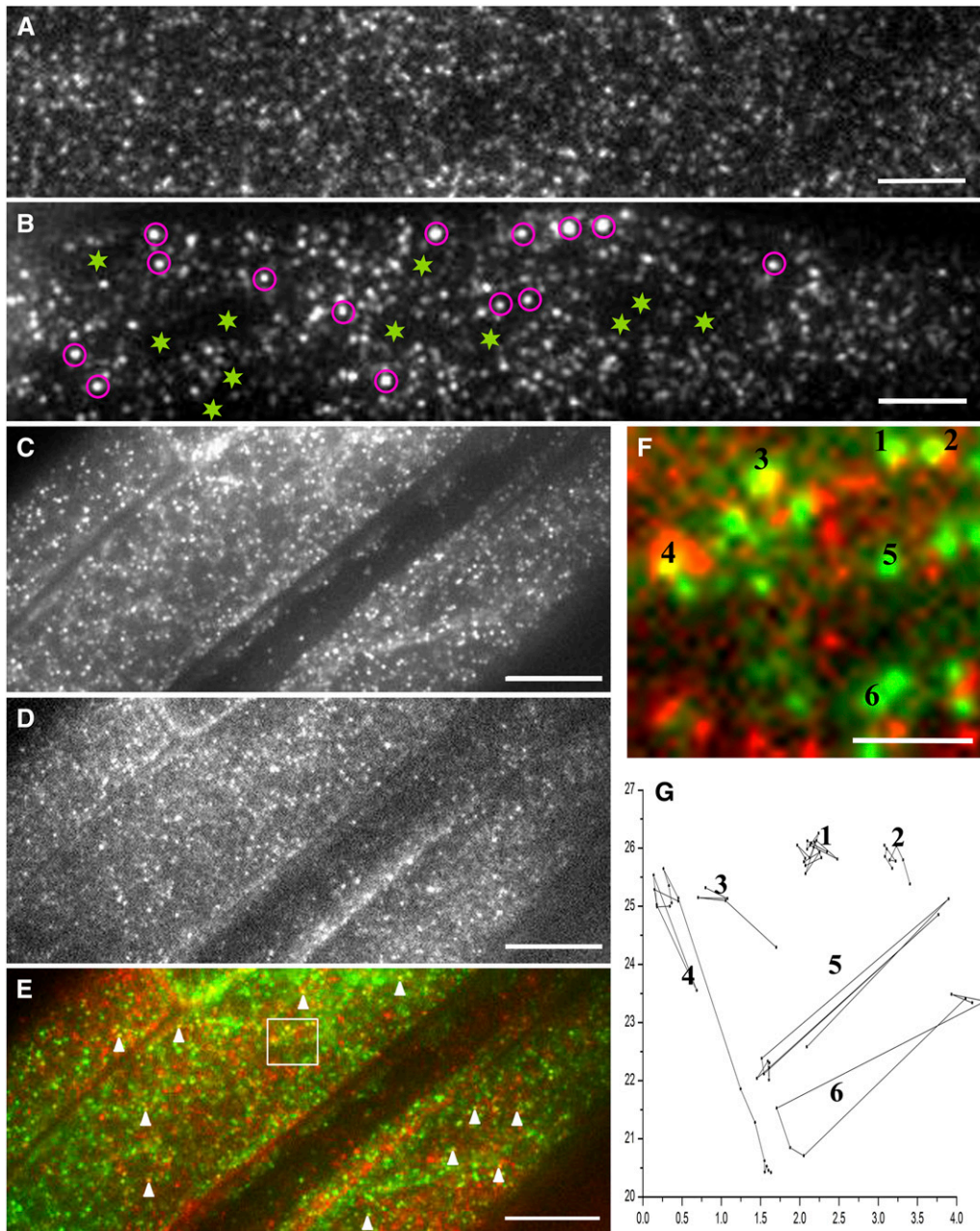


Figure 5. The Partitioning of GFP-PIP2;1 on the Plasma Membrane Is Associated with Membrane Rafts.

(A) The partitioning of GFP-PIP2;1 on the plasma membrane of epidermal cells bathed in half-strength MS medium.

(B) Effects of sterol depletion induced by a M β CD treatment on the plasma membrane partitioning of GFP-PIP2;1. Some GFP-PIP2;1 molecules assembled into small clusters (indicated in purple circles) to yield dots that were larger and brighter than diffraction-limited spots. Disappearance of PIP2;1 molecules in certain areas was also observed, as highlighted with asterisks.

(C) to (E) The first frame from a dual-color EWM movie of GFP-PIP2;1 **(C)**/mCherry-Flot1 **(D)**/merged images **(E)** of the same epidermal cells bathed in half-strength MS medium. Arrowheads indicate the colocalization fluorescent foci.

(F) Higher magnification of the boxed area in **(E)**.

(G) Lateral diffusion trajectories of the corresponding GFP-PIP2;1 signal in **(F)**. Movements of spots 1 to 3 colocalized with mCherry-Flot1 and were confined to certain areas, while spot 4 covered a larger range after a transient trapping. Nonoverlapped spots 5 and 6 covered a longer range compared with spots 1 and 2.

Bars = 5 μ m in **(A)** and **(B)**, 10 μ m in **(C)** to **(E)**, and 2 μ m in **(F)**.

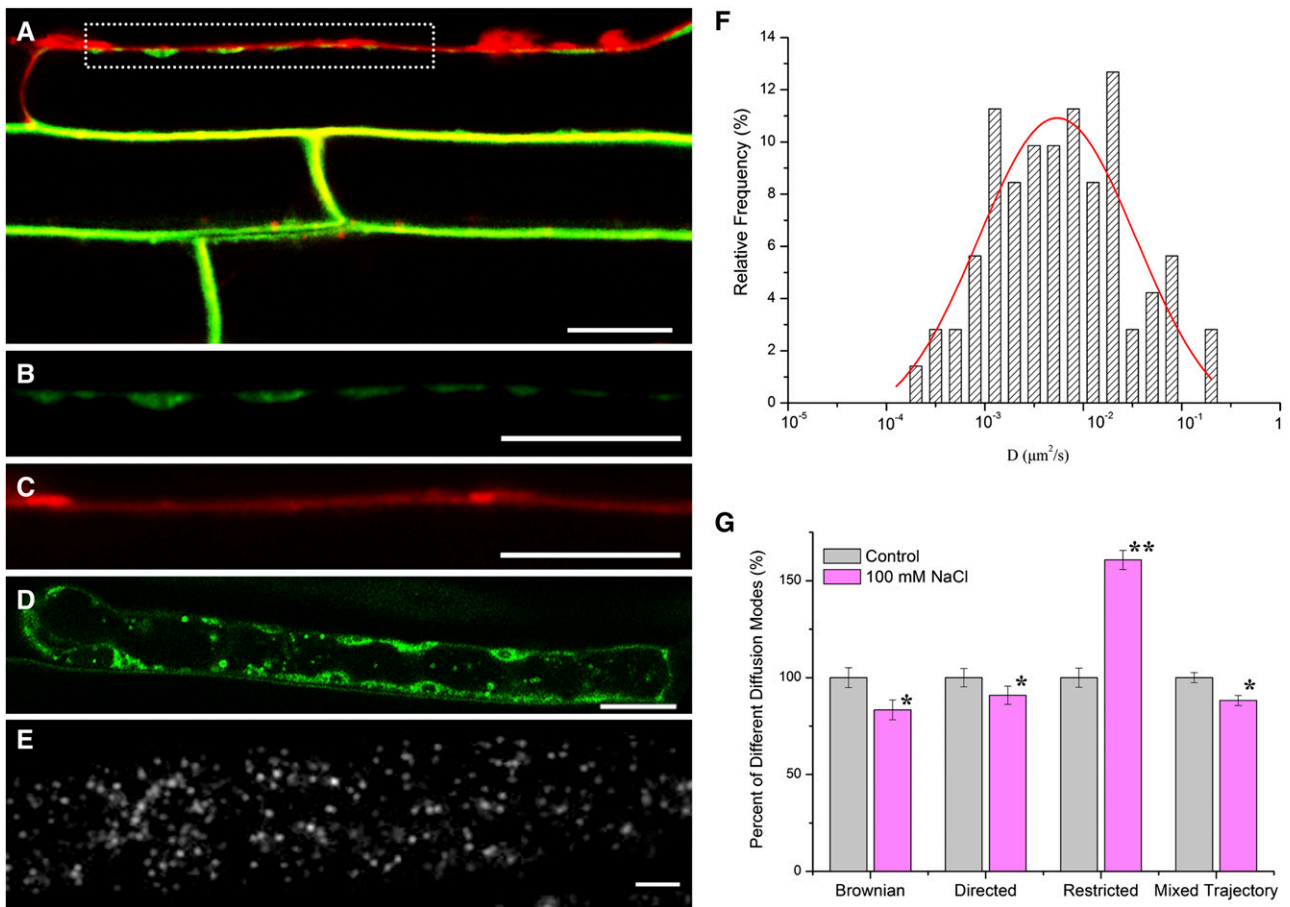


Figure 6. Confocal Images and EWM Analysis of GFP-PIP2;1 after NaCl Treatment.

(A) The plasma membrane of an epidermal cell from GFP-PIP2;1 seedlings stained with FM4-64 after treatment with NaCl. (B) Detail of the plasma membrane indicated discontinuous labeling by GFP-PIP2;1, as highlighted by the white box in (A). (C) Corresponding FM4-64 staining of the plasma membrane to (B) indicates that the membrane was intact and unperturbed. (D) Labeling of intracellular structures by GFP-PIP2;1. (E) EWM image of NaCl-treated epidermal cells. (F) Histogram showing the distribution of diffusion coefficients of GFP-PIP2;1 in NaCl-treated epidermal cells ($n = 171$ spots). (G) Percentage of different diffusion modes in NaCl-treated cell ($n = 80$ individual trajectories) compared with those in control cells bathed in half-strength MS medium. Values given are mean \pm SD. **Significantly different from the control at $P < 0.01$; *significantly different from the control at $P < 0.05$, t test. Bars = $20 \mu\text{m}$ in (A) to (D) and $5 \mu\text{m}$ in (E).

light chain (CLC) and Flot1, two commonly used endocytic markers for the clathrin-dependent pathway and membrane raft-associated pathway, respectively. Cells coexpressing GFP-PIP2;1/mCherry-Flot1 or GFP-PIP2;1/mCherry-CLC were imaged using dual-color EWM. Instead of diffraction-limited fluorescent foci with lateral diffusion on the membranes, we detected green and red particles or clusters that were localized in the cytoplasm region proximal to the plasma membrane and that exhibited movements of departing from membranes. For quantification, two particles were arbitrarily considered as codiffusing when at least one pixel of their fluorescence signals overlapped during at least five consecutive frames acquired within a 200-ms interval. As illustrated in Figure 7, GFP-PIP2;1 was found to colocalize with mCherry-CLC and gradually codiffused away from the focus, indicating that the internalization of PIP2;1 was associated with the

clathrin-dependent pathway. As shown in Figure 8, partial colocalization and codiffusion of GFP-PIP2;1 and mCherry-Flot1 were also detected, suggesting that, under normal conditions, the internalization of PIP2;1 was also associated with membrane rafts but to a lesser extent than with clathrin.

To understand at a quantitative level how both recycling pathways contribute to GFP-PIP2;1 internalization, we examined the temporal interactions using live-cell fluorescence cross-correlation spectroscopy (FCCS). The fluorescence fluctuation of GFP and mCherry gave rise to cross-correlation signals in both seedlings expressing GFP-PIP2;1/mCherry-CLC or GFP-PIP2;1/mCherry-Flot1. The relative cross-correlation amplitude was 0.53 ± 0.11 for GFP-PIP2;1/mCherry-CLC, while the value was 0.42 ± 0.13 for GFP-PIP2;1/mCherry-Flot1, suggesting that the interaction between GFP-PIP2;1 and mCherry-CLC was

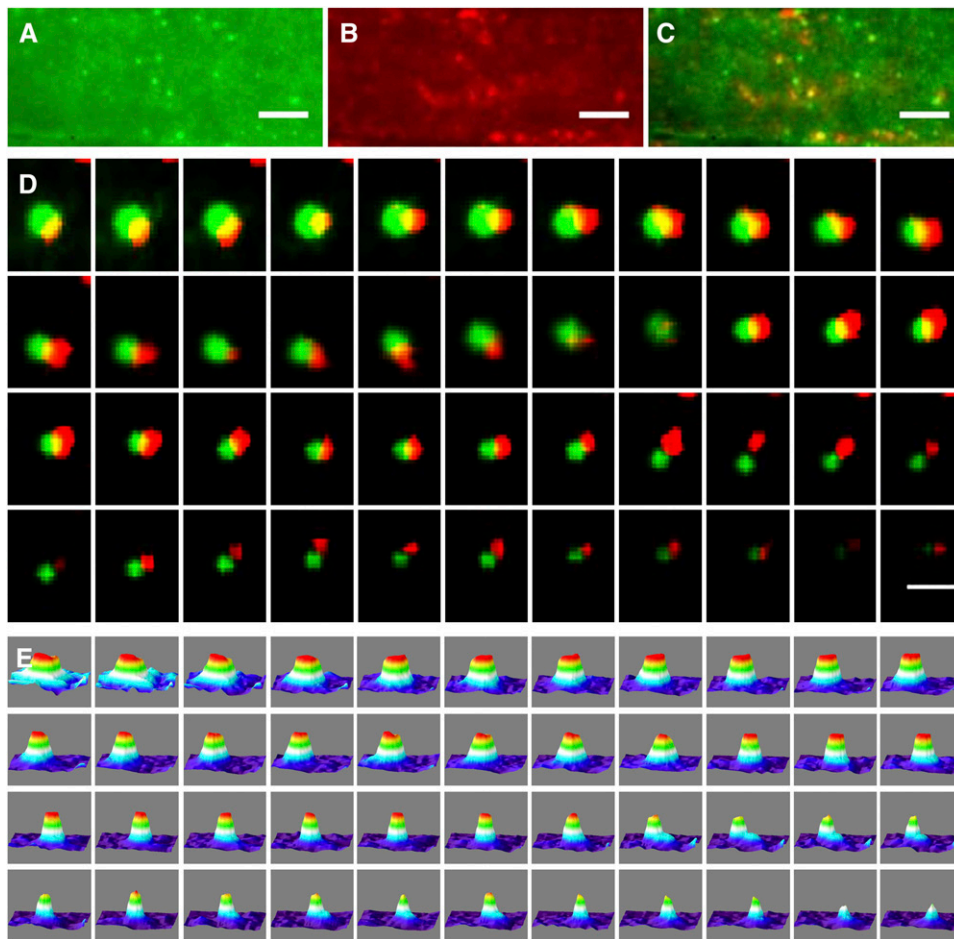


Figure 7. Colocalization and Codiffusion Analysis of PIP2;1 and CLC.

- (A) EWM image of GFP-PIP2;1 clusters proximal to the plasma membrane.
 (B) EWM image of mCherry-CLC clusters proximal to the plasma membrane.
 (C) Merged image of (A) and (B); the yellow dots indicate the colocalization particles.
 (D) Time lapse showing an example of one overlapped GFP-PIP2;1 and mCherry-CLC spot codiffusion away from the focus.
 (E) Three-dimensional luminance plots of the corresponding spots in (D).
 Bars = 5 μm in (A) to (C) and 1 μm in (D).

stronger than that between GFP-PIP2;1 and mCherry-Flot1, consistent with the results obtained by EWM. When the seedlings were exposed to 100 mM NaCl, the interactions between GFP-PIP2;1/mCherry-CLC and GFP-PIP2;1/mCherry-Flot1 significantly increased. The relative cross-correlation amplitude was 0.59 ± 0.14 ($P < 0.01$) and 0.52 ± 0.08 ($P < 0.05$), revealing that the correlation between GFP-PIP2;1 and endocytic pathways became much stronger under hypertonic stress. Note that the increase in cross-correlation amplitude of GFP-PIP2;1/mCherry-Flot1 (23.8%) was higher compared with that of GFP-PIP2;1/mCherry-CLC (11.3%).

We then investigated the effects on GFP-PIP2;1 movement of tyrphostin A23 (TyrA23), a well-characterized inhibitor of the clathrin-mediated endocytic pathway (Dhonukshe et al., 2007). TyrA23 is thought to block specifically the interaction of endocytic cargo motifs with the clathrin medium chain. This interac-

tion is crucial for establishing a link between the cytosolic domains of membrane proteins to the clathrin coat involved in vesicle formation (Banbury et al., 2003). Exposure of seedlings to TyrA23 led to an overall decrease in GFP-PIP2;1 diffusion coefficients, with \hat{G} reduced to $1.59 \times 10^{-3} \mu\text{m}^2/\text{s}$ (SE 1.41 to $1.78 \times 10^{-3} \mu\text{m}^2/\text{s}$) (Figure 9A; see Supplemental Movie 6 online). The percentage of mixed trajectory after treatment with TyrA23 increased notably to twofold that of untreated control cells at the expense of Brownian and restricted diffusion, which decreased to 46 and 71%, respectively, of those in untreated control cells (Figure 9C). No obvious change in directed diffusion was detected (102% that of untreated control cells). Also, the effects of TyrA23 were found to be reversible; at 20 min after washout, the \hat{G} value had increased to $2.20 \times 10^{-3} \mu\text{m}^2/\text{s}$ (SE 1.88 to $2.58 \times 10^{-3} \mu\text{m}^2/\text{s}$) (see Supplemental Figure 8A online), comparable to that of the control cells. When tyrphostin A51, an

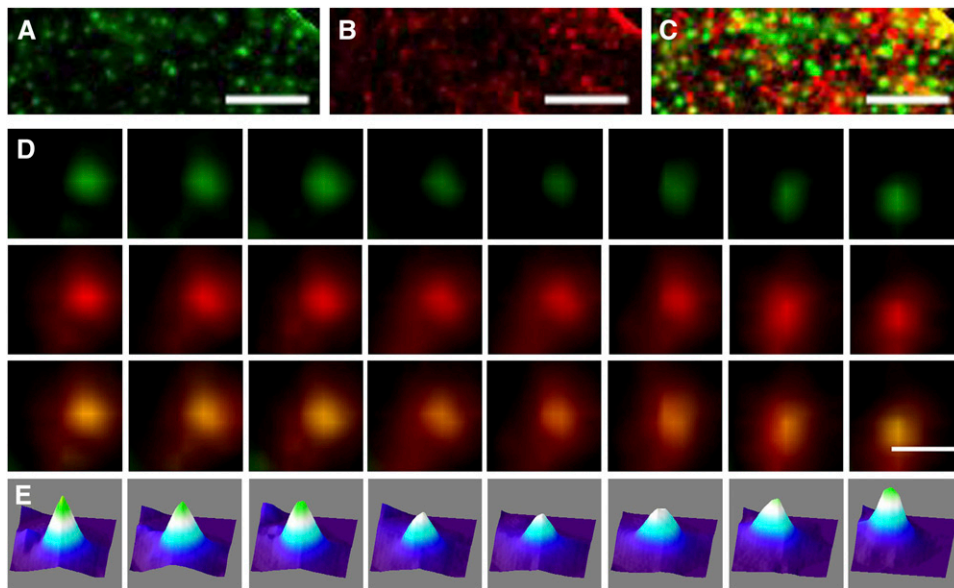


Figure 8. Colocalization and Codiffusion Analysis of PIP2;1 and Flot1.

- (A) EWM image of GFP-PIP2;1 clusters proximal to the plasma membrane.
 (B) EWM image of mCherry-Flot1 clusters proximal to the plasma membrane.
 (C) Merged image of (A) and (B); the yellow dots indicate the colocalization particles.
 (D) An example of real-time dynamic observation of the GFP-PIP2;1 and mCherry-Flot1 molecule codiffusion.
 (E) Three-dimensional luminance plots from the merged fluorescence of the corresponding spots in (D).
 Bars = 5 μm in (A) to (C) and 1 μm in (D).

analog of TyrA23 that does not interfere with the clathrin–cargo interaction, was used (Banbury et al., 2003; Konopka et al., 2008), the diffusion coefficient of GFP-PIP2;1 did not change (see Supplemental Figure 8B online). The recovery experiment and noneffective analog treatment clearly suggested that the concentrations of TyrA23 used in this study were within the physiological range and its effect is rather specific.

Unlike in the presence of TyrA23, the histogram of diffusion coefficients after M β CD treatment showed a broad, bimodal distribution (Figure 9B; see Supplemental Movie 7 online), suggesting the existence of two subpopulations of diffusing GFP-PIP2;1 molecules. One subpopulation would correspond to molecules with a modal diffusion coefficient ($\hat{G} = 2.51 \times 10^{-3} \mu\text{m}^2/\text{s}$, SE 2.32 to $2.73 \times 10^{-3} \mu\text{m}^2/\text{s}$) comparable to that observed under normal conditions. By contrast, most other GFP-PIP2;1 molecules diffused slowly with $\hat{G} = 1.26 \times 10^{-4} \mu\text{m}^2/\text{s}$ (SE 1.01 to $1.57 \times 10^{-4} \mu\text{m}^2/\text{s}$), which was ~ 20 times lower. Among the GFP-PIP2;1 molecules analyzed after M β CD treatment, the percentage of Brownian diffusion declined to 67% of the untreated control cell value, and no obvious changes in the directed diffusion and mixed trajectory were detected (91 and 112% that of untreated control cells, respectively). In contrast with treatment with TyrA23, M β CD treatment increased the restricted diffusion to 164% that of untreated control cells (Figure 9C). These results demonstrate that treatment with TyrA23 and M β CD induced qualitatively different changes in GFP-PIP2;1 dynamic characteristics, suggesting that clathrin-dependent endocytosis and membrane rafts exerted different effects on PIP2;1 membrane movements under normal conditions.

The effects of TyrA23 and M β CD were also investigated in cells exposed to the salt treatment. When the roots were pretreated with TyrA23, the \hat{G} of GFP-PIP2;1 decreased to $2.95 \times 10^{-3} \mu\text{m}^2/\text{s}$ (SE 2.62 to $3.33 \times 10^{-3} \mu\text{m}^2/\text{s}$) (Figure 9D; see Supplemental Movie 8 online) ($\hat{G} = 5.62 \times 10^{-3} \mu\text{m}^2/\text{s}$ in the presence of salt alone). Brownian diffusion and restricted diffusion decreased to 78 and 67%, respectively, of the control treatment with salt alone; by contrast, the mixed trajectory increased to 183% of the control treatment with salt alone. No obvious change in directed diffusion was observed (Figure 9F). The tendencies for dynamic changes after treatment with TyrA23 under NaCl exposure were comparable to those after treatment with TyrA23 under normal conditions (cf. Figures 9C and 9F). When the roots were pretreated with M β CD, the bimodal repartition of the diffusion coefficient disappeared and \hat{G} decreased to $2.63 \times 10^{-3} \mu\text{m}^2/\text{s}$ (SE 2.34 to $2.96 \times 10^{-3} \mu\text{m}^2/\text{s}$) (Figure 9E; see Supplemental Movie 9 online). In addition, Brownian diffusion and restricted diffusion decreased to 88 and 78% of the control treatment with salt alone, respectively. While the mixed trajectory increased to 150% of the control treatment with salt alone (Figure 9F), the percentage of directed diffusion was equal to the control treatment with salt alone. The tendencies in dynamic changes after treatment with M β CD under NaCl exposure were different from those after treatment with M β CD under normal conditions. However, they were similar to those after TyrA23 treatment under NaCl exposure, implying that inhibition of clathrin-dependent and membrane raft-associated endocytosis induced similar changes in PIP2;1 movement.

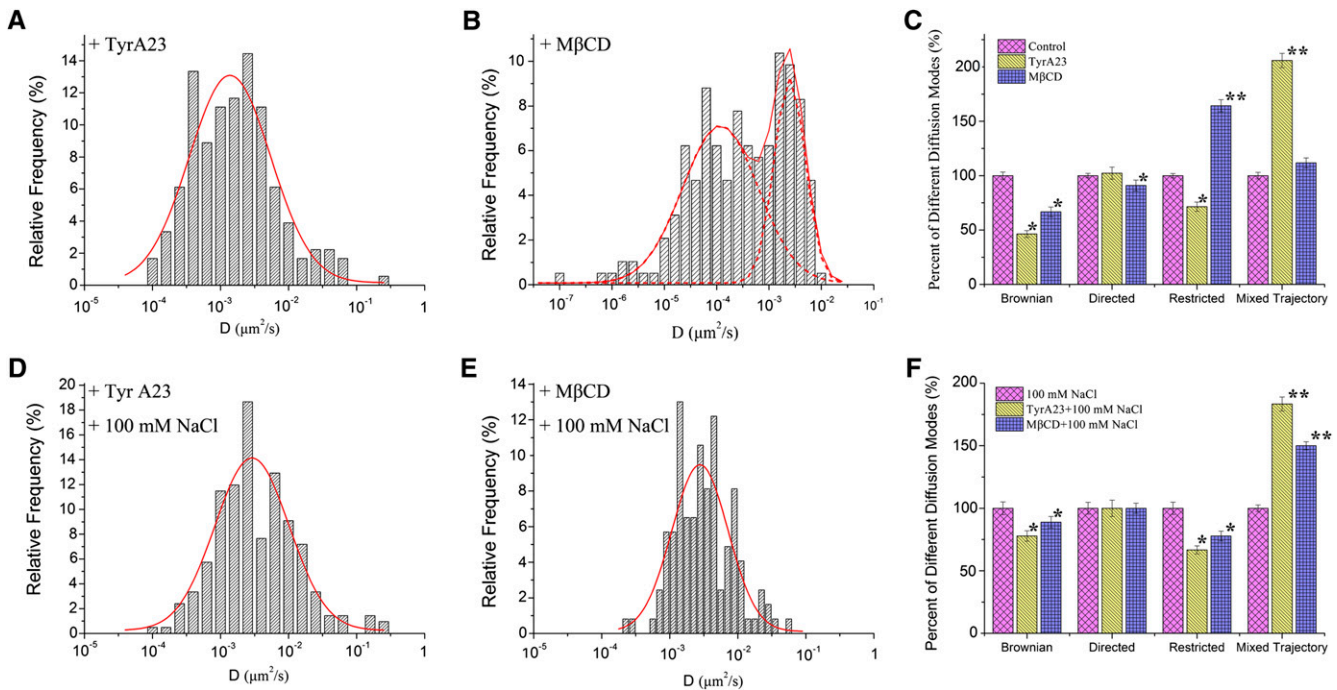


Figure 9. Histograms Showing the Dynamic Characteristics of GFP-PIP2;1 Molecules.

(A) Distribution of diffusion coefficients after treatment with TyrA23 ($n = 180$ spots).

(B) Distribution of diffusion coefficients after treatment with M β CD ($n = 193$ spots); the two peaks (dashed lines, Gaussian fit) indicate that the distribution of diffusion coefficients bifurcated.

(C) Percentage of different diffusion modes under TyrA23 ($n = 96$ individual trajectories) or M β CD treatment ($n = 80$ individual trajectories) compared with the percentage of control cells bathed in half-strength MS medium. Values given are mean \pm SD.

(D) Distribution of diffusion coefficients after treatment with TyrA23 prior to exposure to 100 mM NaCl ($n = 210$ spots).

(E) Histogram showing the distribution of diffusion coefficients after treatment with M β CD coupled with 100 mM NaCl stimulus ($n = 162$ spots).

(F) Percentage of different diffusion modes of GFP-PIP2;1 in cells treated with TyrA23/M β CD prior to 100 mM NaCl exposure ($n = 80$ individual trajectories, respectively) compared with control cells bathed in 100 mM NaCl alone. **Significantly different from the control at $P < 0.01$; *significantly different from the control at $P < 0.05$, t test.

[See online article for color version of this figure.]

Disturbing the Endocytic Pathway Induces Accumulation of PIP2;1 on Plasma Membranes

To reveal the partitioning of PIP2;1 between the plasma membrane and its recycling pathways, FCS was used to measure the density of GFP-PIP2;1 in the plasma membrane under different conditions. FCS measurement was established by focusing an excitation laser beam onto the membrane and then monitoring fluorescence fluctuations within the focal volume of the laser beam (Figure 10A). Applying the parameters of Equation 4 gave an average density for GFP-PIP2;1 of 30.3 ± 5.1 molecules μm^{-2} (Figure 10B), indicating that an average of 11.5 GFP-PIP2;1 molecules occupied the $0.38\text{-}\mu\text{m}^2$ area covered in the confocal volume. A higher GFP-PIP2;1 density (40.1 ± 7.2 molecules μm^{-2} ; 32% increase with respect to control cells; $P < 0.05$, t test) was detected after treatment with TyrA23 (Figure 10B), indicating that more GFP-PIP2;1 molecules dwell on the membrane after the inhibition of clathrin-dependent endocytosis. By contrast, the density of PIP2;1 did not significantly change after treatment with M β CD (32.2 ± 5.4 molecules μm^{-2} ; $P > 0.05$), Fen (30.2 ± 7.1 molecules μm^{-2} ; $P > 0.05$), or PPMP (33.8 ± 8.2 molecules

μm^{-2} ; $P > 0.1$) (Figure 10B), suggesting that under normal conditions, disturbance of membrane rafts did not alter the amount of GFP-PIP2;1 molecules on the membrane. When the roots were exposed to 100 mM NaCl, the GFP-PIP2;1 density dropped to 14.0 ± 3.2 molecules μm^{-2} ($P < 0.001$; Figure 10B), implying that salt exposure induced internalization of PIP2;1. We also measured GFP-PIP2;1 molecular density after disturbing the endocytic pathways prior to exposure to 100 mM NaCl. Under TyrA23 pretreatment, and with respect to 100 mM NaCl alone, the density of GFP-PIP2;1 on plasma membranes significantly increased by $\sim 50\%$ to 21.1 ± 4.4 molecules μm^{-2} ($P < 0.01$; Figure 10B). After disrupting the membrane raft-associated endocytic pathway by a M β CD pretreatment, the density also significantly increased to 18.4 ± 3.0 molecules μm^{-2} ($P < 0.01$; Figure 10B), $>30\%$ higher than that of cells with salt alone. Pretreatments with Fen and PPMP also increased the density of GFP-PIP2;1 to 18.7 ± 7.0 molecules μm^{-2} ($P < 0.01$; Figure 10B) and 25.2 ± 6.2 molecules μm^{-2} ($P < 0.0001$; Figure 10B). These data indicate that both the clathrin-dependent and raft-associated endocytic pathways influenced endocytosis under 100 mM NaCl exposure conditions.

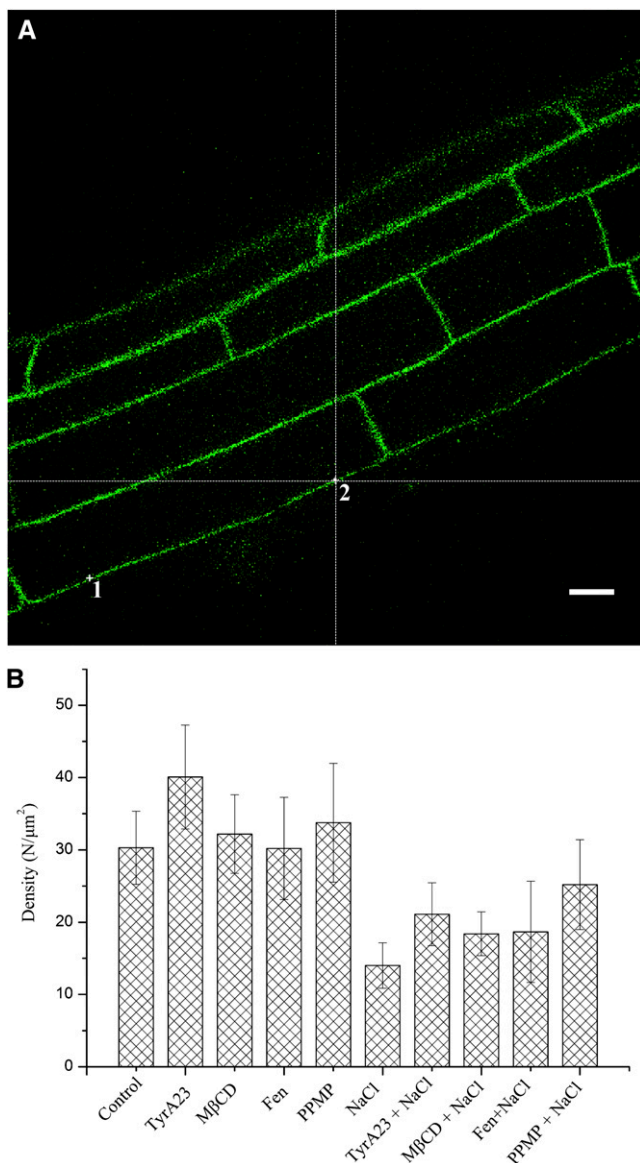


Figure 10. The Density of GFP-PIP2;1 Molecules under Different Conditions as Acquired with FCS.

(A) A confocal image detected by FCS; points 1 and 2 show the location where the laser beam was focused to monitor the fluorescence fluctuations. Bar = 10 μm.

(B) Density of GFP-PIP2;1 on the plasma membrane of epidermal cells under different conditions. Values given are mean ± SD.

[See online article for color version of this figure.]

DISCUSSION

Considering the complex and dynamic architecture of cell plasma membranes, the spatial and temporal dynamics of membrane proteins are definitely closely linked to many fundamental cellular processes (Shinozaki et al., 2009; Zhang et al., 2009b). In this respect, tracking protein dynamics using a single-molecule approach can be advantageous in deciphering the

respective influence of protein interaction or microdomains on the lateral mobility of biomolecules, rather than submerging them into an assembly of characteristics. In this study, we used a high numerical aperture objective and varied the incident angle of the laser beam to obtain an exponentially decaying wave, exciting only fluorophores within 70 to 400 nm proximal to a glass cover slip. In terms of the signal-to-noise ratio, an evanescent wave microscope is up to 10-fold better than a confocal microscope (Wang et al., 2006). Equipped with a high-resolution EMCCD camera, which has extremely high temporal resolution, EWM could obtain near real-time images. Thus, EWM or variable-angle epifluorescence microscopy is an ideal tool for tracking the two-dimensional motion of cell membrane proteins in intact multicellular organisms (Konopka and Bednarek, 2008). This approach has provided valuable and complementary information about spot trafficking, especially in living cells, over lengthy observation periods (Konopka and Bednarek, 2008; Hern et al., 2010). In this investigation, we examined the dynamics and motion of GFP-labeled PIP2;1 molecules in living root cells of *Arabidopsis*. Thus, we achieved visualization of channel proteins at a single-molecule level in living plant cell membranes using EWM.

Since the discovery of aquaporins in plants, the study of these proteins has provided a unique perspective into multiple aspects of plant biology. Integrative (Ehlert et al., 2009) and cellular aspects (Van Wilder et al., 2008; Maurel et al., 2009; Gattolin et al., 2009) of plant-water relations and nutrition have been extensively investigated. However, the characteristics of plant aquaporins at the single-molecular level have remained unclear. Although the structure of aquaporins has been clarified using x-ray crystallography and cryoelectron microscopy (Jap and Li, 1995; Fotiadis et al., 2001; Törnroth-Horsefield et al., 2006), no studies had reported on the oligomeric state of PIPs in the plasma membrane of living plant cells. Here, we imaged GFP-labeled PIP2;1 in the plasma membrane of root cells to determine its oligomeric state. Since the fluorescence signals after expression using a native promoter were too weak to be detected for single-molecule analysis, overexpression of a fluorescently tagged construct was mandatory for this work. The genetic attachment of GFP to PIP2;1 obviated nonspecific labeling that might occur with antibodies and guaranteed that each PIP2;1 polypeptide was labeled with one, and only one, fluorophore. To interpret the oligomeric state of PIP2;1, we counted the photobleaching steps for each of the chosen fluorescent spots. In other channels or receptors (Ulbrich and Isacoff, 2007; Ji et al., 2008; Zhang et al., 2009c), the subunit number and stoichiometry of membrane-bound proteins can be determined from the statistical analysis of bleaching steps of GFP fused to the proteins. As shown in Figure 2, the number of elemental GFP photobleaching steps in an individual punctum was not uniform and ranged from one to four. Since the maximum number was four, a reasonable and conservative conclusion is that PIP2;1 exists on the membrane as a tetramer, in agreement with previous crystallographic studies (Törnroth-Horsefield et al., 2006). Moreover, as the fluorescence intensity distribution was skewed to intensities lower than four fluorophores, it may stem from endogenous unlabeled PIPs or some GFP-PIP2;1 with immature GFP being part of the oligomer. However, another possibility that cannot be excluded is that besides as a tetramer on the plasma membrane,

PIP2;1 exists in various multimeric forms, such as monomers, dimers, or trimers.

The lateral mobility of a molecule is of particular importance as it can be correlated with the molecular state as well as with environmental conditions (Pinaud et al., 2009). Although lateral diffusive mobility on the membrane of living cells has been measured by several means, such as fluorescent recovery after photobleaching, these methods provide only ensemble averaged information regarding the subpopulations, and determining the transition kinetics of diffusion mobility is impossible (Matsuoka et al., 2009). By applying EWM and SPT analysis, we found that the diffusion regime of PIP2;1 in plant cells could be classified into four categories: pure Brownian diffusion, restricted diffusion, directed diffusion, and mixed trajectory. The large dispersion of the diffusion coefficient distribution further confirmed that the diffusion of PIP2;1 on the membrane of root cells was highly heterogeneous. We also found that most of the fluorescent spots with low fluorescence intensity did not have a high diffusion coefficient, and there was no close correlation between the diffusion modes and the fluorescence intensity. However, this does not exclude the possibility that the oligomeric state exerts some effects on the protein motility. Considering that the separation of the membrane in distinct phases has significant effects on the lateral diffusion of a molecule (Korlach et al., 1999; Marguet et al., 2006), we can deduce that PIP2;1 is not uniformly localized in different plasma membrane microdomains. More importantly, PIP2;1 could move into or out of these microdomains, suggesting that the partitioning of PIP2;1 was dynamic. By tracking the motion of GFP-LTI6a, a small integral plasma membrane protein, we found that the diffusion coefficients of GFP-PIP2;1 and GFP-LTI6a were well within the range of various membrane intrinsic proteins reported previously (Cho et al., 1999), confirming that EWM and SPT analyses initially developed in mammalian cells (Loerke et al., 2009) can be similarly applied to plant cells. Comparison of diffusion coefficients of both proteins also revealed that GFP-LTI6a displayed strikingly faster lateral diffusion than GFP-PIP2;1. Whereas the diffusion mode of both proteins shares some common features, PIP2;1 exhibits some unique factors, which require further examination.

Current models of the plasma membrane predict the existence of a patchwork of specialized and dynamic microdomains coordinating a variety of cellular functions (Raffaele et al., 2009). Among the well-characterized plasma membrane microdomains are the membrane rafts formed by the preferential association of certain lipids and proteins into sterol- and glycosphingolipid-rich liquid ordered phases (also called detergent-resistant membranes) (Pinaud et al., 2009). Previous proteomic studies revealed a tendency of PIPs to partition in detergent-resistant membranes (membrane rafts) (Mongrand et al., 2004; Borner et al., 2005); however, whether this corresponds to an enrichment in true plasma membrane microdomains in living plant cells remained to be determined. To acquire a more detailed understanding of PIP2;1 partitioning in native membranes, we used the sterol-depleting drug, M β CD, and more specific inhibitors, Fen and PPMP, which affect the biosynthesis of sterol and sphingolipids. After treatment with these compounds, we observed a remarkable clustering effect of fluorescent foci and the disappearance of PIP2;1 molecules in certain areas, indicating that

the partitioning of GFP-PIP2;1 is closely related to sterols and sphingolipids. Considering that sterols and sphingolipids promote the formation of membrane rafts and affect lipid dynamics on membranes, we speculated that the partitioning of PIP2;1 in the plasma membrane was associated with membrane rafts. To determine further if PIP2;1 was involved in membrane rafts, we adopted a general method called dynamic single-molecule colocalization, which was used to quantify the associations of single-cell surface molecules labeled with distinct fluorescent proteins, namely, GFP-PIP2;1 and mCherry-Flot1 (taken here as a raft marker). The chief advantages of the new quantitative approach were that in addition to stable interactions, it was capable of measuring nonconstitutive associations and was applicable to situations with low numbers of molecules. In cells that coexpressed GFP-PIP2;1 and mCherry-Flot1, we observed that some PIP2;1 fluorescent foci were colocalizing with Flot1 foci and that the joint movement of these molecules was mainly confined to specific areas, suggesting that it was correlated with entry into or interaction with quasistationary membrane rafts. The results provide strong evidence that lipid microdomains are involved in confining PIP2;1 in the plasma membrane.

Recent studies have pointed to protein trafficking as a critical point in regulating plant aquaporin function. This process contributes to diverse responses, such as nutritional adjustments and modification of the number of active proteins at the plasma membrane (Takano et al., 2005). PIP molecules are subject to constitutive cycling between the plasma membrane and cytoplasm through processes of endo- and exocytosis (reviewed in Maurel et al., 2009). In addition, the alteration of PIP abundance at the plasma membrane through stimulus-induced trafficking of PIPs is a significant mechanism to regulate root water transport (Boursiac et al., 2005, 2008; Maurel et al., 2009). We observed a salt-induced intracellular accumulation of GFP-PIP2;1 and a reduced membrane density. Given that the intracellular accumulation of GFP-LTI6a was much less pronounced, we propose that the enhanced internalization was a specific response of GFP-PIP2;1 under hypertonic stress, acting as a regulator to protect cells or the plant against water-deficit stress. SPT analysis further revealed that under these conditions, the diffusion coefficient and the percentage of restricted diffusion dramatically increased. From these results, we conclude that PIP2;1 undergoing enhanced endocytosis is characterized by an increased diffusion coefficient and that spatially restricted diffusion is an important feature of the endocytic process. In agreement with this, restricted diffusion was reported to be a predominant diffusion mode in internalized QD-NGF complexes (Rajan et al., 2008).

In this work, we also dissected the endocytic pathway(s) of PIP2;1 by analyzing the effects of specific inhibitors. TyrA23 can specifically prevent the interaction between cargo motifs destined for endocytosis and the μ 2 subunit of the clathrin binding AP-2 adaptor complex (Banbury et al., 2003). A recent report showed that TyrA23 efficiently inhibited interaction between the human transferrin receptor and a μ -adaptin subunit and then blocked the internalization of the human transferrin receptor in *Arabidopsis* protoplasts (Ortiz-Zapater et al., 2006). Thus, it is widely used to inhibit clathrin-dependent endocytosis without causing discernible morphological changes (Dhonukshe et al., 2007; Robinson et al., 2008). Previous investigations demonstrated that the

accumulation of PIP2;1 in the Brefeldin A compartment was inhibited by TyrA23, suggesting that clathrin might be involved in PIP2;1 endocytic mechanisms (Dhonukshe et al., 2007). The colocalization of GFP-PIP2;1 with mCherry-CLC and an increase in PIP2;1 density in the plasma membrane after TyrA23 treatment reported in this study further support this conclusion. SPT analysis of diffraction-limited fluorescent spots also showed that the repartitioning of diffusion modes and changes in diffusion coefficients induced by TyrA23 were counteracted in the presence of NaCl. Given the link between NaCl treatment and enhanced internalization of PIP2;1, we inferred that the changes after TyrA23 treatment resulted mainly from the inhibition of endocytosis and that the internalization of PIP2;1 under both normal and salt stress conditions was predominantly associated with the clathrin-dependent pathway.

Besides clathrin-dependent endocytosis, other entry pathways are considered to operate in plant cells, among which membrane raft-associated endocytosis is an important form (Murphy et al., 2005). The raft-associated pathway, defined as a sterol-sensitive and clathrin-independent internalization of cargoes from the plasma membrane, is considered to be a new route of endocytosis (Lajoie and Nabi, 2007). Sterol-dependent endocytosis has been reported to mediate postcytokinetic acquisition of PIN2 auxin efflux carrier polarity in *Arabidopsis* (Men et al., 2008). Since we found that the partitioning of PIP2;1 on the plasma membrane was closely associated with membrane rafts, we were also curious as to whether the uptake mechanism of PIP2;1 from the plasma membrane was related to these membrane domains. SPT analysis showed that in seedlings with M β CD under normal conditions, diffusion coefficients of PIP2;1 became bifurcated, suggesting that two different pools of PIP2;1 were segregated into different membrane domains. Considering that sterol depletion induces different changes in the continuous nonraft phase and stationary microdomains, respectively, the bifurcated diffusion coefficients confirmed the aforementioned conclusion that the partitioning of PIP2;1 was associated with a type of membrane rafts. FCS also indicated that under normal conditions, M β CD treatment did not change PIP2;1 density at the plasma membranes. Thus, in contrast with their important role in

PIP2;1 partitioning, membrane rafts made a low contribution to internalization under normal conditions.

When seedlings were treated with M β CD together with 100 mM NaCl, SPT analysis showed that the repartitioning of different diffusion modes and changes in diffusion coefficients were similar to those observed after a TyrA23 plus NaCl treatment. TyrA23 was somewhat able to counteract the effects of NaCl exposure; similarly, M β CD pretreatment significantly increased the plasma membrane density of PIP2;1 in NaCl-treated cells. Thus, we can reasonably conclude that under salt stress, the membrane raft-associated pathway was stimulated and contributed to the enhanced internalization of PIP2;1. The FCCS quantitative analysis presented in this work also suggested that the contribution of raft-associated components to PIP2;1 cell dynamics is greater under salt stress than under control conditions. In fact, the combined effects of two endocytic pathways have already been observed in animals (Schneider et al., 2008). Our data suggest along these lines that the stimulated endocytosis of PIP2;1 under salt stress depends on the action of clathrin-dependent and membrane raft-associated pathways simultaneously.

In conclusion, this work shows that EWM detection and SPT analysis can substantially enhance our understanding of plant plasma membrane protein dynamics. The study also revealed previously undiscovered associations between membrane dynamics and the regulation properties of PIP2;1, a major plant aquaporin. The behavior of PIP2;1 in the plasma membrane of living cells was highly heterogeneous and could be described using four diffusion categories; moreover, membrane rafts were found to play an important role in the membrane partitioning of PIP2;1. Whereas clathrin-dependent endocytosis of PIP2;1 was predominant under normal conditions, a membrane raft-associated pathway was also involved under NaCl stress. Thus, stress-induced changes in PIP2;1 density at the plant plasma membrane do not rely on a unimodal endocytosis as the mechanism of uptake, as summarized in Figure 11. Taken together, these findings provide new insights into the regulation mechanisms of PIP2;1 through dynamic partitioning on the membrane and alternate recycling pathways.

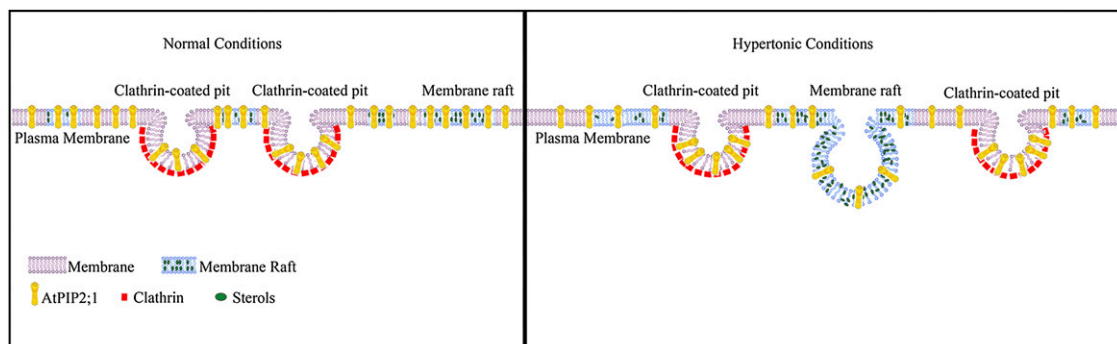


Figure 11. Hypothetical Model Summarizing the Endocytic Pathway of PIP2;1 under Normal and Hypertonic Conditions.

Under normal conditions, the constitutive cycling of PIP2;1 is mediated mainly by clathrin-coated pits. Under hypertonic conditions, however, the enhanced cycling of PIP2;1 depends on simultaneous internalization through clathrin-dependent and membrane raft-associated pathways.

METHODS

Plant Culture and Transformation

A *GFP-PIP2;1* plant expression vector was constructed as follows. The coding sequence for At-PIP2;1 was PCR amplified using the primers 5'-TCTAGAATGGCAAAGGATGTGGAAGCCGTTTC-3' and 5'-GTCGAC-TTAGACGTTGGCAGCACTTCTGAAT-3' and was subcloned as a *Xba*I-*Sal*I fragment into a modified pCAMBIA2300 vector (Hajdukiewicz et al., 1994). The *mCherry-AtFlot1* and *mCherry-CLC* (At2g40060) plant expression vectors were constructed with the coding sequences for Flot1 and CLC, which were PCR amplified using specific primer pairs (*Flot1*, 5'-GGATCCATGTTCAAAGTTGCAAG-3' and 5'-GAATTCCTAGCTGC-GAGTCACTT-3'; *CLC*, 5'-GGATCCATGTCTGCCTTTGAAGACGATT-CCT-3' and 5'-GAATTCCTAAGCAGCAGTAACTGCCTCAGTG-3') and subcloned as *Bam*HI-*Eco*RI fragments into a modified pCAMBIA1200 vector (Hajdukiewicz et al., 1994).

Arabidopsis thaliana ecotype Columbia wild type was transformed with the *GFP-PIP2;1*, *mCherry-Flot1*, and *mCherry-CLC* constructs using the *Agrobacterium tumefaciens*-mediated floral dip method (Clough and Bent, 1998). The preparation of plants expressing a GFP-LTi6a is described elsewhere (Cutler et al., 2000). Transgenic plants were selected on solid medium (1% agar), half-strength Murashige and Skoog (MS) salts medium containing 50 µg/mL kanamycin for *GFP-PIP2;1*, and 70 µg/mL hygromycin for *mCherry-Flot1* and *mCherry-CLC*.

Seeds were surface sterilized for 2 min in 70% ethanol, transferred to 5% (v/v) NaClO for 15 min, and then washed five times with sterilized distilled water. Subsequently, they were transferred to a thin layer of solid medium containing half-strength MS salts with 0.7% plant agar. Plants were cultured at 22°C under long-day conditions (16 h light, 8 h dark) for 4 d.

Drug Treatment

The stock solution of MβCD (Sigma-Aldrich) was prepared in deionized water. TyrA23 (Sigma-Aldrich) was dissolved in 100% DMSO to yield a 50 mM stock solution. The inhibitors were diluted in half-strength MS medium, and the final DMSO concentration was ≤0.1% (v/v) in all EWM analyses. Vertically grown 4-d-old seedlings were incubated in half-strength liquid MS medium containing 50 µM TyrA23 or 10 mM MβCD for 30 min. For the TyrA23 washout experiment, the seedlings were first incubated in half-strength liquid MS medium containing 50 µM TyrA23 for 30 min, transferred to media without TyrA23 for 20 min, then observed under EWM. For the treatment with Fen, seedlings were grown vertically on half-strength MS, 0.7% agar plates with 10 µg/mL Fen for 4 d prior to imaging in half-strength MS media. For treatment with PPMP, the seedlings first grew on half-strength MS agar medium for 2 d and then the 2-d-old seedlings were transferred to MS agar medium with 10 µM PPMP to grow for another 2 d.

The effects of NaCl were studied by supplementing the half-strength MS medium with 100 mM NaCl. Parallel experiments with sorbitol were performed by supplementing the half-strength MS medium with 200 mM sorbitol. The effects of TyrA23 and MβCD under 100 mM NaCl exposure were studied by pretreatment with 50 µM TyrA23 or 10 mM MβCD for 30 min followed by incubation in the same solution but supplemented with 100 mM NaCl. After the indicated times, seedlings were transferred to a glass slide with 150 µL of inhibitor solution and covered with a cover slip.

Confocal Laser Scanning Microscopy Observations

For FM4-64 staining, 4-d-old vertically grown seedlings were transferred to 2.5 µM FM4-64 diluted in half-strength MS medium for 3 min after being exposed to 100 mM NaCl for 10 min. Then these seedlings were observed under confocal laser scanning microscopy.

Single-Molecule Fluorescence Imaging

An objective-type evanescent wave microscope, which was based on an inverted microscope (IX-71; Olympus) with a total internal reflective fluorescence illuminator and a ×100 oil-immersion objective (Olympus; numerical aperture = 1.45), was used for single-molecule fluorescence imaging. The 473-nm/561-nm laser line from a diode laser (Changchun New Industries Optoelectronics Technology) was used to excite GFP and mCherry. Fluorescence signals were collected by the objective and passed through two filters, a BA 510IF long-pass filter (Chroma) and an HQ525/50 band-pass filter (Chroma), before being directed using a back-illuminated, EMCCD camera (ANDOR iXon DV8897D-CS0-VP; Andor Technology) and high-quality filters (band-pass 525/45 and 609/54 nm). We set the gain of our EMCCD camera at 300 throughout all single-molecule imaging experiments; the setting was in the linear dynamic range of the EMCCD camera. Images were acquired with 100-ms exposure time and analyzed with Image J software (NIH).

Image Analysis and Tracking of Single Molecules

Time-lapse series of single particles of *GFP-PIP2;1* images were taken at up to 200 images per sequence. For the analysis of single-molecule fluorescence intensity in a movie acquired from living cells, the background fluorescence was first subtracted from each frame using the rolling ball method in Image J software. Then, the first frame of each movie was used for fluorescent spot (region of interest) selection. After the image processing, the brightest pixel in each fluorescent spot within the diffraction-limited size (3 × 3 pixels) was determined as the central position, and a square of 3 × 3 pixels was enclosed as a region of interest to calculate the integrated fluorescence intensity with Image J.

To analyze dynamic properties, *GFP-PIP2;1* foci were tracked using spatially and temporally global particle assignment, described in detail elsewhere (Jaqaman et al., 2008). We analyzed the MSD of fluorescence-labeled *PIP2;1* spots using the following equation:

$$\text{MSD} = (x - x_0)^2 + (y - y_0)^2 \quad (1)$$

where x_0 and y_0 are the initial coordinates, and x and y are the coordinates at any given time (Haggie and Verkman, 2008).

For calculating the diffusion coefficient, we plotted MSD from each trajectory against time. For each molecule, the slope of the first four time points in the MSD- t plot was used to calculate the diffusion coefficient (D) according to the following equation (Xiao et al., 2008):

$$\text{MSD}_{t \rightarrow 0} = 4Dt \quad (2)$$

In the text, the diffusion coefficients correspond to single (or multiple) Gaussian fit(s) of the D-histograms. The SE values of the position of the peak (noted as \hat{G}) were determined using Origin software (OriginLab) and are given in the form of an upper and lower diffusion coefficient. Determination of the motional modes (Brownian, restricted, directed diffusion, or mixed trajectory) and parameters was performed according to Espenel et al. (2008). For each trajectory, we first linearly fit the MSD. If the MSD- t plot was a straight line with a slope of $4D$, it was a typical trajectory for spots undergoing Brownian diffusion. If the MSD- t plot showed a positive or negative deviation from a straight line with a slope of $4D$, the motion was determined as directed or restricted diffusion. For the mixed trajectory exhibiting a combination of Brownian and apparent restricted diffusion mode, the trajectory was split, and the MSD of each segment was adjusted with a linear or an exponential curve. In a few cases, no convincing MSD- t fits could be obtained, and the trajectories were rejected.

The range of an individual fluorescent spot movement during the time interval (T_n) can be estimated from the following equation:

$$\text{Range}(n) = \sqrt{[x_n - x_{(n-1)}]^2 + [y_n - y_{(n-1)}]^2} \quad (3)$$

The colocalization algorithm was obtained using the Image J plugins Colocalization Test and Colocalization Threshold of T. Collins and

W. Rasband, and BG Subtraction from ROI from M. Cammer and T. Collins (www.uhnresearch.ca/facilities/wcif/imagej). Colocalization was performed as previously described (Zhang et al., 2009a).

FCS Analyses

FCS was performed on a Leica TCS SP5 FCS microscope, equipped with a 488-nm argon laser, in-house coupled correlator, and Avalanche photodiode. After acquiring a scan image of cells in transmitted light mode, FCS was performed in the point-scanning mode. The laser focus was placed at the plasma membrane of a cell. The diffusion of fluorophores into and out of the focal volume alters the local concentration of fluorophores and thus leads to spontaneous fluorescence intensity fluctuations.

The autocorrelation function $G(\tau)$ was calculated with the hardware correlator as $[\delta F(t) \delta F(t + \tau)]/[F(t)]^2$, where $F(t)$ is the fluorescence fluctuation caused by a particle entering the confocal volume and $F(t + \tau)$ is the fluorescence fluctuation by the same particle at time $(t + \tau)$. IgorPro software was used to fit the data to the two-dimensional one particle, one-triplet (2D1P1t) models as follows:

$$G(\tau) = \frac{1}{N} \times \left[\left\{ \frac{1}{(1 + \tau/\tau D)} \right\} \left\{ 1 + \frac{F_{\text{trip}}}{(1 - F_{\text{trip}})} \times e^{-(\tau/\tau_{\text{trip}})} \right\} \right] + 1 \quad (4)$$

where N is the number of particles in the observation volume, F_{trip} is the fraction of particles in the triplet state, and t_{trip} is the triplet relaxation time.

When the volume element was projected onto a single cell, GFP-labeled PIP2;1 localized in the cell membrane was observed. Thus, the parameter N , which could be obtained by fitting the autocorrelation function, characterized the total number of GFP-PIP2;1 proteins in the cell membrane inside the confocal volume. The dimensions of the observation volume element were defined by the half-axes for length (ω_z) and width (ω_{xy}). The waist of the confocal volume ellipsoid was assumed to be situated on the cell membrane such that the highest fluorescence intensity was given. In this case, the surface area on the membrane covered by the focus would be a circular area with a radius equal to ω_{xy} . The circular area covered by the focus volume could be estimated as $\pi (\omega_{xy})^2 = \pi \times (0.35 \mu\text{m})^2 = 0.38 \mu\text{m}^2$. Therefore, the GFP-PIP2;1 density estimated in the confocal volume could be expressed as the total number of GFP-PIP2;1 divided by the area covered as follows:

$$\text{Density} = N / [\pi (\omega_{xy})^2] \quad (5)$$

The GFP-PIP2;1 density was obtained from each individual cell membrane. Two random positions were selected once, and an autocorrelation measurement was performed for 20 s each for every single measurement point. Up to six random points were selected in one cell, three cells were chosen in a root, and at least five representative roots were studied for each measurement.

For quantitatively evaluating the interaction of GFP-PIP2;1/mCherry-Flot1 and GFP-PIP2;1/mCherry-CLC, FCCS was performed. The amplitude of the cross-correlation function was normalized to the amplitude of the autocorrelation function of GFP to calculate the relative cross-correlation ($[Gc(0)]/[Gg(0)]$), as described in a previous investigation (Noda et al., 2008). Up to six random points were selected in one cell, five cells were chosen in a root, and at least three representative roots were studied for each measurement.

Accession Numbers

Sequence data from this article can be found in The Arabidopsis Information Resource database under the following accession numbers: PIP2;1 (At3g53420), Flot1 (At5g25250), and CLC (At2g40060).

Supplemental Data

The following materials are available in the online version of this article.

Supplemental Figure 1. EWM Detection of the GFP Fluorescence Signal.

Supplemental Figure 2. The Dynamic Characteristics of GFP-Labeled PIP2;1 Spots Plotted against the Fluorescence Intensity.

Supplemental Figure 3. Automated Tracking and Statistical Analysis of GFP-LTI6a Spots on the Plasma Membrane.

Supplemental Figure 4. Sterol Content of Plasma Membranes Labeled with Filipin.

Supplemental Figure 5. Organization of the Actin Cytoskeleton in Control (Untreated) and M β CD-Treated Seedlings.

Supplemental Figure 6. Characteristics of the GFP-PIP2;1 Partitioning on the Plasma Membrane after Treatment with Fen and PPMP.

Supplemental Figure 7. Parallel Experiments Using Seedlings Expressing GFP-PIP2;1 or GFP-LTI6a as a Plasma Membrane Marker and Treated with Salt or Sorbitol as a Comparable Osmotic Stress.

Supplemental Figure 8. Distribution of Diffusion Coefficients for GFP-PIP2;1 on the Plasma Membrane of Epidermal Cells after TyrA23 Washout and TyrA51 Treatment.

Supplemental Table 1. Comparison of Actin Dynamic Parameters from Control and M β CD-Treated Root Cells.

Supplemental Movie 1. Dynamics of GFP-Labeled PIP2;1 on the Plasma Membrane Driven by the Native Promoter.

Supplemental Movie 2. Dynamics of GFP-PIP2;1 on the Plasma Membrane under Normal Conditions Detected by EWM.

Supplemental Movie 3. Dynamics of the Actin Cytoskeleton in Control (Untreated) Seedlings.

Supplemental Movie 4. Dynamics of the Actin Cytoskeleton in M β CD-Treated Seedlings.

Supplemental Movie 5. Dynamics of GFP-PIP2;1 on the Plasma Membrane under Salt Stress Detected by EWM.

Supplemental Movie 6. Dynamics of GFP-PIP2;1 on the Plasma Membrane after Treatment with TyrA23 Detected by EWM.

Supplemental Movie 7. Dynamics of GFP-PIP2;1 on the Plasma Membrane after Treatment with M β CD Detected by EWM.

Supplemental Movie 8. Dynamics of GFP-PIP2;1 on the Plasma Membrane after Treatment with TyrA23 Coupled with a 100 mM NaCl Stimulus.

Supplemental Movie 9. Dynamics of GFP-PIP2;1 on the Plasma Membrane after Treatment with M β CD Coupled with a 100 mM NaCl Stimulus.

ACKNOWLEDGMENTS

We thank Wei Ji and Wangxi Luo for technical assistance with EWM as well as Yinglang Wan and Lusheng Fan for their valuable comments on data analysis and early drafts of this manuscript. This work is supported by the National Basic Research Program of China (973 Program 2011CB809103 and 2007CB108703), the Chinese Academy of Sciences/State Administration of Foreign Experts Affairs International Partnership Program for Creative Research Teams (20090491019), the National Natural Science Foundation of China (30730009, 30821007, and 30900072), and the Knowledge Innovation Program of the Chinese Academy of Sciences (KJX2-YW-L08 and KSCX2-EW-J-1).

AUTHOR CONTRIBUTIONS

X.L. and J.L. designed the research. X.L., R.L., D.-T.L., and C.M. performed the experiments. X.L., X.W., and Y.Y. analyzed data. Q.H.

and X.F. contributed new analytic tools. X.L, D.-T.L., C.M., and J.L. wrote the article.

Received September 9, 2011; revised September 9, 2011; accepted October 3, 2011; published October 18, 2011.

REFERENCES

- Banbury, D.N., Oakley, J.D., Sessions, R.B., and Banting, G.** (2003). Tyrothostin A23 inhibits internalization of the transferrin receptor by perturbing the interaction between tyrosine motifs and the medium chain subunit of the AP-2 adaptor complex. *J. Biol. Chem.* **278**: 12022–12028.
- Bhat, R.A., and Panstruga, R.** (2005). Lipid rafts in plants. *Planta* **223**: 5–19.
- Biela, A., Grote, K., Otto, B., Hoth, S., Hedrich, R., and Kaldenhoff, R.** (1999). The *Nicotiana tabacum* plasma membrane aquaporin NtAQP1 is mercury-insensitive and permeable for glycerol. *Plant J.* **18**: 565–570.
- Borner, G.H., Sherrier, D.J., Weimar, T., Michaelson, L.V., Hawkins, N.D., Macaskill, A., Napier, J.A., Beale, M.H., Lilley, K.S., and Dupree, P.** (2005). Analysis of detergent-resistant membranes in *Arabidopsis*. Evidence for plasma membrane lipid rafts. *Plant Physiol.* **137**: 104–116.
- Boursiac, Y., Boudet, J., Postaire, O., Luu, D.T., Tournaire-Roux, C., and Maurel, C.** (2008). Stimulus-induced downregulation of root water transport involves reactive oxygen species-activated cell signalling and plasma membrane intrinsic protein internalization. *Plant J.* **56**: 207–218.
- Boursiac, Y., Chen, S., Luu, D.T., Sorieul, M., van den Dries, N., and Maurel, C.** (2005). Early effects of salinity on water transport in *Arabidopsis* roots. Molecular and cellular features of aquaporin expression. *Plant Physiol.* **139**: 790–805.
- Chaumont, F., Moshelion, M., and Daniels, M.J.** (2005). Regulation of plant aquaporin activity. *Biol. Cell* **97**: 749–764.
- Cho, M.R., Knowles, D.W., Smith, B.L., Moulds, J.J., Agre, P., Mohandas, N., and Golan, D.E.** (1999). Membrane dynamics of the water transport protein aquaporin-1 in intact human red cells. *Biophys. J.* **76**: 1136–1144.
- Clough, S.J., and Bent, A.F.** (1998). Floral dip: A simplified method for *Agrobacterium*-mediated transformation of *Arabidopsis thaliana*. *Plant J.* **16**: 735–743.
- Cutler, S.R., Ehrhardt, D.W., Griffiths, J.S., and Somerville, C.R.** (2000). Random GFP:cDNA fusions enable visualization of subcellular structures in cells of *Arabidopsis* at a high frequency. *Proc. Natl. Acad. Sci. USA* **97**: 3718–3723.
- Dahan, M., Lévi, S., Luccardini, C., Rostaing, P., Riveau, B., and Triller, A.** (2003). Diffusion dynamics of glycine receptors revealed by single-quantum dot tracking. *Science* **302**: 442–445.
- Dhonukshe, P., Aniento, F., Hwang, I., Robinson, D.G., Mravec, J., Stierhof, Y.D., and Friml, J.** (2007). Clathrin-mediated constitutive endocytosis of PIN auxin efflux carriers in *Arabidopsis*. *Curr. Biol.* **17**: 520–527.
- Douglass, A.D., and Vale, R.D.** (2005). Single-molecule microscopy reveals plasma membrane microdomains created by protein-protein networks that exclude or trap signaling molecules in T cells. *Cell* **121**: 937–950.
- Ehler, C., Maurel, C., Tardieu, F., and Simonneau, T.** (2009). Aquaporin-mediated reduction in maize root hydraulic conductivity impacts cell turgor and leaf elongation even without changing transpiration. *Plant Physiol.* **150**: 1093–1104.
- Espenel, C., Margeat, E., Dosset, P., Arduise, C., Le Grimmellec, C., Royer, C.A., Boucheix, C., Rubinstein, E., and Milhiet, P.E.** (2008). Single-molecule analysis of CD9 dynamics and partitioning reveals multiple modes of interaction in the tetraspanin web. *J. Cell Biol.* **182**: 765–776.
- Fetter, K., Van Wilder, V., Moshelion, M., and Chaumont, F.** (2004). Interactions between plasma membrane aquaporins modulate their water channel activity. *Plant Cell* **16**: 215–228.
- Foresti, O., Gershlick, D.C., Bottanelli, F., Hummel, E., Hawes, C., and Denecke, J.** (2010). A recycling-defective vacuolar sorting receptor reveals an intermediate compartment situated between prevacuoles and vacuoles in tobacco. *Plant Cell* **22**: 3992–4008.
- Fotiadis, D., Jenő, P., Mini, T., Wirtz, S., Müller, S.A., Fraysse, L., Kjellbom, P., and Engel, A.** (2001). Structural characterization of two aquaporins isolated from native spinach leaf plasma membranes. *J. Biol. Chem.* **276**: 1707–1714.
- Gattolin, S., Sorieul, M., Hunter, P.R., Khonsari, R.H., and Frigerio, L.** (2009). *In vivo* imaging of the tonoplast intrinsic protein family in *Arabidopsis* roots. *BMC Plant Biol.* **9**: 133.
- Haggie, P.M., and Verkman, A.S.** (2008). Monomeric CFTR in plasma membranes in live cells revealed by single molecule fluorescence imaging. *J. Biol. Chem.* **283**: 23510–23513.
- Hajdukiewicz, P., Svab, Z., and Maliga, P.** (1994). The small, versatile pZP family of *Agrobacterium* binary vectors for plant transformation. *Plant Mol. Biol.* **25**: 989–994.
- Hern, J.A., Baig, A.H., Mashanov, G.I., Birdsall, B., Corrie, J.E., Lazareno, S., Molloy, J.E., and Birdsall, N.J.** (2010). Formation and dissociation of M1 muscarinic receptor dimers seen by total internal reflection fluorescence imaging of single molecules. *Proc. Natl. Acad. Sci. USA* **107**: 2693–2698.
- Jap, B.K., and Li, H.** (1995). Structure of the osmo-regulated H₂O-channel, AQP-CHIP, in projection at 3.5 Å resolution. *J. Mol. Biol.* **251**: 413–420.
- Jaqaman, K., Loerke, D., Mettlen, M., Kuwata, H., Grinstein, S., Schmid, S.L., and Danuser, G.** (2008). Robust single-particle tracking in live-cell time-lapse sequences. *Nat. Methods* **5**: 695–702.
- Ji, W., Xu, P., Li, Z., Lu, J., Liu, L., Zhan, Y., Chen, Y., Hille, B., Xu, T., and Chen, L.** (2008). Functional stoichiometry of the unitary calcium-release-activated calcium channel. *Proc. Natl. Acad. Sci. USA* **105**: 13668–13673.
- Joo, C., Balci, H., Ishitsuka, Y., Buranachai, C., and Ha, T.** (2008). Advances in single-molecule fluorescence methods for molecular biology. *Annu. Rev. Biochem.* **77**: 51–76.
- Katsuhara, M., Hanba, Y.T., Shiratake, K., and Maeshima, M.** (2008). Expanding roles of plant aquaporins in plasma membranes and cell organelles. *Funct. Plant Biol.* **35**: 1–14.
- Konopka, C.A., Backues, S.K., and Bednarek, S.Y.** (2008). Dynamics of *Arabidopsis* dynamin-related protein 1C and a clathrin light chain at the plasma membrane. *Plant Cell* **20**: 1363–1380.
- Konopka, C.A., and Bednarek, S.Y.** (2008). Variable-angle epifluorescence microscopy: A new way to look at protein dynamics in the plant cell cortex. *Plant J.* **53**: 186–196.
- Korlach, J., Schwille, P., Webb, W.W., and Feigenson, G.W.** (1999). Characterization of lipid bilayer phases by confocal microscopy and fluorescence correlation spectroscopy. *Proc. Natl. Acad. Sci. USA* **96**: 8461–8466.
- Lajoie, P., and Nabi, I.R.** (2007). Regulation of raft-dependent endocytosis. *J. Cell. Mol. Med.* **11**: 644–653.
- Lee, H.K., Cho, S.K., Son, O., Xu, Z., Hwang, I., and Kim, W.T.** (2009). Drought stress-induced Rma1H1, a RING membrane-anchor E3 ubiquitin ligase homolog, regulates aquaporin levels via ubiquitination in transgenic *Arabidopsis* plants. *Plant Cell* **21**: 622–641.
- Loerke, D., Mettlen, M., Yarar, D., Jaqaman, K., Jaqaman, H.,**

- Danuser, G., and Schmid, S.L. (2009). Cargo and dynamin regulate clathrin-coated pit maturation. *PLoS Biol.* **7**: e57.
- Marguet, D., Lenne, P.F., Rigneault, H., and He, H.T. (2006). Dynamics in the plasma membrane: how to combine fluidity and order. *EMBO J.* **25**: 3446–3457.
- Martre, P., Morillon, R., Barrieu, F., North, G.B., Nobel, P.S., and Chrispeels, M.J. (2002). Plasma membrane aquaporins play a significant role during recovery from water deficit. *Plant Physiol.* **130**: 2101–2110.
- Matsuoka, S., Shibata, T., and Ueda, M. (2009). Statistical analysis of lateral diffusion and multistate kinetics in single-molecule imaging. *Biophys. J.* **97**: 1115–1124.
- Maurel, C., Santoni, V., Luu, D.T., Wudick, M.M., and Verdoucq, L. (2009). The cellular dynamics of plant aquaporin expression and functions. *Curr. Opin. Plant Biol.* **12**: 690–698.
- Maurel, C., Verdoucq, L., Luu, D.T., and Santoni, V. (2008). Plant aquaporins: Membrane channels with multiple integrated functions. *Annu. Rev. Plant Biol.* **59**: 595–624.
- Mayor, S., and Pagano, R.E. (2007). Pathways of clathrin-independent endocytosis. *Nat. Rev. Mol. Cell Biol.* **8**: 603–612.
- Men, S., Boutté, Y., Ikeda, Y., Li, X., Palme, K., Stierhof, Y.D., Hartmann, M.A., Moritz, T., and Grebe, M. (2008). Sterol-dependent endocytosis mediates post-cytokinetic acquisition of PIN2 auxin efflux carrier polarity. *Nat. Cell Biol.* **10**: 237–244.
- Mongrand, S., Morel, J., Laroche, J., Claverol, S., Carde, J.P., Hartmann, M.A., Bonneau, M., Simon-Plas, F., Lessire, R., and Bessoule, J.J. (2004). Lipid rafts in higher plant cells: purification and characterization of Triton X-100-insoluble microdomains from tobacco plasma membrane. *J. Biol. Chem.* **279**: 36277–36286.
- Murphy, A.S., Bandyopadhyay, A., Holstein, S.E., and Peer, W.A. (2005). Endocytotic cycling of PM proteins. *Annu. Rev. Plant Biol.* **56**: 221–251.
- Noda, Y., et al. (2008). Reciprocal interaction with G-actin and tropomyosin is essential for aquaporin-2 trafficking. *J. Cell Biol.* **182**: 587–601.
- Ortiz-Zapater, E., Soriano-Ortega, E., Marcote, M.J., Ortiz-Masiá, D., and Aniento, F. (2006). Trafficking of the human transferrin receptor in plant cells: Effects of tyrphostin A23 and brefeldin A. *Plant J.* **48**: 757–770.
- Otto, B., et al. (2010). Aquaporin tetramer composition modifies the function of tobacco aquaporins. *J. Biol. Chem.* **285**: 31253–31260.
- Pérez-Gómez, J., and Moore, I. (2007). Plant endocytosis: It is clathrin after all. *Curr. Biol.* **17**: R217–R219.
- Pinaud, F., Michalet, X., Iyer, G., Margeat, E., Moore, H.P., and Weiss, S. (2009). Dynamic partitioning of a glycosyl-phosphatidylinositol-anchored protein in glycosphingolipid-rich microdomains imaged by single-quantum dot tracking. *Traffic* **10**: 691–712.
- Postaire, O., Tournaire-Roux, C., Grondin, A., Boursiac, Y., Morillon, R., Schäffner, A.R., and Maurel, C. (2010). A PIP1 aquaporin contributes to hydrostatic pressure-induced water transport in both the root and rosette of *Arabidopsis*. *Plant Physiol.* **152**: 1418–1430.
- Prak, S., Hem, S., Boudet, J., Viennois, G., Sommerer, N., Rossignol, M., Maurel, C., and Santoni, V. (2008). Multiple phosphorylations in the C-terminal tail of plant plasma membrane aquaporins: role in subcellular trafficking of AtPIP2;1 in response to salt stress. *Mol. Cell. Proteomics* **7**: 1019–1030.
- Raffaele, S., et al. (2009). Remorin, a solanaceae protein resident in membrane rafts and plasmodesmata, impairs *potato virus X* movement. *Plant Cell* **21**: 1541–1555.
- Rajan, S.S., Liu, H.Y., and Vu, T.Q. (2008). Ligand-bound quantum dot probes for studying the molecular scale dynamics of receptor endocytic trafficking in live cells. *ACS Nano* **2**: 1153–1166.
- Robinson, D.G., Jiang, L., and Schumacher, K. (2008). The endosomal system of plants: Charting new and familiar territories. *Plant Physiol.* **147**: 1482–1492.
- Schneider, A., Rajendran, L., Honsho, M., Gralle, M., Donnert, G., Wouters, F., Hell, S.W., and Simons, M. (2008). Flotillin-dependent clustering of the amyloid precursor protein regulates its endocytosis and amyloidogenic processing in neurons. *J. Neurosci.* **28**: 2874–2882.
- Shinozaki, Y., Sumitomo, K., Tsuda, M., Koizumi, S., Inoue, K., and Torimitsu, K. (2009). Direct observation of ATP-induced conformational changes in single P2X4 receptors. *PLoS Biol.* **7**: e103.
- Siefritz, F., Tyree, M.T., Lovisolo, C., Schubert, A., and Kaldenhoff, R. (2002). PIP1 plasma membrane aquaporins in tobacco: from cellular effects to function in plants. *Plant Cell* **14**: 869–876.
- Sommer, A., Geist, B., Da Ines, O., Gehwolf, R., Schäffner, A.R., and Obermeyer, G. (2008). Ectopic expression of *Arabidopsis thaliana* plasma membrane intrinsic protein 2 aquaporins in lily pollen increases the plasma membrane water permeability of grain but not of tube protoplasts. *New Phytol.* **180**: 787–797.
- Sorieul, M., Santoni, V., Maurel, C., and Luu, D.T. (2011). Mechanisms and effects of retention of over-expressed aquaporin AtPIP2;1 in the endoplasmic reticulum. *Traffic* **12**: 473–482.
- Takano, J., Miwa, K., Yuan, L., von Wirén, N., and Fujiwara, T. (2005). Endocytosis and degradation of BOR1, a boron transporter of *Arabidopsis thaliana*, regulated by boron availability. *Proc. Natl. Acad. Sci. USA* **102**: 12276–12281.
- Törnroth-Horsefield, S., Wang, Y., Hedfalk, K., Johanson, U., Karlsson, M., Tajkhorshid, E., Neutze, R., and Kjellbom, P. (2006). Structural mechanism of plant aquaporin gating. *Nature* **439**: 688–694.
- Ulbrich, M.H., and Isacoff, E.Y. (2007). Subunit counting in membrane-bound proteins. *Nat. Methods* **4**: 319–321.
- Van Wilder, V., Miecielica, U., Degand, H., Derua, R., Waelkens, E., and Chaumont, F. (2008). Maize plasma membrane aquaporins belonging to the PIP1 and PIP2 subgroups are *in vivo* phosphorylated. *Plant Cell Physiol.* **49**: 1364–1377.
- Vera-Estrella, R., Barkla, B.J., Bohnert, H.J., and Pantoja, O. (2004). Novel regulation of aquaporins during osmotic stress. *Plant Physiol.* **135**: 2318–2329.
- Verdoucq, L., Grondin, A., and Maurel, C. (2008). Structure-function analysis of plant aquaporin AtPIP2;1 gating by divalent cations and protons. *Biochem. J.* **415**: 409–416.
- Wang, X., Teng, Y., Wang, Q., Li, X., Sheng, X., Zheng, M., Samaj, J., Baluska, F., and Lin, J. (2006). Imaging of dynamic secretory vesicles in living pollen tubes of *Picea meyeri* using evanescent wave microscopy. *Plant Physiol.* **141**: 1591–1603.
- Xiao, Z., Ma, X., Jiang, Y., Zhao, Z., Lai, B., Liao, J., Yue, J., and Fang, X. (2008). Single-molecule study of lateral mobility of epidermal growth factor receptor 2/HER2 on activation. *J. Phys. Chem. B* **112**: 4140–4145.
- Zelazny, E., Borst, J.W., Muijlaert, M., Batoko, H., Hemminga, M.A., and Chaumont, F. (2007). FRET imaging in living maize cells reveals that plasma membrane aquaporins interact to regulate their subcellular localization. *Proc. Natl. Acad. Sci. USA* **104**: 12359–12364.
- Zhang, D., Manna, M., Wohland, T., and Kraut, R. (2009a). Alternate raft pathways cooperate to mediate slow diffusion and efficient uptake of a sphingolipid tracer to degradative and recycling compartments. *J. Cell Sci.* **122**: 3715–3728.
- Zhang, Q., Li, Y., and Tsien, R.W. (2009b). The dynamic control of kiss-and-run and vesicular reuse probed with single nanoparticles. *Science* **323**: 1448–1453.
- Zhang, W., Jiang, Y., Wang, Q., Ma, X., Xiao, Z., Zuo, W., Fang, X., and Chen, Y.G. (2009c). Single-molecule imaging reveals transforming growth factor- β -induced type II receptor dimerization. *Proc. Natl. Acad. Sci. USA* **106**: 15679–15683.

Mechanisms and Effects of Retention of Over-Expressed Aquaporin AtPIP2;1 in the Endoplasmic Reticulum

Mathias Sorieul[†], Véronique Santoni,
Christophe Maurel and Doan-Trung Luu*

Biochimie et Physiologie Moléculaire des Plantes, Institut de Biologie Intégrative des Plantes, UMR 5004 CNRS/UMR 0386 INRA/Montpellier SupAgro/Université Montpellier 2, F-34060 Montpellier Cedex 2, France

*Corresponding author: Doan-Trung Luu,
luu@supagro.inra.fr

[†]Present address: Department of Biological Sciences, University of Warwick, Warwick, UK.

Plasma membrane intrinsic proteins (PIPs) are aquaporins that mediate water transport across the plant plasma membrane (PM). The present work addresses, using *Arabidopsis* AtPIP2;1 as a model, the mechanisms and significance of trafficking of newly synthesized PIPs from the endoplasmic reticulum (ER) to the Golgi apparatus. A functional diacidic export motif (Asp4-Val5-Glu6) was identified in the N-terminal tail of AtPIP2;1, using expression in transgenic *Arabidopsis* of site-directed mutants tagged with the green fluorescent protein (GFP). Confocal fluorescence imaging and a novel fluorescence recovery after photobleaching application based on the distinct diffusion of PM and intracellular AtPIP2;1-GFP forms revealed a retention in the ER of diacidic mutated forms, but with quantitative differences. Thus, the individual role of the two acidic Asp4 and Glu6 residues was established. In addition, expression in transgenic *Arabidopsis* of ER-retained AtPIP2;1-GFP constructs reduced the root hydraulic conductivity. Co-expression of AtPIP2;1-GFP and AtPIP1;4-mCherry constructs suggested that ER-retained AtPIP2;1-GFP may interact with other PIPs to hamper their trafficking to the PM, thereby contributing to inhibition of root cell hydraulic conductivity.

Key words: aquaporins, endoplasmic reticulum exit motifs, root hydraulic conductivity, stably transformed *Arabidopsis*

Received 6 September 2010, revised and accepted for publication 21 December 2010, uncorrected manuscript published online 23 December 2010, published online 1 February 2011

Aquaporins define a multigenic family of transmembrane proteins found virtually throughout the whole living kingdom, and involved in water, gas and solute transport (1–4). In *Arabidopsis thaliana*, 35 members have been identified. Thirteen isoforms belong to the plasma membrane intrinsic protein (PIP) group which is subdivided into two homology subgroups, AtPIP1 and AtPIP2 (5,6).

PIPs are principally localized at the plasma membrane (PM). Reverse genetics and pharmacological approaches have established their critical contribution to plant water homeostasis in a variable environment (2,4,7,8). In roots in particular, their intrinsic activity and density in the PM can be modulated in response to hormonal and environmental stimuli to determine cell water permeability (9).

Like other PM proteins, PIPs are thought to traffic from the endoplasmic reticulum (ER) to the PM through the secretory pathway. Thus, their export out of the ER is a key step. Cytosolic domain signals have been demonstrated to be required in membrane proteins of yeast, mammals and plants to determine their export out of the ER (10). In plants, however, knowledge of these mechanisms is just emerging (11–21). ER export signals are usually divided into dihydrophobic motifs (FF, YY, LL or FY) comprising two adjacent hydrophobic residues, dibasic motifs, diacidic motifs with two acidic residues separated by another one (10,22,23) and lastly, a few, and less differentiated motifs (24–28).

Various diacidic motif sequences have so far been identified, such as DXE (13,15,16,29–31), DXD (32,33) and EXE (34). Recently, an atypical diacidic EXXD motif and a triacidic DXDXE motif have been uncovered (19,20). Any mutation in these signals resulted in an ER retention and a reduction of protein abundance at the cell surface. Finally, homologues of coat protein II (COPII)-vesicle coat components that recognize diacidic motifs have been identified in plants, suggesting ER export molecular mechanisms similar to those of yeast and mammals (35).

In maize aquaporins *ZmPIP2;4* and *ZmPIP2;5*, truncation and mutation of their N-terminal tail allowed identification of a DXE motif that is essential for their ER export (16). Previous studies had also shown that injection of *Xenopus* oocytes with *ZmPIP2* cRNA, but not *ZmPIP1* cRNA, resulted in an increase in membrane water permeability. However, *ZmPIP1*s were found to be properly expressed in the PM only when co-expressed with *ZmPIP2*s and consequently an increase in oocyte membrane water permeability was observed (36). Similar observations were made upon transient expression in maize mesophyll protoplasts: when expressed alone, *ZmPIP1*s were retained in the ER and co-expression of *ZmPIP1*s with *ZmPIP2*s resulted in the correct targeting of *ZmPIP1*s to the PM. Physical interactions of *ZmPIP1*s with *ZmPIP2*s were also demonstrated by means of fluorescence resonance energy transfer/fluorescence lifetime imaging microscopy (FRET/FLIM) analyses. These data suggested that heterooligomerization with *ZmPIP2*s is required for proper targeting of *ZmPIP1*s to the PM (37,38).

Whereas previous studies have addressed the ER export of PIPs using heterologous or transient expression systems, in the present work, we investigated this process in stably transformed *Arabidopsis* plants. We first identified a diacidic motif in AtPIP2;1 and determined its role in aquaporin trafficking and in the dynamics of its subcellular compartmentation. We then investigated the effects of over-expressed ER-retained AtPIP2;1 constructs. We describe how these constructs interfere with other AtPIP isoforms at the subcellular level, and how this may lead to alteration of the root water transport capacity of transformed plants.

Results

Transgenic expression of AtPIP2;1-GFP constructs mutated on a putative diacidic motif

Amino acid sequence analysis of AtPIP2;1 predicts a potential diacidic motif, DVE, at position 4–6 in the N-terminal tail (see Figure S1). To address its trafficking mechanisms, AtPIP2;1 was fused to the green fluorescent protein (AtPIP2;1-GFP) and the resulting construct was expressed constitutively in *A. thaliana* plants under the control of a double enhanced *CaMV35S* promoter. A series of site-directed mutations was conducted to investigate the role of the DVE motif in the trafficking of AtPIP2;1-GFP (Table S1). Substitutions of Asp⁴ or/and Glu⁶ by Ala neutralize the DVE diacidic motif to AVE, DVA and AVA sequences, respectively. Substitutions of Asp⁴ or Glu⁶ by Glu or Asp, respectively, alter the primary amino acid sequence but maintain the diacidic properties of the sequence.

In an attempt to check the expression of constructs, total proteins of transgenic plantlets were subjected to Western blot analysis with an anti-GFP antibody. The calculated molecular weight of the constructs is about 57 kD. As shown in Figure S2, we detected a double band with apparent masses of 50 and 55 kD that probably indicates a partial proteolysis of AtPIP2;1-GFP. Protein extraction performed in the absence of anti-protease cocktail resulted in a severe degradation (data not shown), indicating that the AtPIP2;1-GFP proteolysis observed in Western blots occurred at the protein extraction step. Nevertheless, in Figure S2, no free GFP was detected. This result suggested that confocal microscopy observations of GFP signals described later are associated with the expression of AtPIP2;1-GFP constructs.

Effect of mutations of a diacidic motif on the subcellular localization of AtPIP2;1-GFP constructs

Wild-type (WT) AtPIP2;1-GFP expression resulted in a homogeneous signal located mostly at the periphery of the cell, consistent with the expected localization of this construct at the PM (Figure 1). In marked contrast, constructs with any mutation at Asp⁴ or/and Glu⁶ positions showed a strong GFP-labelling of intracellular compartments mainly observed as a reticulated network

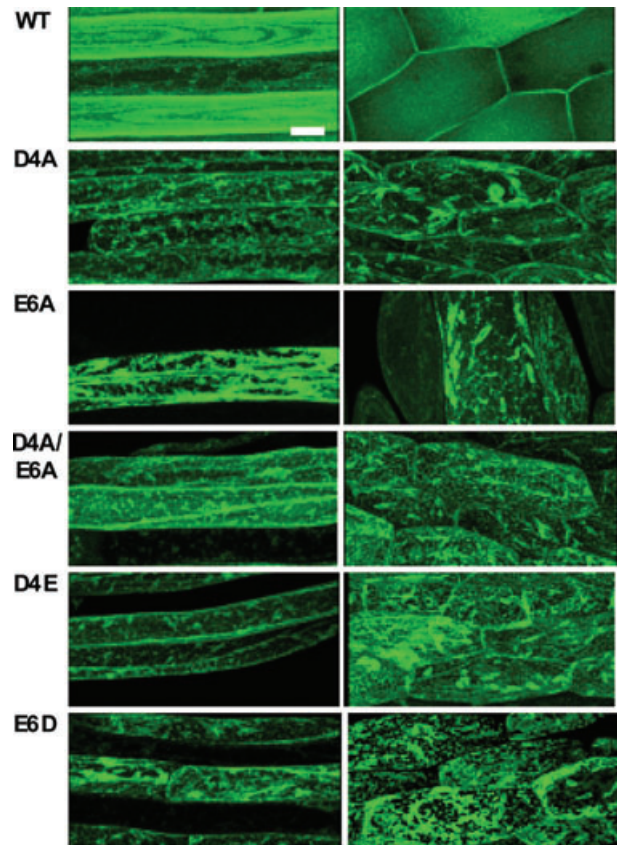


Figure 1: Effects of mutations in the N-terminal cytosolic domain of AtPIP2;1-GFP constructs on their subcellular localization. Z-stack projections of optical sections of epidermal root (left) and hypocotyl (right) cells expressing AtPIP2;1-GFP constructs, either WT or carrying the indicated mutation. Bar = 10 μ m.

in epidermal cells of roots and hypocotyls (Figure 1) as well as leaves (see Figure 4). We also noticed GFP labelling of fusiform bodies (see Figure S3) (39). Such a reticulate network and fusiform body labelling have been extensively described and are associated with the ER compartment (40,41). ER-Tracker dye was previously used as a selective marker for this compartment (42). We found that in the root epidermal cells the WT AtPIP2;1-GFP construct and the ER-Tracker dye showed only a partial colocalization, whereas an extensive co-labelling with the dye was observed for the whole set of diacidic mutants (see Figure S4). Co-expressions of AtPIP2;1-GFP constructs with YFP-HDEL, another marker of the ER (43), were performed to confirm the nature of the compartment labelled by diacidic mutants of AtPIP2;1-GFP construct (Figure 2A). In root epidermal cells YFP-HDEL labelled a perinuclear area and a reticulate network, corresponding to the ER, but also motile dots tentatively identified as Golgi apparatus. Whereas the WT AtPIP2;1-GFP construct did not colocalize with YFP-HDEL, the whole set of diacidic mutant constructs showed an overlapping localization pattern. The possible localization of the diacidic mutant

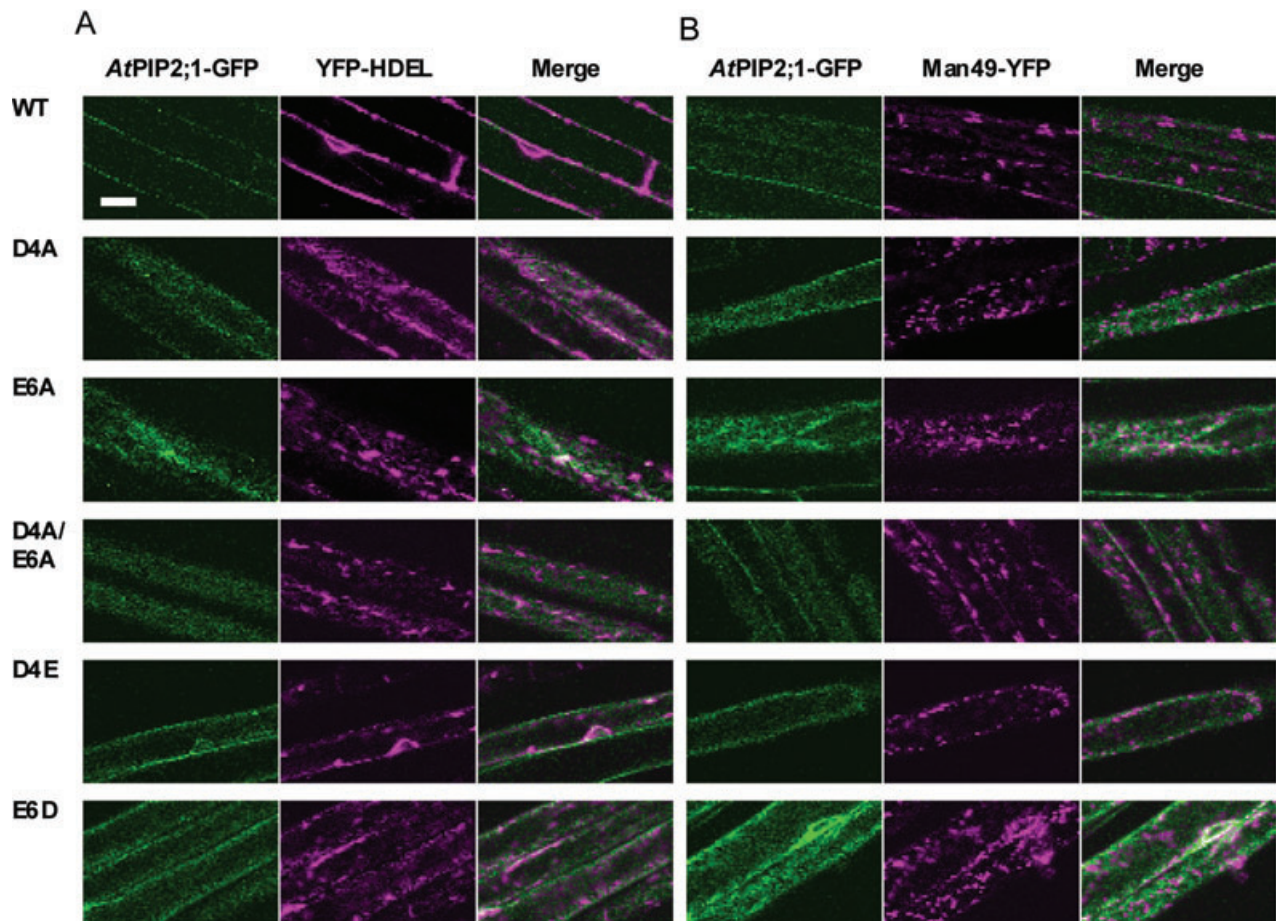


Figure 2: Diacidic mutant of *AtPIP2;1-GFP* constructs colocalize with YFP-HDEL but not with Man49-YFP. Epidermal root cells expressing the indicated *AtPIP2;1-GFP* constructs and either YFP-HDEL (A) or Man49-YFP (B) constructs were observed for GFP (left column) and YFP fluorescence (central). A) YFP-HDEL protein fusion (central column), an ER marker, shows fluorescence located in a reticulate network which is extended throughout the cell and also in dots tentatively identified as Golgi apparatus. The merged image shows that all diacidic mutants colocalize with YFP-HDEL but are excluded from Golgi apparatus. Bar = 10 μm . B) Man49-YFP fusion, combining the cytoplasmic tail and the transmembrane domain (first 49 aa) of soybean α -1,2-mannosidase I (GmMan1) with YFP, is a marker of Golgi apparatus. Man49-YFP does not colocalize with *AtPIP2;1-GFP* constructs (merge image). Bar = 10 μm .

constructs in the Golgi apparatus was investigated by means of a Man49-YFP marker (43). Observation of plants co-expressing this and the diacidic mutant constructs revealed no Golgi colocalization (Figure 2B). As YFP-HDEL labels both the ER and the Golgi apparatus, whereas Man49-YFP specifically labels the Golgi apparatus, mutant constructs appear to be strictly localized in the ER. Similar results were also observed for epidermal leaf cells (Figure S5).

Estimation of *AtPIP2;1-GFP* intracellular labelling

In an attempt to estimate the ratio of diacidic mutant constructs between the intracellular compartments and the PM, we made use of the fluorescence recovery after photobleaching (FRAP) technique. Using this technique, it was demonstrated that the KAT1 K^+ channel, the PMA2 H^+ -ATPase, the *AtBOR1* boric acid/borate exporter and the *AtNIP5;1* boric acid channel, all tagged with

fluorescent markers, did not show any evidence for lateral movement or dispersion within the plane of the PM (44,45). Similar to this, we observed a low rate of lateral mobility for PIP-GFP constructs at the PM (data not shown). Interestingly, GFP-HDEL and GFP-Calnexin constructs marking the ER allowed us to visualize the high mobility (fast rearrangement) of this organelle (46,47). We therefore took advantage of this difference in mobility between fluorescent protein fusions in the PM and in the ER. A region of interest (ROI) was identified in the tangential optical section of epidermal cells expressing WT or mutated *AtPIP2;1-GFP*. This ROI was bleached and recovery of fluorescence was monitored after 5 min. In cells expressing the WT *AtPIP2;1-GFP* (Figure 3A), fluorescence recovery in the ROI was almost not detectable in the ROI. By contrast, a more pronounced fluorescence recovery was observed in cells expressing diacidic mutant constructs. The ratio of fluorescence intensity of bleached

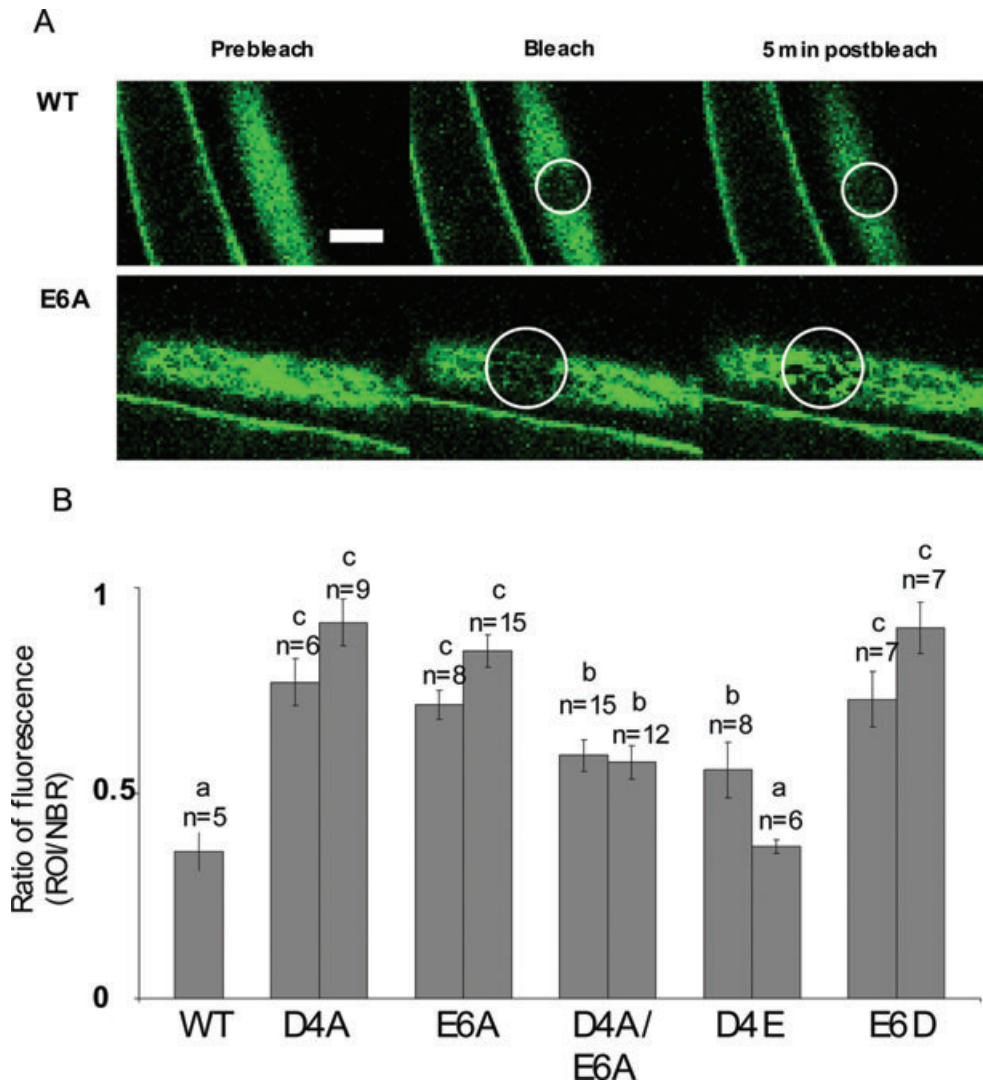


Figure 3: Estimation of AtPIP2;1-GFP intracellular labelling by means of FRAP experiments. A) Tangential optical sections of epidermal cells expressing WT or E6A AtPIP2;1-GFP constructs were recorded prior to, immediately following, or 5 min after photobleaching the ROI (circle). Bar = 10 μ m. B) The fluorescence intensity of a bleached ROI, at 5 min after bleaching, was reported to the fluorescence intensity of a neighbouring nonbleached region (NBR). At this time-point, fluorescence of intracellular compartments in ROI had recovered whereas recovery at the PM was not significant (see A). Thus, intensities of ROI and NBR correspond to intracellular and both intracellular and PM labelling, respectively. The ratio of fluorescence intensity (ROI/NBR) gives an estimate of relative intracellular labelling. Except for WT, two independently transformed lines were analysed for each construct. Standard error values, the number of independent cells studied (*n*) and significant differences between mutants and WT, based on Student's *t*-test, are shown.

ROI to the neighbouring nonbleached region was used as an estimate of the relative intracellular labelling (Figure 3). Comparison of the fluorescence intensity ratios showed that the WT AtPIP2;1-GFP construct had significantly lower values than its mutant counterparts. For instance, ratio values of two independent D4A lines were 2.15- or 2.56-fold higher than that of the WT AtPIP2;1-GFP line. Of the fluorescence ratios of two D4E lines, only one was different from the control. The ratios of fluorescence of D4A-, E6A- and E6D AtPIP2;1-GFP constructs were similar, and higher than the ratio of either D4A/E6A- or D4E

AtPIP2;1-GFP construct. Taken together, these results suggested that independent D4A, E6A and E6D mutations provoked similar and marked intracellular retention of AtPIP2;1-GFP constructs and also that the D4A/E6A or D4E mutants showed a lesser intracellular accumulation.

Estimation of AtPIP2;1-GFP construct protein turn-over

This issue was addressed by using cycloheximide, a protein synthesis inhibitor. As a positive control for the effect of cycloheximide, we treated leaves of

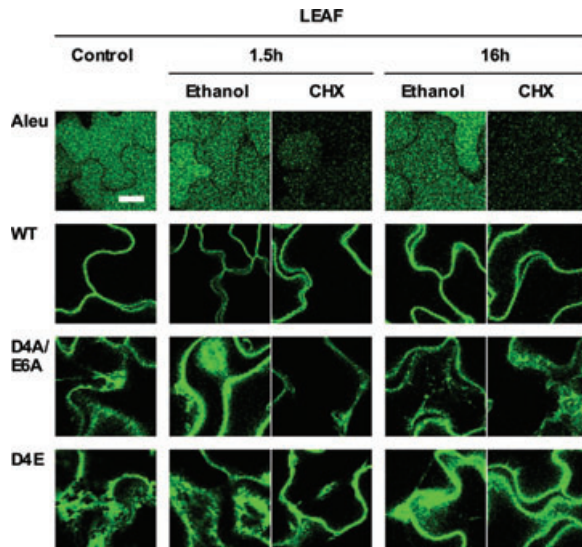


Figure 4: Effect of a cycloheximide treatment on GFP-protein fusion signal. Aleurain (Aleu), or WT and mutated forms of AtPIP2;1 expressed as protein fusions to GFP were monitored in leaf epidermal cells or in root. Plants were immersed in a $\frac{1}{2}$ MS medium supplemented with either cycloheximide (100 μ M; CHX) or ethanol, as a control for the solvent effect, for the indicated duration. GFP fusion signal was then monitored by means of confocal microscopy. Bar = 10 μ m.

Arabidopsis plantlets expressing an Aleurain-to-GFP fusion (Aleu-GFP) (48,49). After 1.5 h of cycloheximide treatment, the fluorescent signal of Aleu-GFP in epidermal cells had almost completely vanished (Figure 4). By contrast, the signal of the WT AtPIP2;1-GFP construct at the periphery of the epidermal cells, previously identified as the PM compartment, was not significantly reduced after either 1.5 or 16 h treatment. Likewise, the whole set of AtPIP2;1-GFP diacidic mutants did not show any fluorescence decrease even after 16 h of cycloheximide treatment. Yet, cytosolic streaming was observed after such a long treatment, suggesting that the cells were still viable. Similar results were also observed in mature root epidermal cells (data not shown).

The peripheral or intracellular labelling observed with the WT or mutant AtPIP2;1-GFP constructs after 16 h of cycloheximide treatment suggested that WT and mutant AtPIP2;1-GFP proteins are highly stable at the cell surface and in the ER, respectively.

Impact of ER retention of diacidic mutant AtPIP2;1-GFP constructs on root water transport

Data from the literature indicate possible interactions between PIP1s and PIP2s during trafficking to the PM (16,36,37). As more than 70% of the *Arabidopsis* root hydraulic conductivity (L_{pr}) is mediated by AtPIP aquaporins (50,51), any major localization faults of AtPIPs should impact this parameter. This prompted us to study the effect of ER-retained AtPIP2;1-GFP constructs on root

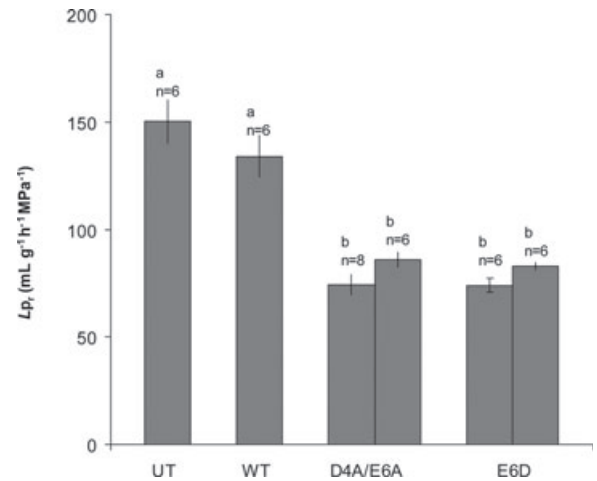


Figure 5: Root hydraulic conductivity (L_{pr}) of plants expressing various AtPIP2;1-GFP constructs. Pressure chamber measurement in roots of *Arabidopsis* plants either untransformed (UT) or transformed with WT or mutated forms of AtPIP2;1 fused to GFP. For the two latter genotypes, two independently transformed lines were analysed. Standard error values, the number of independent plants investigated (n) and significant differences between genotypes, based on Student's t -test, are shown.

water transport. *Arabidopsis* plants, either untransformed or expressing WT or a mutated form of AtPIP2;1-GFP, were grown hydroponically and their L_{pr} was determined by pressure chamber techniques (Figure 5). No significant difference in L_{pr} was found between untransformed plants and plants expressing WT AtPIP2;1-GFP. By contrast, plants expressing diacidic mutated forms of AtPIP2;1-GFP (D4A/E6A and E6D) exhibited 36–45% L_{pr} reduction when compared to that of the WT form.

Impact of ER retention of AtPIP2;1-GFP on the subcellular localization of transgenic fusions of aquaporins

To investigate a possible physical interaction between over-expressed ER-retained AtPIP2;1-GFP constructs and endogenous AtPIPs, we studied the effect of these constructs on the trafficking of selected aquaporin isoforms. For this, we co-expressed WT or diacidic mutant forms of AtPIP2;1-GFP with either PIP2;1-mCherry or AtPIP1;4-mCherry (Figure 6). WT AtPIP2;1-GFP was observed to colocalize with either AtPIP2;1-mCherry or AtPIP1;4-mCherry at the periphery of the cells (Figure 6A,B upper panels). This subcellular localization was attributed to the PM. When co-expressed with E6D AtPIP2;1-GFP, AtPIP2;1-mCherry and AtPIP1;4-mCherry colocalized in intracellular compartments (Figure 6A,B lower panels). This suggested that the ER-retained AtPIP2;1-GFP mutants induced the intracellular retention of both PIP2;1-mCherry and AtPIP1;4-mCherry. Next, the specificity of these changes in subcellular localization pattern was checked in similar experiments with plants co-expressing either WT or mutated AtPIP2;1-GFP but with the tonoplastic aquaporin AtTIP1;1 fused to

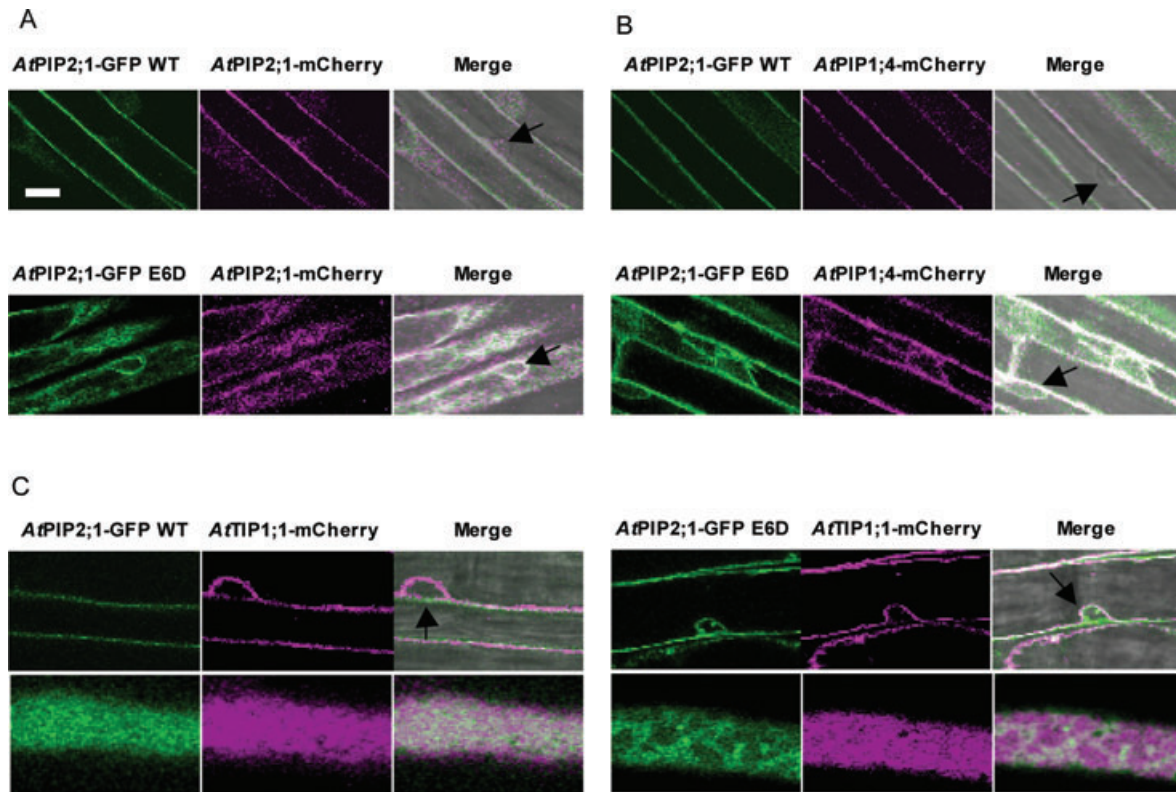


Figure 6: *AtPIP2;1-mCherry* and *AtPIP1;4-mCherry* colocalize with diacidic mutants of *AtPIP2;1-GFP*, but *AtTIP1;1-mCherry* does not. Epidermal root cells expressing WT or E6D forms of *AtPIP2;1-GFP* together with *AtPIP2;1-mCherry* (A), *AtPIP1;4-mCherry* (B) or *AtTIP1;1-mCherry* (C). Constructs were observed for GFP (left column) and mCherry fluorescence (central). The merge image with or without bright field (right column) shows that all *AtPIP-GFP* constructs colocalize with either *AtPIP2;1-mCherry* or *AtPIP1;4-mCherry*. Note that nuclei (arrows) are faintly or strongly labelled when *AtPIP2;1-GFP* WT or E6D isoform is expressed, respectively. In C, the co-expression of *AtTIP1;1-mCherry* with the WT or E6D forms of *AtPIP2;1-GFP* leads in both cases to an mCherry signal that skirts the nucleus (arrow; upper panels). Note that the mCherry signal is distinct from the GFP one in the region of the nucleus (arrow; upper panels) when *AtTIP1;1-mCherry* was co-expressed with E6D *AtPIP2;1-GFP*. In tangential optical sections (lower panels), note that the mCherry signal does not label a reticulate network when *AtTIP1;1-mCherry* was co-expressed with E6D *AtPIP2;1-GFP*. Bar = 10 μ m.

mCherry (Figure 6C). *AtTIP1;1* fusion to fluorescent proteins localizes to the tonoplast (50,52,53). A similar tonoplast localization was established for *AtTIP1;1-mCherry* from peripheral staining of the cell with intracellular invaginations that skirted the nucleus. When *AtTIP1;1-mCherry* was co-expressed with WT or the E6D *AtPIP2;1-GFP* mutant, the same localization was observed. In particular, *AtTIP1;1-mCherry* did not colocalize in perinuclear area with the E6D mutant (Figure 6C). To summarize, this set of data suggested that the expression of an ER-retained *AtPIP2;1-GFP* construct disturbed the trafficking to the PM of fusions of *AtPIP2;1* or *AtPIP1;4* to fluorescent proteins.

Discussion

A DXE motif is involved in *AtPIP2;1* ER export

Several recent studies have uncovered the function of diacidic motifs in the intracellular transport of plant membrane proteins, by transient expression of site-directed mutant forms (15,16,18,20,21,54). Here, we

extended the knowledge of diacidic motif functions to stabilized plant lines. We also addressed the functionality of this motif by altering the amino acids while keeping the diacidic property of the sequence.

More specifically, replacement of the DXE motif of *AtPIP2;1* by either AVE, DVA, AVA, EVE or DVD led to strong intracellular labelling (Figure 1; see Figure S3). Thus, any modification of either the Asp⁴ or Glu⁶ had a deleterious effect on the subcellular targeting of *AtPIP2;1*. These results strongly argue in favour of a strict DXE motif in *AtPIP2;1* instead of a so-called diacidic motif. Examples from mammals support this notion. Mutations of the DIE motif of vesicular stomatitis virus glycoprotein to either EIE or DID prevented ER export in the same manner as mutations to either AIE or DIA or AIA (55). Moreover, mutations of ENE motif of the inwardly rectifying potassium Kir2.1 channel to either DNE or END also abolished ER export in the same manner as mutations of this motif to either ANE or ENA or ANA (34). Interestingly, a DXE motif has already been shown to be involved

in the ER export of plant membrane proteins (13,15,16). Moreover, among the described DXE motifs in plants, the middle residue was either an Ala, a Val, a Leu or an Ile. In maize aquaporins, the middle residue is an Ile at position 5 of the N-terminal tail of *ZmPIP2;4* and *ZmPIP2;5* (16). Thus, in plant cells, DXE motifs comprising an aliphatic residue at the middle position may be preferentially recognized by the ER export machinery, but further investigations are needed to assess this assumption.

Diacidic mutated forms of *AtPIP2;1-GFP* constructs colocalized with ER-Tracker dye (see Figure S4) and with YFP-HDEL (Figure 2A; see Figure S5A), two markers of the ER, but not with Man49-YFP, a marker of Golgi apparatus, indicating a predominant localization in the ER (Figure 2B; Figure S5B). As endogenous *AtPIP2;1* is able to traffic properly to the PM, one may wonder about the occurrence and the fate of heterotetramers comprising endogenous *AtPIP2;1* proteins and mutated *AtPIP2;1-GFP* constructs. In our study, however, the strong over-expression of the constructs may have favoured tetramers comprising mutated *AtPIP2;1-GFP* mostly, which therefore appeared as largely unable to traffic toward the PM. Yet, direct observations by confocal fluorescence microscopy are more qualitative than quantitative. In order to estimate the ER retention of *AtPIP2;1-GFP* mutated forms, the FRAP technique was used. In particular, we showed that the DA4 *AtPIP2;1-GFP* constructs exhibited a twofold greater ER/PM fluorescence ratio compared to the WT form. Yet, other mutant forms showed a lesser intracellular accumulation that had not been resolved through direct observation. More generally, this technique suggested that a fraction of this and other mutated PIP-GFP constructs was able to reach the PM.

The retained *AtPIP2;1-GFP* constructs is highly stable

The stability of *AtPIP2;1-GFP* constructs retained in the ER was addressed by treating tissues with cycloheximide. Compared to an Aleu-GFP construct whose signal vanished almost completely after 1.5 h, diacidic mutated *AtPIP2;1-GFP* constructs were still present in intracellular compartments even after a 16-h treatment (Figure 4). The stability of GFP signal in the ER compartment suggests that ER-retained isoforms were not directed to a degradation pathway. Recent work indicated that, when ectopically expressed in *Arabidopsis*, Rma1H1, a hot pepper (*Capsicum annuum*) homologue of a human RING membrane-anchor 1 E3 ubiquitin ligase, accumulated in the ER and induced an accumulation in this compartment of *AtPIP2;1* fused to GFP or mCherry (56). In addition, Rma1H1 over-expression reduced overall *AtPIP2;1-GFP* or -mCherry levels, in a proteasome-dependent manner. In the present study, over-expression of ER-retained *AtPIP2;1-GFP* constructs did not promote any preferential degradation. This suggests that the degradation machinery present in the ER, including Rma homologues, may have been limiting.

Plants over-expressing ER-retained *AtPIP2;1-GFP* constructs exhibit complex mechanisms leading to a reduced *Lp*.

Molecular interactions between PIP1s and PIP2s have been described in maize and tobacco (36–38). Therefore, we considered the possibility of a direct or indirect interaction between ER-retained *AtPIP2;1-GFP* constructs and endogenous *AtPIP* isoforms. Interestingly, plants over-expressing ER-retained *AtPIP2;1-GFP* constructs (D4A/E6A and E6D) exhibited a 36–45% reduction in root water transport activity in comparison to WT genotype (Figure 5). The reduction observed in the present study was in the same order of magnitude compared to previous studies which used antisens approaches to knock-down *AtPIP2* expression (57,58).

A possible hypothesis to explain this reduction in root water transport activity is that *AtPIP2;1-GFP* would interact with endogenous *AtPIPs* and, consequently, a reduction in the density of endogenous *AtPIPs* at the PM would be observed in plants over-expressing ER-retained *AtPIP2;1-GFP*. This mechanism is supported by confocal imaging of *AtPIP1;4-mCherry* which, when co-expressed with the E6D construct, appeared as mainly intracellular. Noteworthy, over-expression of ER-retained *AtPIP2;1-GFP* constructs did not provoke any visible retention in the ER of either Man49-YFP (see Figure 2B) or *AtTIP1;1-mCherry* marker (see Figure 6C), suggesting that potential interactions of ER-retained *AtPIP2;1-GFP* constructs with membrane protein constructs other than PIP constructs were limited. Thus, specific interactions between ER-retained forms of PIP2;1-GFP and endogenous PIP1s and PIP2s occurred in the ER. Yet, we would like to call for a cautious interpretation of the reduction of root hydraulic conductivity in plants expressing ER-retained *AtPIP2;1-GFP* constructs. This reduction could be explained by a number of factors. Our data strongly suggest that it is contributed by a reduced accumulation of endogenous *AtPIPs* at the PM. However, the D4A/E6A *AtPIP2;1-GFP* construct showed a lesser intracellular accumulation than the E6A construct (Figure 3) and, yet, induced a similar reduction in root hydraulic conductivity (Figure 5). Thus, we cannot exclude that an over-accumulation of *AtPIP2;1-GFP* constructs in the ER may have side effects and might in particular disturb the homeostasis of this organelle to provoke a so-called 'ER-stress'. Although this term is restricted to the effect of an increase in misfolded proteins in the ER, such disturbance of ER function might have an indirect impact on root water transport, through cellular mechanisms that remain to be determined.

Materials and Methods

Plant materials and growth conditions

All plants used in this work are *A. thaliana* L. (Heyn.) accession Columbia 0. When grown on plates, plants were germinated on half strength Murashige and Skoog ($\frac{1}{2}$ MS) medium supplemented with sucrose (10 g/L) and agar (7 g/L; $\frac{1}{2}$ MS agar) (59) and then incubated in a growth chamber at 70%

relative humidity with cycles of 16 h of light ($\sim 150 \mu\text{E}/\text{m}^2/\text{second}$) and 8 h of dark at 21°C . When grown on liquid medium, about a hundred of seeds were germinated in an Erlen-Meyer containing 100 mL $\frac{1}{2}$ MS medium under agitation and continuous illumination ($\sim 150 \mu\text{E}/\text{m}^2/\text{second}$) and 24°C . For root water transport measurements, plants were germinated and grown on plates for 10 days before transfer to hydroponic culture, as described in Ref. 64. Plants were further grown for 10–20 days, in a growth chamber at 70% relative humidity with cycles of 16 h of light ($180 \mu\text{E}/\text{m}^2/\text{second}$) at 22°C and 8 h of dark at 21°C .

Mutagenesis and cloning methods

Site-directed mutagenesis of Asp⁴ or/and Glu⁶ of AtPIP2;1-GFP construct were performed by PCR with a fragment of AtPIP2;1 cDNA fused to the GFP (AtPIP2;1-GFP) sequence as a template. Forward primers listed in Table S1 allowed the introduction of a XhoI restriction site. PCRs were performed with Pfu DNA polymerase (Promega) according to the manufacturer's instructions. After purification (GeneClean Kit II; Q.BiOgene), PCR fragments were digested by XhoI and XbaI and subcloned into the pBluescript vector (Stratagene) under the transcriptional control of the double enhanced CaMV35S promoter and the 3' end of the pea ribulose-1,5-bisphosphate carboxylase small subunit gene (*rbcS*) (60). Next, the expression cassette was cloned into the binary vector pGreenII 0179 (61) and transferred into *Agrobacterium tumefaciens* strain GV3101 with pSOUP for *Arabidopsis* flower dip transformation procedure (62).

Western blot

About 100 mg of fresh tissue were ground until homogeneity in a 1.5 mL tube with a piston in a grinding buffer made of 500 mM sucrose; 10% glycerol; 50 mM NaF; 20 mM EDTA; 20 mM EGTA; 5 mM β -glycerophosphate; 1 mM phenanthroline; 0.6% PVP; 10 mM ascorbic acid; 0.5 $\mu\text{g}/\text{mL}$ leupeptine; 1 mM PMSF; 5 mM DTT; 1 mM Na₂Vanadate; 50 mM Tris-HCl, pH 8. After centrifugation (5 min at $10\,000 \times g$), the supernatant was subjected to SDS-PAGE on 12% acrylamide gels. After SDS-PAGE, separated proteins were transferred onto PVDF membrane (Immobilon, Millipore) according to the manufacturer's instructions. For the detection of AtPIP2;1-GFP fusions, anti-GFP antibody (Invitrogen) was used at a dilution of 1/2000 and performed as described in Ref. 63.

Cell imaging procedures

Images were captured with an inverted confocal laser-scanning microscope (Inverse 1 Axiovert 200M Zeiss/LSM 510 META Confocal) with a 40 \times water immersion or a 63 \times oil immersion objective. The emitted fluorescence of co-expressed -GFP and -YFP constructs was captured by alternately switching the 488 and 514 nm excitation lines of an argon ion laser using the multitrack facility of the microscope and the emission fingerprinting mode of the LSM 510 META confocal. The emitted fluorescence of co-expressed -GFP and -mCherry constructs was captured by alternately switching the 488 and 543 nm excitation lines. The emitted fluorescence of plants expressing GFP constructs and stained with ER-Tracker™ Blue-White DPX (Molecular Probes) was captured by alternately switching the 488 and the 405 nm lines of an argon ion laser and a blue diode laser, respectively.

The recovery of fluorescence was measured by means of IMAGE J software (Rasband W., NIH) which allows the measurement of the mean grey value of a ROI.

Confocal observations were performed on epidermal hypocotyl and primary root (about 1 cm distance from apex) of transgenic plantlets cultivated for ~ 10 days.

Root water transport measurements

Hydrostatic water transport in root systems excised from plants grown in hydroponics was measured essentially as described elsewhere (50,64).

Acknowledgments

This work was supported in part by a doctoral fellowship from the French Ministry of Research to M. S. We thank Angélique Adivèze for assistance in *Arabidopsis* transformations, staff members of the Institut de Biologie Intégrative des Plantes for technical assistance in biological material culture, Dr. Gian-Pietro Di Sansebastiano (University of Lecce, Italy) for providing the Aleu-GFP line, Dr. Niko Geldner and Dr. Joanne Chory for providing AtPIP1;4-mCherry line and Dr Robert Spooner for careful reading of the manuscript. Confocal observations were made at the Montpellier RIO Imaging facility.

Supporting Information

Additional Supporting Information may be found in the online version of this article:

Table S1: Point mutations introduced in the N-terminal cytosolic domain of AtPIP2;1. The table shows the first nine residues of AtPIP2;1 constructs, either WT or carrying mutations (underlined) at positions 4 or 6. Sequences of forward primers used for site-directed mutagenesis are also shown. These primers introduced an XhoI restriction site (italics) and the indicated mutations (underlined).

Figure S1: Alignment of amino acid sequences of N-terminal cytosolic domain of *A. thaliana* AtPIP1s and AtPIP2s. The acidic residues conforming to the (D/E)X(D/E) diacidic motifs are highlighted in bold.

Figure S2: Relative abundance of AtPIP2;1-GFP constructs expressed in transgenic *Arabidopsis*. Top. Western blot, using an anti-GFP antibody, of total proteins extracts from untransformed (UT) and transgenic plantlets expressing AtPIP2;1-GFP constructs, either WT or with the indicated mutation. Bottom. Ponceau red stain of the membrane.

Figure S3: Higher magnification of intracellular labelling observed in the diacidic mutant AtPIP2;1-GFP constructs. A labelling of a network (left) and the fusiform bodies (right) was observed in E6A mutant epidermal root and hypocotyl cells, respectively, as shown here as an example. Bar = 10 μm .

Figure S4: Diacidic mutants of AtPIP2;1-GFP constructs colocalize with ER-Tracker staining at the ER. Epidermal root cells expressing the indicated AtPIP2;1-GFP constructs were observed for GFP fluorescence (left column) and stained with ER-Tracker. The dye (central column) shows fluorescence located in a reticulate network which is extended throughout the cell. The merge image shows that all diacidic mutants colocalize with ER-Tracker staining. A faint colocalization of the WT form with the ER-Tracker reticulate network was observed (arrow). Bar = 10 μm .

Figure S5: Co-expression in epidermal leaf cells of AtPIP2;1-GFP constructs and either YFP-HDEL or Man49-YFP. Epidermal leaf cells expressing the indicated AtPIP2;1-GFP and either YFP-HDEL (A) or Man49-YFP (B) constructs were observed for GFP (left column) and YFP fluorescence (central). Same legend as in Figure 3. Bar = 10 μm .

Please note: Wiley-Blackwell are not responsible for the content or functionality of any supporting materials supplied by the authors. Any queries (other than missing material) should be directed to the corresponding author for the article.

References

1. Maurel C, Santoni V, Luu DT, Wudick MM, Verdoucq L. The cellular dynamics of plant aquaporin expression and functions. *Curr Opin Plant Biol* 2009;12:690–698.
2. Maurel C, Verdoucq L, Luu DT, Santoni V. Plant aquaporins: membrane channels with multiple integrated functions. *Annu Rev Plant Biol* 2008;59:595–624.

3. Wudick MM, Luu DT, Maurel C. A look inside: localization patterns and functions of intracellular plant aquaporins. *New Phytol* 2009;184:289–302.
4. Heinen RB, Ye Q, Chaumont F. Role of aquaporins in leaf physiology. *J Exp Bot* 2009;60:2971–85.
5. Quigley F, Rosenberg JM, Shachar-Hill Y, Bohnert HJ. From genome to function: the *Arabidopsis* aquaporins. *Genome Biol* 2002;3:1–17.
6. Johanson U, Karlsson M, Gustavsson S, Sjovald S, Frayse L, Weig AR, Kjellbom P. The complete set of genes encoding major intrinsic proteins in *Arabidopsis* provides a framework for a new nomenclature for major intrinsic proteins in plants. *Plant Physiol* 2001;126:1358–1369.
7. Vander Willigen C, Verdoucq L, Boursiac Y, Maurel C. Aquaporins in plants. In: Blatt MR, editor. *Membrane Transport in Plants*. Oxford, U.K.: Blackwell Publishing; 2004, pp. 221–251.
8. Luu D-T, Maurel C. Aquaporins in a challenging environment: molecular gears for adjusting plant water status. *Plant Cell Environ* 2005;28:85–96.
9. Boursiac Y, Boudet J, Postaire O, Luu DT, Tournaire-Roux C, Maurel C. Stimulus-induced downregulation of root water transport involves reactive oxygen species-activated cell signalling and plasma membrane intrinsic protein internalization. *Plant J* 2008;56:207–218.
10. Sato K, Nakano A. Mechanisms of COPII vesicle formation and protein sorting. *FEBS Lett* 2007;581:2076–2082.
11. Lefebvre B, Batoko H, Duby G, Boutry M. Targeting of a *Nicotiana glauca* H⁺-ATPase to the plasma membrane is not by default and requires cytosolic structural determinants. *Plant Cell* 2004;16:1772–1789.
12. Contreras I, Yang Y, Robinson DG, Aniento F. Sorting signals in the cytosolic tail of plant p24 proteins involved in the interaction with the COPII coat. *Plant Cell Physiol* 2004;45:1779–1786.
13. Hanton SL, Renna L, Bortolotti LE, Chatre L, Stefano G, Brandizzi F. Diacidic motifs influence the export of transmembrane proteins from the endoplasmic reticulum in plant cells. *Plant Cell* 2005;17:3081–3093.
14. Yuasa K, Toyooka K, Fukuda H, Matsuoka K. Membrane-anchored prolyl hydroxylase with an export signal from the endoplasmic reticulum. *Plant J* 2005;41:81–94.
15. Mikosch M, Hurst AC, Hertel B, Homann U. Diacidic motif is required for efficient transport of the K⁺ channel KAT1 to the plasma membrane. *Plant Physiol* 2006;142:923–930.
16. Zelazny E, Miecielica U, Borst JW, Hemminga MA, Chaumont F. An N-terminal diacidic motif is required for the trafficking of maize aquaporins ZmPIP2;4 and ZmPIP2;5 to the plasma membrane. *Plant J* 2009;57:346–355.
17. Contreras I, Ortiz-Zapater E, Aniento F. Sorting signals in the cytosolic tail of membrane proteins involved in the interaction with plant ARF1 and coatamer. *Plant J* 2004;38:685–698.
18. Hanton SL, Chatre L, Renna L, Matheson LA, Brandizzi F. De novo formation of plant endoplasmic reticulum export sites is membrane cargo induced and signal mediated. *Plant Physiol* 2007;143:1640–1650.
19. Mikosch M, Kaberich K, Homann U. ER export of KAT1 is correlated to the number of acidic residues within a triacidic motif. *Traffic* 2009;10:1481–1487.
20. Chatre L, Watelet-Boyer V, Melsner S, Maneta-Peyret L, Brandizzi F, Moreau P. A novel di-acidic motif facilitates ER export of the syntaxin SYP31. *J Exp Bot* 2009;60:3157–3165.
21. Sieben C, Mikosch M, Brandizzi F, Homann U. Interaction of the K(+) channel KAT1 with the coat protein complex II coat component Sec24 depends on a di-acidic endoplasmic reticulum export motif. *Plant J* 2008;56:997–1006.
22. Giraudo CG, Maccioni HJ. Endoplasmic reticulum export of glycosyltransferases depends on interaction of a cytoplasmic dibasic motif with Sar1. *Mol Biol Cell* 2003;14:3753–3766.
23. Renard HF, Demaegd D, Guerriat B, Morsomme P. Efficient ER exit and vacuole targeting of yeast Sna2p require two tyrosine-based sorting motifs. *Traffic* 2010;11:931–946.
24. Farhan H, Korkhov VM, Paulitschke V, Dorostkar MM, Scholze P, Kudlacek O, Freissmuth M, Sitte HH. Two discontinuous segments in the carboxyl terminus are required for membrane targeting of the rat gamma-aminobutyric acid transporter-1 (GAT1). *J Biol Chem* 2004;279:28553–28563.
25. Schoberer J, Vavra U, Stadlmann J, Hawes C, Mach L, Steinkellner H, Strasser R. Arginine/lysine residues in the cytoplasmic tail promote ER export of plant glycosylation enzymes. *Traffic* 2009;10:101–115.
26. Nufer O, Kappeler F, Guldbrandsen S, Hauri HP. ER export of ERGIC-53 is controlled by cooperation of targeting determinants in all three of its domains. *J Cell Sci* 2003;116:4429–4440.
27. Nufer O, Guldbrandsen S, Degen M, Kappeler F, Paccaud JP, Tani K, Hauri HP. Role of cytoplasmic C-terminal amino acids of membrane proteins in ER export. *J Cell Sci* 2002;115:619–628.
28. Fernandez-Sanchez E, Diez-Guerra FJ, Cubelos B, Gimenez C, Zafra F. Mechanisms of endoplasmic-reticulum export of glycine transporter-1 (GLYT1). *Biochem J* 2008;409:669–681.
29. Sevier CS, Weisz OA, Davis M, Machamer CE. Efficient export of the vesicular stomatitis virus G protein from the endoplasmic reticulum requires a signal in the cytoplasmic tail that includes both tyrosine-based and di-acidic motifs. *Mol Biol Cell* 2000;11:13–22.
30. Nishimura N, Balch WE. A di-acidic signal required for selective export from the endoplasmic reticulum. *Science* 1997;277:556–558.
31. Votsmeier C, Gallwitz D. An acidic sequence of a putative yeast Golgi membrane protein binds COPII and facilitates ER export. *EMBO J* 2001;20:6742–6750.
32. Malkus P, Jiang F, Schekman R. Concentrative sorting of secretory cargo proteins into COPII-coated vesicles. *J Cell Biol* 2002;159:915–921.
33. Wang X, Matteson J, An Y, Moyer B, Yoo JS, Bannykh S, Wilson IA, Riordan JR, Balch WE. COPII-dependent export of cystic fibrosis transmembrane conductance regulator from the ER uses a di-acidic exit code. *J Cell Biol* 2004;167:65–74.
34. Ma D, Zerangue N, Lin Y-F, Collins A, Yu M, Jan YN, Jan LY. Role of ER export signals in controlling surface potassium channel numbers. *Science* 2001;291:316–319.
35. Moreau P, Brandizzi F, Hanton S, Chatre L, Melsner S, Hawes C, Satiat-Jeuennetaire B. The plant ER-Golgi interface: a highly structured and dynamic membrane complex. *J Exp Bot* 2007;58:49–64.
36. Fetter K, Van Wilder V, Moshelion M, Chaumont F. Interactions between plasma membrane aquaporins modulate their water channel activity. *Plant Cell* 2004;16:215–228.
37. Zelazny E, Borst JW, Muylaert M, Batoko H, Hemminga MA, Chaumont F. FRET imaging in living maize cells reveals that plasma membrane aquaporins interact to regulate their subcellular localization. *Proc Natl Acad Sci U S A* 2007;104:12359–12364.
38. Otto B, Uehlein N, Sdorra S, Fischer M, Ayaz M, Belastegui-Macadam X, Heckwolf M, Lachnit M, Pede N, Priem N, Reinhard A, Siegfart S, Urban M, Kaldenhoff R. Aquaporin tetramer composition modifies the function of tobacco aquaporins. *J Biol Chem* 2010;285:31253–31260.
39. Hawes C, Saint-Jore C, Martin B, Zheng HQ. ER confirmed as the location of mystery organelles in *Arabidopsis* plants expressing GFP! *Trends Plant Sci* 2001;6:245–246.
40. Saint-Jore CM, Evins J, Batoko H, Brandizzi F, Moore I, Hawes C. Redistribution of membrane proteins between the Golgi apparatus and endoplasmic reticulum in plants is reversible and not dependent on cytoskeletal networks. *Plant J* 2002;29:661–678.
41. Boevink P, Cruz S, Hawes C, Harris N, Oparka KJ. Virus-mediated delivery of the green fluorescent protein to the endoplasmic reticulum of plant cells. *Plant J* 1996;10:935–941.
42. Villarejo A, Buren S, Larsson S, Dejardin A, Monne M, Rudhe C, Karlsson J, Jansson S, Lerouge P, Rolland N, von Heijne G, Grebe M, Bako L, Samuelsson G. Evidence for a protein transported through the secretory pathway en route to the higher plant chloroplast. *Nature* 2005;7:1224–1231.
43. Nelson B, Cai X, Nebenfuhr A. A multicolored set of in vivo organelle markers for co-localization studies in *Arabidopsis* and other plants. *Plant J* 2007;51:1126–1136.
44. Sutter JU, Campanoni P, Tyrrell M, Blatt MR. Selective mobility and sensitivity to SNAREs is exhibited by the *Arabidopsis* KAT1 K⁺ channel at the plasma membrane. *Plant Cell* 2006;18:935–954.
45. Takano J, Tanaka M, Toyoda A, Miwa K, Kasai K, Fuji K, Onouchi H, Naito S, Fujiwara T. Polar localization and degradation of *Arabidopsis* boron transporters through distinct trafficking pathways. *Proc Natl Acad Sci U S A* 2010;107:5220–5225.

46. Runions J, Brach T, Kuhner S, Hawes C. Photoactivation of GFP reveals protein dynamics within the endoplasmic reticulum membrane. *J Exp Bot* 2006;57:43–50.
47. Tolley N, Sparkes IA, Hunter PR, Craddock CP, Nuttall J, Roberts LM, Hawes C, Pedrazzini E, Frigerio L. Overexpression of a plant reticulon remodels the lumen of the cortical endoplasmic reticulum but does not perturb protein transport. *Traffic* 2008;9:94–102.
48. Jaillais Y, Fobis-Loisy I, Miegue C, Gaude T. Evidence for a sorting endosome in Arabidopsis root cells. *Plant J* 2008;53:237–247.
49. Fluckiger R, De Caroli M, Piro G, Dalessandro G, Neuhaus JM, Di Sansebastiano GP. Vacuolar system distribution in Arabidopsis tissues, visualized using GFP fusion proteins. *J Exp Bot* 2003;54:1577–1584.
50. Boursiac Y, Chen S, Luu DT, Sorieul M, van den Dries N, Maurel C. Early effects of salinity on water transport in Arabidopsis roots. Molecular and cellular features of aquaporin expression. *Plant Physiol* 2005;139:790–805.
51. Tournaire-Roux C, Sutka M, Javot H, Gout E, Gerbeau P, Luu DT, Bligny R, Maurel C. Cytosolic pH regulates root water transport during anoxic stress through gating of aquaporins. *Nature* 2003;425:393–397.
52. Beebo A, Thomas D, Der C, Sanchez L, Leborgne-Castel N, Marty F, Schoefs B, Bouhidel K. Life with and without AtTIP1;1, an Arabidopsis aquaporin preferentially localized in the opposing tonoplasts of adjacent vacuoles. *Plant Mol Biol* 2009;70:193–209.
53. Saito C, Ueda T, Abe H, Wada Y, Kuroiwa T, Hisada A, et al. A complex and mobile structure forms a distinct subregion within the continuous vacuolar membrane in young cotyledons of *Arabidopsis*. *Plant J* 2002;29:245–255.
54. Hanton SL, Matheson LA, Brandizzi F. Seeking a way out: export of proteins from the plant endoplasmic reticulum. *Trends Plant Sci* 2006;11:335–343.
55. Nishimura N, Bannykh S, Slabough S, Matteson J, Altschuler Y, Hahn K, Balch WE. A di-acidic (DXE) code directs concentration of cargo during export from the endoplasmic reticulum. *J Biol Chem* 1999;274:15937–15946.
56. Lee HK, Cho SK, Son O, Xu Z, Hwang I, Kim WT. Drought stress-induced Rma1H1, a RING membrane-anchor E3 ubiquitin ligase homolog, regulates aquaporin levels via ubiquitination in transgenic Arabidopsis plants. *Plant Cell* 2009;21:622–641.
57. Martre P, Morillon R, Barrieu F, North GB, Nobel PS, Chrispeels MJ. Plasma membrane aquaporins play a significant role during recovery from water deficit. *Plant Physiol* 2002;130:2101–2110.
58. Kaldenhoff R, Grote K, Zhu JJ, Zimmermann U. Significance of plasmalemma aquaporins for water-transport in Arabidopsis thaliana. *Plant J* 1998;14:121–128.
59. Murashige T, Skoog F. A revised medium for rapid growth and bioassays with tobacco tissue cultures. *Physiol Plant* 1962;15:473–497.
60. Schardl CL, Byrd AD, Benzion G, Altschuler MA, Hildebrand DF, Hunt AG. Design and construction of a versatile system for the expression of foreign genes in plants. *Gene* 1987;61:1–11.
61. Hellens RP, Edwards EA, Leyland NR, Bean S, Mullineaux PM. pGreen: a versatile and flexible binary Ti vector for Agrobacterium-mediated plant transformation. *Plant Mol Biol* 2000;42:819–832.
62. Clough SJ, Bent AF. Floral dip: a simplified method for *Agrobacterium*-mediated transformation of *Arabidopsis thaliana*. *Plant J* 1998;16:735–743.
63. Santoni V, Vinh J, Pflieger D, Sommerer N, Maurel C. A proteomic study reveals novel insights into the diversity of aquaporin forms expressed in the plasma membrane of plant roots. *Biochem J* 2003;373:289–296.
64. Javot H, Lauvergeat V, Santoni V, Martin-Laurent F, Guclu J, Vinh J, Heyes J, Franck KI, Schaffner AR, Bouchez D, Maurel C. Role of a single aquaporin isoform in root water uptake. *Plant Cell* 2003;15:509–522.

Stimulus-induced downregulation of root water transport involves reactive oxygen species-activated cell signalling and plasma membrane intrinsic protein internalization

Yann Boursiac, Julie Boudet[†], Olivier Postaire[†], Doan-Trung Luu[†], Colette Tournaire-Roux and Christophe Maurel^{*}
Biochimie et Physiologie Moléculaire des Plantes, Institut de Biologie Intégrative des Plantes, UMR 5004 CNRS/UMR 0386 INRA/Montpellier SupAgro/Université Montpellier 2, F-34060 Montpellier Cedex 1, France

Received 1 February 2008; revised 24 April 2008; accepted 12 May 2008.

^{*}For correspondence (fax +33 4 67 52 57 37; e-mail maurel@supagro.inra.fr).

[†]These authors contributed equally to this work.

Summary

The water uptake capacity of plant roots (i.e. their hydraulic conductivity, L_p) is determined in large part by aquaporins of the plasma membrane intrinsic protein (PIP) subfamily. In the present work, we investigated two stimuli, salicylic acid (SA) and salt, because of their ability to induce an accumulation of reactive oxygen species (ROS) and an inhibition of L_p , concomitantly in the roots of Arabidopsis plants. The inhibition of L_p by SA was partially counteracted by preventing the accumulation of hydrogen peroxide (H_2O_2) with exogenous catalase. In addition, exogenous H_2O_2 was able to reduce L_p by up to 90% in <15 min. Based on the lack of effects of H_2O_2 on the activity of individual aquaporins in *Xenopus* oocytes, and on a pharmacological dissection of the action of H_2O_2 on L_p , we propose that ROS do not gate Arabidopsis root aquaporins through a direct oxidative mechanism, but rather act through cell signalling mechanisms. Expression in transgenic roots of PIP-GFP fusions and immunogold labelling indicated that external H_2O_2 enhanced, in <15 min, the accumulation of PIPs in intracellular structures tentatively identified as vesicles and small vacuoles. Exposure of roots to SA or salt also induced an intracellular accumulation of the PIP-GFP fusion proteins, and these effects were fully counteracted by co-treatment with exogenous catalase. In conclusion, the present work identifies SA as a novel regulator of aquaporins, and delineates an ROS-dependent signalling pathway in the roots of Arabidopsis. Several abiotic and biotic stress-related stimuli potentially share this path, which involves an H_2O_2 -induced internalization of PIPs, to downregulate root water transport.

Keywords: Aquaporin, stress, reactive oxygen species, salicylic acid, salt, root.

Introduction

Reactive oxygen species (ROS) were initially seen as hazardous byproducts of stress metabolism. More recently, ROS have emerged as signalling intermediates during plant cell responses to hormonal and environmental signals (Apel and Hirt, 2004). In roots, a causal relationship has been established between ROS accumulation and cell growth, during the auxin-induced gravitropic response of maize root tips (Joo *et al.*, 2001), or during the emergence of Arabidopsis root hairs (Foreman *et al.*, 2003). The production of ROS has also been shown to occur following exposure of roots to multiple biotic or abiotic stimuli, such as pathogenic or symbiotic microorganisms (Bais *et al.*, 2003; Peleg-Grossman *et al.*, 2007), salinity (Demidchik *et al.*, 2003; Leshem *et al.*, 2006), hypoxia (Baxter-Burrell *et al.*, 2002),

chilling (Aroca *et al.*, 2005; Lee *et al.*, 2004) or nutrient deficiency (Shin and Schachtman, 2004; Shin *et al.*, 2005). In the case of potassium (K^+) deficiency, hydrogen peroxide (H_2O_2) was shown to mediate the induction of K^+ -uptake systems and genes responsive to K^+ deficiency (Shin and Schachtman, 2004). ROS have also been identified as potential regulators of water transport during chilling stress in maize and cucumber roots (Aroca *et al.*, 2005; Lee *et al.*, 2004).

It is now well established that in most plant species, the uptake of water by roots is in large part mediated by aquaporins, i.e. water channel proteins that facilitate water transport across cell membranes (Kaldenhoff and Fischer, 2006; Maurel *et al.*, 2008; Vandeleur *et al.*, 2005). Plasma membrane intrinsic proteins (PIPs), which represent the

most abundant aquaporins in the plant plasma membrane, seem to control most of the transcellular water flow in roots, and therefore play a predominant role in water uptake. Most importantly, PIP aquaporins provide the plant with the ability to modulate their root hydraulic conductivity (L_p) in response to a large variety of environmental factors (Chaumont *et al.*, 2005; Maurel *et al.*, 2008; Vandeleur *et al.*, 2005). Whereas the mechanisms involved in regulation of root aquaporins during hypoxic or water stresses have been the object of extensive research (Chaumont *et al.*, 2005; Maurel *et al.*, 2008; Vandeleur *et al.*, 2005), the mode of action of chilling stress and/or ROS on the regulation of water transport and aquaporins has remained uncertain. In cucumber roots, chilling induced a rapid accumulation of H_2O_2 at the cell wall/plasma membrane interface, and exogenous H_2O_2 , similar to chilling, reduced the L_p by up to roughly sixfold (Lee *et al.*, 2004), but by unknown mechanisms. In maize roots, a high concentration of H_2O_2 (35 mM) also reversibly blocked the hydraulic conductivity of excised roots or cortical cells *in situ* (Ye and Steudle, 2006). In addition, exogenous H_2O_2 , similar to chilling, induced a differential regulation of L_p between two maize cultivars that differed in their sensitivity to chilling (Aroca *et al.*, 2005). However, neither the osmotic water permeability of isolated root protoplasts nor the changes in abundance of PIPs, or of their phosphorylated forms, matched the differential responses of the two cultivars to H_2O_2 , and a dominating role of H_2O_2 -induced membrane injury was invoked (Aroca *et al.*, 2005). By contrast with root cells, internodal cells of *Chara corallina* have mercury-sensitive water channels that are essentially insensitive to H_2O_2 , even at high (>100 mM) concentrations (Henzler and Steudle, 2000). However, the channels were highly sensitive to minute (nM) concentrations of hydroxyl radicals (OH^*), and it was proposed that OH^* , but not H_2O_2 , would oxidize residues in aquaporins or lipids nearby, therefore leading to channel inactivation (Henzler *et al.*, 2004). The finding that aquaporins can be permeated by H_2O_2 (Bienert *et al.*, 2007; Henzler and Steudle, 2000) has also suggested new connections between aquaporin function and ROS signalling and/or oxidative stress response.

In view of the involvement of ROS in the responses of roots to multiple stress or hormonal signals, we have investigated a general role of ROS in mediating the stimulus-induced regulation of water uptake. We firstly identified two typical abiotic and biotic stress-related stimuli, salicylic acid (SA) and salt, for their ability to induce an accumulation of ROS and an inhibition of water transport concomitantly in *Arabidopsis* roots. We further investigated the general effects and mode of action of H_2O_2 in *Arabidopsis* roots, and show that this compound and/or derived ROS species act as potent inhibitors of water transport, through cell signalling and aquaporin internalization mechanisms. These findings point to a conserved mechanism where ROS

mediate, in part, the stimulus-induced downregulation of aquaporins in plant roots.

Results

ROS-mediated inhibition of root water transport by SA

The accumulation of ROS in roots was investigated by imaging the oxidatively sensitive fluorescence of carboxy-2',7'-dichlorofluorescein (carboxy-DCF) released intracellularly from its acetylated form (carboxy- H_2 DCFDA) (Coelho *et al.*, 2002; Foreman *et al.*, 2003; Shin and Schachtman, 2004). In a general survey of environmental and/or hormonal stimuli, we observed that the exposure of roots to SA for 60 min increased the relative fluorescence of carboxy-DCF by ~60%, and therefore triggered an accumulation of ROS in root cells (Figure S1). We also checked, in agreement with previous reports (Demidchik *et al.*, 2003; Leshem *et al.*, 2006), that the treatment of *Arabidopsis* roots with salt (150 mM NaCl) induced an intracellular ROS accumulation (Figure S1).

Whereas the time- and dose-dependent inhibition of root water transport by salt has already been described in *Arabidopsis* and other species (Boursiac *et al.*, 2005; Carvajal *et al.*, 1999; Martinez-Ballesta *et al.*, 2003), the effects of SA on tissue water transport have remained unexplored. To investigate these effects, the pressure-induced sap flow [$J_v(P)$] was measured in excised *Arabidopsis* roots. Figure 1a shows that the application of 0.5 mM SA, at a constant 320 kPa pressure, induced a time-dependent decrease in $J_v(P)$ of ~25% in ~60 min. Lower SA concentrations (0.01–0.1 mM) had no significant effect on $J_v(P)$ (not shown). The effects of 0.5 mM SA were fully reversed after <50 min after washout. In parallel experiments, we determined pressure–sap flow relationships, and checked that the inhibition of $J_v(P)$ by SA reflected an inhibition of L_p by a similar factor (not shown). Because of the relatively rapid kinetics of inhibition ($T_{1/2 \text{ inhibition}} = 19.8 \pm 4.4$ min; $n = 21$) and reversion ($T_{1/2 \text{ reversion}} = 12.3 \pm 5.2$ min; $n = 7$), the effects of SA on L_p were interpreted to result from the regulation of root aquaporins. Overall, an inhibition of L_p by $29.2 \pm 2.4\%$ ($n = 21$) was observed after exposure for 90 min to 0.5 mM SA, whereas the chemical analogue 4-hydroxybenzoic acid induced a much lower inhibition ($6.4 \pm 2.4\%$; $n = 11$) with a concentration of 0.5 mM. Therefore, the effects of SA on L_p cannot be explained by a direct acid loading resulting from SA intracellular diffusion (Tournaire-Roux *et al.*, 2003).

To determine the role of ROS (and H_2O_2 in particular) in the SA-dependent inhibition of L_p , H_2O_2 accumulation was prevented by treating roots with 400 U ml^{-1} catalase for 30 min prior to exposure to 0.5 mM SA for 90 min. In these experiments, the procedure significantly reduced ($P = 0.007$) the inhibition of L_p by SA from 36.6 to 25.1% (Figure 1b). In contrast, treatment of roots by catalase alone had no effect

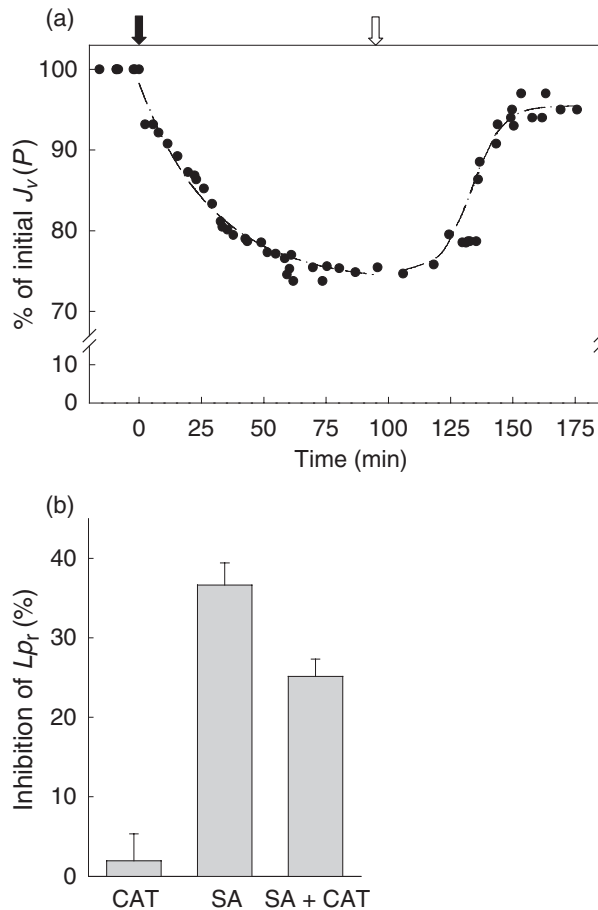


Figure 1. The effects of salicylic acid (SA) on root water transport, and the counteracting effects of catalase.

(a) Pressure-induced sap flow [$J_v(P)$] was measured in excised roots at 320 kPa. After 45 min ($t = 0$), the root bathing solution was complemented by 0.5 mM SA (filled arrow), and the hormone was washed out after 90 min (empty arrow). The figure shows a representative recording, with $J_v(P)$ expressed as a percentage of the mean value in the 10 min preceding treatment with SA.

(b) The independent and combined effects of the treatment of roots by catalase (CAT; 400 u ml^{-1}) or SA (0.5 mM) on the hydraulic conductivity of the roots (L_p). Roots were pre-treated with catalase alone for 30 min, and were further incubated for 90 min with catalase and SA (CAT + SA) or catalase alone (CAT). Treatment of roots with SA alone (SA) was for 90 min. L_p inhibition is expressed as a percentage of the mean L_p value in the 10 min preceding treatment with SA and/or CAT. The mean L_p value in control conditions was $167.7 \pm 5.5 \text{ ml g}^{-1} \text{ h}^{-1} \text{ MPa}^{-1}$. Data were pooled from two independent cultures (CAT, $n = 8$ plants; SA, $n = 16$ plants; CAT + SA, $n = 16$ plants). All treatments are statistically different from each other, with $P \leq 0.008$.

(2% inhibition) on L_p . These data show that the downregulation of root water transport by SA is mediated in part by an enhanced accumulation of H_2O_2 .

Inhibition of root water transport by exogenous H_2O_2

The effects of exogenous H_2O_2 on whole root water transport were investigated using the same approach as has been

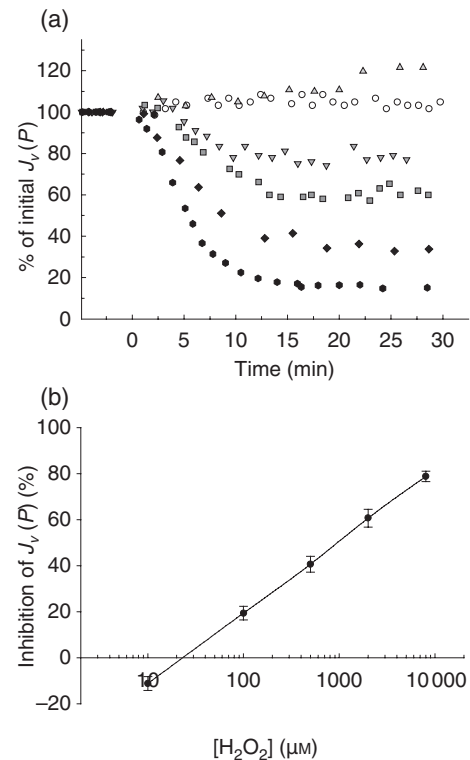


Figure 2. Time- and dose-dependent effects of hydrogen peroxide (H_2O_2) on root water transport.

(a) Time-dependent variations of the pressure-induced sap flow [$J_v(P)$] (expressed as a percentage of the mean value in the 10 min preceding treatment with H_2O_2) in roots bathed in a solution in the absence (\circ) or in the presence of 10 μM (\blacktriangle), 100 μM (∇), 500 μM (\blacksquare), 2 mM (\blacklozenge) or 8 mM (\circ) H_2O_2 .

(b) Final percentage of $J_v(P)$ inhibition. For each plant, $J_v(P)$ was determined prior to and after exposure to the indicated H_2O_2 concentration for $t = 20$ –30 min. Data represent the average value (\pm SE) of $n \geq 5$ plants from at least two independent cultures. The mean value of the hydraulic conductivity of the roots (L_p) in control conditions was $151.4 \pm 8.8 \text{ ml g}^{-1} \text{ h}^{-1} \text{ MPa}^{-1}$.

exemplified for SA. Figure 2a shows that application of H_2O_2 to excised root systems induced a time- and dose-dependent decrease in $J_v(P)$. For instance, exposure for 25 min to 0.1–8 mM H_2O_2 concentrations led to a decrease in $J_v(P)$ of 19–79% (Figure 2b). In the same experiments, the half-time of inhibition showed a tendency ($P = 0.08$) to reduce from 8.8 ± 0.9 min (0.1 mM H_2O_2 ; $n = 5$) to 6.3 ± 0.3 min (8 mM H_2O_2 ; $n = 5$) (Figure 2a and data not shown). The pressure–sap flow relationships determined in parallel indicated that millimolar concentrations of exogenous H_2O_2 reduced $J_v(P)$ and L_p by the same factor (not shown). We note that, because of the presence of transition metals in the apoplast, the molecules acting on root water transport can be either H_2O_2 or related ROS, in particular OH^\bullet , which is produced by a Fenton reaction.

Because aquaporins contribute to more than 70% of the L_p in Arabidopsis (Boursiac *et al.*, 2005; Tournaire-Roux *et al.*, 2003), the marked effects of H_2O_2 on root water transport must be mediated in large part by an inhibition of

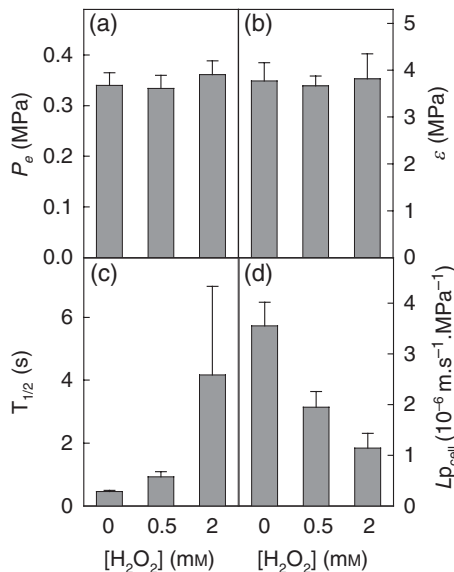


Figure 3. Dose-dependent effects of hydrogen peroxide (H_2O_2) on the water relation parameters of root cortical cells.

Cell pressure probe measurements were performed in cortical cells of root segments that were incubated for 25–45 min in a bathing solution complemented with the indicated H_2O_2 concentration ($[\text{H}_2\text{O}_2]$). The figure shows the mean values (\pm SE) of turgor (P_e ; a), volumetric elastic modulus (ϵ ; b), half-time of hydrostatic relaxation ($T_{1/2}$; c) and hydraulic conductivity (Lp_{cell} ; d). The Lp_{cell} was significantly reduced by the H_2O_2 treatment, with the following P values and number of cells measured: $[\text{H}_2\text{O}_2] = 0$, $n = 8$; $[\text{H}_2\text{O}_2] = 0.5$ mM, $P = 0.007$, $n = 8$; $[\text{H}_2\text{O}_2] = 2$ mM, $P = 0.001$, $n = 6$.

aquaporin activity. To establish this idea further, we investigated the effects of H_2O_2 on the water relation parameters of single root cells *in situ*. Cortical cells are the only cells of the Arabidopsis root that are amenable to cell pressure probe measurements (Javot *et al.*, 2003). Figure 3 shows that the treatment of roots for 25–45 min by up to 2 mM H_2O_2 neither changed the stationary turgor (P_e) nor changed the volumetric elastic modulus (ϵ) of these cells. By contrast, the half-time of water exchange ($T_{1/2}$) was increased from 0.46 to 4.16 sec after treatment with concentrations of H_2O_2 of up to 2 mM. This resulted in a dose-dependent inhibition of cell hydraulic conductivity (Lp_{cell}) by 45 and 68% in response to 0.5 and 2 mM H_2O_2 , respectively ($P < 0.01$). Because, in the Arabidopsis root cortex, Lp_{cell} is in large part determined by aquaporins (Javot *et al.*, 2003; Tournaire-Roux *et al.*, 2003), these data indicate that H_2O_2 markedly reduced aquaporin activity in cortical cells without significantly altering solute accumulation (P_e) or cell wall elasticity (ϵ).

Insensitivity of aquaporins to direct exposure to ROS

To test the hypothesis of an oxidative gating of root aquaporins by ROS (Henzler *et al.*, 2004), the sensitivity of individual aquaporin isoforms to ROS inhibition was investigated after functional expression in *Xenopus* oocytes. We characterized, among the most abundantly expressed

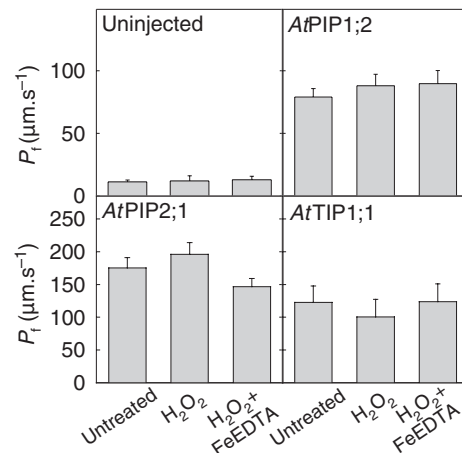


Figure 4. Effects of reactive oxygen species (ROS) on the osmotic water permeability (P_i) of oocytes expressing aquaporin isoforms.

P_i (\pm SE; $n > 7$ cells) was measured in oocytes, either native (uninjected) or injected with cRNAs encoding the indicated aquaporins. Oocytes were either untreated or pre-incubated for 5 min prior to the swelling assay in the presence of 2 mM H_2O_2 (H_2O_2), or 2 mM H_2O_2 and 2 mM FeEDTA ($\text{H}_2\text{O}_2 + \text{FeEDTA}$).

aquaporins from Arabidopsis roots (Alexandersson *et al.*, 2005; Boursiac *et al.*, 2005; Santoni *et al.*, 2003), three different isoforms, AtPIP1;2, AtPIP2;1 and AtTIP1;1, as representative members of three distinct subclasses. Osmotic swelling assays showed that the osmotic water permeability (P_i) of oocytes injected with the corresponding cRNAs was significantly higher than that of native (uninjected) oocytes (Figure 4), showing that each of these aquaporins was functionally expressed in these cells. Incubation for 5 min in the presence of 2 mM H_2O_2 or 2 mM H_2O_2 plus 2 mM FeEDTA did not alter the water transport properties of native oocytes or oocytes expressing plant aquaporins (Figure 4). A longer treatment (25 min) by 2 mM H_2O_2 did not significantly affect the P_i of oocytes either (data not shown). Thus, the water transport activity of AtPIP1;2, AtPIP2;1 and AtTIP1;1 was insensitive to H_2O_2 or derived OH^\bullet .

Dependency of Lp_i inhibition by H_2O_2 on cell signalling events

Exposure of plant cells to ROS can initiate a Ca^{2+} influx and downstream signalling cascades (Demidchik *et al.*, 2007; Kwak *et al.*, 2006; Rentel and Knight, 2004), which could ultimately lead to aquaporin downregulation. To test this hypothesis, plants were cultivated in a Ca^{2+} -free bathing solution for 2 h prior to root excision. Excised roots were then treated with 75 μM LaCl_3 , an inhibitor of calcium channels, and 2 mM EGTA, a divalent cation chelator (Rentel and Knight, 2004; Tavernier *et al.*, 1995). By comparison with control untreated roots, $J_v(P)$ was not altered after Ca^{2+} deprivation and 1 h of the $\text{LaCl}_3/\text{EGTA}$ treatment (not

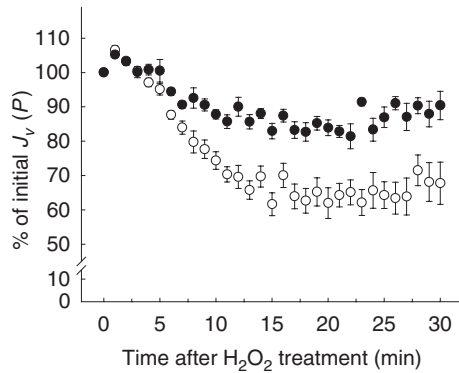


Figure 5. Effects of blockade of Ca²⁺ influx on the inhibition of the pressure-induced sap flow [$J_v(P)$] by hydrogen peroxide (H₂O₂).

In control conditions (○), roots were excised from plants grown in a standard nutrient solution, and $J_v(P)$ was measured for 10 min in the same solution prior to application of 0.5 mM H₂O₂ at $t = 0$. In the treated conditions (●), plants were cultivated in a Ca²⁺-free nutrient medium for 2 h before root excision. $J_v(P)$ was then measured in the same solution for 10 min, and for 10 min in the presence of 75 μM LaCl₃ and 2 mM EGTA, prior to application of 0.5 mM H₂O₂ at $t = 0$. In both conditions, $J_v(P)$ was expressed as a percentage of its initial value prior to treatment with H₂O₂. The figure shows averaged data from $n \geq 7$ individual plants.

shown). By contrast, when added after 10 min of this treatment, 0.5 mM H₂O₂ induced a significant time-dependent decrease in $J_v(P)$ (Figure 5). However, the percentage of inhibition by H₂O₂ ($18.6 \pm 2.8\%$; $n = 8$) was decreased two-fold with respect to that of control roots that were bathed in a standard solution containing Ca²⁺ ($42.9 \pm 4.6\%$; $n = 9$) (Figure 5). The $T_{1/2}$ inhibition resulting from treatment with 0.5 mM H₂O₂ was similar between control roots ($T_{1/2}$ inhibition = 7.5 ± 0.5 min) and roots submitted to the LaCl₃/EGTA pre-treatment ($T_{1/2}$ inhibition = 6.7 ± 0.6 min). The overall results are interpreted to mean that extracellular Ca²⁺, and probably a primary influx of Ca²⁺ in root cells, contributed at least one half of the H₂O₂-induced inhibition of root water transport.

In supplementary experiments we probed for the involvement of phosphorylation events in the downstream response of roots to H₂O₂. Treatment of excised roots with 2 μM staurosporine, a general blocker of protein kinases, for 10 min prior to the addition of 0.5 mM H₂O₂, did not affect the final percentage of the H₂O₂-induced inhibition of $J_v(P)$ (Figure S2). By contrast, $T_{1/2}$ inhibition was significantly increased, from 6.8 min (control) to 9.9 min (staurosporine-treated) (Figure S2). Altogether, our data point to H₂O₂-induced signalling mechanisms, which would be mediated through both primary Ca²⁺ influx and phosphorylation events.

Effects of H₂O₂ on aquaporin subcellular localization

The rapidity of Lp_r inhibition by H₂O₂ suggested that aquaporin regulation might primarily occur at the post-transla-

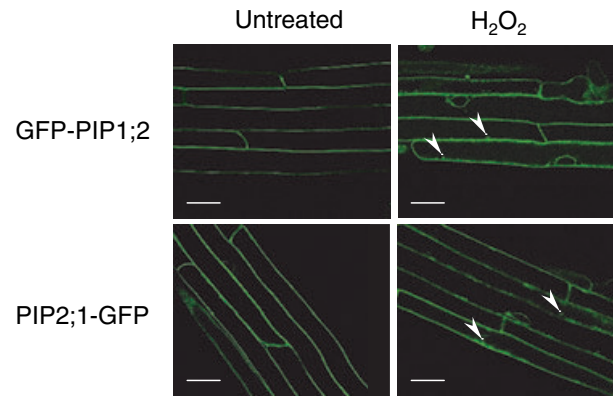


Figure 6. Effects of hydrogen peroxide (H₂O₂) on the subcellular localization of plasma membrane intrinsic protein (PIP) aquaporins in root epidermal cells.

Roots of plants expressing GFP-PIP1;2 or PIP2;1-GFP were incubated for 15 min in the absence (Untreated) or in the presence of 2 mM H₂O₂ (H₂O₂), and images of epidermal cells were taken at 15 min (GFP-PIP1;2) or 30 min (PIP2;1-GFP) from the root apex. Arrowheads indicate the labelling of small intracellular spherical bodies. Scale bar: 20 μm.

tional level. Although a gating of aquaporins in response to cytosolic factors, namely altered phosphorylation, H⁺ or free Ca²⁺, may be involved, here we evaluated the possible contribution of a stimulus-induced relocalization of aquaporins. For this, we used transgenic plants that express fusions of GFP with PIP1;2 and PIP2;1, taken here as representative PIP aquaporins. Laser scanning confocal microscopy of root epidermal cells revealed, in plants grown in standard conditions, a peripheral labelling pattern, indicating predominant expression of the GFP fusions at the plasma membrane (Figure 6). In cells distal from the root apex (20–30 mm), a slight reticulate, perinuclear labelling was occasionally observed, suggesting a partial retention of the fusion proteins in the secretory pathway. Labelling of small intracellular spherical bodies (hereafter referred to as spherical bodies) was occasionally observed in $3.0 \pm 1.5\%$ ($n = 100$ cells) and $6.9 \pm 2.5\%$ ($n = 107$ cells) of epidermal cells expressing GFP-PIP1;2 or PIP2;1-GFP, respectively. Although these bodies might be related to the late endosome/pre-vacuolar compartment (Müller *et al.*, 2007), their precise nature remains undetermined. Treatment of roots expressing the GFP fusions with 2 mM H₂O₂ for 15 min resulted in a marked alteration of this labelling pattern, with a strong enhancement of intracellular staining, either diffuse or localized on discrete structures (Figure 6). In particular, the percentage of GFP-PIP1;2 or PIP2;1-GFP cells showing a labelling of spherical bodies was raised to $27.4 \pm 6.7\%$ ($n = 146$ cells) and $66.4 \pm 13.5\%$ ($n = 87$ cells), respectively. To further quantify the effects of H₂O₂, longitudinal optical sections of epidermal cells were taken at 3, 15 or 30 mm from the apex, and average gray values were integrated from delimited image surfaces corresponding to the cell

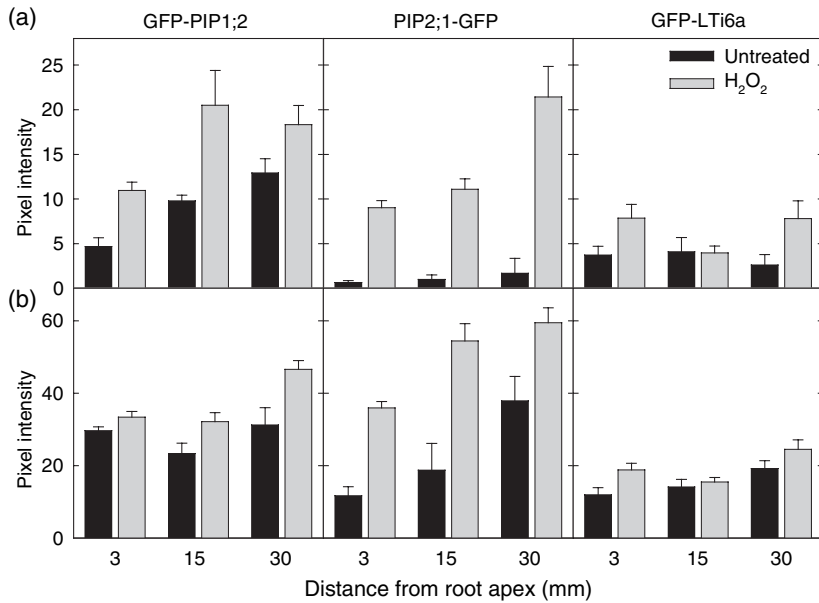


Figure 7. Effects of hydrogen peroxide (H₂O₂) on the intracellular accumulation of plasma membrane intrinsic protein (PIP) aquaporins in epidermal and cortical cells.

Roots of plants expressing GFP-PIP1;2, PIP2;1-GFP or GFP-LTI6a were incubated for 15 min in the absence (black bars) or in the presence of 2 mM H₂O₂ (grey bars). Laser scanning confocal images of epidermal (a) or cortical (b) cells were taken at the indicated distance from the root apex, and the average pixel intensity corresponding to the cell interior was quantified as explained in the text. For each distance, analysis was performed on 3–6 control and 9–17 H₂O₂-treated epidermal cells, and on 5–6 control and 11–20 H₂O₂-treated cortical cells.

periphery and the cell interior, respectively. Images were acquired in conditions where the labelling intensity of the cell surface was close to saturation, and appeared constant between control and H₂O₂-treated cells (not shown). In contrast, H₂O₂ treatment induced an increase by 40–140% and >1000% (11.2–14.3-fold) in the overall intracellular labelling in epidermal cells expressing GFP-PIP1;2 and PIP2;1-GFP, respectively (Figure 7a). Transgenic plants expressing a GFP-low-temperature-inducible protein 6a (GFP-LTI6a) fusion, used here as an independent marker of the plasma membrane, also showed, although less pronounced than with PIP2;1-GFP, an increase in intracellular labelling in response to H₂O₂, by up to 110% (Figure 7a). We also observed a qualitatively similar response to 2 mM H₂O₂ in root cortical cells, with enhanced intracellular labelling by GFP-PIP1;2 (+12–49%), PIP2;1-GFP (+59–209%) or GFP-LTI6a (+10–57%) fusions (Figure 7b). We note that, in resting conditions, the apparent intracellular labelling of cortical cells was higher than in epidermal cells, probably because of a lower resolution of plasma membrane confocal imaging in the former cells. Therefore, the relative effects of H₂O₂ on intracellular labelling might have been more difficult to resolve.

To get an enhanced resolution of the cell membrane responses to H₂O₂, an ultrastructural analysis of epidermal cells was performed by transmission electron microscopy. Immunocytochemistry on control, untreated roots using an anti-PIP2;1 antibody revealed a dense immunogold labelling along the plasma membrane, and occasionally in local invaginations of the cytosol within the vacuolar space (Figure 8a). Treatment of roots with 2 mM H₂O₂ for 15 min did not result in any significant morphological change of cell

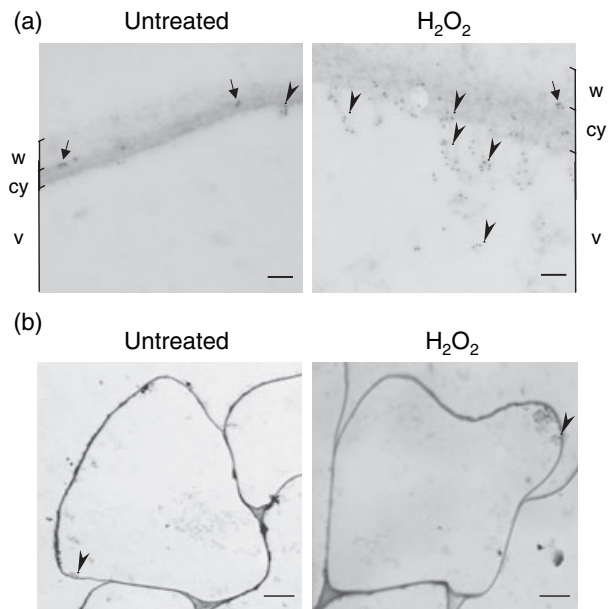


Figure 8. Ultrastructural analysis and expression of plasma membrane intrinsic protein 2 (PIP2) aquaporins in hydrogen peroxide (H₂O₂)-treated epidermal cells.

(a) Immunogold transmission electron microscopy of epidermal cells of roots incubated for 15 min in the absence (Untreated) or in the presence of 2 mM H₂O₂ (H₂O₂). For clarity, the image areas corresponding to the wall (w), cytoplasm (cy) and vacuolar space (v) are indicated. Incubation with a primary anti-PIP2;1 antibody, which cross-reacts with AtPIP2;1, AtPIP2;2 and AtPIP2;3 (Santoni *et al.*, 2003), leads to gold labelling along the plasma membrane (arrows), and in intracellular vesicular structures (arrowheads). No gold labelling was observed in the absence of the primary antibody. Scale bar: 100 nm.

(b) Low-magnification visualization of epidermal cells by transmission electron microscopy. Arrowheads indicate intracellular structures that possibly correspond to spherical bodies. Scale bar: 2 μ m.

membranes (Figure 8b). However, immunogold labelling was more diffuse along the cell surface, and a marked expression of PIP2 in the intracellular compartments was observed (Figure 8a).

Altogether, the microscopic data support the idea that exogenous H_2O_2 enhances the accumulation of PIP aquaporins in intracellular membranes, possibly through relocalization from the plasma membrane.

Dependency of stimulus-induced aquaporin intracellular accumulation on ROS

These findings prompted us to evaluate in closer detail the effects of SA and NaCl on aquaporin subcellular localization, and a possible role of ROS in mediating these effects. Treatment of roots of the aquaporin-GFP reporter lines by SA (0.5 mM, 1 h) resulted in marked changes in the intracellular labelling pattern of epidermal cells, similar to those observed in response to H_2O_2 . A diffuse localization of GFP-PIP1;2 or PIP2;1-GFP along the cell periphery, and in spherical bodies, was observed (Figure 9a). In PIP2;1-GFP plants, and at 30 mm from the root apex, the proportion of epidermal cells with labelled spherical bodies, used here as a reliable indicator of intracellular accumulation of the GFP fusion, was increased from $7.7 \pm 3.8\%$ (untreated) to $32.5 \pm 3.3\%$ (+SA) (Figure 9b). Treatment of roots by 400 U ml^{-1} catalase alone did not significantly alter the PIP2;1-GFP labelling pattern of root epidermal cells. However, when it was provided for 30 min prior to the SA treatment, catalase was able to counteract the SA effects by $\sim 90\%$ ($P = 0.006$), with the percentage of cells with labelled spherical bodies ($10.4 \pm 4.4\%$) being similar to that of control untreated roots. These results suggest that the effects of SA on PIP2;1 subcellular localization are mediated via a pathway involving H_2O_2 .

Exposure of Arabidopsis roots expressing PIP2;1-GFP to 150 mM NaCl for 45 min also enhanced the intracellular staining of epidermal cells. These effects were similar in nature, but were more rapid and pronounced than those previously observed in response to 100 mM NaCl (Boursiac *et al.*, 2005). At 30 mm from the root apex, the proportion of PIP2;1-GFP cells showing a labelling of spherical bodies was increased by about threefold from 9% (untreated) to 27% by treatment with salt (Figure 10). However, the pre-treatment of roots with catalase for 30 min was able to reduce the salt enhancement of the labelling of spherical bodies by 71% ($P = 0.002$), suggesting that these effects were mediated in large part through extracellular H_2O_2 (Figure 10).

Altogether, these observations show that exposure of roots to SA and salt leads to an accumulation of PIP aquaporins in intracellular structures that is qualitatively similar to that induced by exogenous H_2O_2 . The effects of salt and SA on aquaporin localization are mediated in part through ROS, the accumulation of which is enhanced by

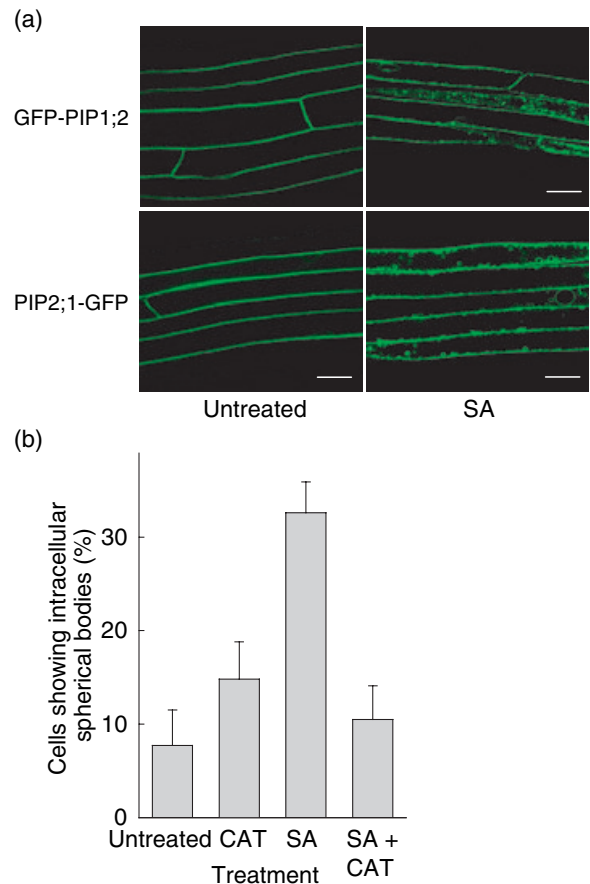


Figure 9. Effects of salicylic acid (SA) on the localization of plasma membrane intrinsic proteins (PIPs) and the counteracting effects of catalase.

(a) Fluorescent images of epidermal cells expressing GFP-PIP1;2 or PIP2;1-GFP, and incubated for 1 h in the absence (Untreated) or in the presence of 0.5 mM SA (SA). Images were taken at 30 mm from the root apex. Note the labelling of spherical bodies in SA-treated cells. Scale bar: 20 μm .

(b) The roots of plants expressing PIP2;1-GFP were untreated (Untreated), treated with 400 U ml^{-1} catalase for 90 min (CAT), treated with 0.5 mM SA for 1 h (SA) or were treated with catalase for 30 min prior to the addition of 0.5 mM SA for one additional hour (CAT + SA). Intracellular spherical bodies were counted in epidermal cells at 30 mm from the root apex. Data from two independent biological experiments, with $n = 9\text{--}12$ plants and $n \geq 120$ cells for each treatment. The treatment with SA was statistically different from all other treatments ($P \leq 0.002$), with no difference between the latter treatments.

these two treatments (Figure S1). These chains of events may contribute to the inhibitory effects of the two stimuli on root water transport.

Discussion

ROS are potent inhibitors of root water transport

Our finding that exogenous H_2O_2 can inhibit Lp_r by up to 80% within 15–20 min of exposure, and can therefore serve as a potent blocker of water transport in Arabidopsis roots, extends previous observations in cucumber (Lee *et al.*, 2004)

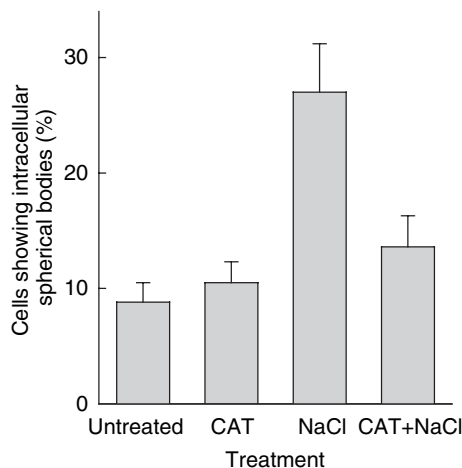


Figure 10. Effects of NaCl on the localization of PIP2;1 can be counteracted by catalase.

Roots expressing PIP2;1-GFP were untreated (Untreated), treated with 400 U ml⁻¹ catalase for 75 min (CAT), treated with 150 mM NaCl for 45 min (NaCl) or were treated with catalase for 30 min prior to the addition of 150 mM NaCl for 45 additional min (CAT + NaCl). Intracellular spherical bodies were counted in epidermal cells at 30 mm from the root apex. Data were from three independent biological experiments, with $n \geq 20$ plants and $n \geq 240$ cells for each treatment. The NaCl treatment was statistically different from all other treatments ($P \leq 0.002$), with no difference between the latter treatments.

and maize (Aroca *et al.*, 2005; Ye and Steudle, 2006). The dose dependency of H₂O₂ effects on Arabidopsis Lp_r , with significant inhibition in the mM range, was consistent with H₂O₂ concentrations reported in the apoplast of root cells under normal (elongating) and stress conditions (Demidchik *et al.*, 2007; Lee *et al.*, 2004; Liszky *et al.*, 2004). We are aware, however, that because transition metals are present in the nutrient solution and the cell walls, H₂O₂ may be converted into other ROS species, such as OH^{*}, which may act as the blocking agents. We also observed a partial, spontaneous reversion of Lp_r inhibition after 1 h of exposure of roots to moderate H₂O₂ concentrations (<0.5 mM, data not shown), indicating a basal ROS detoxification capacity of roots. At higher H₂O₂ doses, the possible saturation of the detoxification machinery may have prevented any detectable reversion of Lp_r inhibition, even after washout of external H₂O₂. Interestingly, 10 μM H₂O₂ had a slight (+11%) stimulatory effect on Lp_r (Figure 2). These effects could be interpreted in line with the signalling mechanism described below, and reflect a balance between water transport activation and inhibition mechanisms.

ROS do not gate Arabidopsis root aquaporins through a direct oxidative mechanism, but instead act through cell signalling mechanisms

The rapidity and amplitude of inhibition of Lp_r by H₂O₂, together with specific effects on the hydraulic conductivity of cortical cells (Figure 3), provided strong evidence that the

inhibition of water transport by H₂O₂ resulted from a marked downregulation of root aquaporins. Most importantly, we could discard a general cytotoxicity of H₂O₂ that did not alter cell turgor, wall properties or cell ultrastructure (Figures 3 and 8).

A primary effect expected to result from ROS reacting with aquaporins is the oxidation of residues with reduced side chains, such as cysteines (Kourie, 1998), which in turn may alter aquaporin structure, thereby leading to channel closure. To investigate such a direct oxidation mechanism, we considered representative root aquaporin homologues, that is two PIPs (AtPIP1;2, AtPIP2;1) and one TIP (AtTIP1;1), with four and a single cysteine residue, respectively. Their water transport activity, as assayed after functional expression in *Xenopus* oocytes, was insensitive to treatments by H₂O₂ alone, or in combination with FeEDTA, suggesting that these aquaporins were primarily insensitive to oxidation by ROS. These ideas are corroborated by independent data obtained in plasma membrane vesicles purified from Arabidopsis roots. Here again, we found that the membrane water permeability was unaltered after exposure of the vesicles to H₂O₂ or derived OH^{*} (YB and CM, unpublished data). Therefore, a direct oxidative gating of aquaporins in the Arabidopsis root treated with H₂O₂ appears unlikely.

These ideas may appear at variance with the model of aquaporin gating by OH^{*} derived from recent studies in *Chara* internodes and maize roots (Henzler *et al.*, 2004; Ye and Steudle, 2006). The possibility exists that aquaporins in these materials are more susceptible to oxidative inhibition by OH^{*} than their Arabidopsis counterparts. We also note that *Chara* and maize cells may, similar to Arabidopsis root cells, express cell signalling cascades responsive to ROS, which, in turn, would downregulate aquaporins.

As an alternative to a direct oxidative gating, we considered a possible role for H₂O₂-dependent signalling pathways. In support for this, the pre-treatment of roots by LaCl₃ and EGTA, which by itself had no effect on Lp_r , counteracted its inhibition by H₂O₂. We speculate that blockade of a primary Ca²⁺ influx prevented a secondary release of Ca²⁺ from intracellular stores and downstream Ca²⁺ signal propagation (Coelho *et al.*, 2002; Rentel and Knight, 2004). In agreement with this, activation of hyperpolarization-activated calcium conductances by high concentrations of H₂O₂ itself has recently been described in mature epidermal or cortical cells (Demidchik *et al.*, 2007). Yet, one half of the inhibition response of Lp_r to H₂O₂ was insensitive to LaCl₃/EGTA, suggesting that pathways independent of a Ca²⁺ influx are also involved.

Plant cell signalling in response to ROS also involves phosphorylation cascades (Apel and Hirt, 2004). Consistent with this, we observed that staurosporine, a broad-range protein kinase inhibitor, significantly delayed the inhibition response of Lp_r to H₂O₂. Therefore, protein kinase(s) in

Arabidopsis root cells probably act to determine a dynamic balance between activated and inactivated aquaporins.

Inhibition of water transport by H₂O₂ involves effects on aquaporin subcellular localization

Confocal imaging and immunogold labelling both revealed that H₂O₂ treatment induced a marked intracellular accumulation of PIPs. Because they occurred within <15 min, these effects are unlikely to result from enhanced aquaporin synthesis and/or inhibition of their trafficking through the secretory pathway. Rather, we propose that H₂O₂ triggered a relocalization of PIPs from the plasma membrane into intracellular membrane compartments (endosomes). PIPs may in turn be partly redirected towards the multivesicular body/prevacuolar compartment (Müller *et al.*, 2007). The spherical bodies labelled by aquaporin-GFP fusions and the intracellular structures revealed by immunogold, which, however, deserve further characterization, may correspond to the latter compartment. Because GFP-LTi6a, an independent plasma membrane marker, also showed some degree of subcellular relocalization, our observations may point to the activation of a general membrane internalization mechanism.

Within this model, exposure of root cells to H₂O₂ could lead to a reduced abundance of PIP aquaporins on the plasma membrane, and therefore to a reduced cell and whole-root hydraulic conductivity. The relative contribution of this mechanism to the overall regulation of water transport by ROS remains, however, to be determined. We cannot exclude other mechanisms, such as acting on aquaporin gating for instance. In particular, the closure of PIPs may result from the binding of free cytosolic Ca²⁺, following local, H₂O₂-induced bursts, or from changes in aquaporin phosphorylation (Alleva *et al.*, 2006; Gerbeau *et al.*, 2002; Johansson *et al.*, 1998; Tornroth-Horsefield *et al.*, 2006). Because staurosporine did not alter the amplitude of *Lp_r* inhibition, but did, however, alter its kinetics, our data do not support the idea of staurosporine-sensitive protein kinases acting directly on aquaporin gating. Phosphorylation of aquaporins remains, however, a central mechanism for controlling various aspects of plant aquaporin functionality. In these respects, we recently showed that both NaCl and H₂O₂ treatments alter the phosphorylation status of the C-terminal tail of AtPIP2;1 (Prak *et al.*, 2008). One of the two sites considered (Ser283) interferes with aquaporin trafficking (Prak *et al.*, 2008).

Effects of SA on root water transport

Salicylic acid is a signalling molecule that has been initially linked to plant defense and more recently to responses to various abiotic stresses (Scott *et al.*, 2004; Shah, 2003; Yalpani *et al.*, 1994). In particular, a regulating role for SA in

salt stress-induced oxidative damage has been proposed (Borsani *et al.*, 2001; Gunes *et al.*, 2007). Together with previously reported effects of SA on stomatal movements (Mori *et al.*, 2001), the finding that SA can regulate root water transport contributes to a more complete picture of the role of SA in plant water relations. Although a sudden treatment of whole roots by SA does not really match natural exposure of plant tissues to the hormone, this procedure was useful to establish effects of the hormone on water transport at the organ level. The mode of action of SA, in terms of ROS production and aquaporin relocalization, was more specifically addressed at the level of root epidermal cells, which are typically exposed to biotic attacks. Therefore, the mechanisms described here may both apply to systemic responses during abiotic stress or to local responses to high SA concentrations during plant defense.

The SA-induced accumulation of ROS has been observed in other materials than in roots (Mori *et al.*, 2001; Singh *et al.*, 2004), and can be accounted for by multiple mechanisms, including the inhibition of catalases and ascorbate peroxidases, leading to H₂O₂ accumulation, or the extracellular peroxidase-mediated generation of SA radicals and superoxide anions (O₂^{-•}) (Kawano *et al.*, 1998; Klessig *et al.*, 2000). Consistent with its effects on ROS accumulation, SA also markedly altered PIP aquaporin subcellular localization in the root, and enhanced the labelling of spherical bodies by a PIP2;1-GFP fusion. Because externally applied catalase was able to counteract 89% of these effects, our data point to a central role of extracellular H₂O₂ in aquaporin regulation. Catalase also counteracted the SA-induced inhibition of *Lp_r*, but to a lesser extent (32%). Therefore, other intermediates might be involved in SA-dependent aquaporin regulation. In particular, a moderate cell acidosis was observed in response to SA, but not in response to 4-hydroxybenzoic acid (Lebrun-Garcia *et al.*, 2002), which may lead to the H⁺-dependent closure of PIPs (Tournaire-Roux *et al.*, 2003).

Regulation of aquaporin function under salt stress

Salt stress was explored as another context where a significant accumulation of ROS is induced (Demidchik *et al.*, 2003; Leshem *et al.*, 2006). Recent studies have shown that the inhibition of *Lp_r* in response to salinity is mediated through multiple effects on aquaporin expression (Boursiac *et al.*, 2005; Maathuis *et al.*, 2003; Martinez-Ballesta *et al.*, 2003) and phosphorylation (Prak *et al.*, 2008). Besides changes in transcript and protein abundance, salt-induced trafficking of both plasma membrane and tonoplast aquaporins was revealed using aquaporin-GFP reporters (Boursiac *et al.*, 2005; Prak *et al.*, 2008). Here, we showed that, in the distal part of the root (30 mm from the root apex), catalase was able to counteract most of (71%) the salt-induced intracellular accumulation of PIP2;1-GFP. We propose that, similar to the SA response, salt-induced H₂O₂ is largely responsible for PIP

aquaporin internalization under salt stress. Overall, our findings confirm ROS as important components of the response of plant roots to salinity, and contribute to a complex picture, in which the salt-induced downregulation of root water transport results from the integration in time and space of multiple cellular mechanisms for aquaporin regulation.

Our conclusions on salt-induced PIP internalization, however, may appear at variance with a somewhat reversed model proposed by Leshem *et al.* (2007), who suggested that one of earliest effects of salt stress in the *Arabidopsis* root tip is to enhance plasma membrane endocytosis. This would in turn activate the production of intracellular ROS through the transfer of NADPH oxidase into endosomes (Leshem *et al.*, 2006, 2007). This model is based on measurements of salt-dependent changes in membrane lipid endocytosis, as followed by the styryl dye FM4-64 (Leshem *et al.*, 2007). The latter observations have been confirmed in our laboratory (M. Sorieul, D-T. Luu and C. Maurel, *et al.*, unpublished data). In the present work, by contrast, we worked with mature root cells, and followed the much slower dynamics of plasma membrane aquaporins. Our data suggest a retrieval mechanism through endocytic vesicles to dissociate the trafficking of these proteins from bulk lipid membrane flow. More generally, the induction of aquaporin internalization by exogenous H₂O₂, salt and SA, and the counteracting effects of catalase, establish a clear causal relationship between ROS, possibly acting extracellularly, and aquaporin trafficking.

In conclusion, the present work identifies SA as a regulator of aquaporin activity, and points to novel links between plant defense, abiotic stresses and water transport regulation. More generally, this study delineates a signalling path in the *Arabidopsis* root that, in response to H₂O₂, leads to a rapid and significant downregulation of aquaporins. These effects are mediated in part by an ROS-induced relocation of PIP aquaporins in intracellular compartments. We believe that this path could serve in the response of roots to a variety of hormonal and environmental signals, such as SA and salt stress, but also to chilling or to nutrient deprivation, which also induce a concomitant accumulation of ROS and an inhibition of water transport (Lee *et al.*, 2004; Shin and Schachtman, 2004; Shin *et al.*, 2005). Because of the general role of ROS in controlling cell expansion and nutrient uptake in roots (Foreman *et al.*, 2003; Joo *et al.*, 2001; Shin and Schachtman, 2004), the aquaporin regulation mechanism described here could provide a means for coordinating water transport to these other important functions.

Experimental procedures

Plant cultures

Arabidopsis thaliana plants, ecotype Col-0, were germinated and grown *in vitro* for 10 days before transfer to hydroponic culture, as

described in Javot *et al.* (2003). Plants were further grown for 10–20 days in a growth chamber at 70% relative humidity, with cycles of 16 h of light (180 $\mu\text{E m}^{-2} \text{sec}^{-1}$) at 22°C and 8 h of dark at 21°C.

The preparation of plants expressing a PIP2;1-GFP fusion under the control of a CaMV 35S promoter, or plants expressing a GFP-PIP1;2 or a GFP-LTI6a fusion, was described elsewhere (Boursiac *et al.*, 2005; Cutler *et al.*, 2000). Transgenic *Arabidopsis* plantlets were grown *in vitro* for 7–12 days on half-strength MS medium (Murashige and Skoog, 1962).

Water transport assays

All procedures are detailed in Appendix S1. The hydrostatic water transport in root systems excised from plants grown in hydroponics was measured essentially as described by Javot *et al.* (2003) and Boursiac *et al.* (2005). The water relation parameters of root cortical cells were determined using a cell pressure probe, as described by Javot *et al.* (2003). Measurements were performed at a distance of 15–20 mm from the root apex in root tip segments perfused with a nutrient solution complemented with 5 mM Mes-KOH, pH 5.5, and the indicated H₂O₂ concentration. Functional expression of aquaporins in *Xenopus* oocytes was as described by Maurel *et al.* (1993).

Confocal microscopy

Transgenic seedlings expressing GFP fusions were transferred for 15–60 min into a nutrient solution, either standard or complemented with the indicated concentration of H₂O₂, SA, NaCl or catalase (Sigma-Aldrich, <http://www.sigmaaldrich.com>), and the GFP signal was examined on a sample of root tissue under a glass coverslip. All observations were performed using a Zeiss LSM 510 AX70 as described by Boursiac *et al.* (2005). To enable comparison of the pixel intensity of images taken from the same transgenic line, but under different treatments, images were taken under identical exposure conditions. Average grey values within selected image areas corresponding to the cell surface or interior were obtained using IMAGEJ software (<http://rsb.info.nih.gov/ij/>). For detection of intracellular spherical bodies, epidermal cells were examined individually through a stack of images at 2- μm spacing along the z-axis.

Immunoelectron microscopy

Samples were fixed with 0.5% formaldehyde in 0.1 M PBS (pH 7.4) for 1 h at 20°C, dehydrated, embedded in LR White (Sigma-Aldrich), and sectioned according to Luu *et al.* (2000). Sections were then incubated with a 1 : 50 dilution of a rabbit anti-PIP2;1 antibody (Santoni *et al.*, 2003) for 1 h at 20°C, and a goat anti-rabbit secondary antibody conjugated to 20-nm gold particles (Ted Pella Inc., <http://www.tedpella.com>) for 1 h at 20°C. To increase the contrast in specimens, sections were positively stained with uranyl acetate-lead citrate. Sections were observed using a JEOL 1200 EX II microscope operating at 70 kV (JEOL, <http://www.jeol.com>).

Acknowledgements

We thank BiotechMarine (Pontrieux, France) for supporting Julie Boudet. We also thank Drs Graham Noctor, Alain Pugin and David Wendehenne for helpful discussions, and Jean-François Dubremetz, Véronique Richard and Anne-Sophie Frémont for assistance in microscopy. Confocal and electron microscopy observations

were made at the Montpellier RIO Imaging and at the University of Montpellier 2 electron microscopy facilities, respectively, with the financial support of the Federative Research Institute (IFR127) 'Développement, Diversité et Adaptation des Plantes'.

Supplementary Material

The following supplementary material is available for this article online:

Figure S1. Salicylic acid (SA)- and NaCl-induced accumulation of reactive oxygen species (ROS) in *Arabidopsis* roots, as revealed by carboxy-H₂DCFDA-derived fluorescence.

Figure S2. Effects of a blockade of Ca²⁺ influx and protein kinases on the kinetic parameters of the inhibition of pressure-induced sap flow [J_{VP}] by hydrogen peroxide (H₂O₂).

Appendix S1. Supplementary experimental procedures.

This material is available as part of the online article from <http://www3.interscience.wiley.com>.

Please note: Blackwell Publishing are not responsible for the content or functionality of any supplementary materials supplied by the authors. Any queries (other than missing material) should be directed to the corresponding author for the article.

References

- Alexandersson, E., Fraysse, L., Sjøvall-Larsen, S., Gustavsson, S., Fellert, M., Karlsson, M., Johanson, U. and Kjellbom, P. (2005) Whole gene family expression and drought stress regulation of aquaporins. *Plant Mol. Biol.* **59**, 469–484.
- Alleva, K., Niemietz, C.M., Sutka, M., Maurel, C., Parisi, M., Tyerman, S.D. and Amodeo, G. (2006) Plasma membrane of *Beta vulgaris* storage root shows high water channel activity regulated by cytoplasmic pH and a dual range of calcium concentrations. *J. Exp. Bot.* **57**, 609–621.
- Apel, K. and Hirt, H. (2004) Reactive oxygen species: metabolism, oxidative stress, and signal transduction. *Annu. Rev. Plant Biol.* **55**, 373–399.
- Aroca, R., Amodeo, G., Fernandez-Illescas, S., Herman, E.M., Chaumont, F. and Chrispeels, M.J. (2005) The role of aquaporins and membrane damage in chilling and hydrogen peroxide induced changes in the hydraulic conductance of maize roots. *Plant Physiol.* **137**, 341–353.
- Bais, H.P., Vepachedu, R., Gilroy, S., Callaway, R.M. and Vivanco, J.M. (2003) Allelopathy and exotic plant invasion: from molecules and genes to species interactions. *Science*, **301**, 1377–1380.
- Baxter-Burrell, A., Yang, Z., Springer, P.S. and Bailey-Serres, J. (2002) RopGAP4-dependent Rop GTPase rheostat control of *Arabidopsis* oxygen deprivation tolerance. *Science*, **296**, 2026–2028.
- Bienert, G.P., Moller, A.L., Kristiansen, K.A., Schulz, A., Moller, I.M., Schjoerring, J.K. and Jahn, T.P. (2007) Specific aquaporins facilitate the diffusion of hydrogen peroxide across membranes. *J. Biol. Chem.* **282**, 1183–1192.
- Borsani, O., Valpuesta, V. and Botella, M.A. (2001) Evidence for a role of salicylic acid in the oxidative damage generated by NaCl and osmotic stress in *Arabidopsis* seedlings. *Plant Physiol.* **126**, 1024–1030.
- Boursiac, Y., Chen, S., Luu, D.-T., Sorieul, M., van den Dries, N. and Maurel, C. (2005) Early effects of salinity on water transport in *Arabidopsis* roots. Molecular and cellular features of aquaporin expression. *Plant Physiol.* **139**, 790–805.
- Carvajal, M., Martinez, V. and Alcaraz, C.F. (1999) Physiological function of water channels as affected by salinity in roots of paprika pepper. *Physiol. Plant.* **105**, 95–101.
- Chaumont, F., Moshelion, M. and Daniels, M.J. (2005) Regulation of plant aquaporin activity. *Biol. Cell*, **97**, 749–764.
- Coelho, S.M., Taylor, A.R., Ryan, K.P., Sousa-Pinto, I., Brown, M.T. and Brownlee, C. (2002) Spatiotemporal patterning of reactive oxygen production and Ca²⁺ wave propagation in fucus rhizoid cells. *Plant Cell*, **14**, 2369–2381.
- Cutler, S.R., Ehrhardt, D.W., Griffitts, J.S. and Somerville, C.R. (2000) Random GFP::cDNA fusions enable visualization of subcellular structures in cells of *Arabidopsis* at high frequency. *Proc. Natl Acad. Sci. USA*, **97**, 3718–3723.
- Demidchik, V., Shabala, S.N., Coutts, K.B., Tester, M.A. and Davies, J.M. (2003) Free oxygen radicals regulate plasma membrane Ca²⁺- and K⁺-permeable channels in plant root cells. *J. Cell Sci.* **116**, 81–88.
- Demidchik, V., Shabala, S.N. and Davies, J.M. (2007) Spatial variation in H₂O₂ response of *Arabidopsis thaliana* root epidermal Ca²⁺ flux and plasma membrane Ca²⁺ channels. *Plant J.* **49**, 377–386.
- Foreman, J., Demidchik, V., Bothwell, J.H. *et al.* (2003) Reactive oxygen species produced by NADPH oxidase regulate plant cell growth. *Nature*, **422**, 442–446.
- Gerbeau, P., Amodeo, G., Henzler, T., Santoni, V., Ripoche, P. and Maurel, C. (2002) The water permeability of *Arabidopsis* plasma membrane is regulated by divalent cations and pH. *Plant J.* **30**, 71–81.
- Gunes, A., Inal, A., Alpaslan, M., Eraslan, F., Bagci, E.G. and Cicek, N. (2007) Salicylic acid induced changes on some physiological parameters symptomatic for oxidative stress and mineral nutrition in maize (*Zea mays* L.) grown under salinity. *J. Plant Physiol.* **164**, 728–736.
- Henzler, T. and Steudle, E. (2000) Transport and metabolic degradation of hydrogen peroxide in *Chara corallina*: model calculations and measurements with the pressure probe suggest transport of H₂O₂ across water channels. *J. Exp. Bot.* **51**, 2053–2066.
- Henzler, T., Ye, Q. and Steudle, E. (2004) Oxidative gating of water channels (aquaporins) in *Chara* by hydroxyl radicals. *Plant Cell Environ.* **27**, 1184–1195.
- Javot, H., Lauvergeat, V., Santoni, V. *et al.* (2003) Role of a single aquaporin isoform in root water uptake. *Plant Cell*, **15**, 509–522.
- Johansson, I., Karlsson, M., Shukla, V.K., Chrispeels, M.J., Larsson, C. and Kjellbom, P. (1998) Water transport activity of the plasma membrane aquaporin PM28A is regulated by phosphorylation. *Plant Cell*, **10**, 451–460.
- Joo, J.H., Bae, Y.S. and Lee, J.S. (2001) Role of auxin-induced reactive oxygen species in root gravitropism. *Plant Physiol.* **126**, 1055–1060.
- Kaldenhoff, R. and Fischer, M. (2006) Functional aquaporin diversity in plants. *Biochim. Biophys. Acta*, **1758**, 1134–1141.
- Kawano, T., Sahashi, N., Takahashi, K., Uozumi, N. and Muto, S. (1998) Salicylic acid induces extracellular superoxide generation followed by an increase in cytosolic calcium ion in tobacco suspension culture: the earliest events in salicylic acid signal transduction. *Plant Cell Physiol.* **39**, 721–730.
- Klessig, D.F., Durner, J., Noad, R. *et al.* (2000) Nitric oxide and salicylic acid signaling in plant defense. *Proc. Natl Acad. Sci. USA*, **97**, 8849–8855.
- Kourie, J.I. (1998) Interaction of reactive oxygen species with ion transport mechanisms. *Am. J. Physiol.* **275**, C1–C24.
- Kwak, J.M., Nguyen, V. and Schroeder, J.I. (2006) The role of reactive oxygen species in hormonal responses. *Plant Physiol.* **141**, 323–329.
- Lebrun-Garcia, A., Chiltz, A., Gout, E., Bligny, R. and Pugin, A. (2002) Questioning the role of salicylic acid and cytosolic acidification in

- mitogen-activated protein kinase activation induced by cryptogein in tobacco cells. *Planta*, **214**, 792–797.
- Lee, S.H., Singh, A.P. and Chung, G.C.** (2004) Rapid accumulation of hydrogen peroxide in cucumber roots due to exposure to low temperature appears to mediate decreases in water transport. *J. Exp. Bot.* **55**, 1733–1741.
- Leshem, Y., Melamed-Book, N., Cagnac, O., Ronen, G., Nishri, Y., Solomon, M., Cohen, G. and Levine, A.** (2006) Suppression of *Arabidopsis* vesicle-SNARE expression inhibited fusion of H₂O₂-containing vesicles with tonoplast and increased salt tolerance. *Proc. Natl Acad. Sci. USA*, **103**, 18008–18013.
- Leshem, Y., Seri, L. and Levine, A.** (2007) Induction of phosphatidylinositol 3-kinase-mediated endocytosis by salt stress leads to intracellular production of reactive oxygen species and salt tolerance. *Plant J.* **51**, 185–197.
- Liskay, A., van der Zalm, E. and Schopfer, P.** (2004) Production of reactive oxygen intermediates (O₂⁻, H₂O₂, and ·OH) by maize roots and their role in wall loosening and elongation growth. *Plant Physiol.* **136**, 3114–3123.
- Luu, D.T., Qin, X., Morse, D. and Cappadocia, M.** (2000) S-RNase uptake by compatible pollen tubes in gametophytic self-incompatibility. *Nature*, **407**, 649–651.
- Maathuis, F.J., Filatov, V., Herzyk, P. et al.** (2003) Transcriptome analysis of root transporters reveals participation of multiple gene families in the response to cation stress. *Plant J.* **35**, 675–692.
- Martinez-Ballesta, M.C., Aparicio, F., Pallas, V., Martinez, V. and Carvajal, M.** (2003) Influence of saline stress on root hydraulic conductance and PIP expression in *Arabidopsis*. *J. Plant Physiol.* **160**, 689–697.
- Maurel, C., Reizer, J., Schroeder, J.I. and Chrispeels, M.J.** (1993) The vacuolar membrane protein γ -TIP creates water specific channels in *Xenopus* oocytes. *EMBO J.* **12**, 2241–2247.
- Maurel, C., Verdoucq, L., Luu, D.T. and Santoni, V.** (2008) Plant aquaporins: membrane channels with multiple integrated functions. *Annu. Rev. Plant Biol.* in press.
- Mori, I.C., Pinontoan, R., Kawano, T. and Muto, S.** (2001) Involvement of superoxide generation in salicylic acid-induced stomatal closure in *Vicia faba*. *Plant Cell Physiol.* **42**, 1383–1388.
- Müller, J., Mettlich, U., Menzel, D. and Samaj, J.** (2007) Molecular dissection of endosomal compartments in plants. *Plant Physiol.* **145**, 293–304.
- Murashige, T. and Skoog, F.** (1962) A revised medium for rapid growth and bioassays with tobacco tissue cultures. *Physiol. Plant.* **15**, 473–497.
- Peleg-Grossman, S., Volpin, H. and Levine, A.** (2007) Root hair curling and *Rhizobium* infection in *Medicago truncatula* are mediated by phosphatidylinositide-regulated endocytosis and reactive oxygen species. *J. Exp. Bot.* **58**, 1637–1649.
- Prak, S., Hem, S., Boudet, J., Viennois, G., Sommerer, N., Rossignol, M., Maurel, C. and Santoni, V.** (2008) Multiple phosphorylations in the C-terminal tail of plant plasma membrane aquaporins. Role in sub-cellular trafficking of AtPIP2;1 in response to salt stress. *Mol. Cell. Proteomics*, **7**, 1019–1030.
- Rentel, M.C. and Knight, M.R.** (2004) Oxidative stress-induced calcium signaling in *Arabidopsis*. *Plant Physiol.* **135**, 1471–1479.
- Santoni, V., Vinh, J., Pflieger, D., Sommerer, N. and Maurel, C.** (2003) A proteomic study reveals novel insights into the diversity of aquaporin forms expressed in the plasma membrane of plant roots. *Biochem. J.* **372**, 289–296.
- Scott, I.M., Clarke, S.M., Wood, J.E. and Mur, L.A.** (2004) Salicylate accumulation inhibits growth at chilling temperature in *Arabidopsis*. *Plant Physiol.* **135**, 1040–1049.
- Shah, J.** (2003) The salicylic acid loop in plant defense. *Curr. Opin. Plant Biol.* **6**, 365–371.
- Shin, R. and Schachtman, D.P.** (2004) Hydrogen peroxide mediates plant root cell response to nutrient deprivation. *Proc. Natl Acad. Sci. USA*, **101**, 8827–8832.
- Shin, R., Berg, R.H. and Schachtman, D.P.** (2005) Reactive oxygen species and root hairs in *Arabidopsis* root response to nitrogen, phosphorus and potassium deficiency. *Plant Cell Physiol.* **46**, 1350–1357.
- Singh, D.P., Moore, C.A., Gilliland, A. and Carr, J.P.** (2004) Activation of multiple antiviral defence mechanisms by salicylic acid. *Mol. Plant Pathol.* **5**, 57–63.
- Tavernier, E., Wendehenne, D., Blein, J.P. and Pugin, A.** (1995) Involvement of free calcium in action of cryptogein, a proteinaceous elicitor of hypersensitive reaction in tobacco cells. *Plant Physiol.* **109**, 1025–1031.
- Tornroth-Horsefield, S., Wang, Y., Hedfalk, K., Johanson, U., Karlsson, M., Tajkhorshid, E., Neutze, R. and Kjellbom, P.** (2006) Structural mechanism of plant aquaporin gating. *Nature*, **439**, 688–694.
- Tournaire-Roux, C., Sutka, M., Javot, H., Gout, E., Gerbeau, P., Luu, D.T., Bligny, R. and Maurel, C.** (2003) Cytosolic pH regulates root water transport during anoxic stress through gating of aquaporins. *Nature*, **425**, 393–397.
- Vandeleur, R., Niemietz, C., Tilbrook, J. and Tyerman, S.D.** (2005) Role of aquaporins in root responses to irrigation. *Plant Soil*, **274**, 141–161.
- Yalpani, N., Enyedi, A.J., León, J. and Raskin, I.** (1994) Ultraviolet light and ozone stimulate accumulation of salicylic acid, pathogenesis-related proteins and virus resistance in tobacco. *Planta*, **193**, 372–376.
- Ye, Q. and Steudle, E.** (2006) Oxidative gating of water channels (aquaporins) in corn roots. *Plant Cell Environ.* **29**, 459–470.

Dynamic Behavior and Internalization of Aquaporins at the Surface of Plant Cells

Doan-Trung Luu and Christophe Maurel

Abstract Aquaporins, channel proteins that facilitate water transport across the tonoplast and the plasma membrane of plant cells, have classically been used as reference markers for these two membranes. Yet, recent studies have shown that the subcellular localization of aquaporins is constantly adjusted in response to environmental stimuli. This chapter addresses the mechanisms that determine the density at the cell surface of aquaporins of the Plasma Membrane Intrinsic Protein (PIP) subclass. While pharmacological interference coupled to confocal imaging was extensively used in initial studies, single particle tracking of PIPs fused to GFP, fluorescence correlation spectroscopy (FCS), and a novel fluorescence recovery after photobleaching approach have provided unique insights into the peculiarity of PIP cellular dynamics. It was shown in particular that, while endocytosis of PIPs is predominantly clathrin-dependent under standard conditions, PIP cycling is enhanced under salt stress possibly involving a clathrin- and membrane raft-mediated endocytosis. Future research will address the genetic bases of these pathways and their possible control by the plant hormone auxin.

D.-T. Luu · C. Maurel (✉)

Biochimie et Physiologie Moléculaire des Plantes, Institut de Biologie Intégrative des Plantes, Centre National de la Recherche Scientifique, UMR 5004 CNRS/UMR 0386 INRA/ Montpellier SupAgro/Université Montpellier 2, 2 place Viala, 34060 Montpellier Cedex 2, France

e-mail: maurel@supagro.inra.fr

1 Aquaporin Functions and Regulations and the Importance of Aquaporin Trafficking

Aquaporins are water channel proteins that are present in virtually all living organisms and contribute to water transport and equilibration throughout the body of terrestrial plants. The plant aquaporin family is subdivided into seven homology classes (Anderberg et al. 2011). The four classes that are present in all higher plant species can be associated with distinct subcellular localizations. Members of the Tonoplast Intrinsic Protein (TIP) and the Plasma membrane Intrinsic Protein (PIP) classes represent the most abundant aquaporins in the tonoplast and plasma membrane (PM), respectively. The PIP class can be further divided in the PIP1 and PIP2 subclasses. Some isoforms of the Nodulin-26-like Intrinsic Protein (NIP) class have also been found in the PM (Ma et al. 2006; Takano et al. 2006). However, other NIP homologs, similar to members of the fourth class (Small basic Intrinsic Proteins; SIPs), are localized to endoplasmic reticulum (ER) membranes (Ishikawa et al. 2005; Mizutani et al. 2006).

Plants are subjected to multiple biotic and abiotic stresses that impact on their water status and aquaporin-mediated water transport plays an important role in the maintenance of this status (for a review see Maurel et al. 2008). In *Arabidopsis* roots, aquaporins of the PIP class (*AtPIP*) have been shown to be differentially regulated in response to oxygen deprivation, oxidative stress, salinity, and treatments with salicylic acid. These regulations can occur at the transcript level, but more generally at the protein level with changes in pore opening and closing (gating) or changes in aquaporin subcellular localization (Tournaire-Roux et al. 2003; Boursiac et al. 2005; Boursiac et al. 2008; Prak et al. 2008). Elucidating the modes of aquaporin trafficking within the cell or at the cell surface is therefore of prime importance for understanding aquaporin function.

Most of current knowledge on the intracellular trafficking (endocytosis and exocytosis) of plant PM proteins comes from studies on the PIN-FORMED (PIN) auxin transport proteins (see also chapter by Nodzynski et al. in this volume). Other molecular models have been punctually investigated such as the flagellin receptor FLS2 (Robatzek 2007), the boron transporter BOR1 (Takano et al. 2005), the brassinosteroid receptor BRI1 (Vert et al. 2005), the endo-1-4-beta-D-glucanase KOR1 (Robert et al. 2005), and the potassium channel KAT1 (Sutter et al. 2007). Although PIP aquaporins have long been used as canonical PM protein markers, data on their trafficking properties are still scarce. Recent studies (Boursiac et al. 2005, 2008; Zelazny et al. 2007, 2009; Prak et al. 2008; Sorieul et al. 2011; Luu et al. 2012) have shown, however, that PIPs are excellent models for studying the cell biology of plant PM proteins. As an example, data have emerged on PIP export from the ER which is considered as the first step, following synthesis, for transit within the secretory pathway of PM proteins. In the case of maize and *Arabidopsis* PIP2s, this process was shown to be dependent on canonical diacidic ER-export motifs (Zelazny et al. 2009; Sorieul et al. 2011). Using heterologous and transient expression systems, it was also established that

hetero-oligomerization between maize *ZmPIP2s* and *ZmPIP1s* is required for proper export of the latter from the ER (Zelazny et al. 2007). While these studies are crucial for understanding the mechanisms that govern PIP aquaporin biogenesis and proper targeting to the PM, additional mechanisms allow to constantly adjust the density of PIPs in the PM, thereby regulating cell water permeability. This chapter focuses on this topic and addresses the generality and peculiarity of PIP aquaporin dynamics at the cell surface.

2 Constitutive Cycling of PIPs

2.1 Protein Components Involved in the Cycling of PM Cargoes in Plant Cells

Animal cells exhibit various uptake mechanisms for surface proteins, such as clathrin-dependent endocytosis, membrane raft-mediated endocytosis, caveolae-mediated endocytosis, and phagocytosis. In plants, the functional importance of endocytosis has been pioneered demonstrated in the case of cell wall pectins (Baluska et al. 2002) and PIN auxin efflux transporters, using developmental mutant and pharmacological interference analyses (Geldner et al. 2001, 2003). Polarity of auxin transport is achieved by the coordinated localization of PINs to the one end of cells that mediates auxin efflux. In these and other studies, the fungal toxin brefeldin A (BFA), which inhibits the adenosine ribosylation factor (ARF)-guanine nucleotide exchange factor (GEF) GNOM and thus supposedly blocks exocytosis, was crucial to demonstrate the existence and importance of a continuous cycling of PM proteins between the PM and endosomal compartments. Although its precise localization is still unknown, GNOM is assumed to sit in a recycling endosome compartment and thus should act in the interface between the *trans*-Golgi network (TGN) and the PM (Šamaj et al. 2004; Robinson et al. 2008).

Further evidence that internalization mechanisms similar to those in animals exist in plant cells comes from pharmacological interference using the tyrosine (Tyr) analog, Tyrphostin A23 (A23). One of the effects of A23 in mammalian cells is to prevent interaction between the $\mu 2$ subunit of the clathrin-binding Adaptor Protein (AP)-2 complex and cytosolic motifs of cargo PM proteins (Banbury et al. 2003). Tyr-based YXX Φ motifs (where Y is Tyr, X is any amino acid, and Φ is an amino acid with a bulky hydrophobic side chain) mediate cargo recruitment into clathrin-coated vesicles by binding to the μ -subunit of the AP complex and have been identified in animal as well as plant proteins (Happel et al. 2004; Ron and Avni 2004; daSilva et al. 2006; Takano et al. 2010). Although A23 side effects cannot be excluded (see Robinson et al. 2008), several laboratories have shown that inhibition by A23 can be used to dissect membrane trafficking processes in plants (Ortiz-Zapater et al. 2006; Dhonukshe et al. 2007; Konopka et al. 2008; Leborgne-Castel et al. 2008; Fujimoto et al. 2010). More specifically, A23

treatment prevented the labeling of BFA compartments by several PM proteins including PINs, H⁺-ATPase, low temperature inducible protein 6b (LTI6b), and most importantly *AtPIP2;1*, suggesting an inhibition of their endocytosis (Dhonukshe et al. 2007). The synthetic auxin analog, naphthalene-1-acetic acid (NAA), has also been shown to inhibit endocytosis of PINs, *AtPIP2;1* and PM H⁺-ATPase (Paciorek et al. 2005; Dhonukshe et al. 2008; Pan et al. 2009). Wortmannin (Wm), an inhibitor of phosphatidylinositol-3-phosphate (PI-3-P) and phosphatidylinositol-4-phosphate (PI-4-P) kinases, induces in Arabidopsis root cells an enlargement of endosomes labeled with the *AtSORTING NEXIN1* (*AtSNX1*), late endosomal (RabF2a) as well as TGN (RabA1d, RabA1e, RabA4b and VTI12) markers (Jaillais et al. 2006; Takáč et al. 2012). Such endosomes may be assimilated to an intermediate compartment between TGN and the pre-vacuolar compartment (PVC) (Jaillais et al. 2006; Niemes et al. 2010; Takáč et al. 2012). Wm-induced enlarged endosomes (Wm compartment) are also labeled by *AtPIP2;1*, suggesting that this aquaporin may cycle between the PM and the endosomes labeled by *AtSNX1* or may have been detected in the PVC during its route toward vacuolar degradation (Jaillais et al. 2008). Finally, a role for membrane sterols in the endocytosis of PIN proteins and other PM proteins such as *AtPIP2;1* has been proposed (Kleine-Vehn et al. 2006; Men et al. 2008; Pan et al. 2009).

As a complement of the above-mentioned pharmacological approaches, reverse genetics has allowed to identify specific protein components involved in the cycling of plant PM cargoes. For instance, the involvement of clathrin in *AtPIP2;1* endocytosis was demonstrated by means of a dominant-negative mutant strategy (Dhonukshe et al. 2007). When overexpressed in plant cells, the C-terminal part of clathrin heavy chain (CHC) termed “clathrin Hub” binds to and titers away the clathrin light chains, thus making them unavailable for clathrin cage formation. This expression strategy was shown to impair the labeling of BFA compartments by *AtPIP2;1*, indicating a disruption of its endocytosis. More recently, a single *chc2* loss-of-function mutant and dominant-negative *CHC1* (HUB) transgenic lines were shown to be defective in bulk lipid membrane endocytosis as well as in PIN1 subcellular localization (Kitakura et al. 2011). Yet, the phenotypic effects on PIP trafficking remain unknown.

Genetic approaches were also used to dissect the dependency of endocytosis on auxin. In a study using auxin signalling SCF^{TIR1/AFB} mutants, PIN2 and LTI6a but not *AtPIP2;1* were able to label BFA compartments in the presence of NAA (Pan et al. 2009). It was concluded that the corresponding nuclear auxin receptor complex is required for inhibition by auxin of PIN2 and LTI6a endocytosis, but not that of *AtPIP2;1*. In another study, auxin-binding protein 1 (ABP1) was shown to act as a positive factor during clathrin recruitment to the PM (Robert et al. 2010). In the absence of auxin, expression of ABP1 at the plant PM promotes endocytosis of PINs as well as internalization of an ectopically expressed human transferrin receptor. By contrast, binding of auxin to ABP1 impaired the recruitment of clathrin to the PM, and therefore inhibited endocytosis, at least transiently. It remains unknown whether ABP1 affects PIP endocytosis constitutively or only after binding to auxin.

Finally, a plant ortholog of the yeast and mammalian vacuolar protein sorting 29 (VPS29), a member of the retromer complex, has been shown to be required for PIN trafficking (Jaillais et al. 2007). In roots of an *Arabidopsis vps29* mutant, PIN proteins were polarly localized but also showed an additional accumulation in abnormally enlarged compartments. Noticeably, *AtPIP2;1* remained correctly localized at the PM of *vps29* and did not label the enlarged intracellular compartments. This indicates that, in contrast to PINs, the trafficking of PIPs does not involve VSP29 (Jaillais et al. 2007, see also chapter by Zelazny et al. in this volume).

Altogether, these data indicate that PIPs share with other plant PM proteins, and PINs in particular, main subcellular trafficking routes. The data also point to molecular and functional specificities that possibly underlie regulation mechanisms restricted to PIPs (Fig. 1a).

2.2 Novel Approaches for Exploring the Cycling of PIPs

Variable-angle evanescent wave microscopy, also named variable-angle epifluorescence microscopy, was first applied in plants for the visualization of vesicles and proteins within or near the plane of the PM of pollen tubes and epidermal cells (Wang et al. 2006; Konopka and Bednarek 2008; Konopka et al. 2008). In a recent study, this technique was extended to analyzing the lateral mobility of plant PM proteins at a high spatio-temporal resolution. This was achieved by tracking single particles of *AtPIP2;1*-fluorescent protein constructs expressed in epidermal cells of *Arabidopsis* roots (Li et al. 2011). Single particle tracking (SPT) allowed to distinguish for *AtPIP2;1* four types of trajectories and modes of diffusion either Brownian (33.7 ± 3.3 %), directed (27.5 ± 2.4 %), restricted (17.5 ± 2.1 %) or with mixed trajectories (21.2 ± 3.1 %). These analyses also revealed a broad distribution of individual *AtPIP2;1* diffusion coefficients. However, the modal value ($2.46 \times 10^{-3} \mu\text{m}^2\text{s}^{-1}$) was ten times lower than the one for LTI6a ($2.37 \times 10^{-2} \mu\text{m}^2\text{s}^{-1}$), indicating an extremely low lateral diffusion for the aquaporin. In this study, an independent technique, fluorescence correlation spectroscopy (FCS), was used to measure the density of *AtPIP2;1*-fluorescent protein constructs in the PM of root epidermal cells (Li et al. 2011). A value of 30.3 ± 5.1 molecules. μm^{-2} was found for *AtPIP2;1* in cells under resting conditions.

The role in *AtPIP2;1* behavior of various membrane components, such as membrane-raft microdomains or clathrin coats, was first addressed using drug interference (Li et al. 2011). Treatment of root cells with methyl- β -cyclodextrin (M β CD), a sterol disrupting reagent, induced a subpopulation of lowly mobile *AtPIP2;1* particles (diffusion coefficient reduced by 20-fold) and modified the lateral mobility characteristics of *AtPIP2;1* by increasing by 64 % the proportion of particles with a restricted diffusion. These important changes were not accompanied by any change in *AtPIP2;1* density in the PM. When cells were treated by A23, a marked (10-fold) reduction of the diffusion coefficient value was observed ($1.59 \times 10^{-3} \mu\text{m}^2\text{s}^{-1}$), accompanied by a twofold increase of the

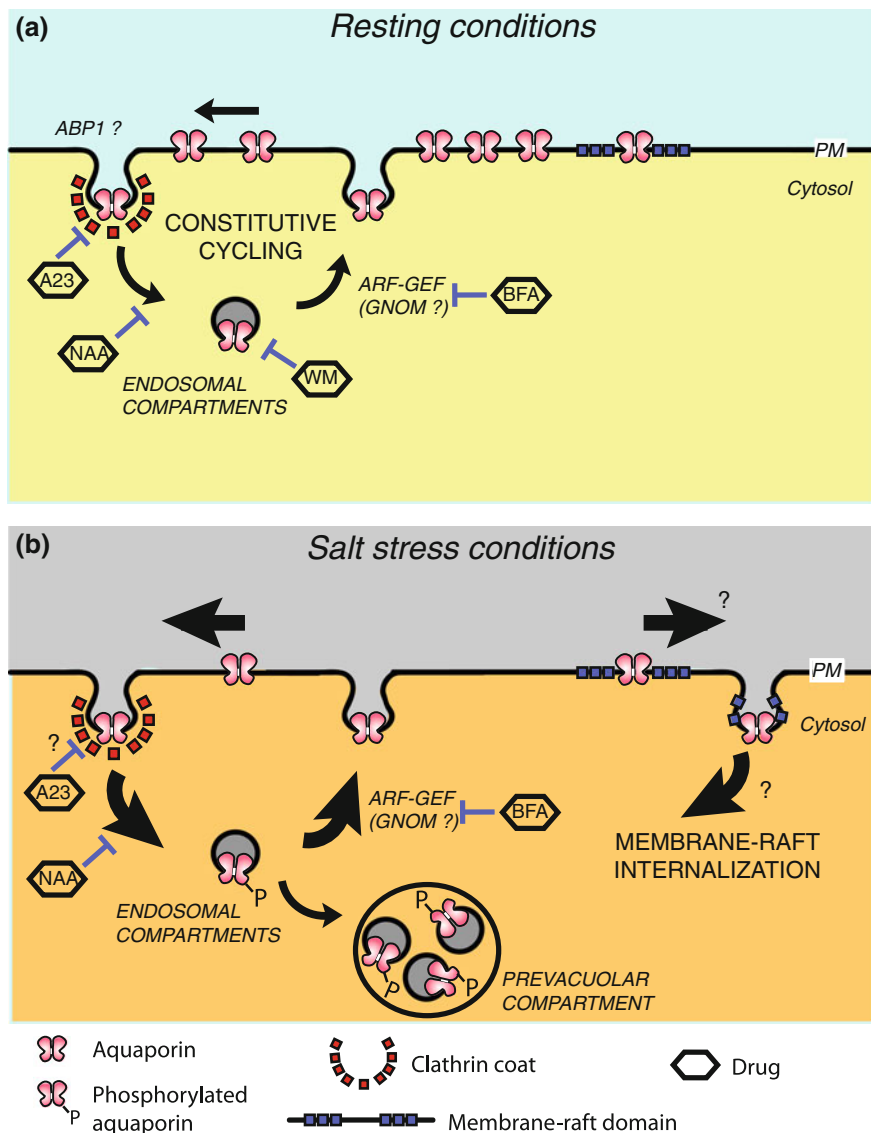


Fig. 1 Tentative model showing the subcellular trafficking mechanisms controlling PIP cycling under resting and stress conditions. **a** In resting conditions, PIP aquaporins exhibit a reduced lateral diffusion and may in part be associated with membrane-raft microdomains. PIPs constitutively cycle between the plasma membrane (PM) and endosomal compartments. Endocytosis is clathrin-mediated and sensitive to A23. Auxin (NAA) or BFA can antagonize PIP cycling at the indicated steps. Functional importance of putative auxin receptor ABP1 in PIP endocytosis is unknown. Enlarged endosomes labeled with PIPs are formed after *Wm* treatments. **b** Under salt stress, the proportion of PIPs with restricted trajectories at the cell surface and the rate of PIP cycling are increased by comparison to resting conditions. Functional importance of clathrin in the salt-induced endocytosis needs to be clarified. A membrane-raft-associated pathway is possibly involved in the internalization of PIPs. Prevacuolar compartments are enriched in phosphorylated forms of *AtPIP2;1* whereas unphosphorylated forms would be confined to undetermined endosomes

proportion of particles with a mixed diffusion mode. Importantly, and consistent with an inhibition of endocytosis, the A23 treatment increased by 32 % the density of GFP-tagged *AtPIP2;1* in the PM. The differential effects of these drugs suggest that both clathrin-dependent endocytosis and membrane microdomains determine the dynamic characteristics of *AtPIP2;1*, but through independent modes. The influence of these two components on *AtPIP2;1* surface behavior was also suggested by co-localizations of the aquaporin with both Flotillin 1 (*AtFlot1*), a marker protein of membrane rafts, and the Clathrin Light Chain (*AtCLC*). These data also confirm previous studies showing that PIPs co-purified with detergent-resistant membranes (Mongrand et al. 2004; Morel et al. 2006).

The low lateral diffusion of *AtPIP2;1* in the plane of the PM described above is reminiscent of the behavior described for the PM K^+ channel, KAT1, and the H^+ -ATPase, PMA2 (Sutter et al. 2006; Sutter et al. 2007). It contrasts with the behavior of proteins resident or retained in the ER, which exhibit an extremely high lateral motion (Runions et al. 2006; Luu et al. 2012). In this kind of studies, fluorescence recovery after photobleaching (FRAP) techniques, and the use of a photo-activable version of GFP (*paGFP*) have been instrumental for monitoring the lateral mobility of membrane proteins. The low lateral diffusion of PIPs was recently examined in Arabidopsis root epidermal cells expressing fusions of GFP with PM (*AtPIP1;2*, *AtPIP2;1*, LTI6a) or tonoplast (*AtTIP1;1*) proteins by using the same set of techniques (Luu et al. 2012). The fluorescence recovery responses were similar for the two *AtPIP* isoforms, fused with GFP either at the N- or C-terminus, suggesting that the position of the fused GFP did not affect the lateral mobility of *AtPIPs*. While the fluorescence signal of GFP-LTI6a had recovered by ~55 % at 50 s and almost completely at 7 min after photobleaching, the relative amplitude of signal recovery of *AtPIP* fusions was below 60 % even after 30 min. A kymographic analysis, allowing to represent as a function of time the recovery of the fluorescence signal along a line which crosses the bleached region, also confirmed the low dynamics of *AtPIPs* in the plane of the PM. Complementary experiments were performed by monitoring the decrease in fluorescent signal, after photo-activation in a region of interest of *paGFP* fused to LTI6a or *AtPIP2;1*. Here again, the decrease in signal was found slower for *AtPIP2;1* than for LTI6a. This series of data indicate a minute, if any, lateral diffusion of GFP-tagged *AtPIPs*, over the 30 min of monitoring in the PM of Arabidopsis root epidermal cells. Therefore, the slow FRAP response observed over the same period of time cannot be explained by the lateral diffusion of the GFP-tagged *AtPIPs* and other processes must be invoked. These findings suggested that the slow FRAP response of the *AtPIP* constructs could be used to dissect their constitutive cycling. A close inspection of the corresponding fluorescence recovery curves showed them to be biphasic, with a fast process completed at 60 s and a slower process that developed for up to 30 min and beyond. It was suggested that the first process is due to a fast cytoplasmic streaming which drags intracellular compartments containing GFP-tagged *AtPIPs* into the initially bleached region. Because of a lack of lateral diffusion of the GFP-tagged *AtPIPs* in the PM, the slower recovery observed during the next 30 min would, by contrast, be due to their recycling from the

endosomal compartments to the PM. As a consequence, the amplitude of the early recovery phase can be used to estimate the labeling intensity of endomembrane compartments (in other words, the abundance of GFP-tagged *AtPIP* in these compartments). The slow recovery phase would report on the cycling of GFP-tagged *AtPIPs* between the endomembrane and PM compartments, including sequential steps in endocytosis, sorting in the endosomes, and exocytosis. This tentative model was validated using a pharmacological dissection of FRAP responses. Consistent with its inhibiting effects on endocytosis, A23 was found to reduce the labeling of endomembrane compartments by GFP-tagged *AtPIPs*. A23 and also NAA and BFA reduced the recovery of fluorescence at 30 min and beyond suggesting an inhibition of the recycling to the PM. Surprisingly, NAA did not change the intensity of endosomal labeling in these experiments. Thus, the site of NAA inhibition may be downstream of endocytic uptake and upstream of the TGN. Nevertheless, the whole set of data validates FRAP as a new technique for studying the cycling of PM proteins, with a higher quantitative resolution than standard confocal imaging (Fig. 1a).

3 Stress-Induced Trafficking of PIPs

3.1 *Physiological Effects of Salinity and Oxidative Stress on Root Water Transport*

Aquaporins contribute to a significant part of the root hydraulic conductivity (L_p) in numerous plant species including *Arabidopsis*, rice, maize, grapevine, or legumes (for review, see Maurel et al. 2008). Therefore, the regulation of L_p in response to multiple abiotic stimuli such as drought, salinity, temperature extremes as well as oxygen and nutrient deprivation provides interesting physiological contexts in which to investigate the molecular and cellular mechanisms of aquaporin regulation. For instance, a treatment with 100 mM NaCl was found to provoke a fast (halftime = 45 min) and strong (–70 %) inhibition of *Arabidopsis* L_p (Boursiac et al. 2005). Salinity was perceived as an osmotic stimulus, since an equivalent osmotic challenge with 200 mM mannitol induced a similar reduction in L_p . A strong reduction (60–75 %) in aquaporin transcript abundance was observed, but at a rather late stage (2–4 h) after exposure to salt. By contrast, *AtPIP1* protein abundance was decreased by 40 % as early as 30 min after salt exposure, whereas *AtPIP2* levels remained constant during the first 6 h of the salt treatment. In addition, salt enhanced the intracellular labeling of root cells expressing *AtPIP1*;2-GFP and *AtPIP2*;1-GFP fusions, as early as 2 h after salt treatment. Internalization of *AtPIPs* and the resulting reduction of aquaporin density at the PM, would therefore contribute to salt-induced reduction of L_p .

In a more general context, exposure of cucumber roots to cold stress (4–8 °C) (Lee et al. 2004), or exposure of *Arabidopsis* to salt (150 mM NaCl) or salicylic acid

(0.5 mM SA) (Boursiac et al. 2008) were all shown to induce a concomitant accumulation of reactive oxygen species (ROS) and inhibition of Lp_r . Exogenous application of hydrogen peroxide (H_2O_2), one of major ROS, was also able to reduce Lp_r by up to 90 % in less than 15 min (Boursiac et al. 2008), suggesting that the effects of cold, salt or SA on Lp_r were mediated through production of ROS. This was partly demonstrated in the case of Arabidopsis by showing that the salt- or SA-induced internalization of *At*PIPs could be counteracted by ROS scavenging using a catalase treatment. Functional expression of *At*PIPs in *Xenopus* oocytes showed, in addition, that the intrinsic water transport activity of these aquaporins was insensitive to ROS. Thus, these experiments establish the central role of a ROS-induced cellular redistribution of aquaporins during the regulation of root water transport in response to multiple hormonal and environmental signals.

3.2 Cell Surface Dynamics and Cycling of PIPs in Response to Salinity and Oxidative Stress

Under biotic or abiotic stresses, regulation of endocytosis is essential in plant cells (Leborgne-Castel and Luu 2009), as it allows a rapid adjustment of membrane transport or stress perception and signalling. For instance, when rice cells were subjected to a saline stress, the endocytosis of biotinylated bovine serum albumin was initially inhibited but activated after a 24 h-extended period (Bahaji et al. 2003). By contrast, a study in Arabidopsis roots (Leshem et al. 2007) demonstrated an enhancement of bulk-flow endocytosis shortly after a massive salt treatment (0.2 M NaCl). More specifically, the salt-induced internalization of aquaporins was found to be strongly dose dependent. Intracellular labeling with *At*PIP-GFP was occasionally observed after 2 h treatment with 100 mM NaCl, whereas a treatment with 150 mM NaCl resulted in a pronounced labeling of fuzzy structures and of spherical bodies, tentatively identified as endomembrane compartments and small vacuoles, respectively (Boursiac et al. 2005, 2008). The same intracellular structures were labeled following SA or H_2O_2 application. While some PM cargoes, such as BOR1 or the iron transporter IRT1 undergo stimulus-induced internalization prior to being targeted to vacuolar degradation (Takano et al. 2005; Barberon et al. 2011), the K^+ -channel *At*KAT1 was shown to be reversibly sequestered upon ABA-induced internalization (Sutter et al. 2007). Whether stress-induced *At*PIP internalization plays a role in degradation and/or intracellular sequestration remains as yet unknown.

The two recent studies partially described in the previous section have brought significant insights into the fundamental effects of salt on the membrane dynamics of PIPs. First, SPT in root epidermal cells expressing *At*PIP2;1-GFP showed that a short-term salt stress (100 mM NaCl for 10 min) increased by twofold the diffusion coefficient of *At*PIP2;1 particles and by 60 % the proportion of particles with a restricted diffusion mode (Li et al. 2011). In addition, FCS showed that these

effects were accompanied by a 46 % decrease of the *AtPIP2;1* density in the PM. The latter decrease could be partly antagonized by both A23 and M β CD. Thus, while endocytosis is predominantly clathrin-dependent under standard conditions, it is enhanced under salt stress and involves both clathrin- and membrane microdomain-mediated endocytic pathways (Fig 1b).

In the second study (Luu et al. 2012), FRAP and photo-activation approaches were used to dissect the cycling properties of *AtPIPs* under salt stress. Kymographic analyses and photo-activation experiments showed that although the diffusion coefficient of *AtPIP2;1* particles was increased by twofold under salt stress (Li et al. 2011), the contribution of lateral diffusion to the recovery of fluorescence was negligible, similar to control conditions (Luu et al. 2012). Yet, the amplitude of fluorescence recovery was increased by twofold by salt treatment, suggesting that salt induced an enhanced cycling of *AtPIPs*. This idea was validated by showing that the kinetics of labeling by GFP-tagged *AtPIPs* of BFA compartments, as well as the reversal of labeling after washout experiment, were accelerated under salt stress conditions. The overall data show that salt stress enhanced both endocytosis and exocytosis of *AtPIPs*, and therefore their cycling. A pharmacological dissection of the FRAP response, similar to the one performed under control conditions, showed that PIP cycling under salt stress was blocked by NAA but had become insensitive to A23. This was interpreted to mean that an enhanced clathrin-mediated endocytosis could overrun the effect of this drug or that, contrary to the standard conditions, an endocytic mechanism, which is insensitive to A23, specifically operates in salt stress conditions. The latter hypothesis is consistent with involvement of a membrane microdomain-dependent pathway, as suggested by FCS measurements (Li et al. 2011).

In mammalian cells, early endosomes comprise two distinct populations: a dynamic population that is highly mobile on microtubules and matures rapidly toward late endosomes, and a static population that matures much more slowly (Lakadamyali et al. 2006). The dynamic population was found to be linked to an AP-2-independent endocytic machinery and transports cargoes such as low-density lipoprotein receptors. Here, we suggest that a similar pathway may be activated in plant cells under salt stress. Interestingly, evidence for a clathrin-independent endocytic pathway has recently been presented in the context of glucose uptake by BY-2 tobacco cells (Bandmann and Homann 2012). Flotillin-dependent endocytosis was also recently described in plant cells (Li et al. 2012). Nevertheless, there is an urging need to know further molecular components involved in these emerging pathway(s) of plant endocytosis.

Phosphorylation has well-identified effects on plant aquaporin gating, but was recently shown to interfere with the subcellular trafficking of PIPs (Prak et al. 2008). Mass spectrometry analyses of membrane protein extracts from Arabidopsis roots allowed the identification of two phosphorylation sites at Ser280 and Ser283 in the C-terminal tail of *AtPIP2;1*. The functional role of these sites was addressed by introducing into a GFP-*AtPIP2;1* fusion, mutations of Ser280 or Ser283 to an Alanine or an Aspartate, to mimic a constitutive dephosphorylation or phosphorylation, respectively, of these two sites. The overall data indicated that

phosphorylation of Ser283 but not of Ser280 is necessary for correct targeting of *AtPIP2;1* to the PM of epidermal root cells. The former site is also involved in the intracellular sorting of *AtPIP2;1* following salt-induced internalization. In brief, the dephosphorylated form (Ser283Ala mutant) was associated with the labeling of “fuzzy” structures whereas the phosphorylated form (Ser283Asp mutant) labeled spherical bodies (Fig. 1b). The protein kinases and phosphatases acting on the two phosphorylation sites and the protein partners involved in the phosphorylation-dependent sorting of *AtPIP2;1* under salt stress are as yet unknown.

4 Conclusions and Future Prospects

While PIPs have been extensively used as canonical and stable markers of the PM, the trafficking of these proteins is now the matter of intense investigations. Data gathered over the last few years have pointed to similarities with the PIN transporters, another intensively studied model for protein subcellular trafficking. For instance, the involvement of clathrin-dependent endocytosis and the similar effects of BFA indicate common constitutive cycling pathways for PIP and PIN homologs (Fig. 1). However, a possible role of ABP1 in the recruitment of clathrin for subsequent endocytosis of PIP remains to be defined. This is a totally open question as recent pharmacological studies (Luu et al. 2012, Wudick et al. 2012 in preparation) indicate that auxin may interfere with PIP trafficking downstream of clathrin-mediated endocytosis. Another important line of research will concern the activation of both clathrin-dependent and -independent endocytic pathways, in cells under oxidative and salt stress. A very useful strategy is to combine pharmacological and genetic interference approaches. Such a strategy has proved to be very informative for the dissection of clathrin-dependent endocytosis of PINs and of course needs to be extended to PIPs. Another component which potentially functions in PIP trafficking is the exocyst complex. This complex tethers secretory vesicles to the PM in yeast and animals (Munson and Novick 2006; He and Guo 2009). By contrast to their mammalian and yeast counterparts, the majority of the eight predicted plant exocyst subunits exist as multiple copies with only a few of these genes having assigned functions in cell–cell interactions, apical cell growth, and development (Synek et al. 2006; Hala et al. 2008; Samuel et al. 2009). Their primary role in exocytosis of PIPs and other PM cargos remains to be determined.

Although providing a very partial knowledge, studies on the trafficking pathways of PIPs have already pointed to significant differences to those described for PINs. These differences might be related to specific PM distributions of the two classes of proteins. Polar targeting of PIN proteins is of fundamental importance for directional auxin transport from cell to cell and for maintaining the auxin gradients that are required for organ development. By contrast, very few aquaporins have been described to be polarly localized in plant cells. For instance, *AtNIP5;1* serves as a boric acid channel and preferentially localizes at the exofacial side of root cells under boron limiting conditions (Takano et al. 2010).

Comparative studies of the trafficking pathways of *AtNIP5;1* and of the non-polar *AtPIP2;1* might reveal specific and common mechanisms. Finally, homologs of the PIP1 and PIP2 subclasses are known to have distinct trafficking abilities within the secretory pathway (Fetter et al. 2004). Yet, these homologs can assemble in heterotetramers and, while PIP1 homotetramers are retained intracellularly, PIP2 homotetramers or PIP1-PIP2 heterotetramers exhibit a facilitated trafficking to the PM (Zelazny et al. 2007). Thus, we anticipate that the PIP1-PIP2 molecular interactions may have specific impacts on the dynamics at the cell surface and endocytosis of each of these PIPs. Complex cellular dynamics of aquaporins would therefore depend on the combinatorial co-expression of numerous PIP isoforms within the same plant cell type.

References

- Anderberg H, Danielson J, Johanson U (2011) Algal MIPs, high diversity and conserved motifs. *BMC Evol Biol* 11:110
- Bahaji A, Aniento F, Cornejo MJ (2003) Uptake of an endocytic marker by rice cells: variations related to osmotic and saline stress. *Plant Cell Physiol* 44:1100–1111
- Baluška F, Hlavacka A, Šamaj J, Palme K, Robinson DG, Matoh T, McCurdy DW, Menzel D, Volkman D (2002) F-actin-dependent endocytosis of cell wall pectins in meristematic root cells. Insights from brefeldin A-induced compartments. *Plant Physiol* 130:422–431
- Banbury DN, Oakley JD, Sessions RB, Banting G (2003) Tyrphostin A23 inhibits internalization of the transferrin receptor by perturbing the interaction between tyrosine motifs and the medium chain subunit of the AP-2 adaptor complex. *J Biol Chem* 278:12022–12028
- Bandmann V, Homann U (2012) Clathrin-independent endocytosis contributes to uptake of glucose into BY-2 protoplasts. *Plant J* (in press)
- Barberon M, Zelazny E, Robert S, Conejero G, Curie C, Friml J, Vert G (2011) Monoubiquitin-dependent endocytosis of the iron-regulated transporter 1 (IRT1) transporter controls iron uptake in plants. *Proc Natl Acad Sci U S A* 108:E450–E458
- Boursiac Y, Boudet J, Postaire O, Luu DT, Tournaire-Roux C, Maurel C (2008) Stimulus-induced downregulation of root water transport involves reactive oxygen species-activated cell signalling and plasma membrane intrinsic protein internalization. *Plant J* 56:207–218
- Boursiac Y, Chen S, Luu DT, Sorieul M, van den Dries N, Maurel C (2005) Early effects of salinity on water transport in Arabidopsis roots. Molecular and cellular features of aquaporin expression. *Plant Physiol* 139:790–805
- daSilva LL, Foresti O, Denecke J (2006) Targeting of the plant vacuolar sorting receptor BP80 is dependent on multiple sorting signals in the cytosolic tail. *Plant Cell* 18:1477–1497
- Dhonukshe P, Aniento F, Hwang I, Robinson DG, Mravec J, Stierhof YD, Friml J (2007) Clathrin-mediated constitutive endocytosis of PIN auxin efflux carriers in Arabidopsis. *Curr Biol* 17:520–527
- Dhonukshe P, Grigoriev I, Fischer R, Tominaga M, Robinson DG, Hasek J, Paciorek T, Petrasek J, Seifertova D, Tejos R, Meisel LA, Zazimalova E, Gadella TWJ Jr, Stierhof Y-D, Ueda T, Oiwa K, Akhmanova A, Brock R, Spang A, Friml J (2008) Auxin transport inhibitors impair vesicle motility and actin cytoskeleton dynamics in diverse eukaryotes. *Proc Natl Acad Sci U S A* 105:4489–4494
- Fetter K, Van Wilder V, Moshelion M, Chaumont F (2004) Interactions between plasma membrane aquaporins modulate their water channel activity. *Plant Cell* 16:215–228

- Fujimoto M, Arimura S-i, Ueda T, Takanashi H, Hayashi Y, Nakano A, Tsutsumi N (2010) Arabidopsis dynamin-related proteins DRP2B and DRP1A participate together in clathrin-coated vesicle formation during endocytosis. *Proc Natl Acad Sci U S A* 107:6094–6099
- Geldner N, Anders N, Wolters H, Keicher J, Kornberger W, Muller P, Delbarre A, Ueda T, Nakano A, Jurgens G (2003) The Arabidopsis GNOM ARF-GEF mediates endosomal recycling, auxin transport, and auxin-dependent plant growth. *Cell* 112:219–230
- Geldner N, Friml J, Stierhof Y-D, Jurgens G, Palme K (2001) Auxin transport inhibitors block PIN1 cycling and vesicle trafficking. *Nature* 413:425–428
- Hala M, Cole R, Synek L, Drdova E, Pecenkova T, Nordheim A, Lamkemeyer T, Madlung J, Hochholdinger F, Fowler JE, Zarsky V (2008) An exocyst complex functions in plant cell growth in Arabidopsis and tobacco. *Plant Cell* 20:1330–1345
- Happel N, Honing S, Neuhaus JM, Paris N, Robinson DG, Holstein SE (2004) Arabidopsis μ A-adaptin interacts with the tyrosine motif of the vacuolar sorting receptor VSR-PS1. *Plant J* 37:678–693
- He B, Guo W (2009) The exocyst complex in polarized exocytosis. *Curr Opin Cell Biol* 21:537–542
- Ishikawa F, Suga S, Uemura T, Sato MH, Maeshima M (2005) Novel type aquaporin SIPs are mainly localized to the ER membrane and show cell-specific expression in *Arabidopsis thaliana*. *FEBS Lett* 579:5814–5820
- Jaillais Y, Fobis-Loisy I, Miege C, Gaude T (2008) Evidence for a sorting endosome in Arabidopsis root cells. *Plant J* 53:237–247
- Jaillais Y, Fobis-Loisy I, Miege C, Rollin C, Gaude T (2006) *AtSNX1* defines an endosome for auxin-carrier trafficking in Arabidopsis. *Nature* 443:106–109
- Jaillais Y, Santambrogio M, Rozier F, Fobis-Loisy I, Miege C, Gaude T (2007) The retromer protein VPS29 links cell polarity and organ initiation in plants. *Cell* 130:1057–1070
- Kitakura S, Vanneste S, Robert S, Lofke C, Teichmann T, Tanaka H, Friml J (2011) Clathrin mediates endocytosis and polar distribution of PIN auxin transporters in Arabidopsis. *Plant Cell* 23:1920–1931
- Kleine-Vehn J, Dhonukshe P, Swarup R, Bennett M, Friml J (2006) Subcellular trafficking of the Arabidopsis auxin influx carrier AUX1 uses a novel pathway distinct from PIN1. *Plant Cell* 18:3171–3181
- Konopka CA, Backues SK, Bednarek SY (2008) Dynamics of Arabidopsis dynamin-related protein 1C and a clathrin light chain at the plasma membrane. *Plant Cell* 20:1363–1380
- Konopka CA, Bednarek SY (2008) Variable-angle epifluorescence microscopy: a new way to look at protein dynamics in the plant cell cortex. *Plant J* 53:186–196
- Lakadamyali M, Rust MJ, Zhuang X (2006) Ligands for clathrin-mediated endocytosis are differentially sorted into distinct populations of early endosomes. *Cell* 124:997–1009
- Leborgne-Castel N, Lherminier J, Der C, Fromentin J, Houot V, Simon-Plas F (2008) The plant defense elicitor cryptogein stimulates clathrin-mediated endocytosis correlated with reactive oxygen species production in bright yellow-2 tobacco cells. *Plant Physiol* 146:1255–1266
- Leborgne-Castel N, Luu D-T (2009) Regulation of endocytosis by external stimuli in plant cells. *Plant Biosyst* 143:630–635
- Lee SH, Singh AP, Chung GC (2004) Rapid accumulation of hydrogen peroxide in cucumber roots due to exposure to low temperature appears to mediate decreases in water transport. *J Exp Bot* 55:1733–1741
- Leshem Y, Seri L, Levine A (2007) Induction of phosphatidylinositol 3-kinase-mediated endocytosis by salt stress leads to intracellular production of reactive oxygen species and salt tolerance. *Plant J* 51:185–197
- Li X, Wang X, Yang Y, Li R, He Q, Fang X, Luu DT, Maurel C, Lin J (2011) Single-molecule analysis of PIP2;1 dynamics and partitioning reveals multiple modes of Arabidopsis plasma membrane aquaporin regulation. *Plant Cell* 23:3780–3797
- Li R, Liu P, Wan Y, Chen T, Wang Q, Mettbach U, Baluška F, Šamaj J, Fang X, Lucas WJ, Lin J (2012) A membrane microdomain-associated protein, Arabidopsis Flot1, is involved in a

- clathrin-independent endocytic pathway and is required for seedling development. *Plant Cell*, (in press, published on line May 15)
- Luu D-T, Martinière A, Sorieul M, Runions J, Maurel C (2012) Fluorescence recovery after photobleaching reveals high cycling dynamics of plasma membrane aquaporins in *Arabidopsis* roots under salt stress. *Plant J* 69:894–905
- Ma JF, Tamai K, Yamaji N, Mitani N, Konishi S, Katsuhara M, Ishiguro M, Murata Y, Yano M (2006) A silicon transporter in rice. *Nature* 440:688–691
- Maurel C, Verdoucq L, Luu DT, Santoni V (2008) Plant aquaporins: membrane channels with multiple integrated functions. *Annu Rev Plant Biol* 59:595–624
- Men S, Boutte Y, Ikeda Y, Li X, Palme K, Stierhof YD, Hartmann MA, Moritz T, Grebe M (2008) Sterol-dependent endocytosis mediates post-cytokinetic acquisition of PIN2 auxin efflux carrier polarity. *Nat Cell Biol* 10:237–244
- Mizutani M, Watanabe S, Nakagawa T, Maeshima M (2006) Aquaporin NIP2;1 is mainly localized to the ER membrane and shows root-specific accumulation in *Arabidopsis thaliana*. *Plant Cell Physiol* 47:1420–1426
- Mongrand S, Morel J, Laroche J, Claverol S, Carde JP, Hartmann MA, Bonneau M, Simon-Plas F, Lessire R, Bessoule JJ (2004) Lipid rafts in higher plant cells: purification and characterization of Triton X-100-insoluble microdomains from tobacco plasma membrane. *J Biol Chem* 279:36277–36286
- Morel J, Claverol S, Mongrand S, Furt F, Fromentin J, Bessoule JJ, Blein JP, Simon-Plas F (2006) Proteomics of plant detergent-resistant membranes. *Mol Cell Proteomics* 5:1396–1411
- Munson M, Novick P (2006) The exocyst defrocked, a framework of rods revealed. *Nat Struct Mol Biol* 13:577–581
- Niemes S, Langhans M, Viotti C, Scheuring D, San Wan Yan M, Jiang L, Hillmer S, Robinson DG, Pimpl P (2010) Retromer recycles vacuolar sorting receptors from the *trans*-Golgi network. *Plant J* 61:107–121
- Ortiz-Zapater E, Soriano-Ortega E, Marcote MJ, Ortiz-Masia D, Aniento F (2006) Trafficking of the human transferrin receptor in plant cells: effects of tyrphostin A23 and brefeldin A. *Plant J* 48:757–770
- Paciorek T, Zažímalová E, Ruthardt N, Petrasek J, Stierhof YD, Kleine-Vehn J, Morris DA, Emans N, Jurgens G, Geldner N, Friml J (2005) Auxin inhibits endocytosis and promotes its own efflux from cells. *Nature* 435:1251–1256
- Pan J, Fujioka S, Peng J, Chen J, Li G, Chen R (2009) The E3 ubiquitin ligase SCFTIR1/AFB and membrane sterols play key roles in auxin regulation of endocytosis, recycling, and plasma membrane accumulation of the auxin efflux transporter PIN2 in *Arabidopsis thaliana*. *Plant Cell* 21:568–580
- Prak S, Hem S, Boudet J, Viennois G, Sommerer N, Rossignol M, Maurel C, Santoni V (2008) Multiple phosphorylations in the C-terminal tail of plant plasma membrane aquaporins: role in subcellular trafficking of *AtPIP2;1* in response to salt stress. *Mol Cell Proteomics* 7:1019–1030
- Robatzek S (2007) Vesicle trafficking in plant immune responses. *Cell Microbiol* 9:1–8
- Robert S, Bichet A, Grandjean O, Kierzkowski D, Satiat-Jeunemaitre B, Pelletier S, Hauser MT, Höfte H, Vernhettes S (2005) An *Arabidopsis* endo-1,4-beta-D-glucanase involved in cellulose synthesis undergoes regulated intracellular cycling. *Plant Cell* 17:3378–3389
- Robert S, Kleine-Vehn J, Barbez E, Sauer M, Paciorek T, Baster P, Vanneste S, Zhang J, Simon S, Covanova M, Hayashi K, Dhonukshe P, Yang Z, Bednarek SY, Jones AM, Luschnig C, Aniento F, Zazimalova E, Friml J (2010) ABP1 mediates auxin inhibition of clathrin-dependent endocytosis in *Arabidopsis*. *Cell* 143:111–121
- Robinson DG, Jiang L, Schumacher K (2008) The endosomal system of plants: charting new and familiar territories. *Plant Physiol* 147:1482–1492
- Ron M, Avni A (2004) The receptor for the fungal elicitor ethylene-inducing xylanase is a member of a resistance-like gene family in tomato. *Plant Cell* 16:1604–1615
- Runions J, Brach T, Kuhner S, Hawes C (2006) Photoactivation of GFP reveals protein dynamics within the endoplasmic reticulum membrane. *J Exp Bot* 57:43–50

- Šamaj J, Baluška F, Voigt B, Schlicht M, Volkmann D, Menzel D (2004) Endocytosis, actin cytoskeleton, and signaling. *Plant Physiol* 135:1150–1161
- Samuel MA, Chong YT, Haasen KE, Aldea-Brydges MG, Stone SL, Goring DR (2009) Cellular pathways regulating responses to compatible and self-incompatible pollen in Brassica and Arabidopsis stigmas intersect at Exo70A1, a putative component of the exocyst complex. *Plant Cell* 21:2655–2671
- Sorieul M, Santoni V, Maurel C, Luu DT (2011) Mechanisms and effects of retention of over-expressed aquaporin AtPIP2;1 in the endoplasmic reticulum. *Traffic* 12:473–482
- Sutter JU, Campanoni P, Tyrrell M, Blatt MR (2006) Selective mobility and sensitivity to SNAREs is exhibited by the Arabidopsis KAT1 K⁺ channel at the plasma membrane. *Plant Cell* 18:935–954
- Sutter JU, Sieben C, Hartel A, Eisenach C, Thiel G, Blatt MR (2007) Abscisic acid triggers the endocytosis of the Arabidopsis KAT1 K⁺ channel and its recycling to the plasma membrane. *Curr Biol* 17:1396–1402
- Synek L, Schlager N, Elias M, Quentin M, Hauser MT, Zarsky V (2006) AtEXO70A1, a member of a family of putative exocyst subunits specifically expanded in land plants, is important for polar growth and plant development. *Plant J* 48:54–72
- Takáč T, Pechan T, Šamajová O, Ovečka M, Richter H, Eck C, Niehaus K, Šamaj J (2012) Wortmannin treatment induces changes in Arabidopsis root proteome and post-Golgi compartments. *J Proteome Res*, (in press, published on line May 10)
- Takano J, Miwa K, Yuan L, von Wiren N, Fujiwara T (2005) Endocytosis and degradation of BOR1, a boron transporter of *Arabidopsis thaliana*, regulated by boron availability. *Proc Natl Acad Sci U S A* 102:12276–12281
- Takano J, Tanaka M, Toyoda A, Miwa K, Kasai K, Fuji K, Onouchi H, Naito S, Fujiwara T (2010) Polar localization and degradation of Arabidopsis boron transporters through distinct trafficking pathways. *Proc Natl Acad Sci U S A* 107:5220–5225
- Takano J, Wada M, Ludewig U, Schaaf G, von Wiren N, Fujiwara T (2006) The Arabidopsis major intrinsic protein NIP5;1 is essential for efficient boron uptake and plant development under boron limitation. *Plant Cell* 18:1498–1509
- Tournaire-Roux C, Sutka M, Javot H, Gout E, Gerbeau P, Luu DT, Bligny R, Maurel C (2003) Cytosolic pH regulates root water transport during anoxic stress through gating of aquaporins. *Nature* 425:393–397
- Vert G, Nemhauser JL, Geldner N, Hong F, Chory J (2005) Molecular mechanisms of steroid hormone signaling in plants. *Annu Rev Cell Dev Biol* 21:177–201
- Wang X, Teng Y, Wang Q, Li X, Sheng X, Zheng M, Šamaj J, Baluška F, Lin J (2006) Imaging of dynamic secretory vesicles in living pollen tubes of *Picea meyeri* using evanescent wave microscopy. *Plant Physiol* 141:1591–1603
- Wudick MM, Geldner N, Chory J, Maurel C, Luu DT (2012) Sub-cellular pathway and role of hydrogen peroxide-induced redistribution of root aquaporins (in preparation)
- Zelazny E, Borst JW, Muylaert M, Batoko H, Hemminga MA, Chaumont F (2007) FRET imaging in living maize cells reveals that plasma membrane aquaporins interact to regulate their subcellular localization. *Proc Natl Acad Sci U S A* 104:12359–12364
- Zelazny E, Miecielica U, Borst JW, Hemminga MA, Chaumont F (2009) An N-terminal diacidic motif is required for the trafficking of maize aquaporins ZmPIP2;4 and ZmPIP2;5 to the plasma membrane. *Plant J* 57:346–355